UNIONE EUROPEA
Fondo Sociale Europeo
Fondo Europeo di Sviluppo Regionale

Ministero dell'Istruzione, dell'Università e della Ricerca

PON RICERCA E INNOVAZIONE 2014 - 2020

University of Naples Federico II

Polytechnic and Basic Sciences School

Ph.D. in Chemical Sciences

Glycolipids with immunomodulant activity and their development as immunotherapy adjuvants and antitumor

Laura Fioretto

Advisors:
Prof. Marina **Della Greca** (Dept of Chemical Sciences, Unina)
Dr. Emiliano **Manzo** (CNR - Biosearch Srl)
Prof. Raymond J. **Andersen** (Dept of Chemistry, UBC)

Examiner:
Prof. Emiliano **Bedini**

XXXII CYCLE 2017-2020
Coordinator: Prof. Angela **Lombardi**

“The PhD candidate wish to thank European Union (FSE, PON Ricerca e Innovazione 2014-2020, Azione I.1 “Dottorati Innovativi con caratterizzazione Industriale”), for funding a Ph.D. grant to Laura Fioretto”

La borsa di dottorato è stata cofinanziata con risorse del
Programma Operativo Nazionale Ricerca e Innovazione 2014-2020 (CCI 2014IT16M2OP005),
Fondo Sociale Europeo, Azione I.1 “Dottorati Innovativi con caratterizzazione Industriale”

UNIONE EUROPEA
Fondo Sociale Europeo

Ministero dell'Istruzione, dell'Università e della Ricerca

PON RICERCA E INNOVAZIONE 2014 - 2020

Index

Abbreviations

AIDS = acquired immunodeficiency syndrome

ANS = 8-Anilinonaphthalene-1-sulfonic acid

APC = Antigen-Presenting cell

BF_3OEt_2 = Boron trifluoride ethyl etherate.

$BnNH_2$ = benzylamine

BODIPY = 4,4-difluoro-4-bora-3a,4a-diaza-s-indacene

CD = Cluster of Differentiation

cDC = conventional Dendritic Cell

CMC = Critical Micellar Concentration

Cryo-TEM = Cryogenic Transmission Electron Microscopy

DAPI = 4',6-diamidin-2-fenilindolo

DBU = 1,8-Diazabiciclo[5.4.0]undec-7-ene

DC = Dendritic cell

DCC = *N,N*-dicyclohexylcarbodiimide

DCM = dichloromethane

DGDG = digalactosyldiacylglycerol

DLS = Dynamic Light Scattering

DMAP = *N,N*-dimethylaminopyridine

DMF = *N,N*-Dimethylformamide

DNA = Deoxyribonucleic Acid

DPH = 1,6-diphenyl-hexatriene

EBV-EA = Epstein-Barr virus-associated early antigen

Et_3N = trimethylamine

FCA = Freund's Complete Adjuvant

FIA = Freund's Incomplete Adjuvant

GM-CSF = granulocyte-macrophage colony-stimulating factor

HEK = Human embryonic kidney

HIV = human immunodeficiency virus

HLA = Human Leukocyte Antigen

HSV = herpes simplex virus

IFN = interferon

Ig = Immunoglobulins

IL = Interleukin

ISCOM = Immune timulating complexes

K_b = Boltzmann constant

LPS = lipopolysaccharide

mAbs = monoclonal Antibodies

MFI = mean fluorescence intensity

MGDG = monogalactosyldiacylglycerols

MHC = major histocompatibility complex

MLR = mixed lymphocyte reaction

MoDC = monocyte-derived dendritic cells

MPLA = Monophosphoryl lipid A

NK = Natural Killer

NMR = Nuclear Magnetic Resonance

NPN = 1-N-phenylnaphthylamine

OVA = Ovalbumin

PAMP = pathogen-associated molecular patterns

pDC = plasmocytoid Dendritic Cell

PPh_3 = Triphenylphosphine

PRR = Pattern Recognition Receptors

R_h = hydrodynamic radius of particles in solution

RT = reverse transcriptase

SQDG = sulfoquinovosyldiacylglycerol

TCR = T cell Receptor

TEM = Transmission Electron Microscopy

Th = T helper

THF = tetrahydrofuran

TLR = Toll-Like Receptor

TM = TiterMax®

TNF = Tumor Necrosis Factor

TPA = 12-*O*-tetradecanoylphorbol-13-acetate

α-Galcer = α-galactosylceramide

η = solvent viscosity

Summary

All vaccinations are based on the common concept of stimulation of an immune response. A vaccine is a preparation consisting of properly treated pathogens (or parts of them) administered with the purpose of providing acquired immunity [1-4]. This process, called vaccination, is able to actively exploit the memory of the immune system, allowing the body to develop a defence system against a bacterium, virus or other microorganism even before they come into contact with it. Long-term protection requires the persistence of specific antibodies above protective thresholds and/or the maintenance of immune memory cells capable of rapid and effective reactivation with subsequent exposure to the antigens [4]. The induction of these mechanisms requires activation by specific Antigen-Presenting Cells (APCs).

Dendritic Cells (DCs) are the most efficient APCs and are often called 'nature's adjuvants' for their ability to capture antigens, process and present them on the cell surface as well as to produce appropriate costimulatory molecules aimed to induce a primary antigen-specific immune response in naïve T lymphocytes [5]. The activation of DCs consist in a transition from an immature state to a mature state and this maturation leads to interleukins production and can be monitored by the detection of some phenotypic surface markers such as CD83 and CD86 molecules [6-7].

Even if vaccine containing highly purified antigens are often less immunogenic, they own an improved safety profile [4] and for this reason vaccine adjuvants are necessary.

Adjuvants are complex molecules or mixture of compounds able to enhance the pathogen recognition as well as to elicit an immune response.

Actually, the exact mechanisms that adjuvants employ to enhance the immune response is unknown and one of the hypothesized mechanisms of action lies in their ability to trigger the maturation of APCs through upregulation of costimulatory

molecules, improving antigen processing and presentation [4, 8-9].

In spite of the enormous efforts in the research of new vaccines and vaccine adjuvants, approved formulations of commercial adjuvants are still the same as fifty years ago, and they are far from being efficient and appropriate for what life requires [10]; therefore, this is still an active field and the identification of new, safe and efficient adjuvants represent the most innovative technology in the identification of new vaccines against challenging diseases.

Among adjuvants, immunomodulators are compounds able to regulate and/or normalize the immune system and they are used to boost immune response.

The present PhD thesis is based on the development of new molecular vaccine adjuvants.

Within the field of marine natural products several studies involved the identification of new candidates able to stimulate the activation of DCs maturation and to prime a specific immune response. In particular, a natural mixture of α-sulfoquinovosyldiacylglycerols (α-SQDGs) isolated from the diatom *Thalassiosira weissflogii* showed an interesting ability to stimulate DCs maturation in *in vitro* biological assays [11].

Starting from these outstanding results, in this PhD thesis the 1,2-*O*-distearoyl-3-*O*-β-D-sulfoquinovosylglycerol, a synthetic analogue of the natural α-SQDGs, named Sulfavant A, was initially prepared

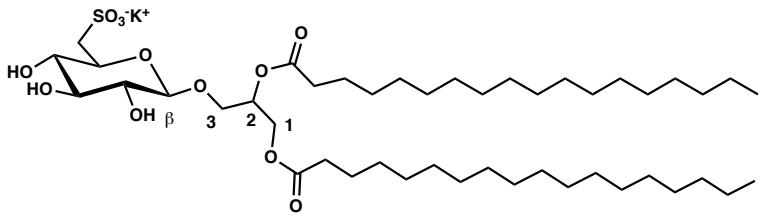

Chemical structure of 1,2-*O*-distearoyl-3-*O*-β-D-sulfoquinovosylglycerol (Sulfavant A)

The chemical structure of Sulfavant A was featured by the characteristic sulfonic group of natural α-SQDGs, combined with the β configuration at the anomeric

carbon, typical of LPS-based glycolipids.

Since saturated fatty acids are characteristic of other immunogenic bacterial glycolipids, such as Monophosphoryl lipid A (MPLA) acyl chains, $C_{18:0}$ acyl chains have been inserted on the glycerol moiety of Sulfavant A [11].

The synthesis of Sulfavant A was achieved by an efficient and versatile synthetic strategy and its immunomodulant activity was tested evaluating its ability to induce DCs maturation, or in other words, monitoring the regulation of the phenotypic surface markers induced by Sulfavant A on DCs [11-12].

Biological assays carried out on Sulfavant A showed an up-regulation of the CD83 molecules as well as the gene expression of proinflammatory cytokines [11], moreover, as mentioned before, it was demonstrated that the mechanism of action of Sulfavant A is TLRs-independent, even though it was plausible considering the similarity with other immunogenic bacterial glycolipids (e.g. LPS) [11].

Even if the mechanism behind Sulfavant A activity was not clarified, these results were positive enough to proceed with further investigation. During this PhD thesis, Sulfavant A was also tested *in vivo*: in a first experiment the antibodies response was evaluated, considering the type and the level of immunoglobulins produced by Sulfavant A in animal model using Ovalbumin (OVA) as antigen; while in a second experiment the adjuvant properties of Sulfavant A was evaluated in an experimental model of vaccination against melanoma in mice using $hgp100_{25–33}$ melanoma antigen [11].

Considering the promising results obtained from these experiments, it was decided to explore the effect of molecule structural changes on biological activity introducing other different acyl chains and/or changing the stereochemistry at carbon 2 of the glycerol moiety.

In particular, making slight modifications of the synthetic strategy planned for the preparation of Sulfavant A, two palmitoyl ($C_{16:0}$) and two nonadecanoyl chains ($C_{19:0}$) were introduced and, for each analogue, both the epimeric mixture at carbon 2 of the glycerol moiety and the diasteropure analogues were synthetized.

This approach led to six different derivatives: three with the $C_{16:0}$ acyl chains, called β-SQDG16 (epimeric mixture at C2), β-SQDG16-R (with *R* configuration at C2) and β-SQDG16-S (with *S* configuration at C2) and three with the $C_{19:0}$ acyl chains named β-SQDG19, β-SQDG19-R and β-SQDG19-S.

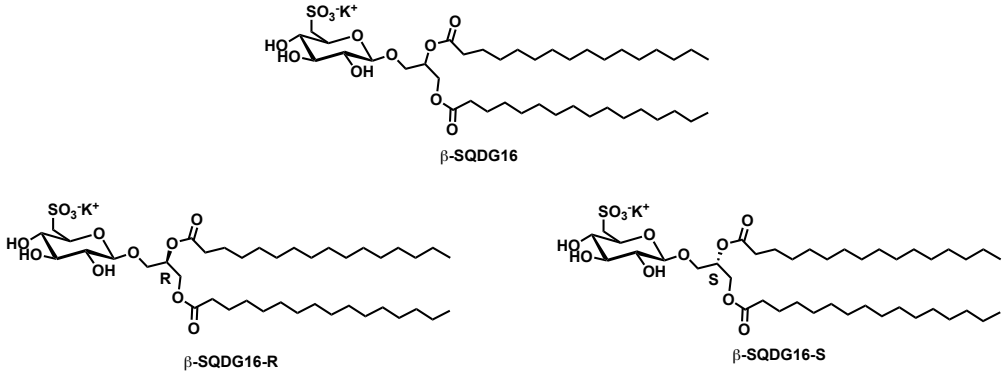

Chemical structure of 1,2-*O*-dipalmitoyl-3-*O*-β-D-sulfoquinovosylglycerol (β-SQDG16), (*R*)-1,2-*O*-dipalmitoyl-3-*O*-β-D-sulfoquinovosylglycerol (β-SQDG16-R) and (*S*)-1,2-*O*-dipalmitoyl-3-*O*-β-D-sulfoquinovosylglycerol (β-SQDG16-S)

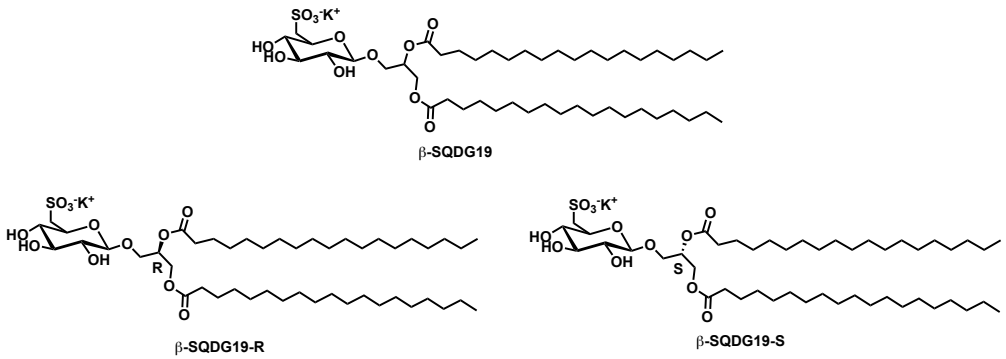

Chemical structure of 1,2-*O*-dinonadecanoyl-3-*O*-β-D-sulfoquinovosylglycerol (β-SQDG19), (*R*)-1,2-*O*-dinonadecanoyl-3-*O*-β-D-sulfoquinovosylglycerol (β-SQDG19-R) and (*S*)-1,2-*O*-dinonadecanoyl-3-*O*-β-D-sulfoquinovosylglycerol (β-SQDG19-S)

As well as for Sulfavant A, also for the other β-SQDGs the immunomodulant activity on DCs maturation was tested. The results suggested that even a small modification in the length of the hydrophobic tails induced partial loss of activity, independently from the stereochemistry of the carbon 2 of the glyceridic moiety.

With the purpose to proceed with further biological investigation on Sulfavant A bioactivity the synthetic strategy previously planned was improved and specifically the number of total steps was reduced from 14 to 11 with an increase of the overall yield from 4% to 11.2% [13].

The new synthetic strategy was also employed for the preparation of the diasteropure analogues of Sulfavant A, called Sulfavant R (with *R* configuration at C2) and Sulfavant S (with *S* configuration at C2) [13], even if, because of a partial epimerization occurred during Sulfavant S preparation, its synthesis was successively optimized in order to achieve the pure Sulfavant S.

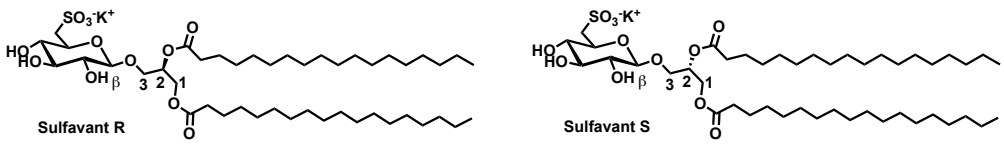

Chemical structure of 1,2-*O*-distearoyl-3-*O*-β-D-sulfoquinovosyl-(*R*)-glycerol (Sulfavant R) and 1,2-*O*-distearoyl-3-*O*-β-D-sulfoquinovosyl-(*S*)-glycerol (Sulfavant S)

The biological evaluation of Sulfavant R and Sulfavant S immunomodulant activity [13] led to surprising different response strictly correlated with stereochemical aspects; in fact, the efficacy of single epimers (Sulfavant S and R) on the up-regulation of DCs maturation phenotypic markers was maximum at concentration 1000-fold lower than that occurred for the Sulfavant A.

Therefore, while Sulfavant A showed maximum activation of DCs maturation at concentration around 10 μM, Sulfavant R and S expressed their maximum activity at concentration around 10 nM, and all curves of activity were featured by a peculiar bell-shaped dose response [13].

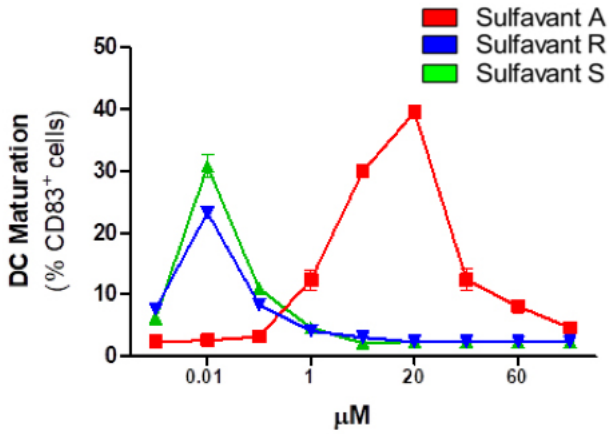

DCs maturation expressed as percentage of $CD83^+$ cells depending on Sulfavants concentration

Within this PhD project, particular attention was focused on the reasons behind the different biological behaviour of Sulfavants on DCs activation and on the characteristic shape of their curves of activation.

Taking into consideration the amphiphilic nature of glycoglycerolipids, a hypothesis was that Sulfavants could self-assemble in hydrophilic environment, arranging themselves in supramolecular structure. If it was true, the formation of aggregates could influence the bioavailability of the molecule to the cellular target and affect the ability to induce DCs maturation [13].

In order to investigate the self-assembling properties of Sulfavants and to correlate it with the relation structure-activity, a detailed study on the chemo-physical properties of Sulfavants was carried out.

In particular, the first evidence that effectively Sulfavants aggregate in aqueous solution was obtained by Dynamic Light Scattering (DLS) measurements. The hydrodynamic radius of the aggregates, evaluated by DLS, also underline the differences between the supramolecular structure formed by each Sulfavant [13].

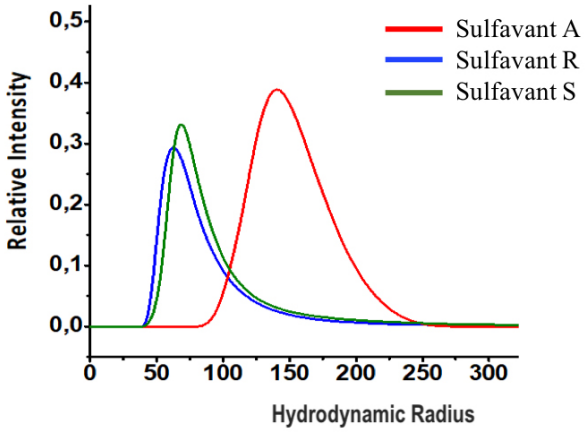

Hydrodynamic radius distribution of particles of Sulfavants in aqueous suspension at 0.2 mM as measured by DLS on three independent measurements.

Despite some difficulties to analyse Sulfavants solution at very low concentrations, in this thesis the Critical Micellar Concentration (CMC) was evaluated by means of two different techniques: surface tension measurements and fluorescence spectroscopy. Since the results obtained were divergent, it was plausible that the ability to detect aggregates depended from the sensitivity of the techniques used for this purpose.

The study on the chemo-physical properties of Sulfavants self-assembling, carried out during this thesis, involved also the evaluation of the effect of a detergent agents on Sulfavant A aqueous solution, that not only confirmed the formation of aggregate at low concentration, but especially it evidences that aggregation negatively affected the immunomodulant activity of these compounds, since by adding a detergent the maximum activation of DCs maturation undergo important shift at lower concentrations.

The only technique suitable for the investigation of Sulfavants solution at the same concentration at which they showed the maximum bioactivity (10 nM and 10 μM) was Cryogenic Transmission Electron Microscopy (cryo-TEM).

Cryo-TEM images showed direct evidences of Sulfavant A and Sulfavant R aggregation at 10 nM and 10 μM concentrations, underlining the differences between their supramolecular structures.

Despite the exact mechanism underlying Sulfavants activity is still not completely clarified, it is possible to assert that they represent a new class of molecular adjuvants able to prime human DCs by a Toll like receptor (TLR2/TLR4) – independent mechanism [11].

Simultaneously to this study on the trend of Sulfavants to aggregate in colloidal structures, the investigation of the biological mechanisms behind their bioactivity and the identification of their cellular targets were a very important topic to be evaluate.

Furthermore, a fluorescent analogue of Sulfavants was synthesised in order to get informations, by bioimaging studies, about the possible mechanisms behind the activity of these sulfolipids. In particular, the fluorescent probe 4,4-difluoro-4-bora-3a,4a-diaza-*s*-indacene dye (BODIPY) was introduced on the hydrophobic moiety of Sulfavant R by a diastereoselective and versatile synthetic strategy.

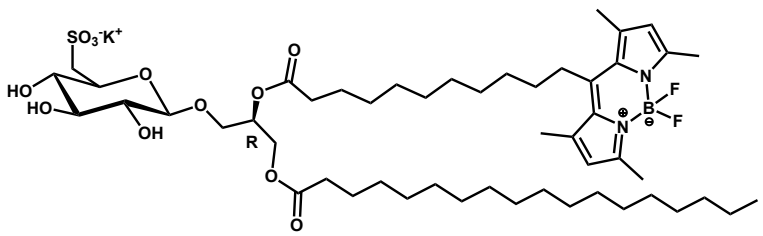

Sulfavant R-Me$_4$ BODIPY

Chemical structure of Sulfavant R-Me$_4$BODIPY

In order to guarantee that the structural modification of the fluorescent Sulfavant derivative did non-affect the biological activity, preliminary test on DCs maturation were performed showing outcomes comparable with immunomodulant activity of Sulfavants.

Considering the potential of these sulfolipids in terms of their possible applications as vaccine adjuvants, further investigations, aimed to their future development, required the preparation of higher amounts of product. With this purpose, during this PhD an improved and scalable procedure that allowed the production of grams of Sulfavant

A was designed. This synthetic procedure was very similar to the previous one, but slight modifications were mandatory in order to avoid decrease of the total yield due to the increased difficulties in the purification of the intermediate products.

Within the huge class of bioactive glycolipids, recently Professor Andersen and coworkers, of the University of British Columbia (Vancouver-Canada), found out an interesting biological activity from a fraction of natural compounds isolated from a Canadian sponge (to be classified), containing as main component the 1-*O*-alkyl-2-*O*-(2'-*O*-β-D-glucopyranosyl-β-D-xylopyranosyl)-glycerol.

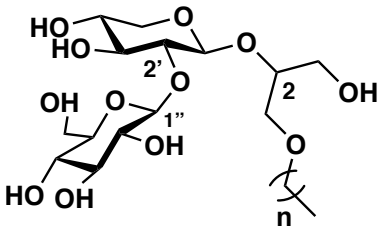

Chemical structure of
1-*O*-alkyl-2-*O*-(2'-*O*-β-D-glucopyranosyl-β-D-xylopyranosyl)-glycerol

According to this PhD thesis, during an internship at the University of British Columbia, a synthetic strategy for the preparation of the above main component has been designed in order to proceed with further investigations on its biological activity. More details about the biological activity of this compound and the nature of the alkyl chains linked to the glycerol moiety are not disclosed because patent submission by Professor Andersen and coworkers is pending.

References

[1] E. Tritto, F. Mosca, E. De Gregorio, E "Mechanism of action of licensed vaccine adjuvants" Vaccine, 27 (25-26) (2009), 3331-3334.

[2] R. Rappuoli, M. Pizza, G. Del Giudice, E. De Gregorio "Vaccines, new opportunities for a new society" Proceedings of the National Academy of Sciences, 111(34) (2014), 12288-12293.

[3] T. Olafsdottir, M. Lindqvist, A. M. Harandi "Molecular signatures of vaccine adjuvants" Vaccine, 33(40) (2015) 5302-5307.

[4] Di Pasquale, S. Preiss, F.T. Da Silva, N. Garcon, "Vaccine Adjuvants: From 1920 to 2015 and Beyond" Vaccines, 3 (2015) 320–343

[5] A.M. Dudek, S. Martin, A.D. Garg, P. Agostinis "Immature, Semi-Mature, and Fully Mature Dendritic Cells: Toward a DC-Cancer Cells Interface That Augments Anticancer Immunity" Frontiers in Immunology, 4 (2013), 438

[6] Mbongue, J. C., Nieves, H. A., Torrez, T. W., Langridge, W. H. (2017). The role of dendritic cell maturation in the induction of insulin-dependent diabetes mellitus. Frontiers in immunology, 8, 327.

[7] Dalod, M., Chelbi, R., Malissen, B., Lawrence, T. (2014). Dendritic cell maturation: functional specialization through signaling specificity and transcriptional programming. The EMBO journal, 33(10), 1104-1116.

[8] Rey-Ladino, J., Ross, A. G., Cripps, A. W., McManus, D. P., Quinn, R. (2011). Natural products and the search for novel vaccine adjuvants. Vaccine, 29(38), 6464-6471.

[9] Vandebriel, R. J., Hoefnagel, M. H. (2012). Dendritic cell-based in vitro assays for vaccine immunogenicity. Human vaccines & immunotherapeutics, 8(9), 1323-1325.

[10] Rappuoli, R., Mandl, C. W., Black, S., De Gregorio, E. (2011). Vaccines for the twenty-first century society. Nature reviews immunology, 11(12), 865.

[11] Manzo, E., Cutignano, A., Pagano, D., Gallo, C., Barra, G., Nuzzo, G., Sansone, C., Ianora, A., Urbanek, K., Fenoglio, D., Ferrera, F., Bernardi, C., Parodi, A., Pasquale, G., Leonardi, A., Filaci, G., De Palma, R., Fontana, A. (2017). A new marine-derived sulfoglycolipid triggers dendritic cell activation and immune adjuvant response. Scientific reports, 7(1), 6286.

[12] Manzo, E., Fioretto, L., Pagano, D., Nuzzo, G., Gallo, C., De Palma, R., Fontana, A. (2017). Chemical synthesis of marine-derived sulfoglycolipids, a new class of molecular adjuvants. Marine drugs, 15(9), 288.

[13] Manzo, E., Gallo, C., Fioretto, L., Nuzzo, G., Barra, G., Pagano, D., Russo Krauss, I., Paduano, L., Ziaco, M., DellaGreca, M., De Palma, R., Fontana, A. (2019). Diasteroselective Colloidal Self-Assembly Affects the Immunological Response of the Molecular Adjuvant Sulfavant. ACS Omega, 4(4), 7807-7814.

Chapter 1: Introduction

1.1 Glycolipids

Glycolipids represent a broad and heterogeneous family of natural products with different essential biological functions [1,2]. They are located in all living organisms, included bacteria and plants, and constitute significant building blocks for cellular membranes [3].

As active compound or as precursors, glycolipids are involved in crucial mechanisms of cellular communication and recognition as well as they are an essential energy reserve. Since their discovery, glycolipids, either intra and extra cellular, have been studied for their important biological properties [4,5].

Albeit they are characterized by a wide structural diversity, glycolipids can be classified on the base of the lipidic fragment in three main groups:

- **Glycosphingolipids**, structurally composed of a mono- di- or oligo-saccharide residue linked to a common ceramide lipid unit, sphingosine or phytosphingosine bound to a fatty acid via an amide bond (Figure 1.1a)
- **Glycoglycerolipids**, made up of a general structure with a mono- di- or oligo-saccharide residue linked to a 1,2-di-*O*-acylglycerol moiety (Figure 1.1b), even if there can be several exceptions including the replacement of the sugar residue with a five-membered cyclitol, or substitution of the 1-*O*-acyl chain bound to glycerol with a 1-*O*-alkyl chain (Crasserides and Isocrasserides) [6] (Figure 1.2)
- **Atypical glycolipids**, those comprising the rest of the glycolipids possessing atypical lipidic moieties linked to the saccharide residues.

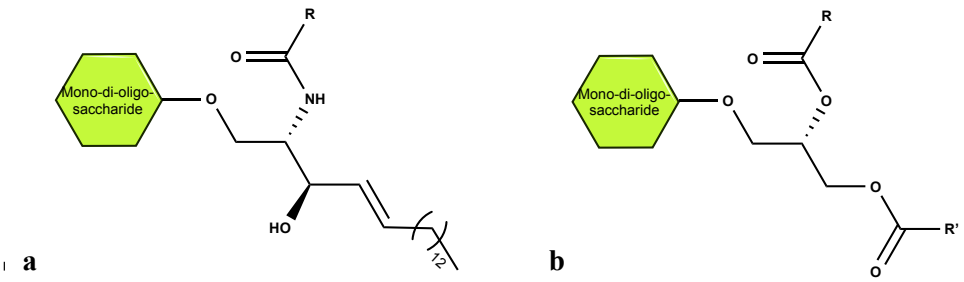

Figure 1.1: General structure of a) Glycosphingolipids and b) Glycoglycerolipids (R and R'=alkyl chains)

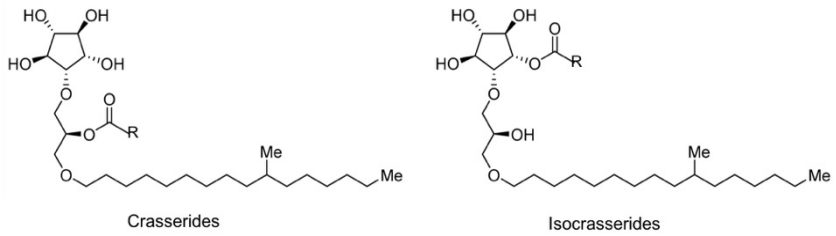

Figure 1.2: Structure of Crasserides and Isocrasserides (R=alkyl chains)

Glycosphingolipids are extensively distributed on the surface of cell membranes of all living organisms where they play crucial activity for cell-cell recognition and cell signalling. An example of these compounds is the α-galactosylceramide, illustrated in Figure 1.3a

In contrast to the glycosphingolipids, glycoglycerolipids are mainly located in micro-organisms and plants. Due to the difficulty of their isolation from natural sources, the importance of this class of metabolites has been underestimated for many years. Even after the improvement of analytical and synthetic approaches, most of the mechanisms behind their biological activity has not been fully clarified.

Finally, the 'atypical glycolipids' include any glycoconjugate that contains a lipid chain not present in the previous groups. Within this huge family there are

Agminosides, Ancorinosides, Caminosides, Erylusamides [7] (Figure 1.3b) and many other compounds.

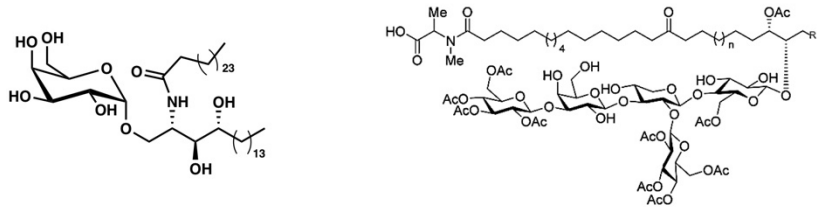

Figure1.3: Chemical structure of the a) α Galactosylceramide and b) Erylusamides [7]

1.1.2 Glycoglycerolipids from marine organisms

Nature has ever been the traditional source for the development of new pharmaceuticals. Today, over 50% of the commercial drugs is inspired by natural products both extracted or, more commonly, synthesised.

Since ancient times, natural medicines were used to treat many diseases including infection, inflammation, pain and neurological disorders.

Drug discovery has changed with the introduction of sophisticated and multidisciplinary methods, but natural products remain the primary source for the development of new therapeutic agents. However, steep technological challenges associated with screening and manufacturing these molecules has stifled their discovery and marketing. To this end, the recent development of metagenomics and ancillary high-throughput screening technologies has exponentiated the volume of useful genetic information for the screening methodologies. Secondly, a new manufacturing paradigm employing metabolic engineering has greatly accelerated the path to market for these molecules. In this frame, the oceans represent a huge reservoir of potential drugs for the future. Marine organisms are used as model systems to address fundamental biology questions [8] about the structure and function of cells, subcellular structures, organelles, organ systems, and whole organisms as well as a huge wealth of recruitment of new therapeutic molecules.

Within marine organisms, microalgae are one of the oldest microorganisms [9] able to grow in different kind of environments, sometimes also in extreme condition (e.g. desert or Antarctica) capable to protecting themselves through the biosynthesis of some secondary metabolites with antibiotic or repellent effects [9-12].

These molecules, including polysaccharides, secondary metabolites and lipids, have gained attention for industrial applications as pharmaceutical, cosmeceutical and nutraceutical products [13-15].

Within this frame, glycoglycerolipids are nowadays extensively studied due to their biological activity. Widely distributed in marine algae, cyanobacteria and higher plants, first glycoglycerolipids were isolated from plants in the second half of the 20th century when it was demonstrated that some of them, namely galactoglycerolipids, were among the main components of the photosynthetic membranes in plants and other photosynthetic organisms [16-17]. Subsequently, a sulfoquinovosyldiacylglycerol (SQDG) molecule was isolated from the alga *Chlorella* [18] and was proved that this glycolipid is a universal plant lipid element [19].

In the first decade after their discovery and characterization, the functions of glycolipids were only correlated with the membrane structuration and as energy source, mainly due to the difficulties to work with this kind of molecules or the minimal amounts of product isolated. Just some years later, the biosynthetic pathways, the role and the distribution of this family of molecules gained attention especially with the increasing necessity to discover new drug entities [20-23].

Plant glycoglycerolipids consist essentially of three main components: monogalactosyldiacylglycerols (MGDGs), digalactosyldiacylglycerols (DGDGs) and sulfoquinovosyldiacylglycerols (SQDGs); even if other homologues have been detected in small amount like tri- and tetra- galactosyldiacylglycerols.

The general structure of glycoglycerolipids from marine organisms consist of a sugar group, mono-, di- or poly-saccharide, linked to a 1,2-diacyl-*sn*-glycerol moiety by α

or β glycosidic bond in anomeric position. To better understand the common structure of these compounds, some examples are given in Figure 1.4.

These compounds are characterized by an amphiphilic nature due to the different polarity of the two main moieties: the polar sugar and the non-polar hydrophobic acyl chains. This feature implicates peculiar characteristics in aqueous environments that affect their biological functions, as it will discuss in this thesis.

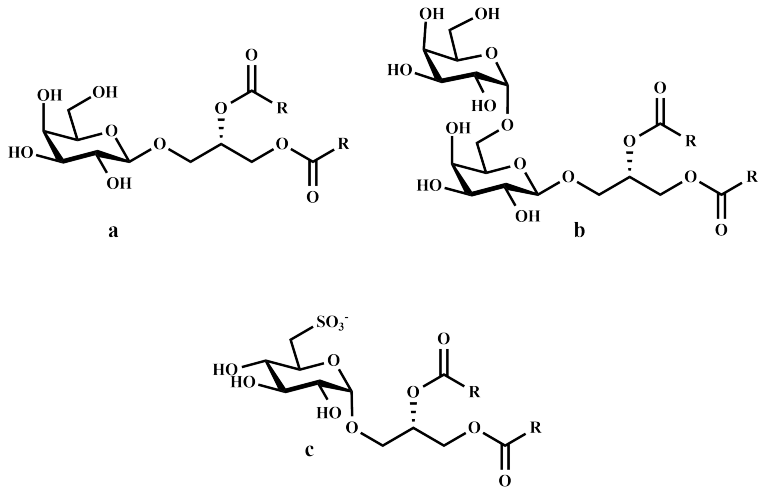

Figure 1.4: General structure of natural a) monogalactosyldiacylglycerols (MGDGs), b) digalactosyldiacylglycerols (DGDGs) and c) sulfoquinovosyldiacylglycerols (SQDGs) (R=alkyl chain)

1.1.3 Glycolipids bioactivity

A quick look at the literature is enough to associate important biological activities with glycoglycerolipids, in fact, these natural compounds often have unusual and sometimes unexpected pharmacological activities which make them interesting targets for drug discovery. Unfortunately, it is not always possible to obtain a sufficient amount of product by isolation from natural sources and it is necessary to turn to synthetic approaches in order to pursue with further studies.

This paragraph will briefly report some studies that highlight the features of glycoglycerolipids which make them promising candidates for drug discovery in several medical fields.

1.1.3.1 Anticancer activity

One of the first evidences of significant anti-tumour activity correlated with glycoglycerolipids was revealed in 1995 from Morimoto and co-workers [24]. Some glycoglycerolipids isolated from marine organisms showed an inhibitory effect on tumour promoting stage of Epstein-Barr virus-associated early antigen (EBV-EA) activation on Raji cells induced by 12-*O*-tetradecanoylphorbol-13-acetate (TPA) (Figure 1.5a).

Recent studies described glycoglycerolipids as potential anticancer drugs whether for their specific proapoptotic activity [25] or they inhibition of replicative DNA polymerase activities, that potently affected cancer cells and tumour growth in *in vivo* and *in vitro* experiments [26].

The glycoglycerolipids ability to inhibit replicative DNA polymerase and their antiproliferative activity toward human cancer cells is widely reported in literature, also for ether-linked glycoglycerolipids (Figure 1.5b) isolated from the marine sponges [27]. For most of these products, the mechanisms of action are still completely unknown.

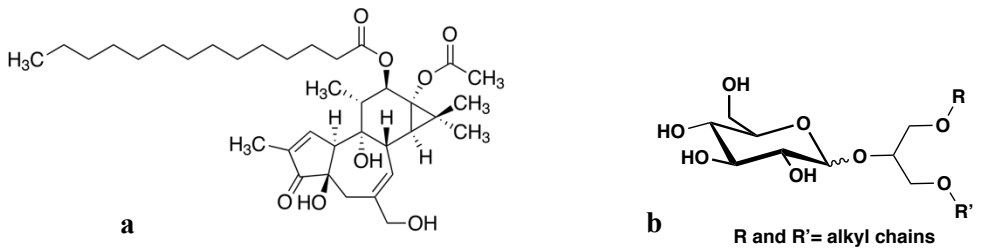

Figure 1.5: a) Chemical structure of TPA and b) generic ether-linked glycoglycerolipids structure

1.1.3.2 Antiviral activity

Despite the great steps that human did in drug discovery and in medicine, viral diseases are still cause of death in whole worldwide. Severe human infections are caused by a large family of viruses called Herpesviridae. The most common subfamilies are the herpes simplex virus-1 (HSV-1) and the herpes simplex virus-2 (HSV-2),

Effective anti-herpes drugs are available for treatment and they are inhibitor of DNA polymerase [28], despite this, some undesirable effects are reported after a long treatment with the commercial drugs as well as a drug-resistant strains emergency [29, 30], therefore, new anti HSV drugs with higher efficacy are essential.

In this frame, marine products are considered as a source with good prospect for the individuation of new anti-HSV therapeutic drugs. In fact, it has been reported that a fraction rich in sulfoquinovosylglycerolipids extracted from marine organisms was active against human herpes simplex virus (HSV) infection [31] and further study demonstrated that pure sulfoquinovosyldiacylglycerols have a potent antiviral activity against HSV-1 and HSV-2 [32, 33].

The inhibitory activity of glycoglycerolipids paved the way to additional studies on their enzymatic activities. The human immunodeficiency virus type 1 (HIV-1), defined as major causative agent of acquired immunodeficiency syndrome (AIDS), is probably one of the most studied viruses in biomedical research, even if the immunopathogenic mechanisms of its infection are complex and still not understood. It is also known that the reverse transcriptase (RT) is the key enzyme in the life cycle of HIV-1 and the main target for AIDS therapy.

In this field, the effect of some glycoglycerolipid extracts on this enzyme are reported and the authors underline a potent inhibitor activity by sulfoglycoglycerolipids fractions and a moderate inhibition by others glycoglycerolipids of the DNA polymerase function of HIV-1 RT. However, the process of this inhibition is still under investigation [34].

1.1.3.3 Anti-inflammatory activity

Several studies describe glycoglycerolipids as anti-oxidant and anti-inflammatory agents for their ability to inhibit the generation of superoxide anion.

One of the most relevant evidence is a study on two *in vivo* models of inflammation: croton-oil-induced mouse ear oedema and carrageenan-induced mouse footpad oedema [35].

In their work, Bruno *et al.* [35], after isolation, purification and identification of some glycoglycerolipids (MGDG, DGDG, SQDG) from the ETS-05 thermophilic blue-green alga, demonstrated that the three compounds act in a dose dependent manner. In particular, MGDG showed an enhanced efficacy respect to the reference drug, indomethacin, strictly correlated with the degree of saturation of the fatty acid chains of MGDG, as its activity was almost entirely abrogated by saturation of its acyl chains.

In addition, several glycoglycerolipids extracted from terrestrial plants were identified as anti-inflammatory agents, like the galactoglycerolipids isolated from the fruit of *Rosa canina* that showed a potent inhibitory effect on chemotaxis of human peripheral blood neutrophils *in vitro*, with clear evidences that the activity is not related to toxicity [36].

1.1.3.4 Immunomodulant activity

Immunomodulators are compounds able to regulate and/or normalize the immune system and they are used to boost immune response.

The numerous biological activities of glycoglycerolipids put them in the spotlight of various field, and the importance of this class of compounds extends to the recognition of their ability to act as immunoregulators. *In vitro* and *in vivo* experiments demonstrated that a synthetic derivative of natural SQDG was able to regulate, or better to inhibit, human mixed lymphocyte reaction (MLR), indispensable for the success of allogeneic transplantation, classifying them as a new class of immunosuppressive agents. [37]

Recent evidences showed the ability of some glycoglycerolipids, natural and not, to prime human dendritic cells (DCs) *in vitro* experiments and to trigger an efficient immune response *in vivo* [38].

The ability to trigger DCs maturation is considered a main tool to control the induction of immune response, and it represents an important tool for the development of adjuvant agent in vaccine formulation.

1.2 Immune System: an overview

Immunity has been defined as the ability to resist infections against bacteria or viruses, but also against everything that is recognized by the organism as 'not-self', generally called antigen.

The immune system is a complex network made up of special cells and proteins that actively fight infections, and the main components of this elaborate system are white blood cells, antibodies, the complement system, the lymphatic system, the spleen, the thymus and the bone marrow.

The immune system can be broadly sorted into two categories based on two different forms of defence: innate immunity and adaptive immunity.

Innate immunity is a natural immune reaction, the one we were born with, and it consist mainly of a non-specific defence mechanism, it does not depend on a previous interaction with foreign threats; innate immunity comes into play immediately or within few hours of the appearance of antigen in the body. The innate immune response is activated by chemical properties of the antigen, it depends only on the nature of the foreign antigen and the host resistance to a particular antigen is not enhanced by repeated exposure (lack of memory).

The first response to pathogens is an inflammatory reaction, followed by cells migration and release of some mediators like cytokines, chemokines and interferons (IFNs).

Components of innate immunity include skin, stomach acid, enzymes found in tears and skin oils, mucus and the cough reflex. There are also chemical components of innate immunity, including substances called interferon and interleukin-1.

Foreign threats are recognized from macrophages and neutrophilic granulocytes that englobe and destroy them by enzymatic activity: this process is called phagocytosis.

It also occurs through the intervention of the complement system, also known as cascade system. It consists of several plasma proteins (numbered from C1 to C9) that interact with each other activating a cascade. The complement system intervenes in

inflammation, in the removal of antigen-antibody complexes, in lysis of cells and microorganisms.

On the other hand, adaptive (or acquired) immunity is based on a specific response stimulated by substances that act as antigens. This immunity is based on the ability of our immune system to distinguish the 'self' from the 'not-self', or rather to recognize structures belonging to the organism (self) and extraneous potentially dangerous structures (not-self). In this way, it can activate an inflammatory response solely with respect to the 'not self' macromolecules. The hallmark of the adaptive system is the specificity of antigen recognition and memory, in other words, the repeated exposure to a specific antigen elicit an intense immune response.

The initial reaction is actually amplified by a series of events that involve all the cells of the immune system such as lymphocytes and macrophages, but also basophils and eosinophils [39].

Adaptive immunity is more complex than innate immunity, in fact after recognition and procession of the antigen, the adaptive immune system creates antibodies specifically designed to this specific antigen and "remembers" it making future responses more efficient.

However, innate and adaptive system are strictly linked, considering that the antigen recognition by innate system is crucial for the adaptive system activity [40].

The adaptive immune response is split in turn in humoral response and cellular response.

The humoral response is mediated by B cells and, depending on the nature of the antigen, can need the costimulatory signals of T helper cells (Th cells) or can go forward in a way independent of T helper cells.

The cellular response is mediated by the activation of naïve T cells as a result of the recognition of pathogen bound to MHC molecules and the delivery of costimulatory signal from Antigen Presenting Cells, like Dendritic Cells and Macrophages that will be described later in this chapter.

1.2.1 Components of Immune System

As mentioned, the immune system is a complex network that include several cooperative cellular and molecular components able to recognize and process foreign agents.

To better understand how new immunomodulant molecules can be developed, a basic knowledge about the main components of the immune system is required, therefore a straightforward description of cellular and molecular elements involved in the immunocompetent reactions is discussed in the next paragraphs.

All cells of the immunocompetent system, belonging to the family of leukocyte, descend from multipotential hematopoietic stem cells of the bone marrow. Each leukocyte surface is provided with several phenotype markers, called *cluster of differentiation* (CD), essential for their identification and characterization. The CD nomenclature has been developed to provide a standard classification of the many monoclonal antibodies (mAbs). Nowadays about 400 CD unique cluster and subcluster have been identified.

1.2.1.1 Lymphocytes

Lymphocytes are one of the several subtypes of a white blood cells in a vertebrate's immune system, each type of white blood cells has a specific function and they collaborate each other to fight antigens.

These cells are made in the bone marrow and about 25% of the new lymphocytes remain in the bone marrow and become B cells (for humoral, antibody-driven adaptive immunity). Whereas, the other 75% travel to thymus and becomes T cells [41] (for cell-mediated, cytotoxic adaptive immunity).

Each B cells produces a specific antibody and each antibody matches an antigen in the same way that a key matches a lock, and when this happens, the antigen is marked for destruction. T cells control the immune response to antigens destroying cells in the body that have been taken over by viruses or become cancerous. B and T cells are

divided in memory B or T cells that help the immune system to remember previously found antigens helping a fast antibody response, and regulatory B or T cells [42, 43], that actually have protective anti-inflammatory or that control/suppress the immune system respectively.

Moreover, T lymphocytes expressing CD4 cell surface molecules are known as T helper (Th) and they are the major source of cytokines. Th can be further subdivided in Th1 and Th2 and the cytokines they produce are called Th1-type and Th2-type cytokines.

Lymphocytes include also a third type of cells known as Natural Killer cells (NK cells), with similar function as T cells but without T cell receptors rearrangements. Some NK cells own a not-specific cytotoxic activity towards virally infected cells and tumor cells. NK cells can also exhibit a specific activity if provided with an antibody [43].

1.2.1.2 Antibodies

Also called immunoglobulins, these proteins recognize antigens in order to remove them. Antigen receptors on B cells' surface interact with an antigen eliciting maturation of these lymphocyte that release countless antibodies into the bloodstream and lymphatic system; the latter attack and neutralize antigens identical to that one that trigger the B cells. This cooperative function between B cells and antibody is the most important part of immunity. There are five main classes of antibodies, according to their structure and their activity: IgG, IgM, IgA, IgD, and IgE [44].

1.2.1.3 Monocytes

Originated from monoblasts, monocytes are fundamental components of the immunocompetent system [45] and belong to the myeloid cell lines. They circulate for few days in the bloodstream before reaching the tissues where they differentiate into macrophages and myeloid dendritic cells. Macrophages play an important role in

the protection of tissues and of some organs like heart and brain. Dendritic cells (DC) are the most important Antigen Presenting Cells that will be discussed later in detail. Mainly functions of monocytes and their progeny are phagocytosis, antigen presentation, and cytokine production, in addition to the ability to kill infected host cells by antibody-dependent cell-mediated cytotoxicity.

1.2.1.4 Granulocytes

Granulocytes are the most abundant leukocytes, they have a role in innate system as well as in adaptive system. Granulocytes move into the site of infection releasing different effector molecules (cytokines, chemokines, enzymes and growth factors [43]). They have a short life span and are continuously produced from stem cells in the bone marrow. Granulocytes' family is divided in four subgroups:

- neutrophils, professional phagocytes that leave the bone marrow only during an infection;
- eosinophils, important cells for immune responses implicated in the pathogenesis of allergic or autoimmune disease;
- basophils, involved in several functions such as antigen presentation, stimulation and differentiation of CD4+ T cells;
- mast cells, mediator of host defence against pathogens, of inflammation and autoimmunity as well as mediator and regulator of neuroimmune system response [46, 47].

1.2.1.5 Cytokines

Cytokines are small proteins secreted by different cells with a clear effect on the interaction and communication between cells [48]. According to their progenitor is possible to distinguish different cytokines:

- lymphokine are cytokines made by lymphocytes;
- monokine are produced from monocytes;
- chemokine are cytokines with chemotactic activities;

- interleukin (IL) derive from one leukocyte and act on other leukocytes.

There are both pro-inflammatory and anti-inflammatory cytokines. Pro-inflammatory cytokines are mainly produced by macrophages and dendritic cells. They are involved in the up-regulation of inflammatory reaction. Anti-inflammatory cytokines are immunoregulatory molecules able to control the pro-inflammatory cytokines response. Cytokines work all together to regulate the human immune response.
In this regard, it is necessary mention Th1-type and Th2-type cytokines, previously introduced: Th1-type cytokines tend to produce the proinflammatory responses while Th2-type cytokines include IL-10 which is associated with anti-inflammatory responses. Humans should produce well balanced Th1 and Th2 response [49].
Within the family of cytokines there are also interferons (IFNs). Interferons are signalling proteins able to 'interfere' with viral replication protecting cells from infection [50]. They up-regulate antigen presentation increasing the expression of major histocompatibility complex (MHC) antigens. IFNs are mainly divided into three class: type I, type II and type III.

1.2.1.6 Complement system

Also called 'cascade system', the complement system is an essential tool of the innate immune response and its main activity is to link innate and adaptive immunity. It is composed by several proteins and is located in the plasma and on cell surfaces. Many of these proteins exist in an inactive precursor form that will be activated at the site of infection triggering a cascade of inflammatory reactions, in other words, this system is activated by a triggered-enzyme cascade. Talking about 'cascade', we mean that the activation of few proteins is hugely amplified by each successive enzymatic reaction, with a consequent fast and greater complement response [51]. The cascade system can be activated by three pathways:

- classical pathway (where the activation is triggered by IgM and IgG antigen-antibody complexes or by danger signals 52, 53]);

- alternative pathway [54] (direct binding of bacteria or yeast to the complement activates the latter, independently from antibodies);
- mannose-binding pathway [55] (where the complement is activated by multimeric lectin complexes).

As well as all the mechanisms involved in the immune response, the cascade reactions are regulated by regulatory protein to avoid any kind of damage due to accidental activation [40].

1.2.1.7 The Major Histocompatibility Complex (MHC)

It is the most complicated set of genes in the whole human genome codifying cell surface proteins involved in the acquired immune system. The MHC molecules have the ability to bind to antigens and display them on cell surface to allow the recognition by appropriate T-cells. In other words, MHC operate as bridge between different leukocyte and its molecules are antigen-binding agent.

In humans, MHC molecules are termed HLA (Human Leukocyte Antigen) and they are highly polygenic (every individual own a group of MHC molecules with various set of peptide-binding specificities) and polymorphic (there are more than one modification of each gene within the population); these features make this complex very efficient in the neutralization of the pathogens.

The core of the MHC complex consists of three major regions and, as a consequence, it is possible to define three group of MHC molecules: class I, class II and class III [56]. Class III molecules are less defined structurally and their functions in immune response are not completely clear; they are not antigen-binding molecules and are mostly signalling molecules in other cell communications [57].

Within the MHC class I molecules there are: HLA-A, HLA-B, HLA-C, HLA-E, HLA-F, HLA-G and they are located almost on all cells but red blood cells [58]. MHC class I molecules are able to link peptides originated from cytosolic proteins [59] and for this reason, the pathway of their antigen presentation is also called *cytosolic pathway* [60].

Class II molecules usually occur on professional antigen-presentation cells, especially on dendritic cells [61]. These molecules bind to antigens from extracellular proteins. In humans, the MHC class II molecules' family is composed of: HLA-DP, HLA-DM, HLA-DOA, HLA-DOB, HLA-DQ, and HLA-DR.

1.2.3 Dendritic cells: Professional Antigen Presenting Cells

Antigen presentation is a mandatory step for the recognition of exogenous antigens by T cells and it is the main role of Antigen Presenting Cells (APCs) [62].
Intact protein antigens are not recognised by antigen-specific T cells, but they must be processed into small peptide fragments by APCs, then, peptide fragments will be presented on the cell surface of APCs allowing the interaction with appropriate cell receptor.Actually, the antigen presentation is a cooperative work between APCs and MHC class II molecules.
APCs can be divided into two main class:

- Nonprofessional APCs, such as endothelial cells, pancreatic β- cells and thyroid cells that perform their antigen presentation only under select conditions and for a briefly time;
- Professional APCs, like monocytes, macrophages, dendritic cells, and B cells that are fully committed to antigen presentation as an integral part of their role in the immune response

1.2.3.1 Dendritic cells origin and differentiation

Since 1973 when Ralph M. Steinman and Zanvil Chon [63] described for the first time these rare peripheral blood cells with a 'stellate' shape, therefore called Dendritic Cells (DCs), the science of immunology profoundly changed even if DCs were underappreciated until the mid-1990s when the scientific community recognized their crucial role in the immune system [64].

Steinman and his co-workers defined DCs as essential sentinels of the immune system able to control and link immune and adaptive response [65].

DCs widely occur in lymphoid and nonlymphoid tissues, in all immune organs and at the interface between our body and the environment.

As aforementioned, DCs are originated from hematopoietic precursor cells in the bone marrow as well as the others cellular components of the immune system and they represent a huge and heterogenous family, where each DC has its own markers and functions.

It is possible to distinguish two big class of DCs: plasmocytoid DCs (pDCs) and conventional DCs (cDCs).

pDCs are involved in the production of type I interferons (IFN) as soon as a viral infection is perceived, and they are also responsible of the immune suppression (tolerance) in their immature state [66, 67].

cDCS are involved in the recognition of bacterial components and in the production of proinflammatory cytokines to activate the primary immune response [66].

The physiological differentiation pathways of DCs (Figure 1.6 [68]) from a unique precursor have been studied for years, especially with the aim to overcome the difficulties to gain a sufficient amount of DCs for deeper studies, in fact, one of the biggest experimental problems is the low number of DCs in tissues and their elaborate incubation.

A general practice to solve this difficulty is to use monocytes as source of DCs because they can differentiate into dendritic cells (MoDCs) in presence of an inflammatory stimulus preserving the mains APCs' features. Blood monocytes cultured with IL-4 and granulocyte-macrophage colony-stimulating factor (GM-CSF) produce monocyte-derived dendritic cells, MoDC.

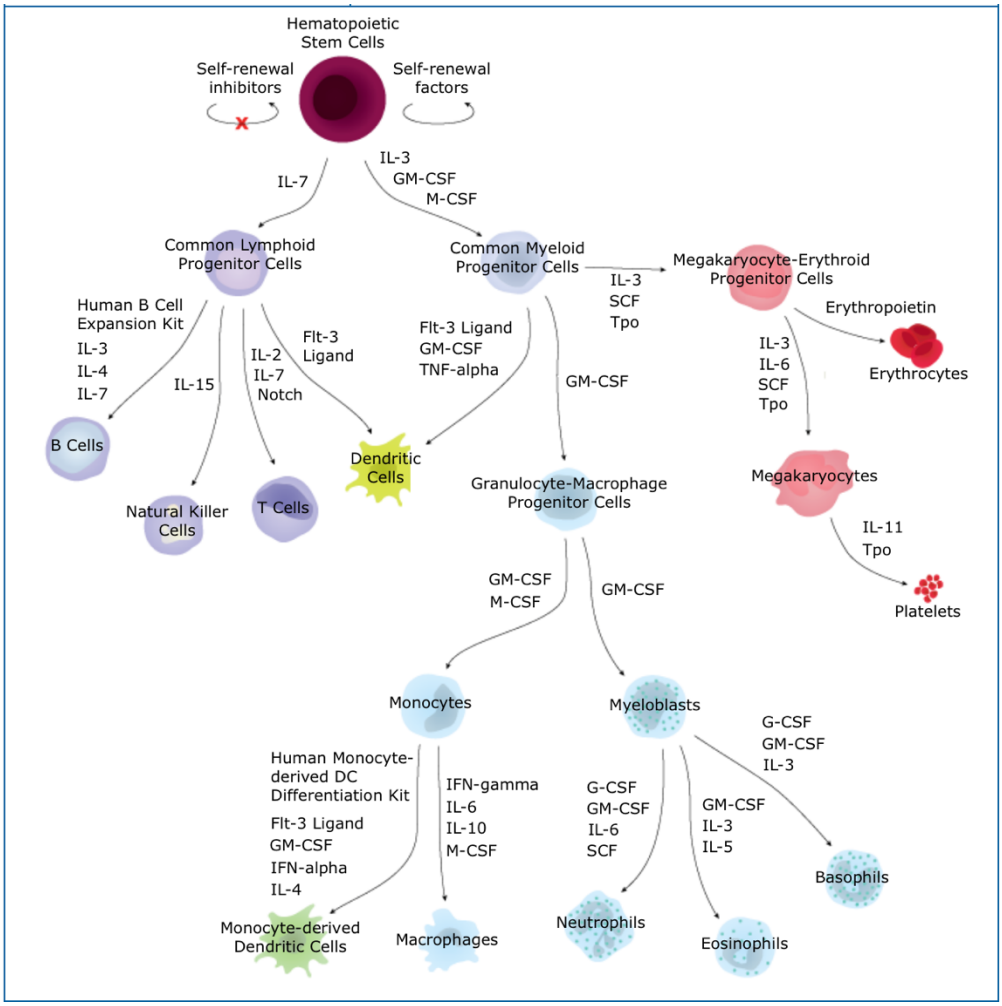

Figure 1.6: Schematic representation of Dentridic Cells differentiation pathways (From: https://www.rndsystems.com/pathways/hematopoietic-stem-cell-differentiation-pathways-lineage-specific-markers [68])

DCs are the only professional APCs able to stimulate naïve T cells proliferation and trigger a primary immune response in vivo. In addition, they are two-fold more potent than other APCs and are also involved in the induction of tolerance.

Nowadays there is a general awareness that DCs are a central point of the immunocompetent system since they represent a crucial connection between innate and acquired system. Currently they are considered a promising tool to activate a robust immune response in immunotherapy for their ability to recognize, capture, process and present antigens.

1.2.3.2 Dendritic Cells maturation

Dendritic cells maturation is a complex heterogeneous process characterized by a change of cells' properties.

DCs in steady-state are called 'immature DCs' and they are defined by low surface expression of MHC class II and co-stimulatory molecules. In presence of stimuli or 'danger signals', DCs take up antigens and go through a maturation process inducing their migration to lymphoid organs [69]. The progression in the maturation state of DCs population involve both changes of the expression of surface receptors and their ability to interact with the environment and surrounding cells.

Maturation signals can be exogenous, mediated by activation of Pattern Recognition Receptors (PRRs), or endogenous, mediated by inflammatory molecules (TNF-α, IL-1, IL-6 and IFN-α), released by damaged tissues or by cells of the immunocompetent system.

The process of DCs maturation trigger a sequence of events that actually supervise the type and the quality of the immune response [70].

Differences between mature and immature DCs are summarized in Figure 1.7 and essentially lie in:

- inclination to capture antigens
- production of cytokines
- ability to antigenic presentation

During their maturation DCs overexpress some chemokines, costimulatory molecules and surface receptors that assist DCs migration to lymphoid tissues and mediate the

interaction between DCs and T cells promoting a transient cluster and allowing DCs to match the appropriated T cell receptor (TCR) [71].
After the antigen presentation, DCs secrete different cytokines, like IL-12 or IL-10, that differentiate T cells into pro- or anti-inflammatory T cell subsets [72, 69].

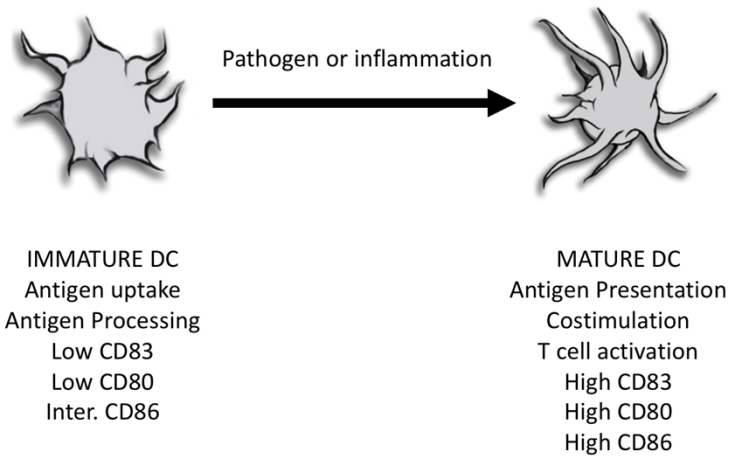

Figure 1.7: Schematic representation of Dendritic Cells maturation [73]

Considering the mentioned peculiarity of this set of cells, the connection between DC and vaccine adjuvants is legitimated and, with the better knowledge about DCs growth and differentiation, therefore with more available quantity of them, several scientists used DCs as adjuvants in humans controlling DCs maturation features as evaluation of the efficacy [74-76].
Nowadays, the DCs maturation is considered a valuable method to screening new efficient immunomodulators [77-79].
Given the noticeable different features between immature and mature DCs and the real opportunities to monitor the maturation process through the evaluation of their phenotypic markers, they can be an excellent tool to estimate the ability of some substances to act as immunomodulant, or in other word to trigger DCs maturation.

1.3. Lipid antigens

Until few years ago, proteins were considered the only class of antigen able to prime an immune response. Recently, it has been shown that glycolipids are strictly involved in the immunologic reaction mechanisms [80].

Endogenous and exogenous lipids can be recognized by the immune system inducing a cascade of immune reaction essential for the defence against infections and diseases. It is clear that all the automatisms by which this class of compound interact and activate the immune system are not completely clear and considering the high impact that it could have on pharmacology, it worth to be investigated, especially for their potential employment as new glycolipid-based vaccine adjuvant [81, 82].

1.3.1 Glycolipids vs Immune System

During the last years, many studies review the glycolipids capability to activate and regulate the complex mechanisms of the immune system [38, 83, 84]. Some of the examined natural and not-natural glycolipids, within the class of α-galactosylceramide (α-Galcer) showed the peculiarity to link the CD1 proteins (cluster of differentiation 1)

The main role of CD1 protein is the antigen presentation to T cells, in particular, these glycolipids are CD1d ligands that activate NKT cells [85].

Another way that glycolipids use to boost an immune response is through Toll Like Receptors (TLRs) [86], even if the mechanisms at the base of this process are still under investigations. An example of glycolipid that act via TLRs is clearly the lipopolysaccharide (LPS) whose Lipid A moiety (Figure 1.8) is a potent stimulator of host defence systems throughout TLR4 activation.

The most recent evidence of the immunomodulatory behaviour of glycolipids is the ability of a synthetic β-sulfoquinovosyldiacylglycerol to trigger DCs maturation via TLRs independent way and to produce an immune adjuvant response *in vitro* and *in*

vivo [38].

The potential pharmacological applications of glycolipids are the driving force to continue to investigate the biological mechanisms behind their activity, even if the complexity of all immune system, and its several interactions, make this field as fascinating as unexplored.

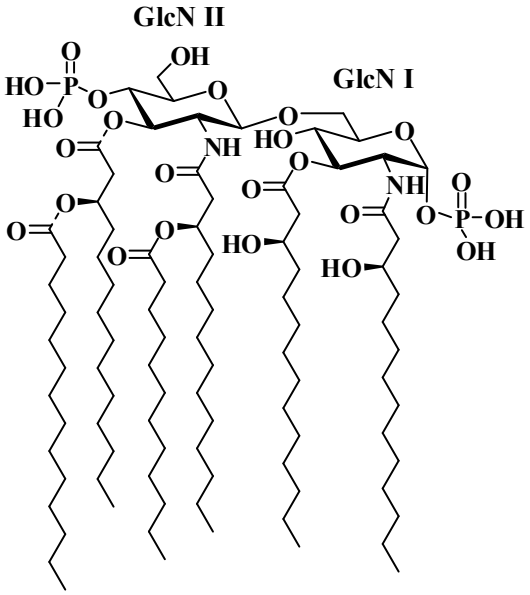

Figure 1.8: Lipid A from *Escherichia coli*.

1.4 Vaccine Adjuvants

All vaccinations are based on the common concept of stimulation of immune response. A vaccine is a preparation consisting of properly treated pathogens (or parts of them) administered with the purpose of providing acquired immunity. This process, called vaccination, is able to actively exploit the immune system's memory, allowing the body to develop a defence system against a bacterium, virus or other microorganism even before they came into contact with it [87-90]. Therefore, vaccines purpose is to activate APCs inducing a protective response to a foreign antigen.

In this regard adjuvants are complex molecules or mixtures that are added to highly purified antigens to enhance their immunostimulatory abilities.

A hypothesised mechanism of action of adjuvant lie in their ability to trigger the maturation of APCs through upregulation of costimulatory molecules, improving antigen processing and presentation; moreover, they could modulate the antibody affinity and stimulate lymphocyte proliferation.

Currently, they represent the most innovative technology in the identification of new vaccines against challenging diseases.

1.4.1 The origin of vaccination

"I shall endeavour still further to prosecute this inquiry, an inquiry I trust not merely speculative, but of sufficient moment to inspire the pleasing hope of its becoming essentially beneficial to mankind" (Edward Jenner 1749-1823)

Edward Jenner is considered the father of immunology for his study on preventing smallpox. He was the first one to demonstrate the control of an infectious disease by the use of vaccination without transmitting the disease itself [91].

Truthfully, he did not discover vaccination, but he gave the first validated scientific proof of the use of vaccine, changing the way medicine was performed.

Vaccines were born from the necessity to survive to one of the most devasting infective disease: smallpox. The virus appeared in Europe between the V and VII century and because of the conquest of territories and the slave trades it spread rapidly. It was known that those who survived smallpox would be immune to the same disease, although nobody understood why.

At the beginning an efficient cure against this disease was the inoculation, often called also variolation, that consisted to a subcutaneous injection of the virus Variola before the individual has incurred the smallpox. Ordinarily, the infection was located for few days closed to the spot site, but many times it came up with fever and/or other infective diseases, like tuberculosis or syphilis [92]. Nonetheless, variolation was the only efficacious method available and it branched out worldwide, from China to India and then to Europe and America [93].

In 1757 variolation was successfully carried on an eight years old boy: Edward Jenner (1749-1823).

During his life Jenner spent a lot of efforts in medicine and in particular in his research on smallpox. His intuition on vaccination came from stories of dairymaids that became immune to smallpox after contamination from cowpox, a virus of the same family of the one that infected humans, but with soft side effects.

Starting from these evidences and with the same basic idea of inoculation, Jenner realized that cowpox could protect against smallpox and also could be transmitted as a mechanism of protection.

He called this method ‘vaccination’ from Latin word for cow, ‘vacca’.

We can surely say that Jenner is the pioneer of all the following studies on infective diseases and of the development of immunology [94].

Vaccination is one of the most implemented public health interventions and continues to be an essential tool in the prevention of infectious diseases worldwide.

The smallpox vaccine, as well as all the early vaccines, can be classified as ‘live-attenuated vaccine’, because it contains pathogens whose virulence is reduced but it is still alive and acts through a transient infection.

Live vaccines still continue to be used to date, but some of them faced several difficulties as reactogenicity, low efficacy and potency [95].
In the 20th century, with the discovery of immunogenic non-toxic bacteria, were introduced the 'inactivated' vaccines, consisting of viruses, bacteria or pathogens grew under controlled condition and killed to reduce their infectivity. Inactivated vaccines are less efficient than live vaccine [96].

1.4.2 Most commonly used adjuvants

Adjuvants can be classified used different criteria, like their physicochemical properties, their origin and their mechanisms of action. Based on the mechanism of action, we can describe two main classes of adjuvant: delivery systems, that localize vaccine components and target vaccines to APCs, and immunostimulatory substances, that increase the immune response [97].
Delivery system are antigen-associated carrier able to promote the interaction of both antigens and immunostimulators with the key cells of the innate immune system, whereas, immunostimulatory substances are able to trigger an innate immune response by Pattern Recognition Receptors (PRRs) or directly by cytokines [98].

Within the class of delivery system (and not only), there are mineral salts, like alum salt-based adjuvant, that is most widely used adjuvant since its introduction by Glenny in 1926. The behaviour of this class of adjuvants is expressed in three main points: a slow release of antigen, the recruitment of APCs after inflammation and the ability to facilitate the uptake of alum-antigen complex on DCs [97]. Alum-based adjuvants induce Th2 type response [99] and upregulation of costimulatory signals, but they have low adjuvant activity for cell-mediated immunity and unfortunately are often associated to allergic reaction [100, 101].
In 1940, Jules Freund introduced a new, potent, immunogenic adjuvant composed of a mixture of mineral oil and heat-killed mycobacteria. Freund's Complete Adjuvant (FCA) is part of the water-in-oil emulsion adjuvants and is used to evaluate the

immunogenicity of antigens in mice, or however for experimental purpose, because, even if it has a potent action in animals, some diseases are associated with its use [102]. Whereas, Freund's Incomplete Adjuvant (FIA) is also a water-in- oil emulsion, but without mycobacteria; it is used in human influenza vaccine [103] and is able to release the antigen continuously, increasing the antigen lifetime and enhancing the potency of the immune response [98]. Although some side effects are linked with the use of FIA, it is still employed in several clinical trials [98].

Immune stimulating complexes (ISCOMs) are delivery systems generally composed by a glycoside (*Quillaja* saponins), cholesterol and phospholipids that support the formulation of these compounds. ISCOMs have a rigid cage-like structure with a strong negative charge. Different variations of these compounds have been developed to improve the antigen incorporation, hence to ensure the intracellular deposition of the vaccine antigen [104].

ISCOMs strongly affect the MHC class II expression on APCs, promoting both humoral and cell-mediated immune responses and its activity is mainly associated to the presence of *Quillaja* saponins [105].

Bacterial DNA is able to activate the innate immune system through the interaction between its unmethylated CpG motif and TLR-9 expressed on cells surface [106] of B cells and pDC. This immunostimulatory activity is reproduced by synthetic oligodeoxynucleotides expressing unmethylated CpG motifs [107].

CpG oligodeoxynucleotides activate the maturation and proliferation of different components of the immunocompetent system, like NK cells, T cells and monocytes, with consequent production of proinflammatory cytokines, chemokines and immunoglobulins. Moreover, they enhance the induction of memory, increasing the duration of humoral and cellular immunity.

Some studies showed the increased effect of CpG oligodeoxynucleotides adjuvants when they are used with plasmid protein antigens or using delivery systems in their formulation [108, 109].

Another class of adjuvants are oil-in-water emulsions based on squalene, an oil that is better metabolized than the oil used in Freund's adjuvant. These adjuvants stimulate a stronger antibody response even using a low dose of antigen, generating a memory response [110, 111].

1.5 Background and aim of thesis

In spite of the enormous efforts put in the research of new vaccines and vaccine adjuvants, it is clear that this is still an active field due to the several challenges that evolution gives us every day. The licensed vaccine adjuvants are far from being efficient and appropriate for what life requires.

Nowadays approved formulations of commercial adjuvants are still the same as fifty years ago, such as alum salts and oil-in-water emulsion [112].

Recently glycoglycerolipids from marine sources are introduced as a novel class of molecular adjuvants [38].

This PhD thesis was inspired by the positive hits obtained from the biological evaluation of a natural mixture of α-sulfoquinovosyldiacylglycerols (α-SQDGs) with interesting immunomodulant activity.

Starting from these evidences, the synthetic analogue 1,2-*O*-distearoyl-3-*O*-β-D-sulfoquinovosylglycerol, named Sulfavant A (Figure 1.9), has been prepared and its immunomodulant activity has been tested for its ability to trigger DCs maturation [38].

Sulfavant A consists of a glycoglycerolipid characterized by a sulfonic functionality on carbon 6' of quinovose linked to a diacylated glycerol moiety by β glycosidic bond.

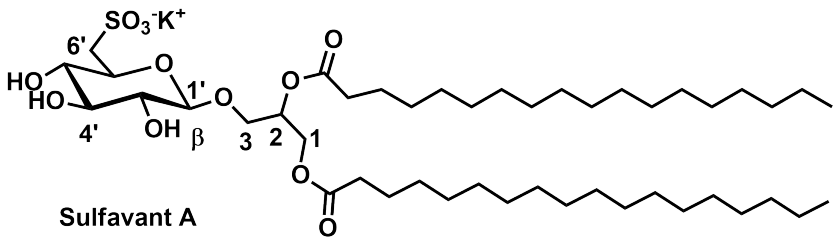

Figure 1.9: Chemical structure of 1,2-*O*-distearoyl-3-*O*-β-D-sulfoquinovosylglycerol (**Sulfavant A**)

This compound exhibited a peculiar ability to trigger the maturation of human DCs with consequent upregulation of T cell co-stimulatory factors, such as HLA-DR,

CD83, CD86, and the gene expression of specific subset of cytokines, like IL-12p40 and INF- γ [38].
Sulfavant A was also tested in two *in vivo* experiments to evaluate its capability to boost immune protection acting as molecular adjuvant.
Once confirmed the bioactivity of Sulfavant A, this study proposed the synthesis of structural analogues of Sulfavant A introducing different acyl chains and/or changing the stereochemistry at carbon 2 of the glycerol moiety.
In order to explain the differences and peculiarities of some synthetic sulfolipids, together with the need to evaluate the structure/activity correlation, a detailed study on the chemo-physical properties of the most promising synthetic compounds was carried out.
Due to their amphiphilic nature, it is plausible that glycoglycerolipids occur in polar solvents as colloidal aggregates and considering that the aggregation process can affect the biological activity and the chemical reactivity of molecules [113, 114], during the PhD thesis this aspect was examined.

The investigation on the biological mechanisms behind glycoglycerolipids bioactivity and the identification of their cellular targets still represent an unexplored field.
In order to clarify some biological aspects of this class of molecules an advantageous tool could be the fluorescence analysis. Actually, the fluorescent labelling of carbohydrates is far from being a usual practice, because of the structural complexity of these molecules, even if recent studies report the synthesis and applications of fluorescently labelled carbohydrates [115].
In this work a fluorescent analogue of β-SQDGs was prepared with the aim to use bio-imaging analysis to increase the knowledge about the interactions of sulfolipids with their biological targets.

Another goal of this PhD project was the preparation of higher amount of product in order to proceed with further and in-depth studies intended to the pharmacological

development of β-SQDGs, therefore, an enhanced and scalable procedure for the preparation of β-SQDG in large scale is proposed.

Within the huge and fascinated world of bioactive glycolipids, Professor Andersen and his co-workers isolated from a Canadian sponge (to be classified) a natural mixture including as main component 1-*O*-alkyl-2-*O*-(2'-*O*-β-D-glucopyranosyl-β-D-xylopyranosyl)-glycerol (Figure 1.10), whose preliminary bioactivity evaluation showed a pharmacological potential.
With the aim to examine the biological activity of the natural mixture and to correlate it with the glycolipid, it was necessary to have a pure molecule to study on. In the framework of to this PhD project, during an internship at University of British Columbia, a synthetic strategy for the preparation of this molecule was designed.
More details about the biological activity of this compound are not disclosed because of patent pending from Professor Andersen and co-workers.

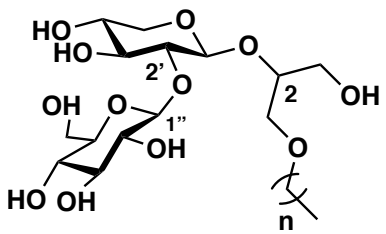

Figure 1.10: Chemical structure of 1-*O*-alkyl-2-*O*-(2'-*O*-β-D-glucopyranosyl-β-D-xylopyranosyl)-glycerol

Chapter 2: Results and Discussion

2.1 Sulfavant A: a new marine-inspired immunomodulant sulfoglycolipid

As extensively discussed in the first chapter, the identification of new vaccine adjuvants is increasingly required today because of the constant evolution of infectious diseases and the need to develop vaccines for non-infectious diseases, such as cancer and autoimmune disease.

In this regard microalgae are a huge tank of immunomodulant substances and, previous to this PhD thesis, extraction and bioassay-guided fractionation of the diatom *Talassiosira weissiflogii* led to an immunomodulatory mixture enriched of α-sulfoquinovosyldiacylglycerols (α-SQDGs) (Figure 2.1) with interesting bioactivity in terms of DC maturation. To confirm this primary evidence, a synthetic α-SQDGs was prepared and *in vitro* assays showed the ability of these molecules to maturate DC inducing the gene overexpression of IL-12 and HLA-DR [38].

Encouraged by these results and motivated by the need to find novel and more potent immunomodulant molecules, in addition to the aim to expand the knowledge about the structure/activity relationship of this type of molecules, a new non-natural SQDG, named Sulfavant A, was synthetized (Figure 2.2)

Sulfavant A is featured by a 6'-sulfo-quinovose linked to a distearoyl glyceridic portion by beta glycosidic bond.

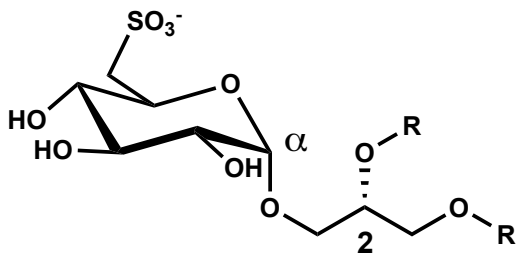

Figure 2.1: General structure of natural α-SQDGs

The design of the structure of Sulfavant A was inspired by the usual β configuration at the anomeric position typical of LPS-based glycolipids [116], combined with the characteristic sulfonic group of natural α-SQDGs. As far as the acyl chains are concerned, saturated fatty acids, characteristic of other immunogenic bacterial glycolipids, such as monophosphoryl lipid A (MPLA), were linked to the glycerol moiety; in particular for the Sulfavant A, progenitor of this new class of non-natural SQDG, $C_{18:0}$ acyl chains have been inserted.

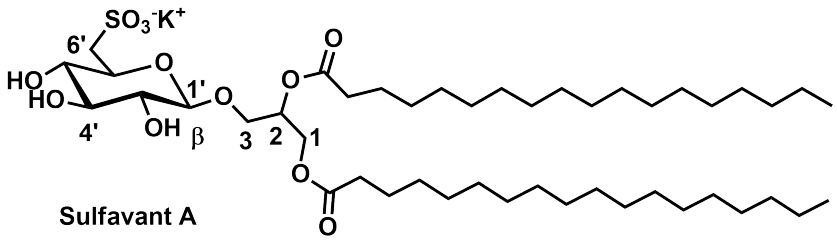

Figure 2.2: Chemical structure of 1,2-*O*-distearoyl-3-*O*-β-D-sulfoquinovosylglycerol (Sulfavant A)

2.1.1 Synthesis of 1,2-*O*-distearoyl-3-*O*-β-D-sulfoquinovosylglycerol (Sulfavant A)

For the preparation of the 1,2-*O*-distearoyl-3-*O*-β-D-sulfoquinovosylglycerol (Sulfavant A), the main challenge was the design of a chemical strategy comprising the β-configuration of the anomeric carbon and the insertion of the sulfonic function on carbon 6' of sugar portion.

In addition, with the aim to make the strategy versatile and accessible to a wide class of β-SQDG analogues, it was useful to find a way to introduce different fatty acid residues on the glycerol moiety.

Furthermore, the whole process had to be suitable for large-scale synthesis aimed to the possible pharmacological optimization and development of β-SQDG derivatives, both with saturated and polyunsaturated acyl chains.

The first crucial point was the choice of orthogonal protecting groups on sugar residue, whose deprotection should not affect the diacylglycerol moiety and the glycosidic bond. In this frame, some protecting groups had already been applied [117-119] but, unfortunately, they were not suitable for the experimental conditions and the goals of the above project.

For these reasons, it was decided to explore the use of acetate as protecting group of the sugar hydroxyl functions, stable under a wide range of conditions and, most importantly, the presence of the acetate at the carbon 2' of the sugar allowed to take advantage of the neighbouring group participation to achieve an excellent stereoselectivity in the formation of the β glycosidic bond.

The planned methodology is also suitable for the preparation of β-SQDG analogues with mixed composition of fatty acids regioselectively linked at carbon 1 and 2 of the glycerol part thanks to an appropriate choice of different experimental conditions [120].

The total synthesis of Sulfavant A (scheme 2.1) [121] starts with acetylation of D-glucose, followed by selective deacetylation at the anomeric position with benzylamine in tetrahydrofuran before the derivatization to trichloroacetimidate intermediate (**3**). The subsequent coupling with 1,2-*O*-isopropylidene glycerol was achieved by Schmidt methodology [122, 123] (using BF_3OEt_2 as catalyst). As expected, the acetate groups determined high stereoselectivity of reaction with the β-orientation of the glycosidic bond (**4**).

The strategy proceeded with the removal of isopropylidene residue under soft acidic conditions and in particular, zinc nitrate hexahydrate in acetonitrile allowed the hydrolysis of the acetonide in quantitative yields preserving the glycosidic linkage (**5**); subsequently the glycerol acylation was carried out through *N,N*-dicyclohexylcarbodiimide (DCC)-mediated condensation with stearic acid (**6**).

An essential point of this strategy is the introduction of the sulfonic group on carbon 6' of the sugar moiety. For this aim, at first it was necessary to remove the sugar acetyl groups without affecting the ester function on glycerol part, obtaining the β-glucosyl-

distearoyl-glycerol (**7**). This step was achieved by an accurate setting of the basic conditions that drove towards the use of monohydrate hydrazine (2.4 moles per acetate unit) at a temperature by 45°C. The tritylation of the primary alcohol of glucose by tritylchloride was followed by one more acetate protection of the sugar and detritylation in order to carry out the introduction of a tosyl group in position 6' (**11**) subsequently replaced by a thioacetate, using potassium thioacetate in 2-butanone. Final oxidation by hydrogen peroxide gave the corresponding sulfonic residue (**13**).
The compound obtained was fully deacetylated by hydrazine, in ethanol/water 85/15, to give Sulfavant A (**14**). Actually, the use of monohydrate hydrazine could be an issue in this methodology because in the usual drastic conditions reported in literature (2–4 equivalents of hydrazine carrying out the reaction for 4-6 hours within a temperature range of 40–80°C), could determine partial removal of acyl groups [124], while milder conditions, such as adding 2.1 equivalents of monohydrate hydrazine and stirring the reaction mixture for 3 hours at 44°C, led to Sulfavant A without the formation of deacylated by-products [113].
The designed synthetic strategy opens possibilities for the preparation of a wide range of analogues, including compounds with mixed composition of saturated and/or unsaturated acyl chains on glycerol moiety.

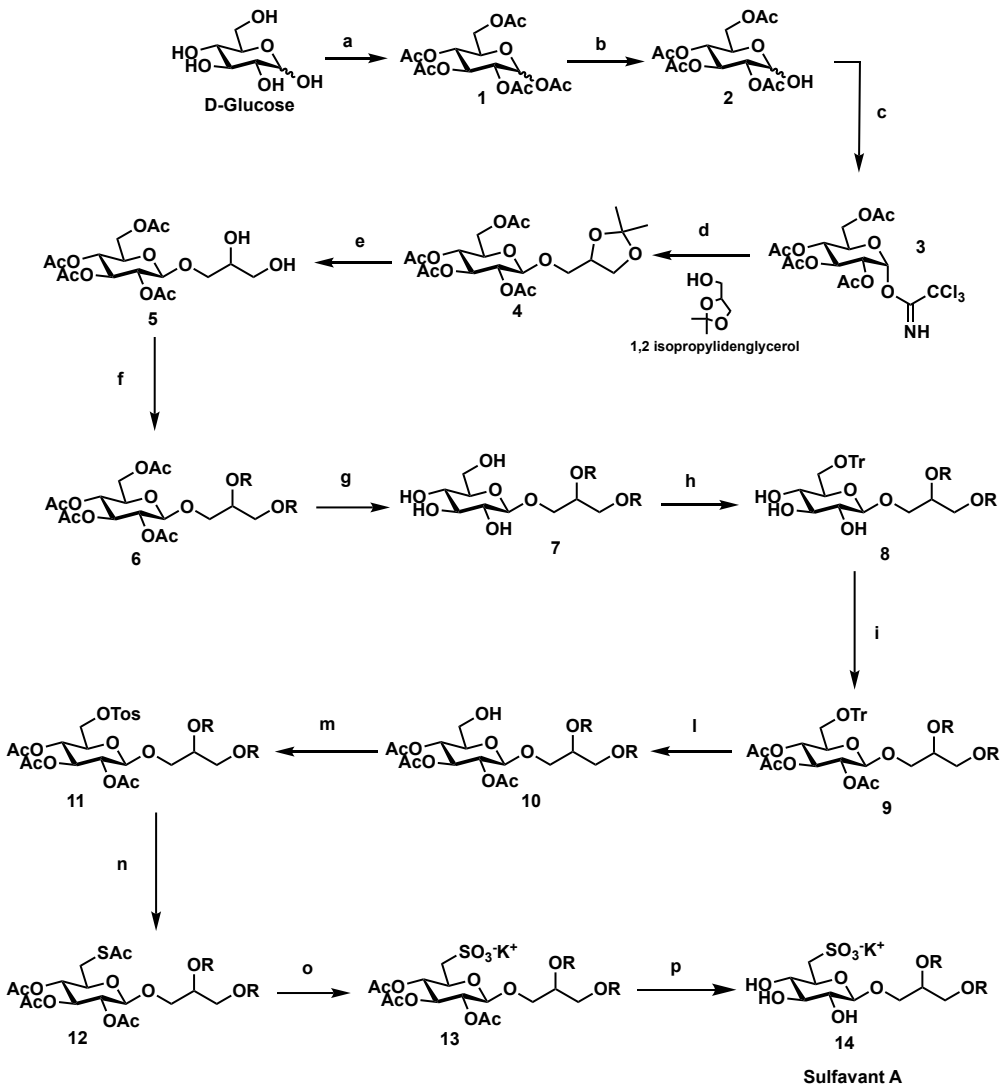

Scheme 2.1 Total synthesis of 1,2-*O*-distearoyl-3-*O*- β-D-sulfoquinovosylglycerol (Sulfavant A)
(all experimental conditions are reported in Chap. 4)

2.1.2 Evaluation of the biological activity of Sulfavant A

Monocytes own the ability to differentiate into DCs (moDCs) under inflammatory stimulus preserving the main features of APCs [125, 126].

In this study, the maturation process of DCs has been evaluated by flow cytometry through the measurement of the expression of MHC-Class II receptor HLA-DR, co-stimulatory molecule CD86 and CD83.

The phenotypic marker CD83 is strictly correlated with a fully maturated state of the DCs [127, 128] and is not detectable in other antigen-presenting cells (APCs) that do not prime naïve T cells, hence, $CD83^+$ DCs are considered a screening tool to detect the ability to prime a protective T cell response and have important clinical implication for vaccines against several infectious diseases, including HIV-AIDS, malaria, and tuberculosis, or for therapeutic treatment of cancers [129].

Moreover, high expression of CD83 avoids the down-regulation of MHC II and CD86 induced by IL-10, enhancing the immunogenicity of vaccine adjuvants [130]. This is a crucial effect for the *in vivo* priming of naïve T cells [131, 132].

In this frame, Sulfavant A was tested *in vitro* assays in order to evaluate its ability to induce DCs maturation, or in other word, to trigger a prime immune response.

Sulfavant A determined an increment of the levels of phenotypic marker CD83 cells even if the expression of the co-stimulatory molecules CD86 was comparable to that induced by Pam2CSK4 that is the TLRs agonist positive control used in this work, as shown in Figure 2.3, where is reported the flow-cytometry analysis of the *in vitro* assays. For a better reading, the up-regulation of CD83 is reported also in Figure 2.4a, that underline the dose dependent manner Sulfavant A promote the maturation of DCs with. Moreover, Sulfavant A induced the gene expression of proinflammatory cytokines like IL-12 and INFγ (Figure 2.4b), that are strictly correlated to the DCs ability to trigger an efficient Th1 cells response [133].

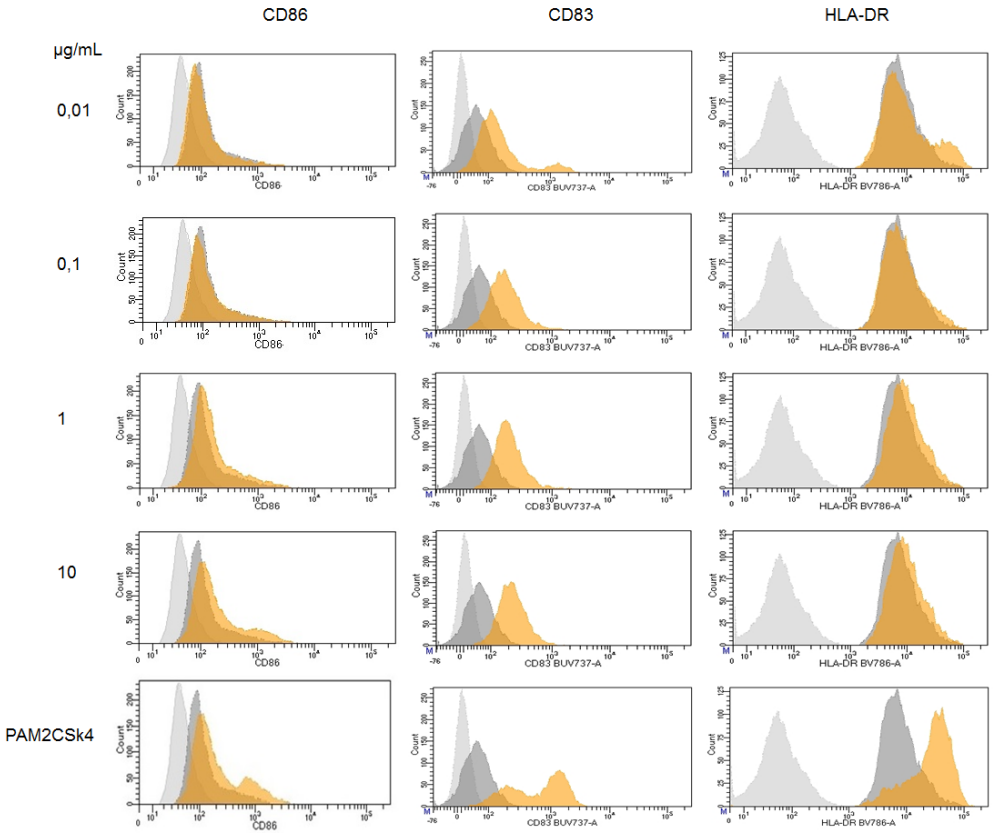

Figure 2.3: Flow-cytometry analysis of the phenotyping markers of DC maturation (HLA-DR, CD83 and CD86) at concentrations between 10 ng/ml to 10 µg/ml of Sulfavant A gray = isotype control; dark gray = unstimulated cells; orange = stimulated cells. Pam2CSK4 (PAM) was used as positive control [38].

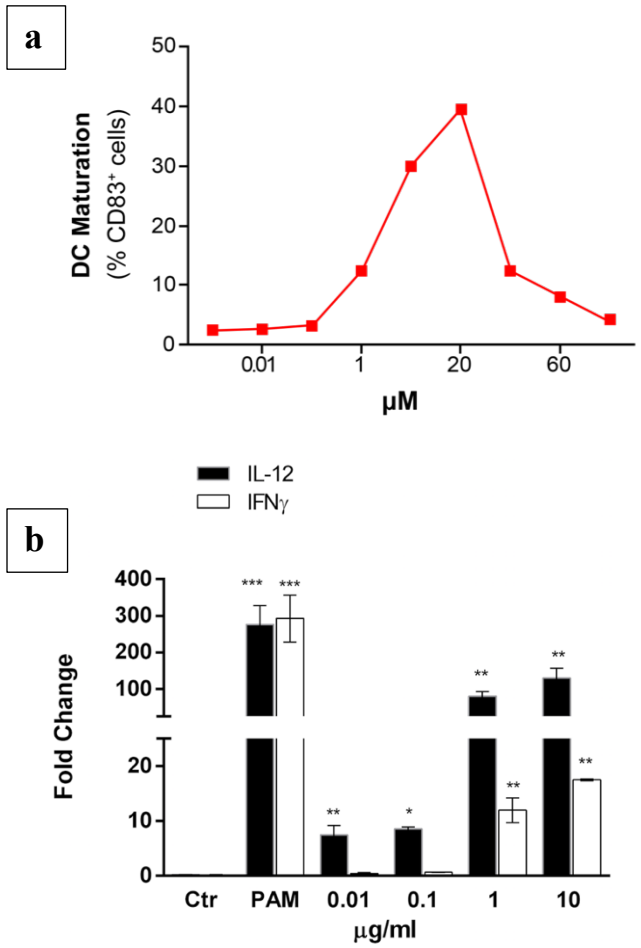

Figure 2.4: a) Percentage of $CD83^+$ cells depending on Sulfavant A concentration; b) Expression of IL-12 and IFN-γ by DC stimulated with Sulfavant A in the same range of concentrations used for the above marker phenotyping

2.1.2.1 TLRs-independent activity of Sulfavat A [38]

In general, the immunological response induced by MPLA and other glycolipids, interesting in terms of vaccine adjuvance, is mainly mediated by TLR-2 and TLR-4 [134]. TLRs are membrane-associated innate receptors expressed on the cell surface

of APCs able to recognize conserved pathogen-associated molecular patterns (PAMPs).

With the aim to investigate the mechanism of action responsible of the immunomodulant activity of Sulfavant A, cell receptor binding assays were run. In this regard Sulfavant A was tested on HEK293 cells co-transfected to express TLR-2 or TLR-4 and the reporter gene of the alkaline phosphatase.

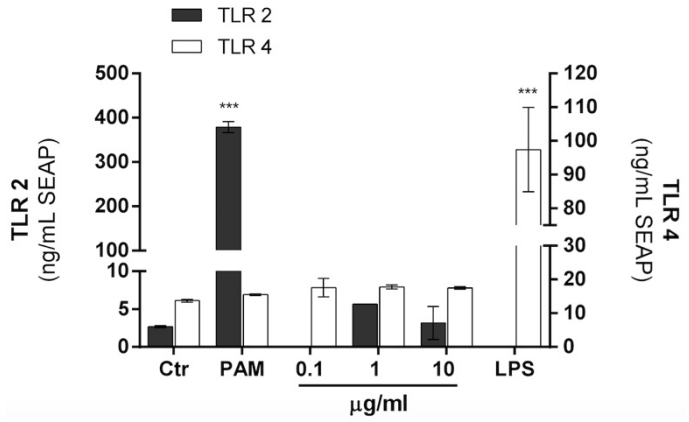

Figure 2.5: Evaluation of the Toll-Like Receptor (TLR) activation by increasing concentration concentrations of β-SQDG18 in TLR-2 and TLR-4 [38]

Figure 2.5 displays the results of this experiment: Pam2CSK4 (PAM) and LPS were used as positive controls for TLR-2 and TLR-4 respectively and it is clear that Sulfavant A had no effect on the activation of both receptors at the same concentration it showed DCs maturation and cytokine production, therefore the mechanisms of action of this sulfolipid is TLR-independent [38].

2.1.2.2 Evaluation of adjuvant activity in immunization assays [38]

In order to obtain further evidences about the Sulfavant A ability to act as adjuvant triggering the immune system, the antibody response in animal model has been evaluated, using Ovalbumin (OVA) as antigen associated with the synthetized

sulfolipid and comparing the results with two commonly used vaccine adjuvants: complete Freund's adjuvant (CFA) and TiterMax® (TM).

OVA is a T cell-dependent antigen used as a model protein in antigen-specific immune responses in studies on animal models. The immune response to OVA with anti-OVA antibodies production has been well characterized and is nowadays used to evaluate the efficiency of a specific protein antigen or adjuvant.

TiterMax® is a squalene-based commercial adjuvant with immunostimulatory activity formulated as water-in-oil emulsion. It is an alternative to CFA (discussed in the paragraph 1.4.2) to investigate cell mediated and humoral responses *in vivo* experiments.

As far as the experiment is concerned, the mice immunization with OVA/Sulfavant A gave a robust enhancement of anti-OVA antibody titres, with high level of murine IgG and IgM (Figure 2.6) and the results were comparable to the antibody response achieved with the approved adjuvants CFA and TM.

Murine IgGs are different from human ones and they include four subclasses (IgG1, IgG2a, IgG2b and IgG3) that work in a synergic manner to supply the right immune responses [135]. Even if the antibodies function in mouse is no completely understand, it is known that IgM and IgG1 are involved in early response and migration of the inflammatory process respectively, moreover, IgG antibodies are linked with the activation of long-lasting memory B-cells and cytotoxic T-cells [136], important requirement for vaccine adjuvant.

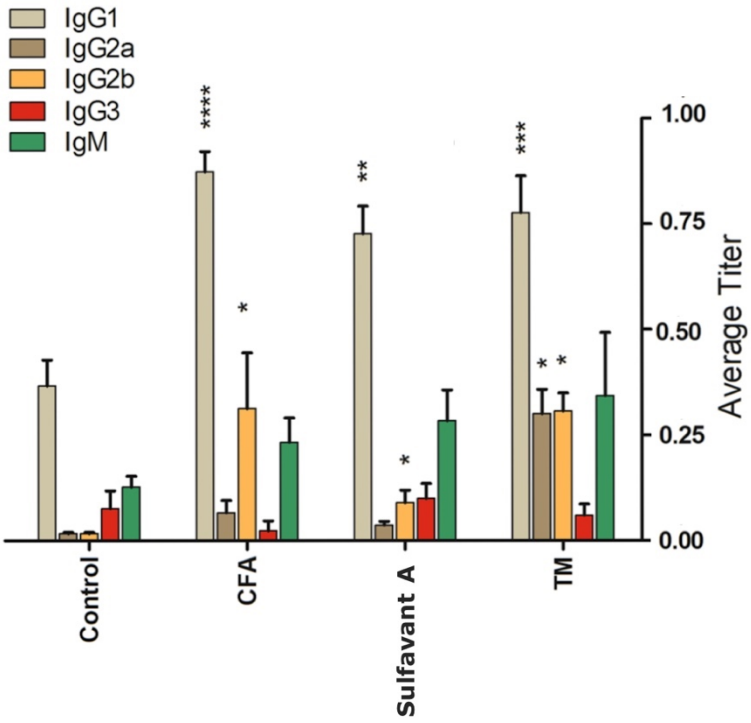

Figure 2.6: Immune response of mice after immunization to ovalbumin formulated with Sulfavant A

2.1.2.3 *In vivo* assay against an experimental melanoma cancer model [38]

As previously discussed, the necessity of new vaccines and therefore vaccine adjuvants come from the exigences to fight against new infectious disease as well as the will to find new and alternative therapies against cancer. Activation of immune system is considered a promising approach in this field, even if, to date, the hard selection of an efficient protocol hinders the clinical application of therapeutic cancer vaccines. Different tumour antigens were overexpressed and isolated from tumorous cells and they could be potentially useful as vaccines in anticancer treatments but

unfortunately, one of the major problems is their poor antigenicity that could be overcome using, in association with them, a strong adjuvant qualified to boost the cell-mediated immune response [137].

In this context, Sulfavant A has been tested in an experimental model of cancer vaccine against a murine B16F10 melanoma cell line using as antigen the human $gp100_{25–33}$ peptide ($hgp100_{25–33}$).

The B16F10 melanoma is a murine tumorous cell line widely used as a model for therapeutic evaluation of metastasis and solid tumour formation of human skin cancers [138], while the antigen $hgp100_{25–33}$ is the amino acids 25-33 fragment of the human melanoma antigen recognized by T cells [139].

In this experiment as the previous one, the adjuvant effect of Sulfavant A was compared with those of CpG Oligodeoxynucleotide and CFA adjuvants (discussed in the first chapter, paragraph 1.4.2). Since vaccination with CpG and $hgp100_{25–33}$ has already shown a protective effect [140], it was used the same protocol.

Mice have been immunized three times with Sulfavant A/ $hgp100_{25–33}$ vaccine before the injection of B16F10 melanoma cells and, after that, the experiment has been monitored in terms of tumor growth. As showed in Figure 2.7, the association of the sulfolipid with the antigen $hgp100_{25–33}$ reduced the tumour development with a consequent prolonged survival compared to the mice stimulated only with B16F10 melanoma cells.

Even if the results of the whole experiment showed a comparable effect between CFA, CpG and Sulfavant A as adjuvants, it is possible to note that these last two, unlike CFA, were able to inhibit the tumour growth during the first ten days [38] of the experiment.

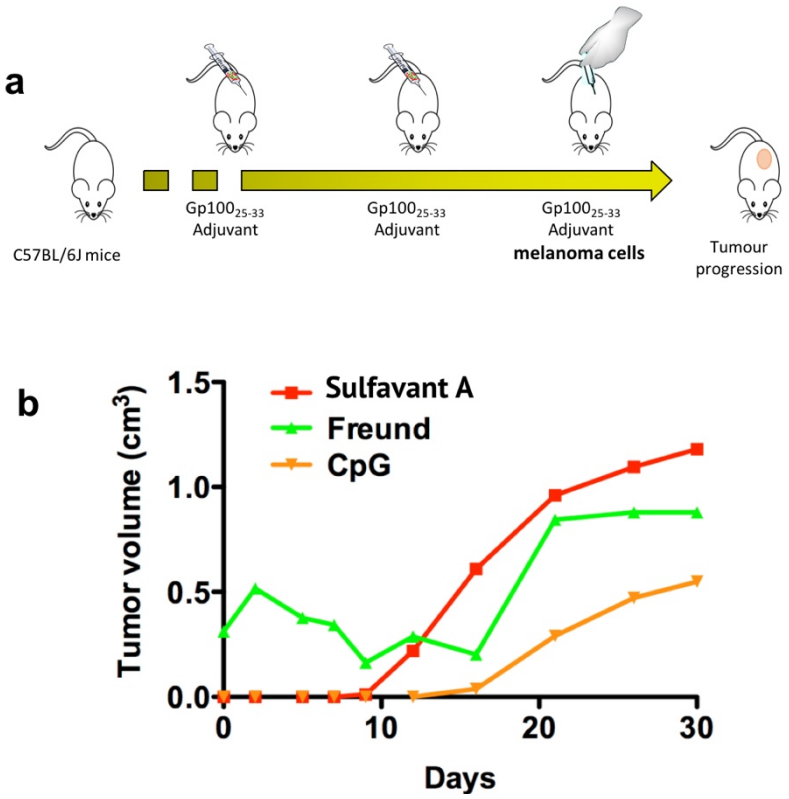

Figure 2.7: Protective effect of hgp100$_{25-33}$ peptide formulated with Sulfavant A as adjuvant in an experimental model of anti-melanoma vaccine. (**a**) Experimental design of immunization and (**b**) Tumour growth during the experiment time [38].

2.1.3 Conclusions

The chemical structure of Sulfavant A is inspired by the natural immunomodulant α-D-sulfoquinovosyl-diacylglycerols (α-SQDGs), featured by a sulfonic group on the carbon 6' of quinovose, linked to a diacyl glycerol portion.

Sulfavant A was prepared by a versatile chemical procedure involving stereoselective glycosylation of trichloroacetimidate-glucose donor with 1,2-*O*-isopropylidene glycerol acceptor. The trichloroacetimidate derivative with the use of acetate as main protecting groups of the sugar moiety allowed to achieve the β configuration of the glycosidic bond with high yield. The efficient designed procedure can be potentially

employed for the preparation of a broad range of regiopure glycoglycerolipids and, moreover, it is easily scalable in order to synthetize large amount of β-SQDGs for further biological, pharmacological and clinical investigations.

Sulfavant A was able to trigger DCs maturation and this effect is a crucial point in the development of new substances potentially useful in vaccines field and in particular in therapeutic vaccine formulations for cancer treatment.

The immunomodulant effect of Sulfavant A was TLR-independent and, even if, considering the chemical analogies between the sulfolipid and the LPS-related adjuvants (e.g. MPLA), this result could be unexpected, another mechanism could be at basis of the DCs maturation without passing through activation of TLRs [141].

The antibodies response induced by Sulfavant A *in vivo* biological assays confirmed the ability of this molecule to activate the immune system, as demonstrated by the Ig production after mice immunization with the sulfolipid associated to OVA antigen.

Sulfavant A showed encouraging results in an experimental model of vaccination against melanoma in mice, with a delayed and reduced tumour growth that hallmark the protective effect of this molecule able to enhance the immunogenicity of $hgp100_{25–33}$ melanoma antigen.

All these data suggest that Sulfavant A is a good candidate and prototype of a new class of molecular adjuvants.

The scale-up of the synthesis of Sulfavant A is required for further investigation as well as the preparation of its analogues with the aim to improve its immunomodulant behaviour; furthermore, optimization of the formulation will probably open the way to meliorated vaccination protocols.

2.2 Sulfavant A analogues with different acyl chains

The biological results obtained on Sulfavant A were particularly promising and further investigation on its biological activity was necessary.

An interesting point was the correlation between the chemical structure of this molecule and its immunomodulant action; in this regard a study on the effect of slight structural modifications on the immunomodulant response could be crucial.

In fact, once established that Sulfavant A modulated immune response by a TLR-independent mechanism, in order to enhance the efficiency and to investigate a possible mechanism of action of this new class of vaccine adjuvants, the chemical synthesis of Sulfavant A analogues was planned; in detail, the crucial topic was to establish the effect of structural changes of Sulfavant A on the activation and maturation of human monocyte-derived dendritic cells (moDCs).

In this regard different motifs of the molecule could be modified, like the configuration of both anomeric and glycerol secondary carbon as well as the type of acyl groups.

Considering the milder biological activity of the natural α-SQDGs, the effectiveness of the presence of a β-configuration at the anomeric position has already proved [38], therefore, in a first approach it was evaluated the influence that different acyl chains and the stereochemistry change at carbon 2 of glycerol moiety could have on moDCs maturation.

2.2.1 Synthesis of 1,2-*O*-dipalmitoyl-3-*O*-β-D-sulfoquinovosylglycerol and its diasteropure analogues

As first structural change on Sulfavant A, the effect of shorter acyl chains on glycerol moiety was evaluated by replacing the two $C_{18:0}$ with two $C_{16:0}$ to obtain 1,2-*O*-dipalmitoyl-3-*O*-β-D-sulfoquinovosylglycerol (β-SQDG16); at the same time the impact of the modification on the configuration of carbon 2 of the aglycon part was assessed with the synthesis of (*R*)-1,2-*O*-dipalmitoyl-3-*O*-β-D-

sulfoquinovosylglycerol (β-SQDG16-R) and (*S*)-1,2-*O*-dipalmitoyl-3-*O*-β-D-sulfoquinovosylglycerol (β-SQDG16-S)

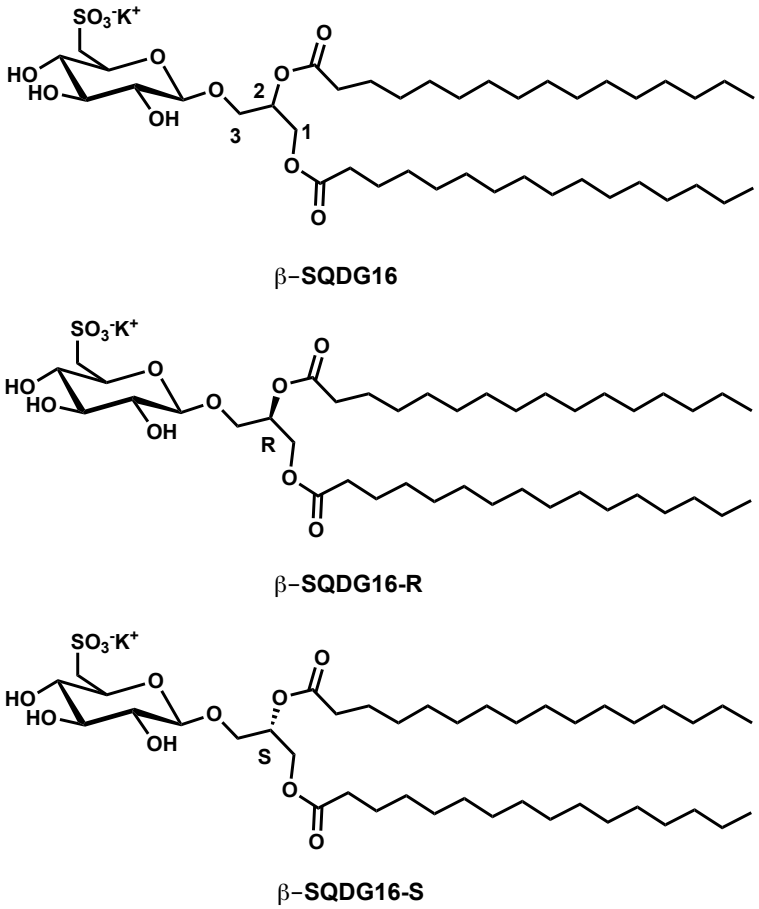

β−**SQDG16**

β−**SQDG16-R**

β−**SQDG16-S**

Figure 2.8: Chemical structure of 1,2-*O*-dipalmitoyl-3-*O*-β-D-sulfoquinovosylglycerol (β-SQDG16), (*R*)-1,2-*O*-dipalmitoyl-3-*O*-β-D-sulfoquinovosylglycerol (β-SQDG16-R) and (*S*)-1,2-*O*-dipalmitoyl-3-*O*-β-D-sulfoquinovosylglycerol (β-SQDG16-S)

The good versatility of the synthetic strategy for the preparation of Sulfavant A, allowed to obtain a wide range of its analogues without strong modifications; for the synthesis of β-SQDG16 the only required amendment was the choice of the fatty acids to link at the glycerol moiety. Therefore, β-SQDG16 has been prepared with the same

method previously described (Scheme 2.1) except for the reaction **f** where the stearic acid was substituted by palmitic acid (Scheme 2.2).

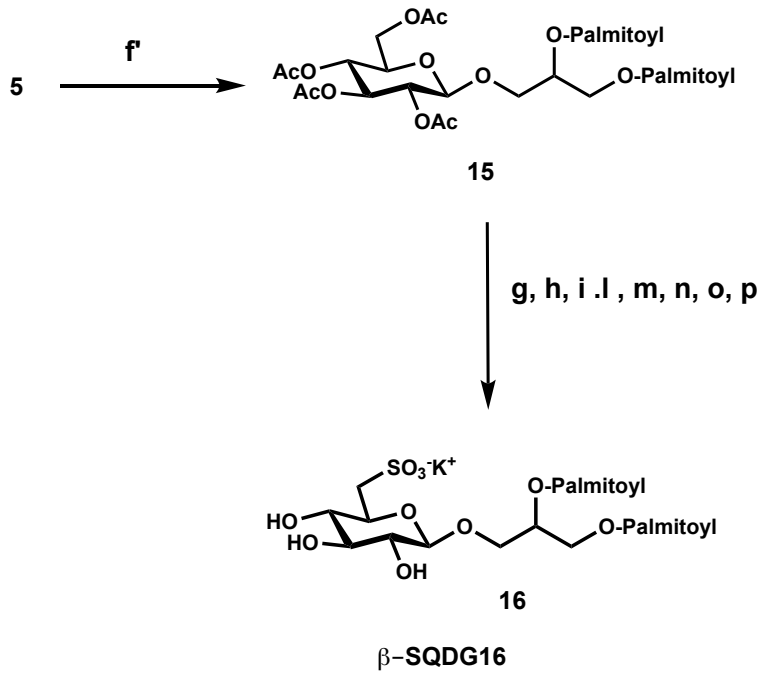

Scheme 2.2: Modification of synthetic strategy of Sulfavant A in order to obtain β-SQDG16 (all experimental conditions are reported in Chap. 4)

Together with the chain length, another structural modification was therefore the introduction of a specific configuration at the glyceridic carbon 2: carrying out the coupling reaction (**d**) (Scheme 2.1) with the (*R*) or (*S*) enantiomer of 1,2-*O*-isopropylidene glycerol, the preparation of β-SQDG16-R and β-SQDG16-S was achieved (scheme 2.3)

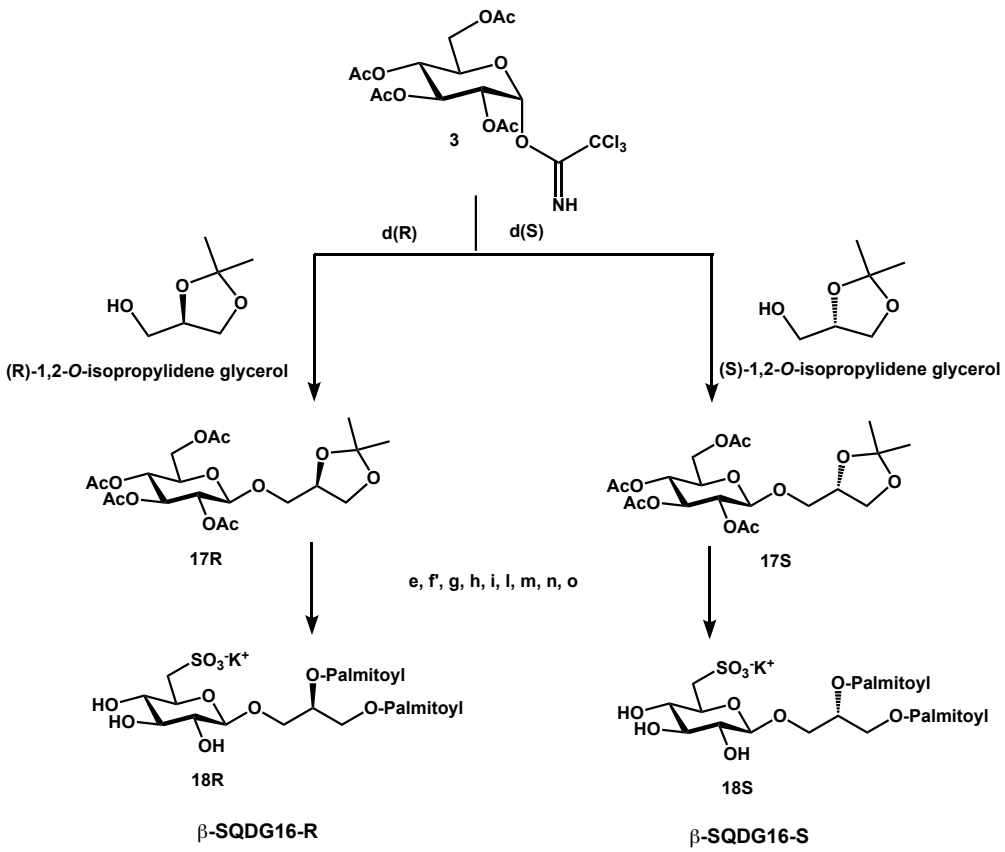

Scheme 2.3: Modification at the synthetic strategy previous discussed for the preparation of β-SQDG16-R and β-SQDG16-S
(all experimental conditions are reported in Chap. 4)

2.2.2 Synthesis of 1,2-*O*-nonadecanoyl-3-*O*-β-D-sulfoquinovosylglycerol analogues

In order to explore also the effect of a longer hydrophobic tail, the sulfolipid structure was modified introducing two saturated $C_{19:0}$ acyl chains (β-SQDG19) (Figure 2.9).

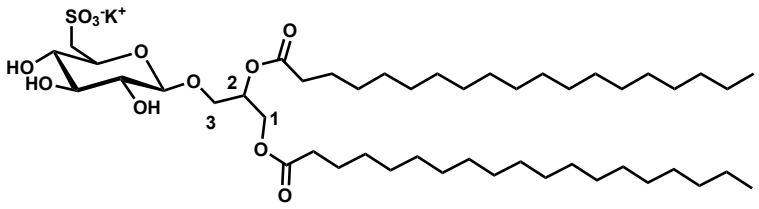

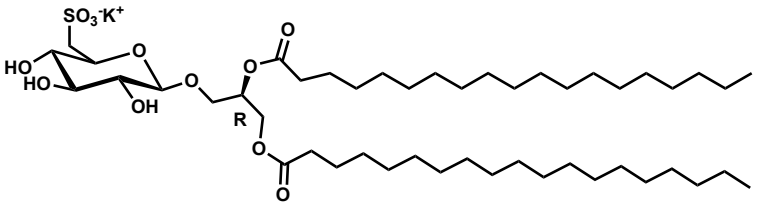

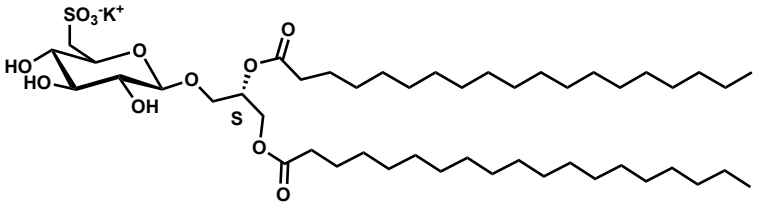

Figure 2.9: Chemical structure of 1,2-*O*-dinonadecanoyl-3-*O*-β-D-sulfoquinovosylglycerol (β-SQDG19), (*R*)-1,2-*O*- dinonadecanoyl-3-*O*-β-D-sulfoquinovosylglycerol (β-SQDG19-R) and (*S*)-1,2-*O*- dinonadecanoyl-3-*O*-β-D-sulfoquinovosylglycerol (β-SQDG19-S)

In this case, as well as for β-SQDG16, using the same synthetic strategy of Scheme 2.2 and Scheme 2.3, after the coupling reaction of the trichloroacetimidate derivative with the (*R/S*), (*R*) or (*S*)-1,2-*O*-isopropylideneglycerol, the use of nonadecanoic acid in the DCC-mediated esterification led to β-SQDG19 (Scheme 2.4), β-SQDG19-R and β-SQDG19-S (Scheme 2.5) featured by two hydrophobic $C_{19:0}$ chains.

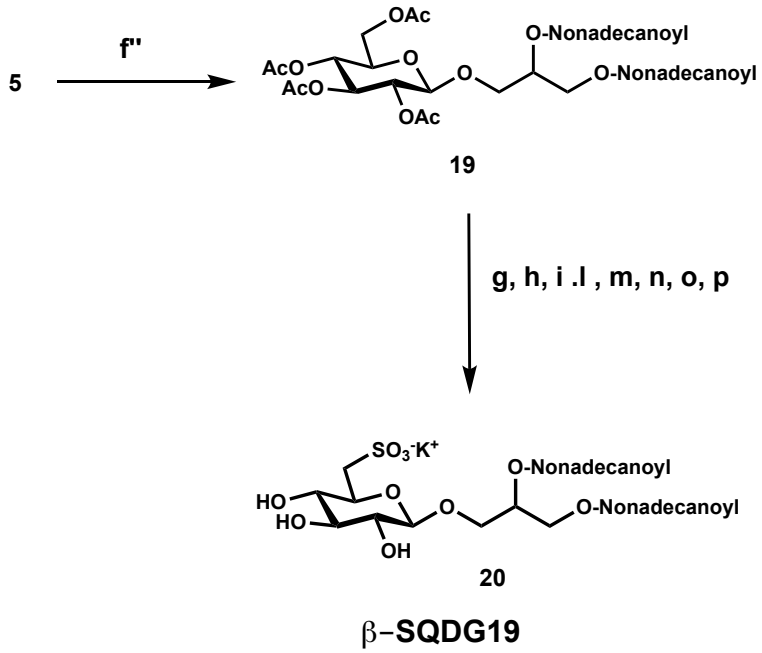

Scheme 2.4: Modification of synthetic strategy of Sulfavant A in order to obtain β-SQDG19 (all experimental conditions are reported in Chap. 4)

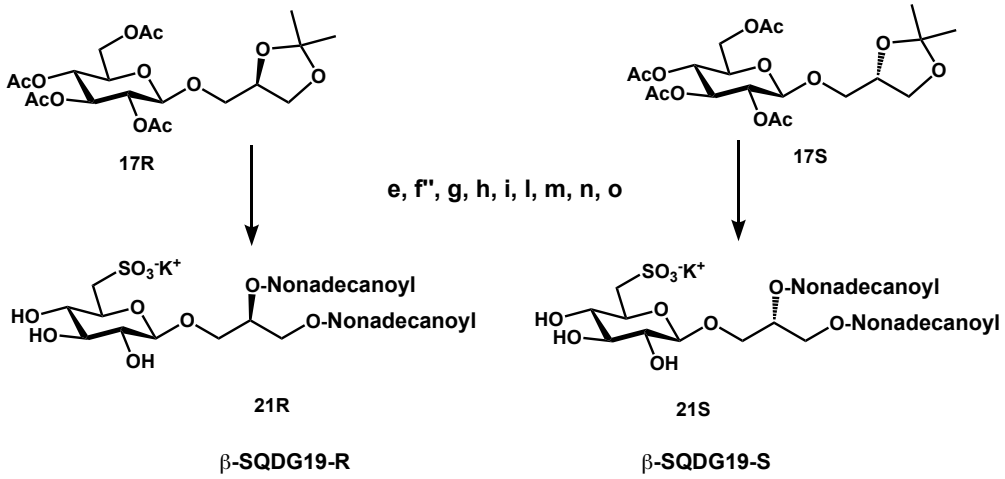

Scheme 2.5: Modification at the synthetic strategy previous discussed for the preparation of β-SQDG19-R and β-SQDG19-S (all experimental conditions are reported in Chap. 4)

2.2.3 Evaluation of the *in vitro* biological response of β-SQDG16, β-SQDG16-R, β-SQDG16-S and β-SQDG19, β-SQDG19-R, β-SQDG19-S

β-SQDG16 and β-SQDG19, as well as Sulfavant A, are an epimeric mixtures, but they differ from Sulfavant A in the length of the hydrophobic tails.

β-SQDG16-R, β-SQDG16-S, β-SQDG19-R and β-SQDG19-S are diasteropure analogues of β-SQDG16 and β-SQDG19 that combine the effect of different (shorter for β-SQDG16 and longer for β-SQDG19) acyl chains with the stereochemistry at glycerol carbon 2.

The immunomodulant behaviour of the synthetized compounds was evaluated as their ability to elicit immature DCs maturation that was monitored throughout the percentage of the phenotypic marker surface, CD83, strictly correlated with a completely mature DCs.

As shown in Figure 2.10 and in Figure 2.11 β-SQDG16, β-SQDG16-R, β-SQDG16-S and β-SQDG19, β-SQDG19-R, β-SQDG19-S derivatives, despite the slightly structural differences from Sulfavant A, proved an unexpected relevant negative effect on the moDCs assay, whether they were characterized by only shorter/longer acyl chains or both different length of chains and the stereochemistry of glycerol C2.

Sulfavant A resulted to be, among these, the most active molecule and for this reason our interest has been totally focused on the chemical and biological study of this molecule.

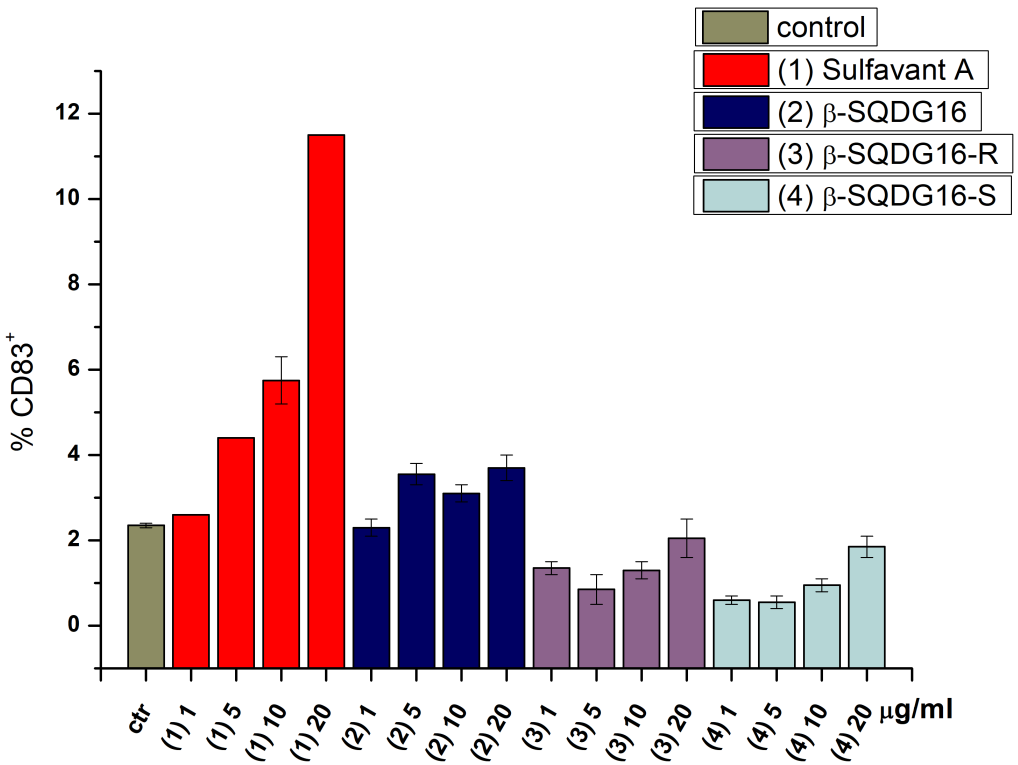

Figure 2.10: Percentage of $CD83^+$ determined by FACS analysis after 24 hours incubation with β-SQDG16 analogues derivatives at concentrations of 1, 5, 10, 20 µg mL^{-1}. Data are expressed as mean and standard deviation from duplicates of two independent experiments and compared to cells treated with only vehicle (DMSO) and to Sulfavant A.

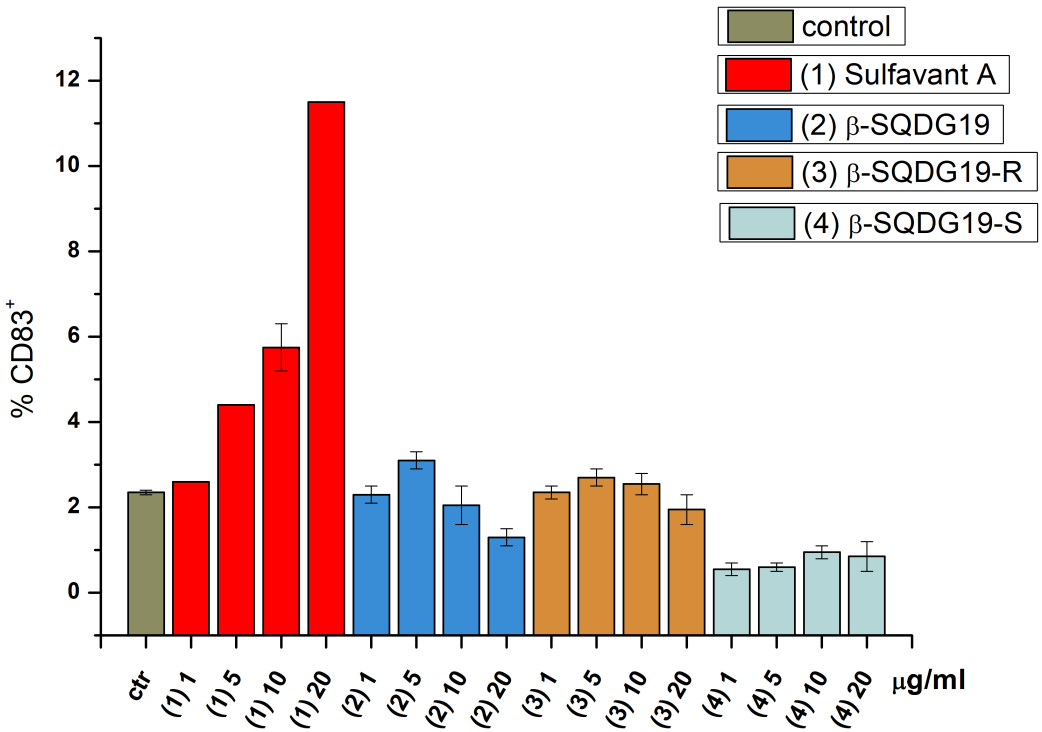

Figure 2.11: Percentage of $CD83^+$ determined by FACS analysis after 24 hours incubation with β-SQDG19 analogues derivatives at concentrations of 1, 5, 10, 20 µg mL^{-1}. Data are expressed as mean and standard deviation from duplicates of two independent experiments and compared to cells treated with only vehicle (DMSO) and to Sulfavant A.

2.2.4 Conclusions

The effect of structural changes on immunomodulant activity of Sulfavant A was evaluated. In particular, modifications on the lipidic part of the molecule concerning variations of acyl chains and glyceridic configuration were performed. For this purpose, the synthesis of different analogues of Sulfavant A was carried out with the same methodology previously designed, as evidence of its great versatility. Derivatives of Sulfavant A, with modifications on acyl chains length and C2 configuration, were prepared. In particular, β-SQDG16 and β-SQDG19, have been synthetized replacing the stearoyl acyl chains with the palmitoyl and the nonadecanoyl acyl chains, respectively, in the DCC-mediated condensation; furthermore, the use of the enantiomers (*R)* or (*S*)-1,2-O-isopropylidene glycerol acceptors, in the coupling reaction, allowed the preparation of the diasteropure epimers β-SQDG16-R, β-SQDG16-S, β-SQDG19-R and β-SQDG19-S.

As far as the biological assay is concerned, the influence of the stereochemistry of glycerol moiety and the nature of acyl chains on the immunomodulatory activity of β-SQDG16, β-SQDG16-R, β-SQDG16-S, β-SQDG19, β-SQDG19-R and β-SQDG19-S were evaluated comparing their capability to activate the DCs maturation with that of Sulfavant A. It was evident that minimal structural modifications in the β-SQDGs basic structure induced significant changes of the immunomodulant activity and in this context Sulfavant A still resulted as the most promising molecule from a biological point of view.

2.3 Improvement of the synthetic strategy and synthesis of diasteropure analogues of Sulfavant A [114]

Sulfavant A is an epimeric mixture at glyceridic carbon 2 with a ratio R/S about 1.3:1. As described before, this molecule has been prepared employing a chemical strategy based on the trichloroacetamidate methodology for the coupling reaction between the sugar moiety with 1,2-*O*-isopropylidene glycerol acceptor.

The first synthetic approach for the preparation of Sulfavant A, fully described in the paragraph 2.1.1, involved multiple protection and deprotection steps for the insertion of sulfonic group at carbon 6' of quinovose (Scheme 2.1). Unfortunately, these steps affected negatively the overall synthetic yield and, in order to overcome these limits, some modifications to the previous strategy were carried out.

The goals were clean and efficient approach, with easy work-up and applicable to a subsequent scale-up phase, sufficiently versatile for the preparation of other analogues also. The versatility of the synthetic strategy was already achieved by the previous method and in this new strategy it was convenient to ameliorate only the steps with a low yield.

As far as the improvement is concerned, in agreement with Traboni and co-workers [142], a direct sulfonation of the carbon-6′ of the compound **7** through the formation of an iodinate derivative was tested (Scheme 2.6). In particular, from 1,2-distearoyl-3-*O*-β-D-glucosyl glycerol (**7**), the selective iodination (I_2, PPh_3, 2,6-Lutidine) of carbon 6' followed by thioacetylation allowed to reduce the number of total steps from 14 (of previous strategy) to 11, with a consequent increase of the overall yield from 4% (of previous strategy) to 11.2% [114].

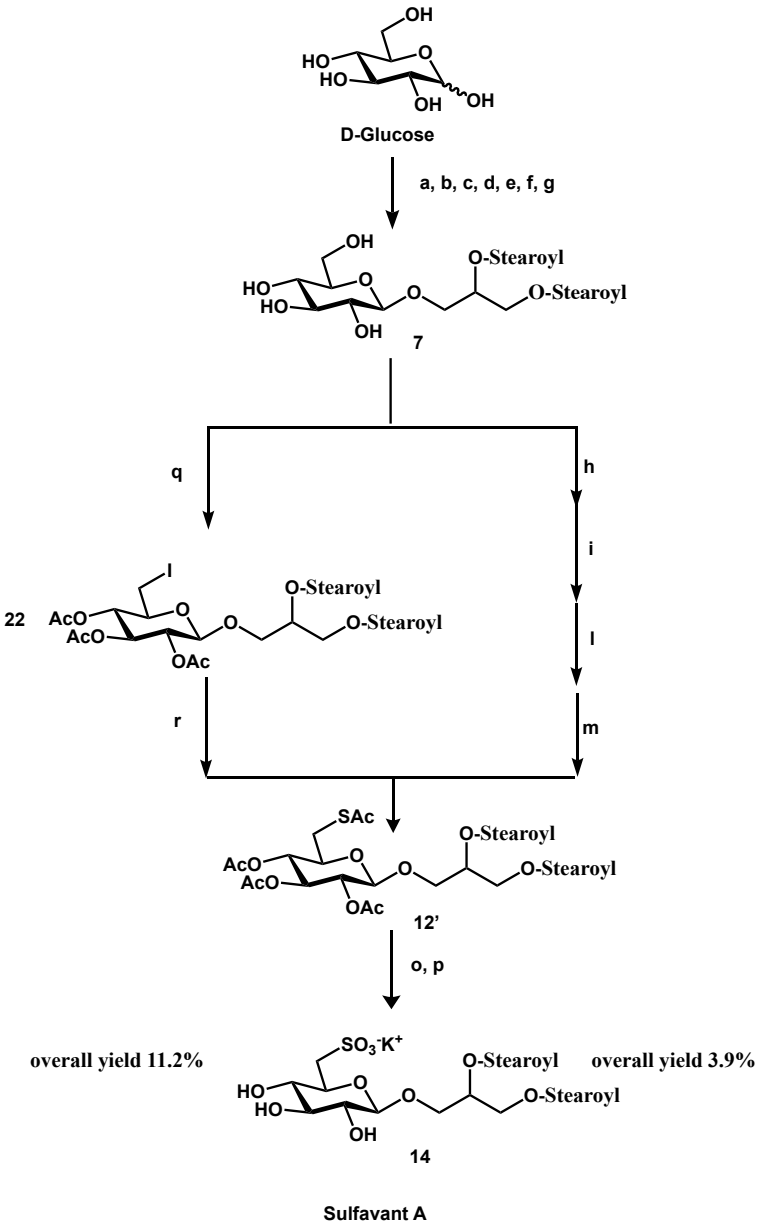

Scheme 2.6: Synthesis of Sulfavants, A: on the right is showed the first synthetic strategy employed; on the left is showed the improved synthesis of Sulfavant A [114].
(all experimental conditions are reported in Chap. 4)

In addition to Sulfavant A, the new approach was employed also for the preparation of its two diasteropure analogues (Sulfavant R and S).

2.3.1 Synthesis of two diasteropure analogues of Sulfavant A: Sulfavant R and Sulfavant S

The very promising results obtained in the biological assays carried out on Sulfavant A opened the way to a lot of questions that, considering the relevance of the topic, was worth to be investigated.

One of the most difficult challenge in drug discovery is to address the relationship between structure and activity of the potential drugs. In this frame, in order to understand the complex mechanisms beyond the sulfolipid activity and the cell target involved, it was decided to add a minor structure modification regarding the stereochemistry of the carbon 2 of the glycerol part.

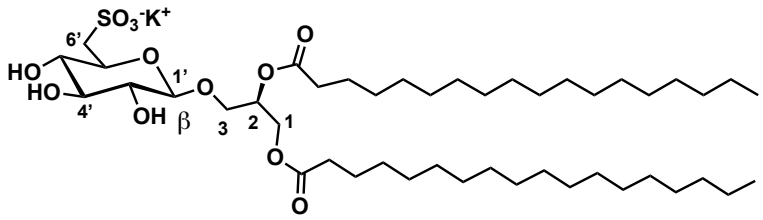

Sulfavant R

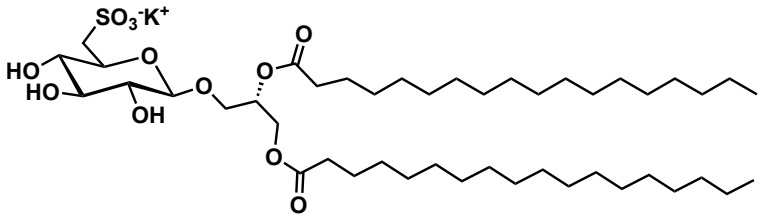

Sulfavant S

Figure 2.12: Chemical structure of 1,2-*O*-distearoyl-3-*O*-β-D-sulfoquinovosyl-(*R*)-glycerol (Sulfavant R) and 1,2-*O*-distearoyl-3-*O*-β-D-sulfoquinovosyl-(*S*)-glycerol (Sulfavant S)

As already mentioned, the new, and more efficient synthetic strategy preserved the versatility of the first one and it was suitable for the preparation of the two enantiopure epimers of Sulfavant A. In particular, using the (*S*)-1,2-O-isopropylidene glycerol in the coupling step, the 1,2-*O*-distearoyl-3-*O*-β-D-sulfoquinovosyl-(*S)*-glycerol (Sulfavant S) was obtained, whereas using the *R* enantiomer of 1,2-*O*-isopropylidene glycerol the strategy led to 1,2-*O*-distearoyl-3-*O*-β-D-sulfoquinovosyl-(*R*)-glycerol (Sulfavant R). As illustrate in Scheme 2.6, the overall yields of the total synthesis for both the diastereomers was about 11%.

MS and NMR data of the two new products were identical to Sulfavant A (that is an epimeric mixture at carbon 2 with a ratio R/S about 1.3:1) in all aspects but for the signals of the protons H_2-1 that resonate at δ 4.40 (1H, dd, J = 2.7, 12.0 Hz, H-1a) and 4.24 (1H, dd, J = 6.9, 12.0 Hz, H-1b) for the *S* epimer and at δ 4.45 (1H, dd, J = 2.6, 12.1 Hz, H-1a) and 4.17 (1H, dd, J = 6.7, 12.1 Hz, H-1b) for the *R* epimer (Figure 2.13)

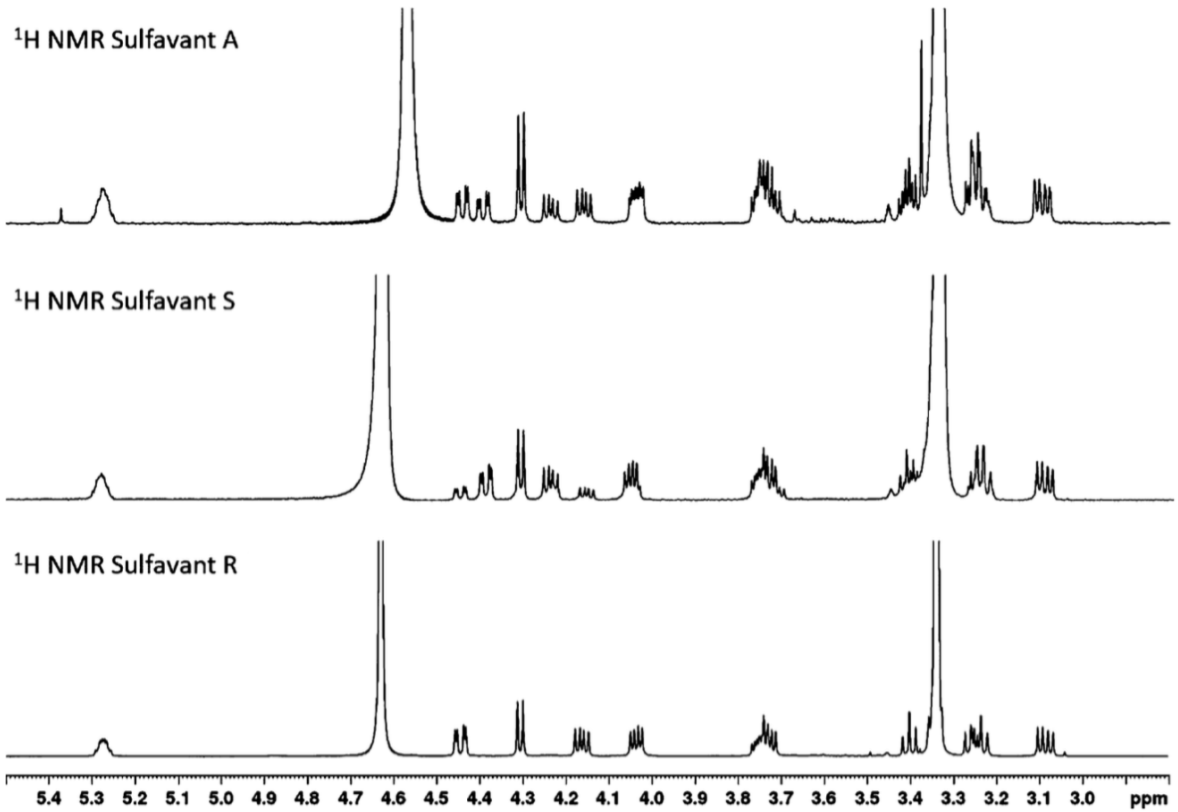

Figure 2.13: section of ^{1}H-NMR (400 MHz, $CD_3OD/CDCl_3$ 1/1) spectra of Sulfavant A, S and R. Partial epimerization of Sulfavant S is clearly detectable by the presence of the doublet of doublets at 4.45 and 4.17 ppm due to the *R* epimer.

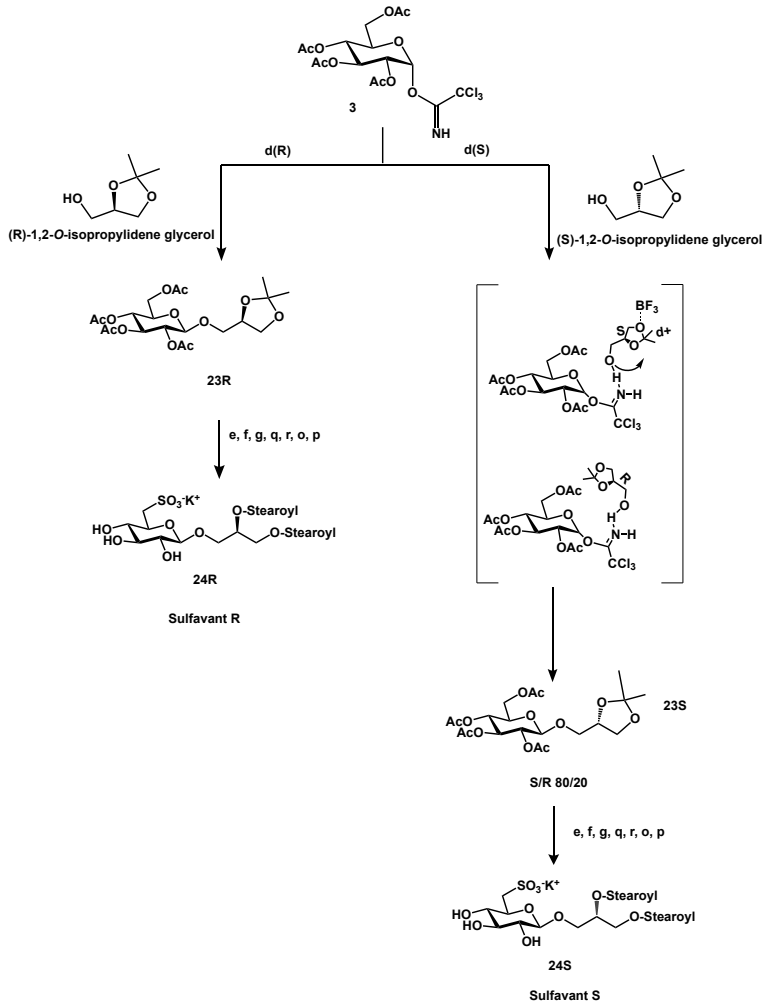

Scheme 2.7: Synthesis of Sulfavant R and Sulfavant S.
(all experimental conditions are reported in Chap. 4)

Scheme 2.7 summarizes the total synthesis of Sulfavant R and Sulfavant S, including the mechanisms hypothesized for the epimerization of Sulfavant S, that is better illustrate in Figure 2.14

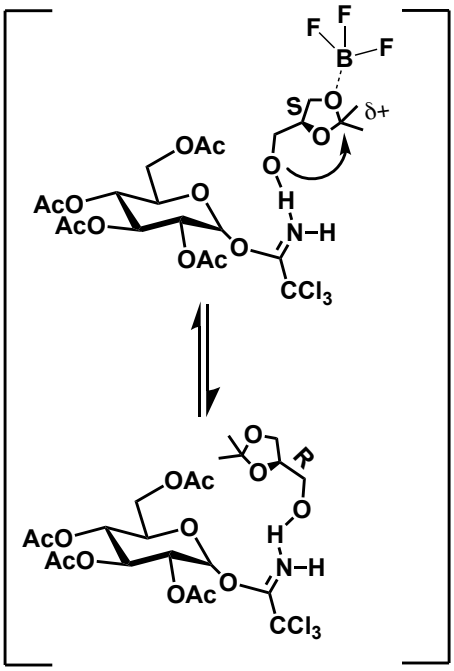

Figure 2.14: Mechanisms proposed for the epimerization of Sulfavant S

As illustrate in scheme 2.7, the configuration at carbon 2 was preserved throughout the synthetic procedure of Sulfavant R, whereas, because of diastereoselective opening and subsequent closure of the *S*-glycerol acetonide during the coupling step (favoured by the probable formation of a complex with BF_3), the synthesis of Sulfavant S led to a partial epimerization of carbon 2. Therefore, while Sulfavant R was 100% a pure epimer, Sulfavant S was composed by 80% *S* and 20% *R* diastereomers at C-2.

2.3.2 Evaluation of the biological activity of Sulfavant S and R

The crucial relevance of DCs in the immune response has been widely discussed before and, as well as for Sulfavant A, the immunomodulant effects of Sulfavant R and S have been evaluated in terms of their ability to induce DCs maturation considering the expression of MHC-Class II receptor HLA-DR, co-stimulatory molecule CD86 and CD83 as well as for Sulfavant A.

Cultured DCs treated with Sulfavant R and Sulfavant S showed an up-regulation of the expression of the DCs maturation phenotypic markers in a dose-dependent manner like Sulfavant A but at different concentrations range.

In fact, Sulfavant R and Sulfavant S surprisingly primed activation of DCs maturation at concentration drastically lower than that reported for Sulfavant A: Sulfavant A gave clear differentiation only of the CD83 DC population at 10 μM [38], while Sulfavant R and S were able to promote the maturation of DCs at 10 nM (Figure 2.15).

At higher concentration, the activity of both epimers *R* and *S* gradually decreased even if Sulfavant S stimulated residual overexpression of CD83 in the whole range of explored concentration (up to 10 μM).

Figure 2.16 illustrates the same data of the flow-cytometry about the production of CD83, underling the bell-shaped dose response of Sulfavants and the strong differences in the concentration at which they expressed their maximum activity, comparing the results of the same experiment on the three Sulfavants.

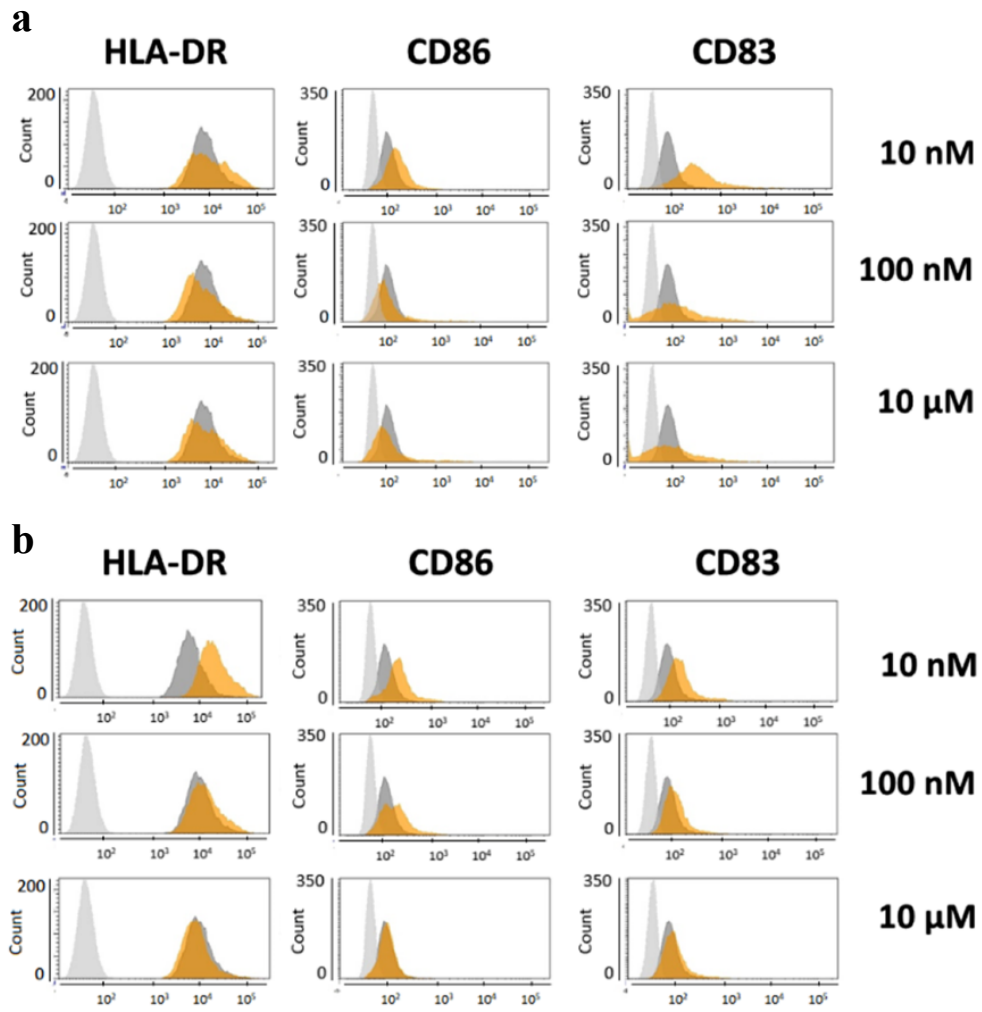

Figure 2.15: Flow-cytometry analysis of the phenotyping markers of DC maturation (HLA-DR, CD83 and CD86) at concentrations between 10 nM to 10 µM a) Sulfavant S and b) Sulfavant R (grey = isotype control; dark grey = unstimulated cells; orange = stimulated cells) Pam2CSK4 (PAM) was used as positive control [114].

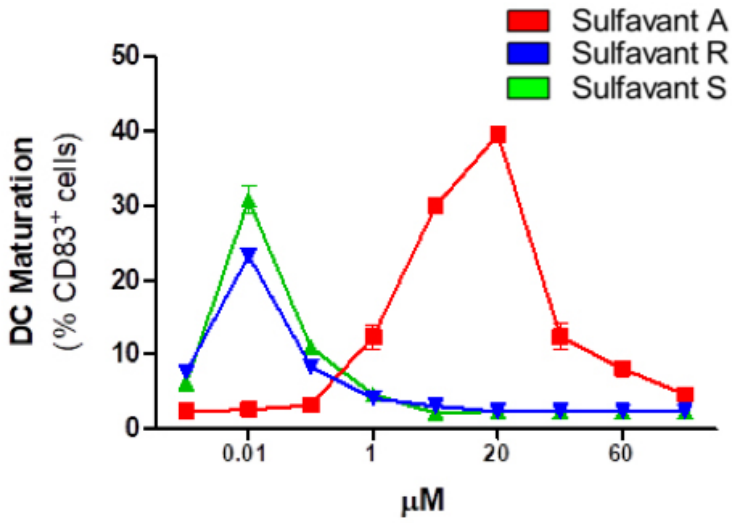

Figure 2.16: Percentage of $CD83^+$ cells depending on Sulfavants concentration

Moreover, after 24 h, Sulfavant S and Sulfavant R enhanced IL-12p40 gene expression (Figure 2.17a) without any effect on the expression of IL-10 (just as it was for Sulfavant A [38]). IL-12 is a pro-inflammatory cytokine released by DC in response to infection of bacteria and virus [143, 144], whereas IL-10 downregulates immune and inflammatory responses mediating several tolorogenic action linked to DCs [145, 146].

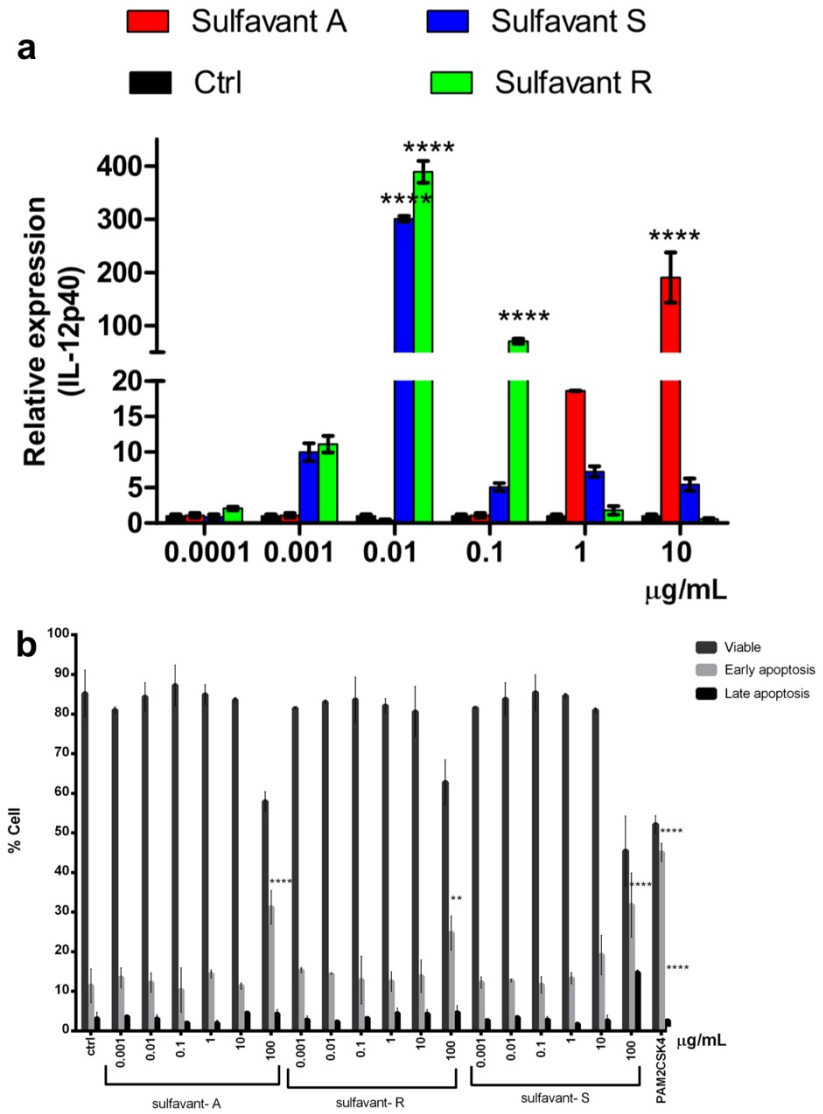

Figure 2.17: a) Gene expression analysis of IL-12p40 in DCs by stimulation with increasing dose of Sulfavants; b) Cytotoxic assay on moDcs. Percentage of viable, early apoptotic and late apoptotic cells stimulated with Sulfavants [114]

On the whole, the experiments suggest that the correlation of Sulfavant S and Sulfavant R with the gene expression of the mentioned cytokines is qualitatively comparable to the results obtained with Sulfavant A but the new epimeric analogues

are featured by a maximal activation at 10 nM on DCs whereas Sulfavant A showed the strongest effect only at 10 μM [121].
Cytotoxic assay on moDCs (Figure 2.17b) underlined that the three compounds did not show toxic activity on DCs at concentration up to 105-fold higher than the effective dose.

2.3.3 Conclusions

The necessity to assess the structure/immunomodulant activity relationship for Sulfavant A led to the need to make some structural modifications and in the same moment to ameliorate the synthetic strategy. In order to improve the total yield of the previous applied strategy, some adjustments were developed allowing to reduce the total steps from 14 to 11 and tripling the overall yield (up to 11%).
The improved synthetic strategy was exploited for the preparation of two analogues of Sulfavant A, Sulfavant R and Sulfavant S, epimers at carbon 2 of aglycon moiety, in order to proceed in the research of improved immunomodulant agents, applicable in the contest of vaccine adjuvants, and to estimate the structure activity correlation of this class of sulfolipids.
The versatility of this synthetic approach permitted the coupling between the sugar and the glycerol moiety by using the two enantiomers *R* or *S* of 1,2-*O*-isopropylidene glycerol to achieve Sulfavant R or Sulfavant S respectively, without any loss of the strategy efficiency.
While it was possible to preserve the glyceridic configuration for Sulfavant R, this was not possible for Sulfavant S, subject to a partial epimerization during the above-mentioned coupling reaction, obtaining in this case, a *S/R* epimeric mixture with a ratio of 80/20.
With the aim to obtain Sulfavant S, a substantial change of the synthetic approach was introduced in order to avoid the partial epimerization. This aspect will be discussed later in this thesis.

Biological properties of Sulfavant R and S were evaluated throughout the screening of specific phenotypic markers strictly correlated with the activation of DCs, as well as Sulfavant A.

In vitro assays underlined that this class of molecules, named 'Sulfavants', including the above illustrated Sulfavant A, Sulfavant S and Sulfavant R, is a non-toxic activator of DCs, but also showed a surprising different response tightly correlated with stereochemical aspects: Sulfavant R and Sulfavant S differ each other for the configuration of Carbon 2 of the aglycon moiety, while Sulfavant A represent a mixture of them.

Efficacy of single epimers (Sulfavant S and R) proved to arise at concentration 1000-fold lower that that occurred for the Sulfavant A and this fact was amazing.

In addition to this difference, another important feature is that the Sulfavants activity did not increase with a sigmoid trend related to concentration but followed a peculiar 'bell-shaped' curve of activity (Figure 2.16). Bell-shaped dose–response curves are not the rule, but several lipophilic drugs show this behaviour not often only due to problems related to interactions with cell receptors. Recently, the 'bell-shaped' response has been addressed to the formation of colloidal aggregates of the active agent [147] and it has been also reported that sulfoquinovosides in aqueous or polar environment tend to self-assemble affecting the biological activity [148-150] and chemical reactivity [113].

Considering this point of view, the explanation beyond the 'bell-shaped' response and the differences of activity concentration of Sulfavants could lie in their chemo-physical properties in polar solvents because of the natural ability of these glycolipids to form supramolecular aggregates.

2.4 Chemo-Physical Characterization of Sulfavants Self-Assembling

Due to their amphiphilic nature, molecules like Sulfavants can aggregate in supramolecular structure in aqueous environment by a thermodynamically driven process. In general, these amphiphilic substances are commonly named 'surface-active agents' or 'surfactants', and they represent an important and versatile class of chemicals employed in several industrial field [151].

Depending upon the type of molecule and the solution conditions, colloidal structures can assume different forms and properties: closed aggregates with completely hydrophobic environment within itself are called micelles, while spherical bilayer encapsulating aqueous solution are called vesicles [152]. (Figure 2.18)

A feature of aqueous surfactants solutions is their ability to enhance the solubility of an agent that otherwise would be poorly soluble in water [153].

The common ability of Sulfavant A, R and S to trigger DCs maturation make them valuable immunomodulator agents for potential pharmacological applications as vaccine adjuvants. The peculiar features of these molecules to have a different concentration of activity and to give bell-shaped dose-dependent curves deserved to be studied.

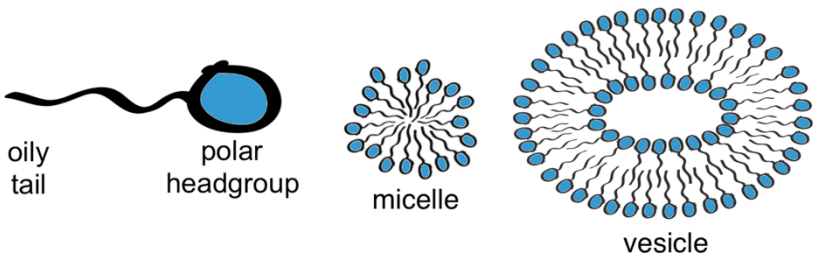

Figure 2.18: Simple illustration of micelle and vesicle

Considering the amphiphilic nature of this class of molecules, their tendency to organize themselves in more complex structures, in polar solvents, to avoid the contact between the hydrophobic acyl chains and the solvent itself, is evident.

As already reported by Shoichet and co-workers [147], bell-shaped dose–response curves are distinctive of many amphiphilic bioactive compounds and it has been addressed to the formation of colloidal species.

Moreover, in the field of sulfoquinovosides it has been reported that the occurrence of aggregates affects the biological activity [113, 149, 154] and their reactivity, therefore, in order to clarify some aspects linked with the biological response of Sulfavants, a study on the chemo-physical properties of these molecules in aqueous solution, has been carried out.

2.4.1 Dynamic Light Scattering measurements

In this regard, the first technique used to analyse and confirm the Sulfavants self-assembling and to evaluate the differences between diastereomeric mixture and its enantiopure analogues was the Dynamic Light Scattering (DLS).

DLS is a very useful technique for studying the diffusion property of macromolecules in solution. In a classic DLS experiment, a source of monochromatic light collides with the sample and the scattered light is collected and detected by an appropriate detector.

At the base of scatter phenomenon there is the theory of Brownian motion, introduced for the first time by Robert Brown in 1827 and explained some years later by Einstein (1905): Brownian motion can be described as random motion of particles suspended in a fluid due to their collision with the other molecules in the solution [155].

Few years later, Einstein introduced also a relationship between the diffusion coefficient and the translational friction of the particles, including the theory of Stokes about the proportionality between the friction exerted by a particle in motion and their radius as well as the viscosity of the solvent 156].

Only after the development of laser optics and further detailed studies, light scattering technique acquire great importance and in 1969 the first experiment to diffusion coefficient determination was carried out [157].
When a laser light collides on a solution, containing macromolecules or aggregates, the incident light scatters in all direction and the scattered light will result from constructive and destructive phenomena producing fluctuations of the detected signal that are related to the time: the correlation Fluctuation/Time strictly depend on the diffusion behaviour of the molecules in solution, or rather on their size [156].
Particle size is correlated with diffusion coefficient by the Stokes-Einstein (Eq. 2.1):

$$D = \frac{K_b T}{f} \qquad f = 6\pi R_h \eta \qquad \text{(Eq. 2.1)}$$

Where:
K_b= Boltzmann constant
R_h= hydrodynamic radius of particles in solution
η= solvent viscosity

In a DLS experiment is important to define the autocorrelation function of the electric field of the scattered light in the time, that after rigorous mathematical analysis of the process of light scattering by noninteracting small Brownian particles leads to the following expression for the normalized field correlation function:

$$g^{(1)}(\tau) = e^{-Dq^2\tau} \qquad \text{(Eq. 2.2)}$$

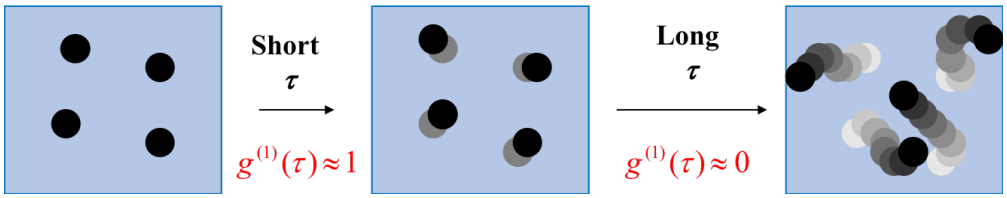

Figure 2.19: Schematic representation of the function g $^{(1)}$ in the time

As schematically illustrated in Figure 2.19, for an ideal measure, for long time, the autocorrelation function tends to zero.

Considering all the properties of this technique, DLS was really useful to determine the presence of colloidal particle in Sulfavants aqueous solution.

Preliminary tests (conducted in the laboratories of Professor Luigi Paduano, University of Naples Federico II, Dept of Chemical Sciences) were carried out to find out the better experimental conditions. Even if our purpose was to evaluate the physical aspects of Sulfavants in the same concentration range of the biological activity assays (from 5 nM to 100 µM), unfortunately DLS measures of too low concentrations solution were indeterminable because of the instrument detection limit and on the other hand DLS analysis with high concentration solution were unworkable for the presence of big aggregates that precipitated making a great background noise or creating unwanted multiple scattering.

Another issue to resolve before making the experiments was to find the right protocols for the preparation of the samples: the solution had to be sufficiently transparent in order to avoid that incident and scattered light will be drastically attenuated by absorption.

After some attempts, including sonication with immersion probe or ultrasonic bath, changing temperature and time of sonication, the samples were suspended using Millipore water filtered on 0.22 µm pore size syringe filter and sonicated for 40 minutes at 35ºC in ultrasonic bath. With this procedure several solutions with different concentrations were prepared for each compound: 0.3 mM, 0.2 mM and 0.1 mM;

moreover, for every sample DLS analysis at various time after sonication were performed: immediately after preparation and after 2, 4, 24, 48 hours.

As shown in Figure 2.20, where is reported, as an example, the autocorrelation function of Sulfavant A 0.2 mM at different time after sonication, the samples are quite unstable within the first 24 hours (the autocorrelation function should go at zero) while after 24 hours they can be considered stable.

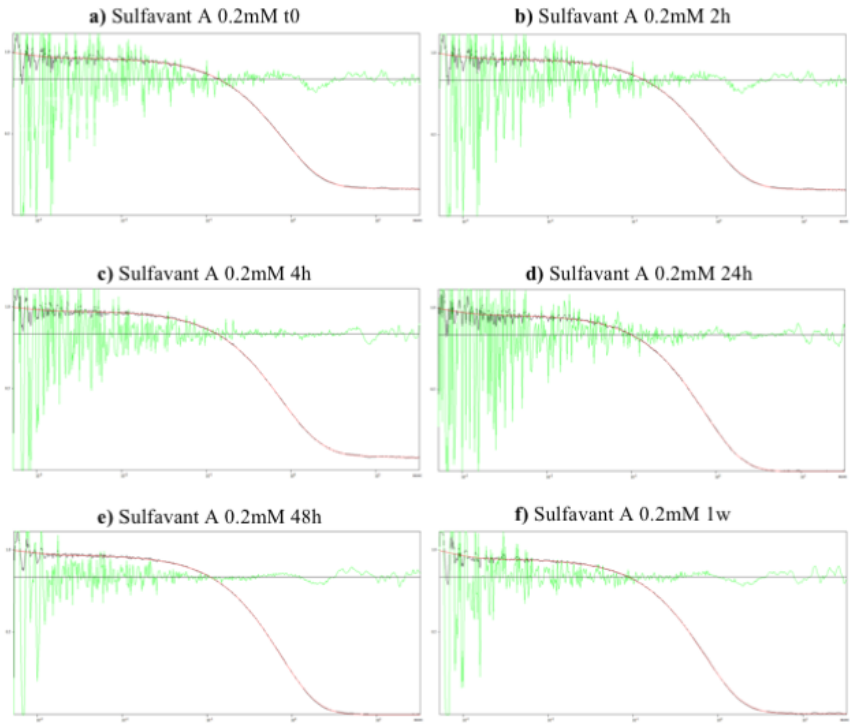

Figure 2.20: Autocorrelation functions of DLS measurements performed on 0.2 mM Sulfavant aqueous solution at different times after sonication of the sample. a) t0 (immediately after sonication); b) 2h; c) 4h; d) 24h; e) 48h; f) 1 week.

As far as the concentration is concerned, solutions at 0.2mM gave the best results in all experiments. Hence, the DLS results reported in this paragraph are referred at

Sulfavants 0.2 mM solutions, that was the lower concentration measurable for all compounds with a good resolution.

The first evidence obtained with DLS analysis was that actually Sulfavant A, R and S in aqueous solution form aggregates, although it was foreseeable by the nature of these molecules. In addition to that, the hydrodynamic radius (R_h) of the colloidal particles formed by Sulfavant A, S and R at 0.2 mM in Millipore was different for each molecule: self-aggregation of Sulfavant R and Sulfavant S gave a R_h around 50 nm, slightly different from each other, whereas Sulfavant A led to aggregates with a R_h of 150 nm with higher size dispersity (Figure 2.21a).

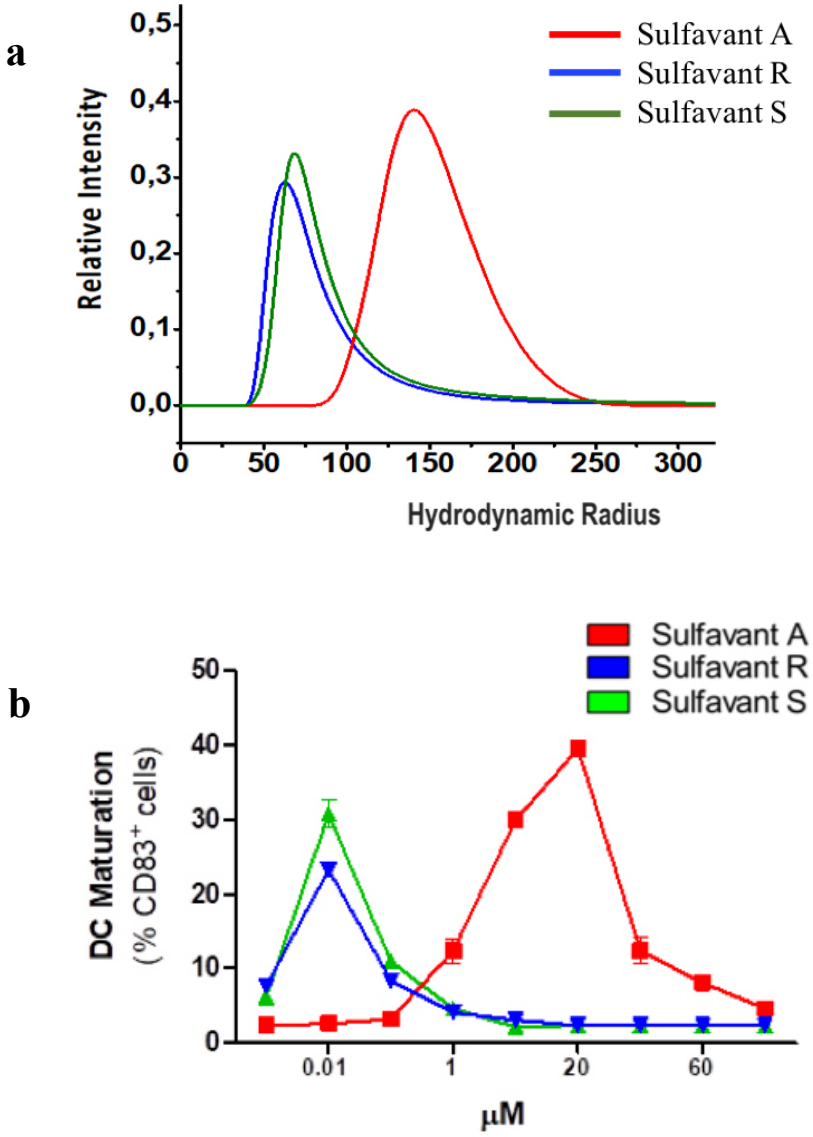

Figure 2.21: Correlation of immunomodulatory activity vs colloidal behaviour of Sulfavant A, S and R. a) Hydrodynamic radius distribution of particles of Sulfavants in aqueous suspension at 0.2 mM as measured by DLS on three independent measurements. b) Percentage of mature Dendritic cells after stimulation by Sulfavants [114]

As proved by these data, even a little structural modification, like a single carbon configuration, can strongly affects the supramolecular organization of this class of compounds.

Comparing the DLS results with the biological activity of Sulfavants (in terms of DCs maturation) it was possible to underline an unambiguously parallelism between self-assembling behaviours and biological responses (Figure 2.21). In agreement with Shoichet and co-workers [147], all these data suggested that the bell-shaped dose response curves were determined by a decrease of effective concentration of the free sulfolipid monomers at the receptor site due to the formation of colloidal species. Increasing the concentration, the size of aggregates changes, monomers are tied up and the biological activity decreases thus leading to the bell-shaped curves measured experimentally, around 10 nM with Sulfavant S and R and around 10 μM with Sulfavant A.

Figure 2.22 shows as an example the difference between two solution of Sulfavant A at different concentration: 0.2 mM and 0.3 mM, to underline that the size of aggregates is strictly related to the amount of compound in solution.

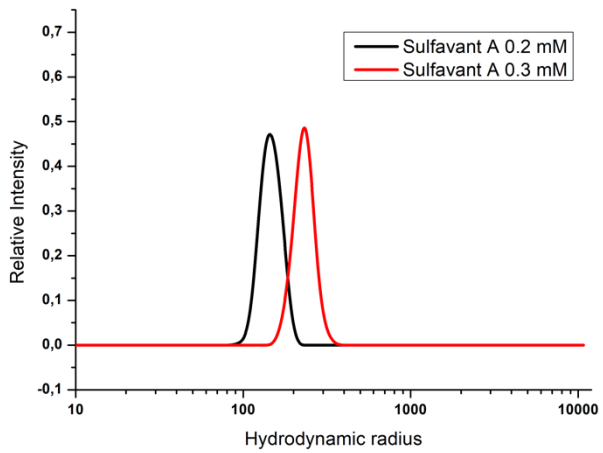

Figure 2.22: Hydrodynamic radius of two solution of Sulfavant A at different concentration: 0.2 mM (black line) and 0.3 mM (red line)

2.4.2 Micellization process and CMC evaluation

Further investigation about the trend of Sulfavants to organize themselves in aggregates structure were carried out by the evaluation of their Critical Micelle Concentration (CMC) throughout the measurement of surface tension (γ). The Critical Micelle Concentration (CMC) is defined as the concentration of surfactants above which micelles start to self-assemble forming a colloidal solution.

Surfactants are amphiphilic molecules that exhibit divergent behaviours when interacting with polar solvents like water. The polar part of the molecule interacts with water while the non-polar part escape from interaction with water. Below a well-defined concentration (CMC), surfactants in aqueous solution tend to arrange themselves on the water surface so that the polar moiety interacts with the water and the non-polar part is held above the surface oriented to the air or to a non-polar solvent (Figure 2.23a). The presence of these molecules on the water surface damages its cohesive energy inducing a reduction of the surface tension (γ) [158].

When the surfactants reach their CMC, micellization or, in wider terms, aggregation process takes place orienting the hydrophobic portions within the aggregate and the hydrophilic portions to the solvent.

Figure 2.23b reports an illustrative example of a spherical micelle.

Aggregation is energetically favourable because it allows to minimize the contact water-hydrophobic groups whereas alkyl–alkyl interactions are maximized, and hydrophilic head groups remain surrounded by water.

The thermodynamics of micellization is based on Gibbs– Helmholtz equation:

$$\Delta G_{mic} = \Delta H_{mic} - T\Delta S_{mic} \qquad \text{(Eq. 2.3)}$$

Even if at room temperature the process has a small positive enthalpy (ΔH_{mic}), the driving force of the whole phenomenon is the large positive entropy (ΔS_{mic}).

Despite high positive value of ΔS_{mic} could be surprising, since the aggregation process lead to an apparent enhancement of order, when hydrophobic moieties are

surrounded by water, the latter forms a cage increasing both the strength and the number of effective hydrogen bonds, with a consequent lower entropy of the whole system: this is one of the main features of the hydrophobic effect. When micellization occur, the water cages around each hydrophobic chain collapse back to ordinary bulk water augmenting the total entropy [159].

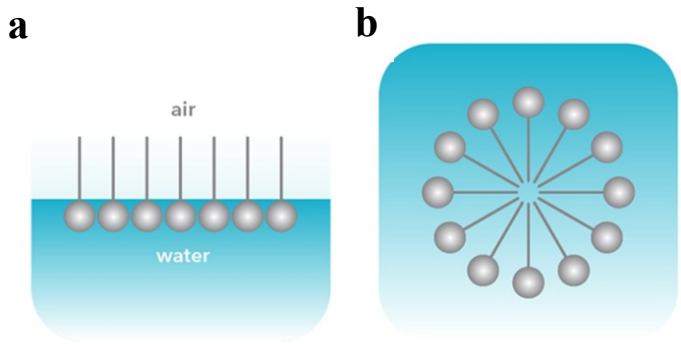

Figure 2.23: Representation of amphiphilic molecule **a**) before the CMC and **b**) after micelles formation

The evaluation of CMC is an important issue in drug discovery, especially when dealing with poorly water-soluble drugs [160].

Several methods have been developed for CMC determination, including measurements of surface tension, conductivity, fluorescence and other techniques [161-164].

In this work the CMC of Sulfavant A, R and S has been evaluate by measuring surface tension (γ) using the DuNouy ring which is the most standard and acceptable method [165].

Measurement of CMC, where the tension surface depending on surfactant concentration, consist of three phases:

- small amount of analyte is located on the surface and the γ does not chance (Figure 2.24a)
- additional surfactant decreases the γ before the CMC (Figure 2.24b)

- the surface is saturated of free monomers, micellization process starts and the γ no longer change (Figure 2.24c).

The Critical Micellar Concentration corresponds with the intersection between the plateau reached at the minimal surface tension and the slope where surface tension gradually decreases.

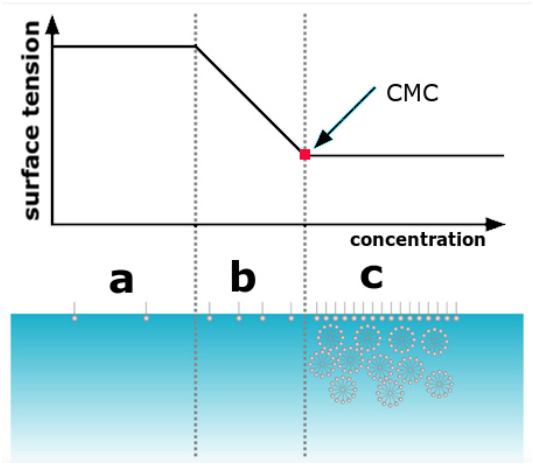

Figure 2.24: Schematization of the three phases in CMC determination experiment

The Du Noüy method is based on the interaction of a platinum ring with the solvent surface and is ordinarily used for measuring surface tension at a liquid/air interface. This technique is also known as pull-force method because during the measurement the ring is submerged in the solution and then raised from it and the force exerted passes through minimum and maximum. This process is illustrated in Figure 2.25. The maximum force, F, required to raise the ring from the surface of the liquid is measured by a tensiometer and related to the tension surface of the solution γ.

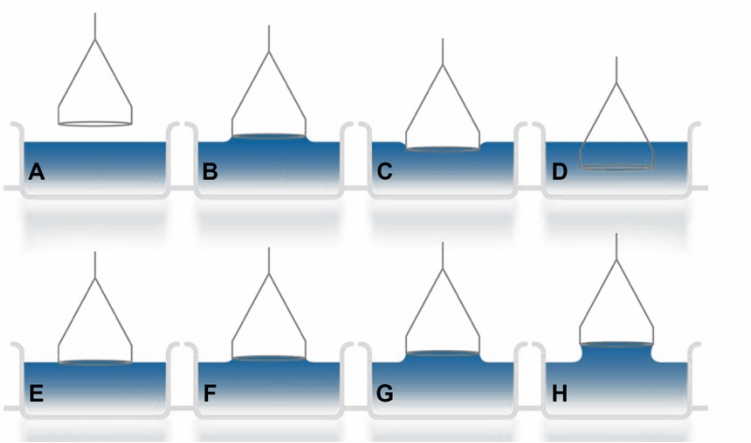

Figure 2.25: Simplified illustration of the Du Noüy method in the surface tension determination. A) The ring is above the surface (the force is zeroed); B) The ring hits the surface (slight positive force); C) The ring must be pushed through the surface (small negative force); D) The ring breaks through the surface (small positive force); E) When lifted through the surface the measured force starts to increase; F) The force keeps increasing until the maximum force is reached; G) After the maximum there is a small decrease of in the force until the lamella breaks.

The adsorption of Sulfavant A, R and S at the water/air interface has been conveniently investigated by measuring the surface tension decrease as a function of surfactant concentration. The curve obtained by these measures is called 'surface tension isotherm' and it has been measured at constant temperature. Figure 2.26 shows the surface tension isotherms for the three compounds under investigation, while in Table 2.1 the results obtained from these measures are reported.

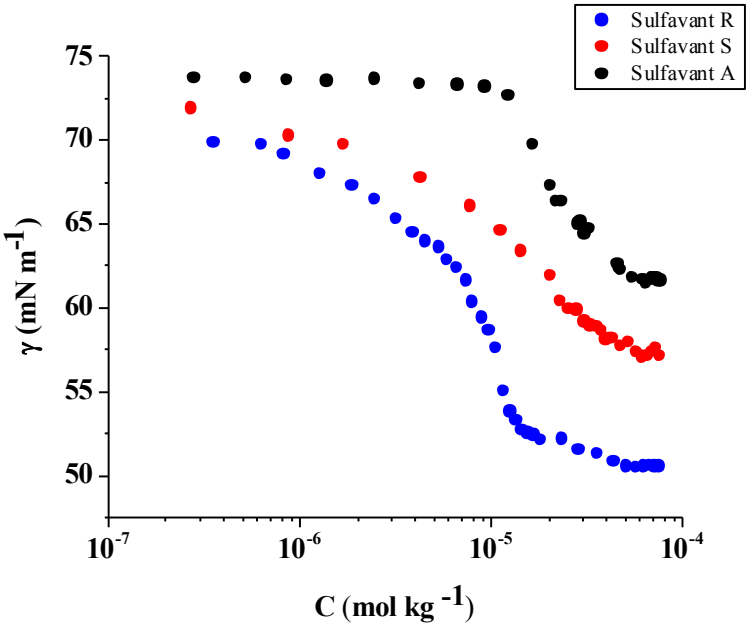

Figure 2.26: Surface tension vs. total concentration of Sulfavant A, R and S

Sulfavant	*Concentrazione Iniziale (mmol/Kg)*	*Concentrazione finale (mmol/Kg)*	*CMC mmol/Kg*	A_{min} *(Å²)*	ΔG^0_{mic} *(KJ/mol)*
A	**$2.8 \cdot 10^{-4}$**	**$7.8 \cdot 10^{-2}$**	**$70 \cdot 10^{-3}$**	**175±10**	**-24.119**
R	**$3.6 \cdot 10^{-4}$**	**$7.6 \cdot 10^{-2}$**	**$15 \cdot 10^{-3}$**	**76±10**	**-27.551**
S	**$2.7 \cdot 10^{-4}$**	**$7.6 \cdot 10^{-2}$**	**$60 \cdot 10^{-3}$**	**200±10**	**-24.098**

Table 2.1: Data obtained with the surface tension measurements

Taking a look at these results, it seems evident that Sulfavant R tends to aggregate at concentration clearly lower (about 15 μM) than that of Sulfavant S (about 60 μM) and Sulfavat A (about 70 μM). Moreover, from the value of CMC the ΔG of the micellization process has been calculated, considering that

$$\Delta G^0_{mic} = RTlnCMC \qquad \text{(Eq.2.4)}$$

Therefore, Sulfavant R, not only forms aggregates at lower concentration, but also that aggregates seem to be more stable than those formed by Sulfavant A and S.
Despite these results, once again, underline that there was a clear difference between the self-assembling of the three compounds, considering that theoretically below the CMC there should be only free monomers in solution, and the CMC for all Sulfavants is over their activity concentrations; how could aggregation affect their bioactivity?
To answer at this question, there was the need to evaluate the chemo-physical features of Sulfavants at nanomolar and micromolar concentration, in other words at the same concentration at which they express their higher activity.

2.4.3 Effect of detergent agents on aqueous solution of Sulfavants

As above mentioned the dynamic light scattering technique did not allow to obtain information about nanomolar and micromolar concentrations of these compounds because of the instrument detection limit.
Comparing the data obtained by the biological assay and the surface tension, the explanation hypothesized, that whether the bell-shaped curves or the different concentration where Sulfavants showed their maximum activity depended by supramolecular structures, collapsed because of the resulting CMCs that were higher than the activity concentration of all the three compounds.

The necessity to explore a lower range of concentrations drove this research to the use of other techniques or methods for the measurements of possible aggregates at these concentrations.

The first approach used to investigate on the hypothetical aggregation of Sulfavants at concentration lower than the CMC previously measured, was the evaluation of the effects of detergent agents on aqueous solution of Sulfavants.

2.4.3.1 ^{1}H NMR investigation

Nuclear Magnetic Resonance (NMR) spectroscopy is a powerful tool with huge application in many different scientific fields, including drug delivery, oil recovery, detergency, elucidation of mechanisms of chemical reactions, biological membrane modelling and other branch correlated with the study of colloidal aggregates [166, 167]: in fact, high resolution NMR can be applied to understand different aspects of self-assembling phenomenon, like structure, size, interactions with solutes and ion exchange [166].

Taking advantage of the NMR properties, the effect of a detergent on the NMR spectrum of Sulfavant A in water has been investigated.

For this experiment has been used Triton X100 (Figure 2.27): non-ionic surfactant commonly used in laboratories as detergent.

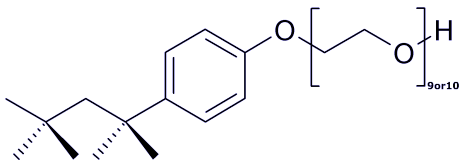

Figure 2.27: Chemical Structure of Triton X100

Figure 2.28a (red line) shows the NMR spectra of Sulfavant A 5 μM in $CDCl_3/CD_3OD$ 1:1 and Figure 2.28c (blue line) shows the NMR spectra of Sulfavant A 5μM in D_2O. As conceivable, in D_2O the NMR signals related to Sulfavant A were broadly and

poorly defined. Since this result was due to the supramolecular structure that determined the slowing down of the molecule movements that enormously changing relaxation times, adding a detergent it tends to disrupt these supramolecular structures and these signals had to get better.

In this regard an NMR spectrum was performed on the same Sulfavant A solution, adding an excess of Triton X100.

Figure 2.28c (blue line) shows the NMR spectrum of Sulfavant A without the detergent where is clear that there is a knocking down of the signals, whereas Figure 2.28b shows the spectrum of Sulfavant A 5 μM in D_2O with Triton X100.

In this latter, at chemical shift around 5.2 ppm is possible to note the increment of the signal related to the carbon 2 of the glycerol moiety that was completely absent in the NMR spectrum of the only Sulfavant A in D_2O, as well as the signal related to the anomeric proton become to be recognisable.

Because of the low concentration of the sample for this experiment and high signals of the detergent, it was not possible to have a clear evidence of an improvement of the whole spectrum, but this result could be a preliminary proof that Sulfavant A forms supramolecular structure at concentration lower than the CMC calculated by surface tension.

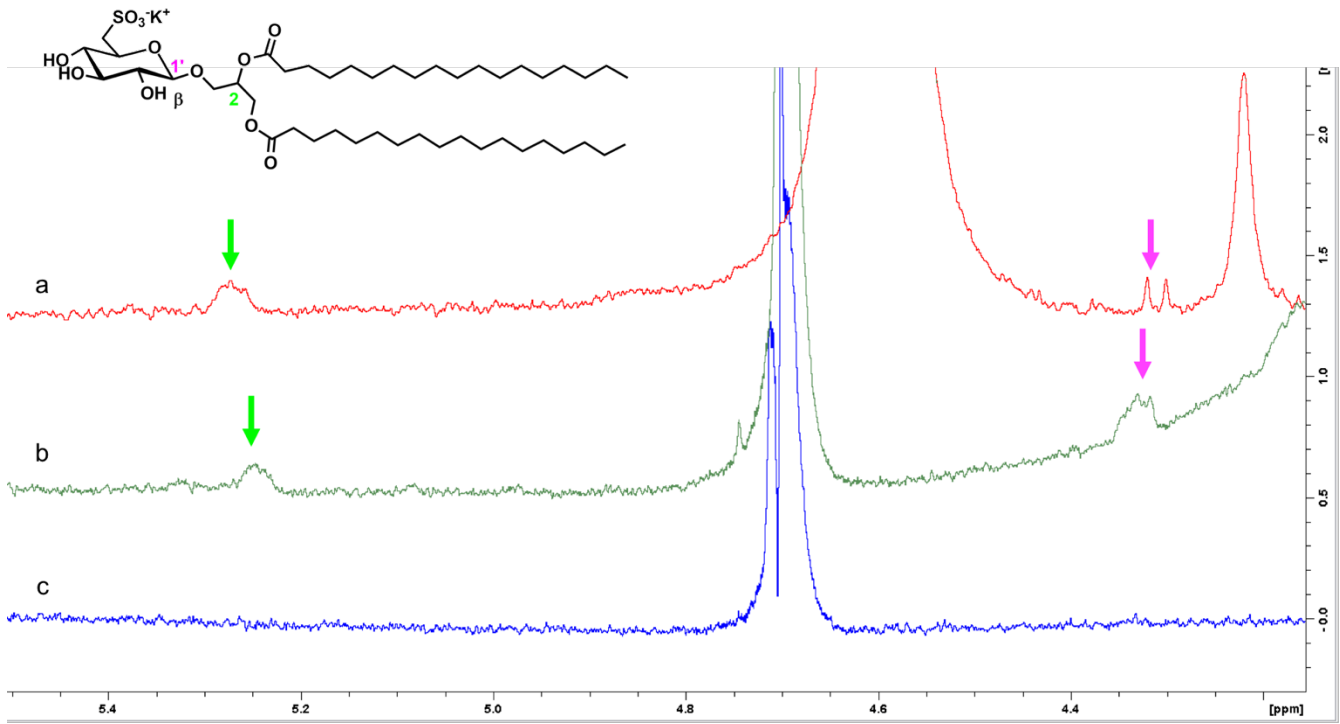

Figure 2.28: Section of NMR spectra of Sulfavant A 5 μM in $CDCl_3/CD_3OD$ 1/1 (red line) in D_2O (blue line) and in D_2O adding Triton X100 as detergent (green line)

2.4.3.2 Biological assays investigation

With the aim to understand the complexes biological mechanisms at the basis of immunomodulant activity of this class of compounds, a similar experiment, in terms of effect of adding a detergent to a Sulfavant A aqueous solution, was carried out in the assay of bioactivity evaluations. The biological activity of Sulfavant A, as previous tested, was compared with the activity of the same compound in presence of a detergent.

For this experiment, Kolliphor RH 40 (Figure 2.29) has been employed as detergent. Surfactants are often used to improve the delivery and the solubility of drugs [168]. Generally, the non-ionic surfactants are less toxic then ionic surfactant [169], and Kolliphor RH 40, together with Kolliphor EL are widely used as pharmaceutical excipients, even if a full documentation about their cytotoxicity on all cellular system is not available and some side effects sometimes could occur [170, 171].

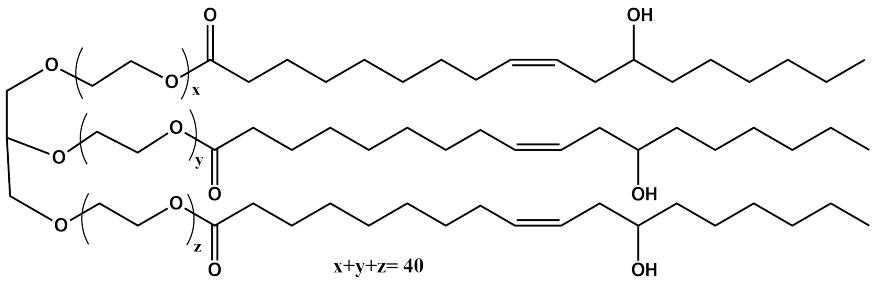

Figure 2.29: Chemical structure of kolliphor RH 40

For the purpose of this work, it was decided to explore the cytotoxicity of both Kolliphor and their effect on the DCs maturation in order to define the best choice for *in vitro* biological assays.

Although whether Kolliphor RH40 or Kolliphor EL did not show toxicity at concentration of interest, Kolliphor EL induced a small increment of HLA-DR and CD54 at higher concentration that moved the selection on Kolliphor RH40 that was

not active on DCs in the whole range of concentration and was already reported in literature [148].

The results of this biological assay are reported in Figure 2.30, where is clear that adding the detergent to the solution of Sulfavant A, there is a modification of the activity concentration.

In fact, whereas without Kolliphor RH40, the maximum activity express by Sulfavant A was around 10 μg/ml, adding the detergent, this concentration was reduced to 0.1 μg/ml. This decrement can be explained with the increase of quantity of free monomers in solution at lower concentration due to the disaggregating effect of Kolliphor RH40.

With the data obtained by NMR spectroscopy and this biological assay, it is clear that Sulfavant A tends to aggregate before reaching the CMC evaluated through the measurement of surface tension. It is plausible that below the calculated CMC the Sulfavant A exists as different and smaller aggregates, all in equilibrium with each other and the experimental CMC represents nothing more than a change of physical state relative to a transition between two different colloidal particles formed by these compounds.

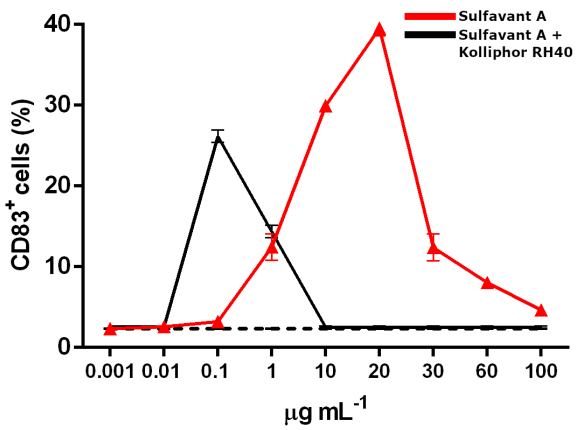

Figure 2.30: Percentage of mature $CD83^+$ cells after stimulation by Sulfavant A without (red line) and with (black line) Kolliphor RH40 as detergent

Increasing the awareness that aggregation occurs below the experimental CMC, it is possible to confirm that these compounds own a Critical Aggregation Concentration (CAC) lower than the CMC, in fact, while the CMC defines the concentration above which larger spherical aggregates are formed (measurable by surface tension measurements), CAC could be defined as the concentration at which premicellar aggregates occur [172].

Even if these data do not clearly explain how aggregation can affect the biological behaviour of Sulfavants, however they underline the existence of colloidal particles at concentration closed to that one at which Sulfavants express their maximum biological activity.

2.4.4 Fluorescence techniques for evaluation of CMC

Confirmed that Sulfavants aggregation starts at concentration much lower than the one evaluated by tension surface, in fact the effect of adding a detergent underlined the presence of supramolecular structure already below 5μM, in order to appreciate the exact concentration below which Sulfavants exist as monomers, another technique was employed to try to determine the real CMC: the fluorescence.

Fluorescence techniques have been often used to determine CMC basing on the fact that some emission bands of different fluorescent probes change deeply in intensity or wavelength, depending on the environment of the probe (e.g. viscosity and polarity of the surrounding solvent) [173, 174].

Under the CMC a fluorescent non-polar molecule will be mainly surrounded by the aqueous solution, while above the CMC it will be trapped inside the aggregate whose internal part is apolar.

By exploiting that type of probes with higher emission quantum yield in a non-polar environment compared to a polar solvent, such as water, and by plotting the intensity of the emission band versus the concentration of the surfactant under analysis, it is possible to extrapolate the CMC.

A representative illustration of CMC determination by fluorescence technique is reported in Figure 2.31, where is possible distinguish the three phases of the fluorescence emission:

I) fluorescent probe in polar solvent→no fluorescent emission

II) fluorescent probe starts to be included in non-polar inner of aggregates→ improvement of the fluorescence emission

III) fluorescent probe all included in non-polar inner of aggregates→ maximum fluorescence emission

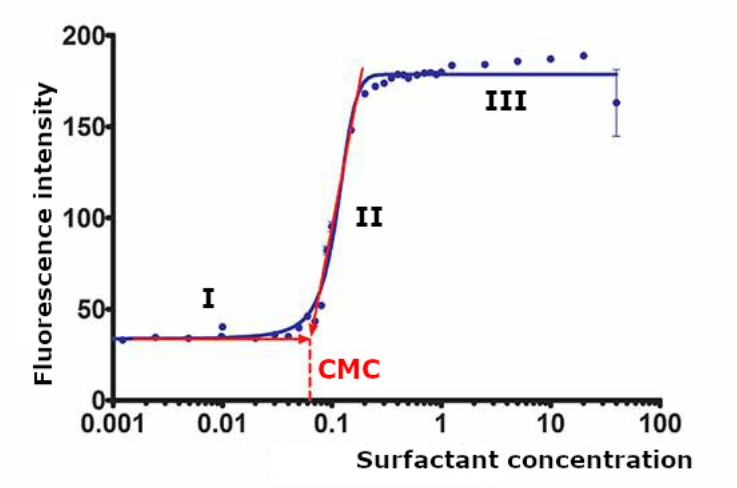

Figure 2.31: Illustration of the data analysis of CMC determination by fluorescence

2.4.4.1 Fluorescent measurement using 1,6-diphenyl-hexatriene (DPH)

Different fluorescent probes own the peculiarity to increase their fluorescent emission in non-polar solvent being insoluble in water (or polar solvent). Among these, well known examples of fluorescent molecule employed for the determination of CMC are: 8-Anilinonaphthalene-1-sulfonic acid (ANS), 1-N-phenylnaphthylamine (NPN) and 1,6-diphenyl-hexatriene (DPH) [175] (Figure 2.32).

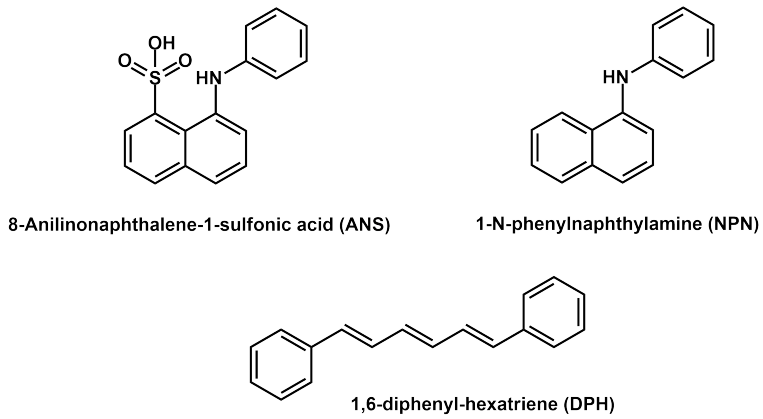

Figure 2.32: Chemical structure of fluorescent probes

Where, ANS is high soluble in water and the fluorescence of NPN in water is quite appreciable, with an enhancing of the fluorescence of only 20-fold when internalized in the aggregate structure, while DPH is more suitable for this type of fluorescence assays in water because of its insolubility that allow a very low background fluorescence and a strong enhancement of the emission bands when it is surrounded by non-polar environment [163, 175].

Taking advantage of the strongly enhancement of the DPH fluorescence above the CMC, depending on its intercalation into the hydrophobic moiety of the aggregates, it was determined the dependence of DPH fluorescence intensity from the Sulfavant A concentration.

Figure 2.33 shows the emission bands of different solutions of Sulfavant A containing DPH, and the increase in intensity with the concentration of the surfactant is clear.

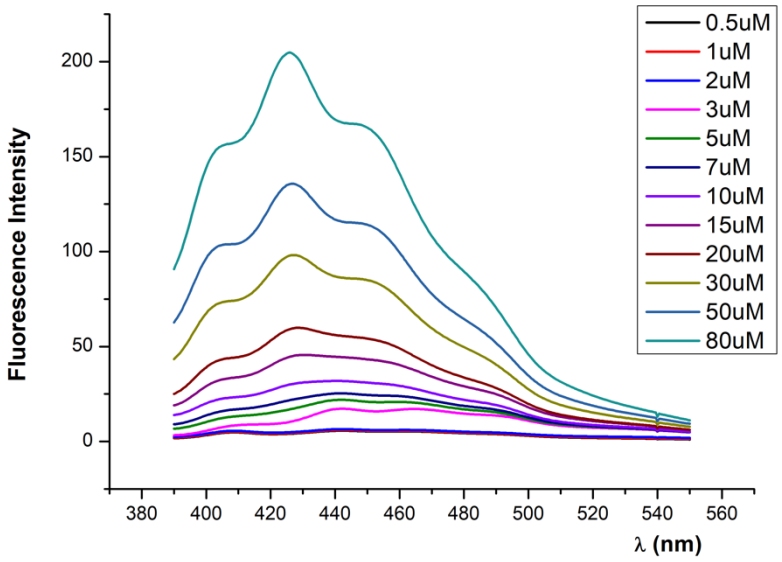

Figure 2.33: Dependence of the fluorescent emission bands of DPH with different concentration of Sulfavant A

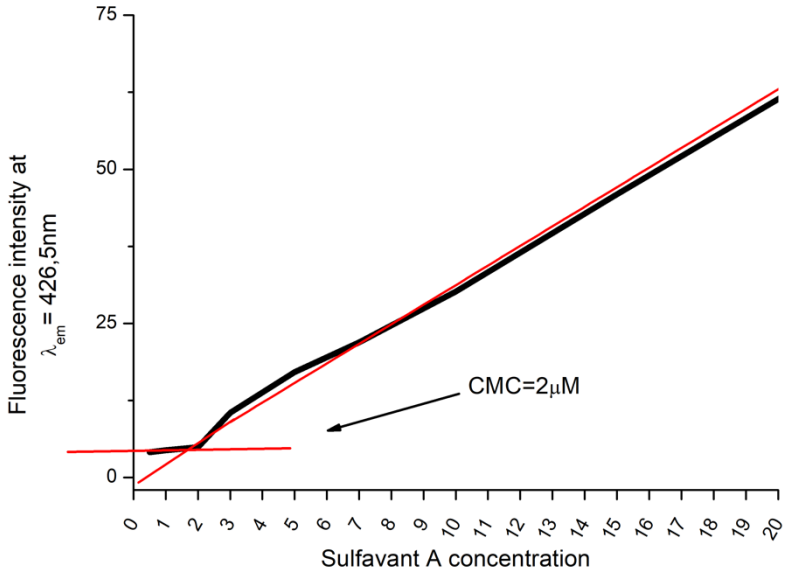

Figure 2.34: CMC determined by fluorescence data analysis

Data elaboration is reported in Figure 2.34, where the CMC determined is specified. As clear, with fluorescence technique it was possible to investigate Sulfavant A solution at lower concentration than surface tension and NMR, and also at this concentration aggregates were already formed.

2.4.5 Cryo-TEM experiments

Analysis with Cryogenic Transmission Electron Microscopy (cryo-TEM) were performed to investigate on aqueous solutions of Sulfavant A and R at low concentration (10 nM and 10 μM), which is, as explained before, a range of concentration difficult to investigate by other analysis techniques.

Transmission Electron Microscopy (TEM) is an essential and powerful technique that allow to obtain structural information on nanomaterials and is an emerging tool for the characterization of soft matter and supramolecular chemistry [176, 177].

The application field of TEM is wide in biology, in organic or polymer chemistry; in fact, it can be employed to study biological systems, like cells or proteins, as well as materials, like the self-assembling of surfactants.

Nowadays, this technique is widely used for the study of colloidal particles and it consist of three main different methods: drying, staining and cryo-TEM. In particular, cryo-TEM is the most useful method that avoids possible misinterpretations related to a not correct evaluation of the nature of a colloidal aggregation.

The sample preparation is a crucial issue of this technique and since it was developed, many sample preparations have been applied: drying, freeze-drying, freeze fracture, negative or positive stain, quick-freeze deep-etch and cryo-TEM.

Cryo-TEM is particularly useful and suitable for the investigation of the supramolecular aggregates in aqueous environment since the analysis carried-out is based on a precise image of what actually happens in solution.

In cryo-TEM experiments the sample is exposed to a very low temperatures in order to rapidly vitrify it in a thin layer of solvent on the grid [178]. The procedure is performed in a humidity-controlled environment to prevent dehydration and because

of the really fast vitrification cryo-TEM images can suffer from ice contamination [179]. Despite this, nowadays, cryo-TEM is the microscopy with highest resolution power.

Considering all these properties, in this work it was take advantage from cryo-TEM to investigate on the self-assembling of Sulfavant A and R. Further investigation on Sulfavant S has been postponed because of the partial epimerization discussed in the paragraph 2.3.1.

Figure 2.35 shows the images obtained by cryo-TEM analysis on Sulfavant A and R at the concentrations of interest for the biological activity (cryo-TEM measurements were conducted in laboratories of Professor Pietro Lupetti, University of Siena, Dept of Life Sciences and in collaboration with Professor Luigi Paduano, University of Naples Federico II, Dept of Chemical Sciences and Dr. Marie-Sousai Appavou of Jülich Centre for Neutron Science JCNS at Heinz Maier-Leibnitz Zentrum (MLZ) - Garching - Germany). In particular, first tests were carried out on Sulfavants solution at concentration of 10 nM in Millipore water filtered on 0.22 μm pore size syringe filter and sonicated for 40 minutes at 35ºC in ultrasonic bath.

Regarding Sulfavant R (Figure 2.35b), active at this concentration, it formed small spherical particles of few nm (about 3-5 nm) characteristic of micelles, whereas Sulfavant A (Figure 2.35a), not active at this concentration, aggregated in larger vesicular colloidal particles (around 40 nm).

So, considering that at concentration of 10 nM Sulfavant R expressed its maximum activity while Sulfavant A was inactive, it seems quite clear that the ability of these compounds to trigger DCs maturation depends on monomers or very small aggregates (dimers/trimers). This hypothesis was justified considering that, as well defined by Aniansson [180], micellar systems are characterized by rapid equilibrium with their free monomers in the bulk solution: the exchange process micelles/monomers generally occurs in a range of time from nanoseconds to microsecond [181, 182]; whereas, the situation is a bit more complex for vesicular systems: the stronger hydrogen bonds on the inner and outer surface slow down both insertion and release

of monomers from the aggregate. The same equilibrium monomers/aggregates for vesicles involve many more molecules than micelles enhancing the kinetic of the process [151, 181].

Obviously, this discussion makes sense only in the absence of external perturbations such as high temperatures, addition of salts to the solution, modification of the pH, etc.

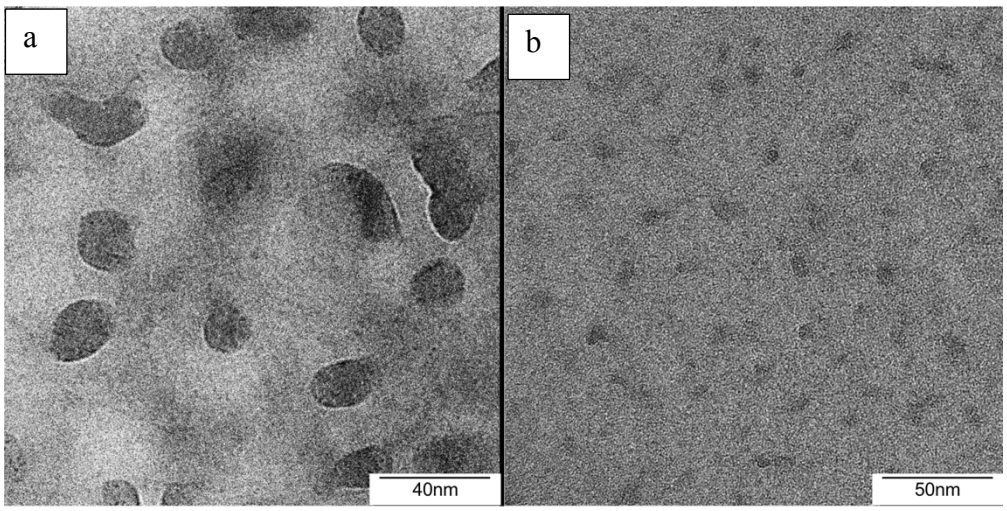

Figure 2.35: Cryo-TEM images of aqueous solution of a) Sulfavant A and b) Sulfavant R 10 nM

In a second cryo-TEM experiment two different solutions of Sulfavant A and R were analysed changing the concentration (10 μM) and preparation procedure.

The samples subjected to these experiments were:

- Sulfavant A 10 μM in Millipore water filtered on 0.22 μm pore size syringe filter and sonicated for 40 minutes at 35ºC in ultrasonic bath (Figure 2.36a);
- Sulfavant R 10 μM in Millipore water filtered on 0.22 μm pore size syringe filter and sonicated for 40 minutes at 35ºC in ultrasonic bath (Figure 2.36b);
- Sulfavant A 10 μM in Millipore water filtered on 0.22 μm pore size syringe filter and sonicated for 40 minutes at 65ºC in ultrasonic bath (Figure 2.36c);

- Sulfavant R 10 μM in Millipore water filtered on 0.22 μm pore size syringe filter and sonicated for 40 minutes at 65 ºC in ultrasonic bath (Figure 2.36d).

After making sure of the stability of the Sulfavants when sonicated for 40 minutes at 65ºC in ultrasonic bath, it was decided to investigate also the influence of temperature, in the procedure of solubilization, on the shape and size of the aggregates.
Comparing the TEM images previously discussed, with the ones regarding Sulfavants at different concentration (10 nM before and 10 μM now) but with the same sample preparation, the first evidence was the higher size of aggregates for both compounds: Sulfavant R showed spherical vesicles with a diameter about 30-40 nm, while Sulfavant A appeared as larger vesicles of about 150-160 nm.
The augment of dimensions was not a surprise since it was already demonstrated by DLS measurements at higher concentrations (Paragraph 2.4.1, Figure 2.22).
For the Sulfavant R, not only an enhancement of the particles size, but also a changing of the type of aggregates (vesicular) occurred at 10 μM and this could explain the decrease of its biological activity. Sulfavant A still resulted to be as vesicles but with a greater diameter.
Remembering the surface tension experiments, the calculated CMC had the same order of magnitude of the concentration of this TEM analysis, and it resulted that Sulfavant A was less stable than Sulfavant R ($\Delta G°_{mic}(Sulfavant\ R) < \Delta G°_{mic}\ (Sulfavant\ A)$) and, on the base of these data, it is possible that at this concentration the amount of free monomers of Sulfavant A (in equilibrium with aggregates) is enough to interact with its target and activate the DCs maturation, unlike Sulfavant R which monomers are strongly tied up.
Regarding the water solutions of Sulfavants at 10 μM prepared at 65 ºC, the cryo-TEM images showed something quite imperceptible but small, low defined particles in Sulfavant A solution, while for Sulfavant R nothing was visible (Figure 2.36c and Figure 2.36d)

This scenario let think that preparing the sample by ultrasound at higher temperatures reduces the particle size of the aggregates and if so, it should have consequences on the dose-response curves of activity of Sulfavants.

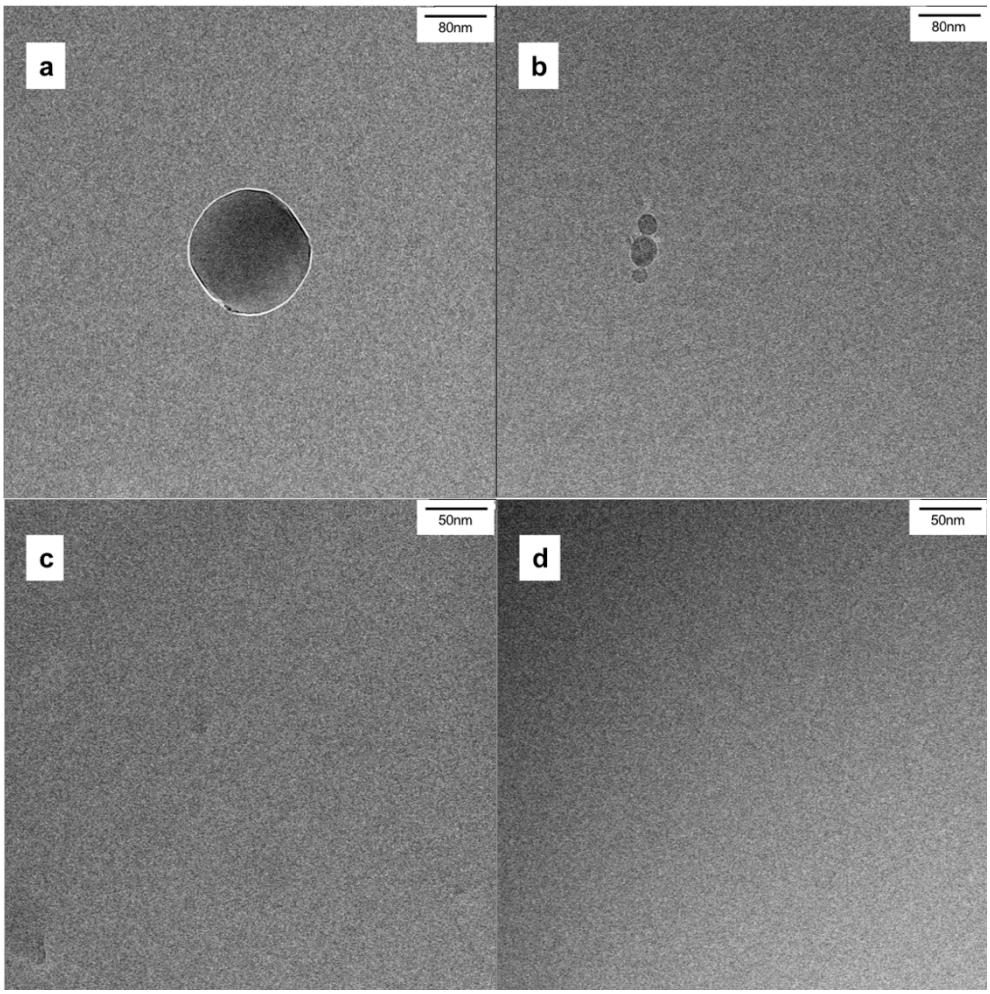

Figure 2.36: Cryo-TEM images of aqueous solution 10 μM of a) Sulfavant A sonicated for 40 minutes at 35º C in ultrasonic bath; b) Sulfavant R sonicated for 40 minutes at 35º C in ultrasonic bath; c) Sulfavant A sonicated for 40 minutes at 65º C in ultrasonic bath; d) Sulfavant R sonicated for 40 minutes at 65º C in ultrasonic bath

2.4.6 Effect of the sample preparation protocol on biological activity

Considering the effects produced by a different protocol of sample preparation on particles size, it was worthwhile investigate if also the biological response was affected by this procedure.

Data obtained by DLS, surface tension and, above all, cryo-TEM analysis, allowed to correlate the bell-shaped dose–response curves to the nature of Sulfavants self-assembling. The use of higher temperatures in the sample preparation changed the aggregation state, leading to a 'minor' aggregation or to the formation of very small particles as shown by cryo-TEM data, as consequence this protocol of Sulfavants solubilization should affect the concentration at which they express their maximum activity.

In order to confirm or not this hypothesis, aqueous solutions of Sulfavant A and Sulfavant R have been prepared throughout sonication for 40 minutes at 65ºC. Several dilutions from these stock solutions have been performed in order to evaluate the DCs maturation by Sulfavants in terms of up-regulation of the surface markers CD83.

Figure 2.37 shows the results of the biological assays carried out on Sulfavant A and Sulfavant R with the new samples preparation.

Both samples prepared with sonication at 65ºC showed a maximum of activity at lower concentrations than the previous experiments (sample preparations conducted at 35ºC). While Sulfavant A prepared by sonication at 35ºC showed a maximum around 10 µg/ml, the maximum of activity moved at 10 ng/ml with this new method of preparation, and for Sulfavant R the shift of concentration was from 10 ng/ml to 0.1 ng/ml.

The reduction of the maximum concentration of activity, obtained with this experiment, was plausible Considering the deep decrease of the size of the self-assembling colloidal structures shown by the cryo-TEM images (Figure 2.36c-d).

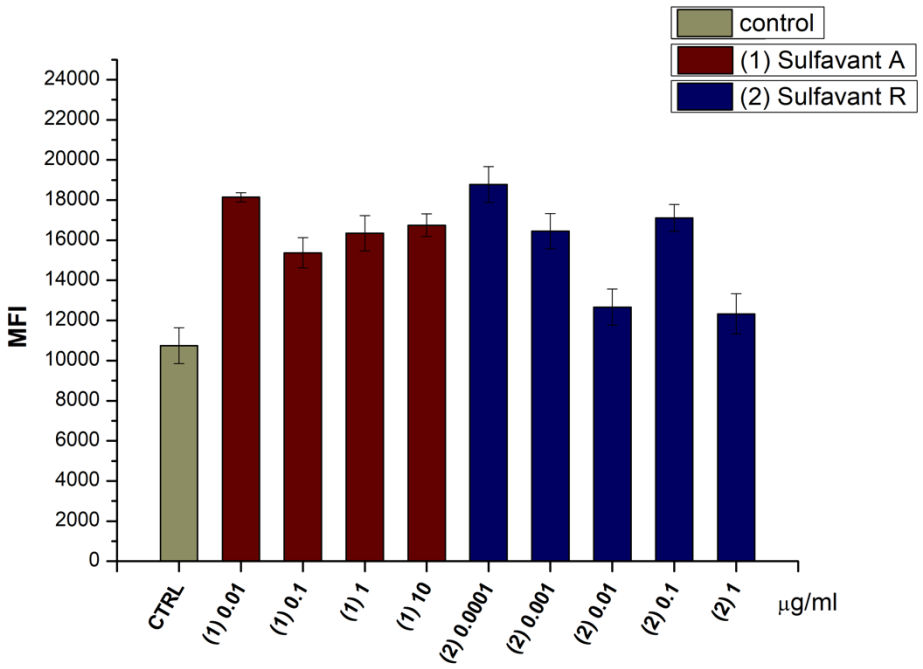

Figure 2.37: Flow cytometric analysis of moDCs stimulated with Sulfavant A and Sulfavant R prepared by sonication at 65ºC, at different concentration; data are expressed as the mean fluorescence intensity (MFI) of the specific antibody.

2.4.7 Conclusions

The chemical-physical characterization of Sulfavants has provided great help for a better understanding of their biological behaviour.

Pronounced differences in the concentration at which Sulfavants expressed their maximum activation, in terms of DCs maturation, were underlined in paragraph 2.3.2. Dynamic Light Scattering was the first technique employed in this work to highlight the tendency of Sulfavants to self-assemble into colloidal particles and to demonstrate that the nature of the aggregation was strictly correlated with the structural features of these molecules; in fact, small structural differences, such as the different configuration of a single chiral centre, have led to different supramolecular organizations.

Despite some difficulties to analyse very low concentrations, some experiments carried out on more concentrated aqueous solution gave interesting results.

At first, these experiments showed that the sulfolipids are able to organize themselves in supramolecular structures in order to avoid the direct interaction between water and their hydrophobic moiety. Moreover, it has been shown that a small variation in their chemical structure led to different colloidal particles with different hydrodynamic radius; in particular, Sulfavant A formed larger particles (about 150 nm) than Sulfavant R and S (about 50 nm).

In addition to these results, comparing the DLS data with the curves obtained from the evaluation of biological assays, the correlation between the immunomodulant activity and the hydrodynamic radius seems to be clear (Figure 2.21), and it could also explain the way the curves decrease with at higher concentration, assuming a bell-shape profile.

The evaluation of CMC by surface tension measurements suggested that all the three Sulfavants started their self-assembling at concentration higher than 10 μM and the aggregates formed by a pure apimer as Sulfavant R were, at this concentration, more stable than the aggregates formed by Sulfavan A; on the other hand, these data did not explain the different behaviour at lower concentrations, at which they showed their immunomodulant activity.

In order to find a way to explore the behaviour of Sulfavants at lower concentrations, the effect of a detergent on the Sulfavant A 5 μM aqueous solution was tested by ^{1}H-NMR and biological assay. The ^{1}H-NMR signals relating to Sulfavant A in D_2O were absent because of the slowing down of the movements of the molecule which changed the relaxation times; comparing the latter spectrum with the ^{1}H-NMR of Sulfavant A mixed with Triton X100 detergent, an improvement of diagnostic signals was displayed, proving that even at concentrations lower than the CMC, calculated by means of surface tension measurements, colloidal particles were present in the solution.

These preliminary data were confirmed by the biological evaluation of Sulfavant A in the presence of a detergent (Kolliphor RH40), with which the maximum bioactivity was showed at lower concentrations than those without Kolliphor RH40, proving that the biological response was influenced by the presence of aggregates also under the CMC estimated by the surface tension.

Further experiments for the evaluation of CMC of Sulfavant A were carried out by means of fluorescence analysis, that highlighted the presence of supramolecular structure already at 2 μM. Evidently, the ability to detect aggregates depended from the sensitivity of the techniques utilized for this purpose.

The most undeniable evidence has been achieved by electron microscopy analysis of Sulfavant A and Sulfavant R 10 nM and 10 μM solutions: in fact, for both Sulfavants, at both concentrations, cryo-TEM images clearly showed the presence of aggregates that differ in size and in nature for the two molecules.

More in detail, at 10 nM concentration Sulfavant R formed micellar aggregates with a diameter around 3-5 nm, while Sulfavant A showed vesicular particles of 40 nm.

Considering that only Sulfavant R was active at a concentration of 10 nM, it is possible to confirm that the ability of these compounds to trigger DCs maturation depends on the occurrence of monomers or very small aggregates (dimers and/or trimers).

As far as higher concentration (10 μM) is concerned, both Sulfavants formed vesicles; Sulfavant R not only undergo to an enhancement of the particles size (30-40 nm), but also to a changing of the shape, and this can explain the decrease of biological activity; on the other hand Sulfavant A still resulted to be as vesicles but with a greater diameter (150-160 nm) and less stable than those of Sulfavant R, and it was possible that at this concentration the equilibrium monomers/aggregates could ensure enough monomers to elicit the DCs maturation.

A final experiment was aimed at evaluating the effect of a different sample preparation on the self-assembling and biological response of this class of molecules. By solubilizing the sample at higher temperatures (65ºC), differently from the standard procedure (35ºC), the cryo-TEM images showed an evident reduction in the particle

size, so much that Sulfavant R was undetectable. By exploring this effect on biological response, the curves of activity of Sulfavants solutions prepared at higher temperature showed a clear shift of the biological activity at lower concentrations, and this was an additional proof that the ability of this molecule to trigger an immune response depended on monomers (or very small aggregates like dimers/trimers).

Albeit all these results have in part explained why the immunomodulatory activity of Sulfavant A, Sulfavant R and Sulfavant S is so different, they do not clearly explain what happens at the molecular level. A reasonable hypothesis is that the colloidal particles of the two diasteropure epimers, having a regular composition, form a more efficient molecular packing than the epimeric mixture, leading to smaller structures.

Future molecular docking experiments could be a great help to confirm this hypothesis and to explore this field.

2.5 Fluorescent analogue of Sulfavant R

As extensively discussed, Sulfavants can be considered as potential candidates as vaccine adjuvants [38, 114] for their efficiency to boost an immune response with the advantage to not produce side effects.

The development of their pharmacological application requires an in depth understanding about the complex biological mechanisms underlying their immunomodulant activity, including interactions with cellular target as well as the biodistribution of these compounds *in vivo* and *in vitro*.

As reported in paragraph 2.3.2, Sulfavant R displayed an interesting immunomodulant activity at very low concentration.

The insertion of a fluorescence probe on Sulfavants can be a powerful tool to acquire more information about their mechanism of action and correlated studies.

With this aim, a fluorescent analogue of Sulfavant R was synthesised in the framework of this thesis.

The fluorescent labelling is largely applied in several field, especially for detailed studies on proteins and nucleic acids, but it is still low developed in association with glycolipids, maybe for their structural complexity and the numerous issues in the labelling of one of their specific functional group [183].

Even if slowly, in the last years, the chemical development of glycolipids coupled with fluorescent probes is advancing [184, 188].

2.5.1. Choice of fluorescent probe

Advances in drug discovery have accelerated the development of increasingly precise therapies aimed at detecting pharmacological targets and the biological consequences of drug / target interaction in *in vitro* and *in vivo* experiments. One of the most powerful techniques to reach these purposes is the molecular bioimaging [189].

In this regard, the choice of an appropriate fluorescent probe to link to the β-SQDGs represents a crucial challenge for the use of this technique on this class of molecules.

Although pyrene and anthracene have been extensively used as probes in bioimaging investigations [190, 191], numerous new compounds have been developed recently and great attention has been paid to 4,4-difluoro-4-bora-3a,4a-diaza-*s*-indacene dye (BODIPY) [192-198] (Figure 2.38)

BODIPY was described by Treibs and Kreuzer in 1968, but only lately its biological application was expanding for its suitable features, like high absorption and fluorescence quantum yield, tight absorption and emission bands, good stability in physiological environment (scarce sensitivity to polarity and pH), good photo- and chemical-stability, high solubility, and resistance to self-aggregation [199-200].

In addition, even though the insertion of a fluorescent moiety in the sulfolipid structure could have effects on its biological properties, BODIPY has been already employed to label sphingolipids in order to study the metabolism and traffic in animal cells [201], without greatly modify its biological features.

BODIPY family is a group of fluorescent molecules composed of a dipyrrin structure with a BF_2 core characterized by sharp fluorescent emissions (λ_{abs}~496 nm/λ_{emiss}~515 nm)

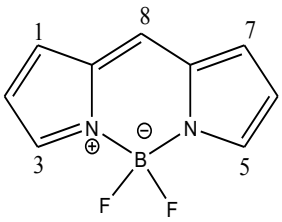

Figure 2.38: BODIPY

In this thesis, the Me_4BODIPY probe has been linked to the glycerol moiety in order to avoid and excessive influence on the chemical-physical properties due to amphiphilic nature of Sulfavant R (Figure 2.39).

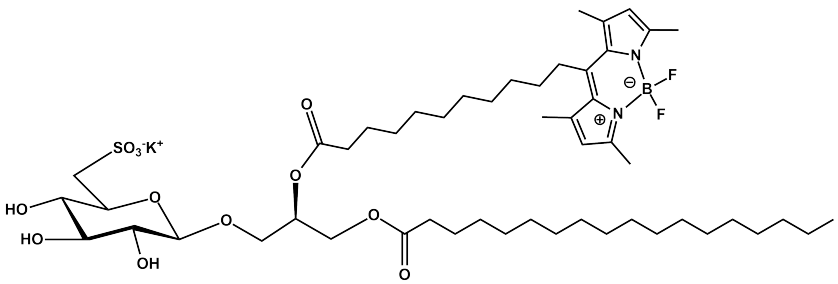

Figure 2.39: Chemical structure of Sulfavant R-Me$_4$BODIPY

2.5.2 Synthesis of Sulfavant R-Me$_4$Bodipy

The synthetic strategy employed to prepare Sulfavant A was enough versatile to allow its application for the preparation of several analogues with different acyl chains, for this reason, the first approach used for the synthesis of Sulfavant R-Me$_4$BODIPY was based on a similar methodology (Scheme 2.1).

Inspired by Boldyrev and Molotkovsky [202], the strategy involved the synthesis of a Me$_4$BODIPY-undecanoic acid (Scheme 2.8) that has been successively introduced on the glycerol moiety.

Because of the Me$_4$BODIPY-undecanoyl instability with respect to the previously planned oxidative conditions (Scheme 2.1 reaction step **o**) [121], it was necessary to find an alternative method to avoid that fluorines were replaced by hydroxyl groups: for this reason, as illustrated in the Scheme 2.9, the oxidative reaction, to give the sulfonic function in position 6', was carried out before the introduction of the fluorescent probe.

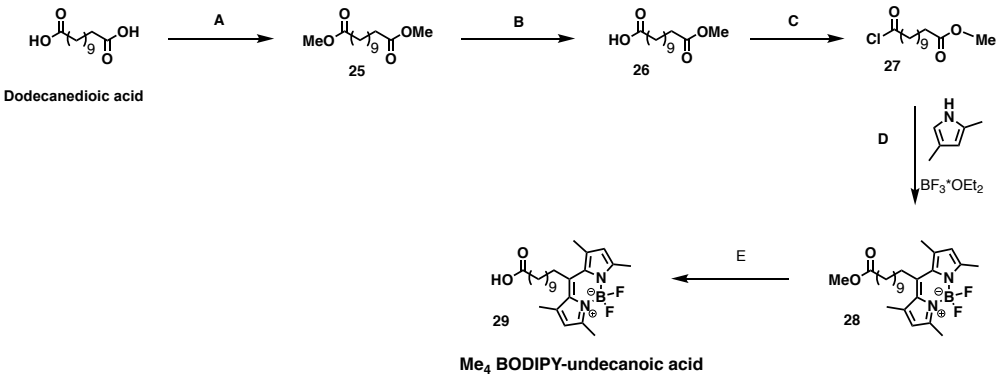

Scheme 2.8: Synthetic procedure employed for the preparation of Me_4BODIPY-undecanoic acid.

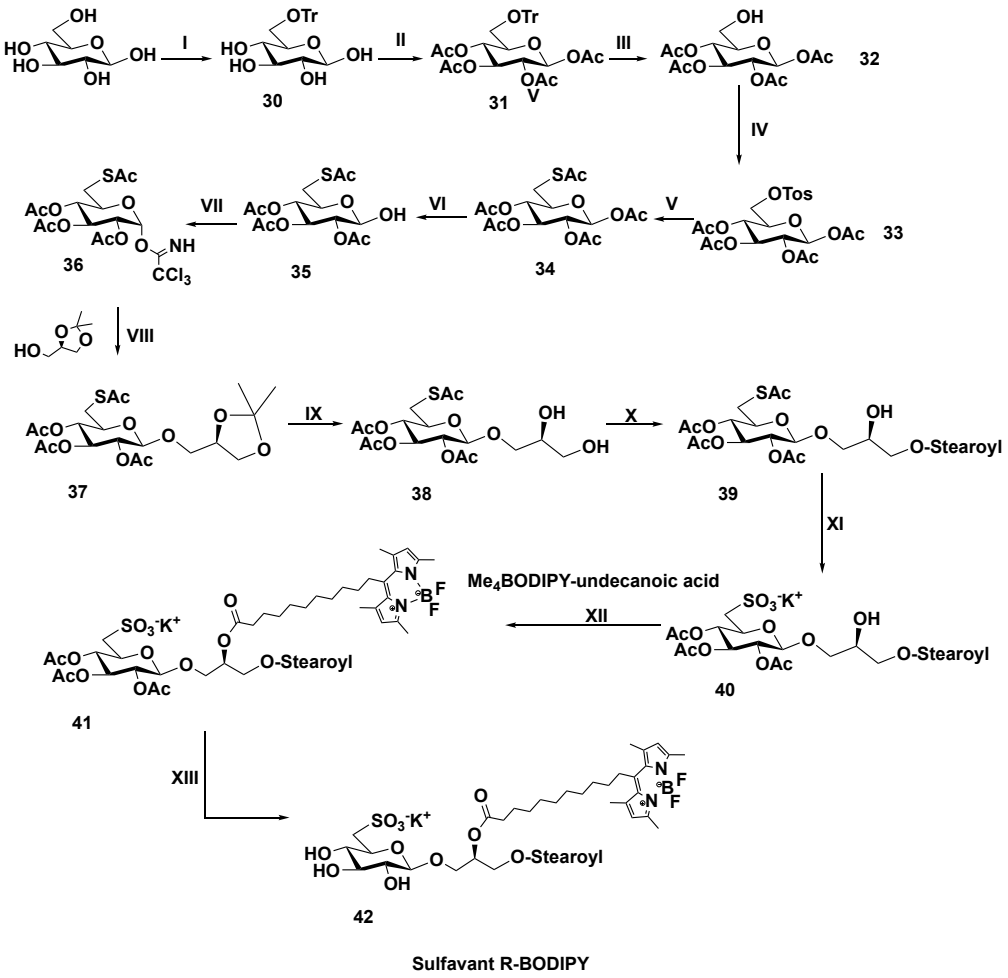

Scheme 2.9: Synthetic strategy for the preparation of Sulfavant R- Me4BODIPY
(all experimental conditions are reported in Chap. 4)

The introduction of the sulfonate group was achieved by tritylation followed by detritylation of the hydroxyl group in position 6' and the β configuration was obtained stereoselectively taking advantage of the neighbouring group participation of the acetate using the trichloroacetamidate as leaving group. In order to prepare the Sulfavant R fluorescent analogue, the coupling reaction was performed using the (*R*)-1,2-*O*-isopropylidene glycerol as acceptor.

The synthesis started with the tritylation and acetylation of D-glucose (**I-II**), followed by selective detritylation (**III**) and subsequent tosylation at carbon 6'(**IV**). The introduction of a thioacetate group by potassium thioacetate (**V**) has been carried out just before the selective deacetylation at the anomeric position (**VI**) in order to proceed with the derivatization with trichloroacetimidate (**VII**), used as leaving group in the reaction of glycosylation with (*R*)-1,2-*O*-isopropylidene glycerol acceptor (**VIII**) performed by Schmidt methodology [122, 123].

The use of soft acid conditions (acidic resin DOWEX-H^+ in methanol/water) allowed to hydrolyse the isopropylidene residue (**IX**), preserving the glycosidic linkage.

In this case, a crucial step was the introduction of two different acyl chains on the glycerol moiety. For this purpose, the *N,N*-dicyclohexylcarbodiimide (DCC)-mediated condensation was made in different conditions comparing with the previous case (Scheme 2.1 reaction step **f**): the condensation with two or one equivalents of free fatty acids yielded gave di- or mono-acyl derivatives respectively.

Equimolar amounts of reagents at 4°C gave only esterification at carbon-1 of the glycerol, as indicated by the reported NMR spectra (Figure 2.40). In this way, the procedure allowed step-wise introduction of different acyl residues at C-1 and C-2 of glycerol, thus permitting to control fatty acid regiospecificity of the synthetic glycolipid [121].

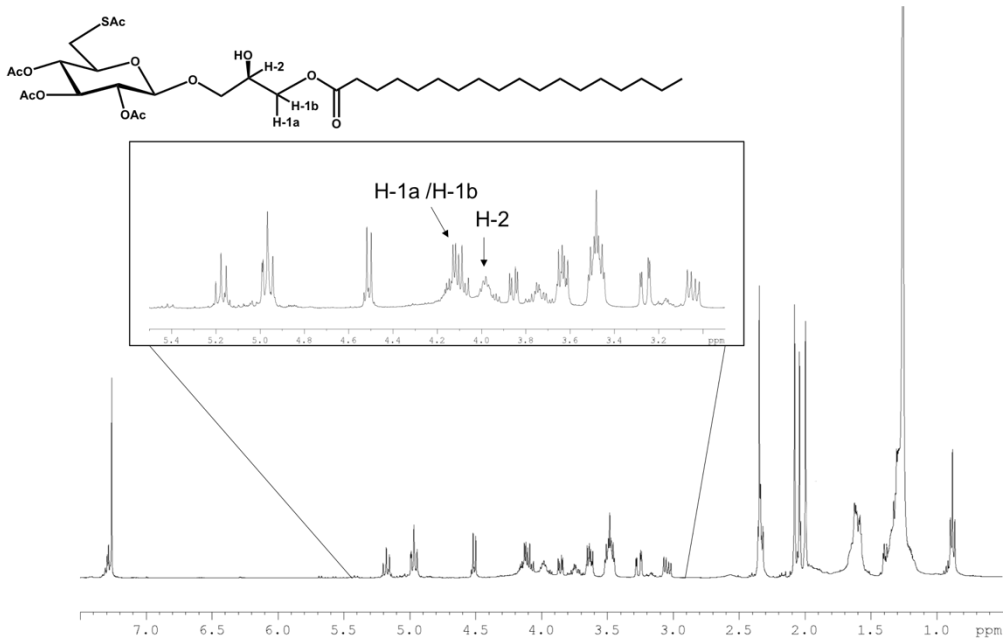

Figure 2.40: Section of the ^{1}H NMR spectrum of compound **39**

Before the introduction of Me_4BODIPY-acyl moiety, for the reasons above discussed, the oxidation reaction by hydrogen peroxide was performed.

The acylation of the secondary hydroxyl group on glyceridic part with Me_4BODIPY-8-undecanoic acid (**XII**) and the final deacetylation of the sugar (**XIII**) lead to the fluorescent Sulfavant R-Me_4BODIPY adduct (**42**).

This strategy is particularly versatile and opens the way for the preparation of other fluorescent BODIPY β-sulfoquinovosylacylglycerol analogs with different acyl chains and/or different configuration at carbon 2 of glycerol.

2.5.3 Evaluation of the biological activity of Sulfavant R-Me$_4$BODIPY

Sulfavant A, R and S were able to trigger the maturation of moDCs in vitro throughout the up-regulation of phenotypic markers involved in T cells priming [203], like CD86 and CD83, and the gene expression of some cytokines (IL-12p40, IFNγ) in the range of concentration 10 nM-10 μM.

The introduction of the BODIPY probe into the bioactive Sulfavant R could produce some alteration of the biological response, therefore the immunomodulant effect of Sulfavat R-Me$_4$BODIPY on DC maturation was evaluated.

As showed in Figure 2.41a, Sulfavant R-Me$_4$BODIPY determined the up-regulation of the phenotypic markers CD83 and CD86 and, moreover, it induced the gene expression of proinflammatory cytokines like IL-12 and INFγ (Figure 2.41b). The stimulation was quite linear with the increment of the compound concentration and as well as Sulfavants, Sulfavant R-Me$_4$BODIPY had no effect on IL-10 expression (anti-inflammatory cytokine).

Considering these results, the ability of Sulfavant R-Me$_4$BODIPY to activate the DCs maturation was comparable with the one of Sulfavant R, highlighting a preservation of the biological activity even after introduction of the BODIPY group.

In preliminary studies, confocal microscopy image (Figure 2.41c) showed the ability of the fluorescent molecule to move across the membrane; in fact, the compound was spread in all the cell, even if, marking the nuclei with DAPI (4',6-diamidin-2-fenilindolo), it was possible to exclude localization of Sulfavant R-Me$_4$BODIPY in the nucleus.

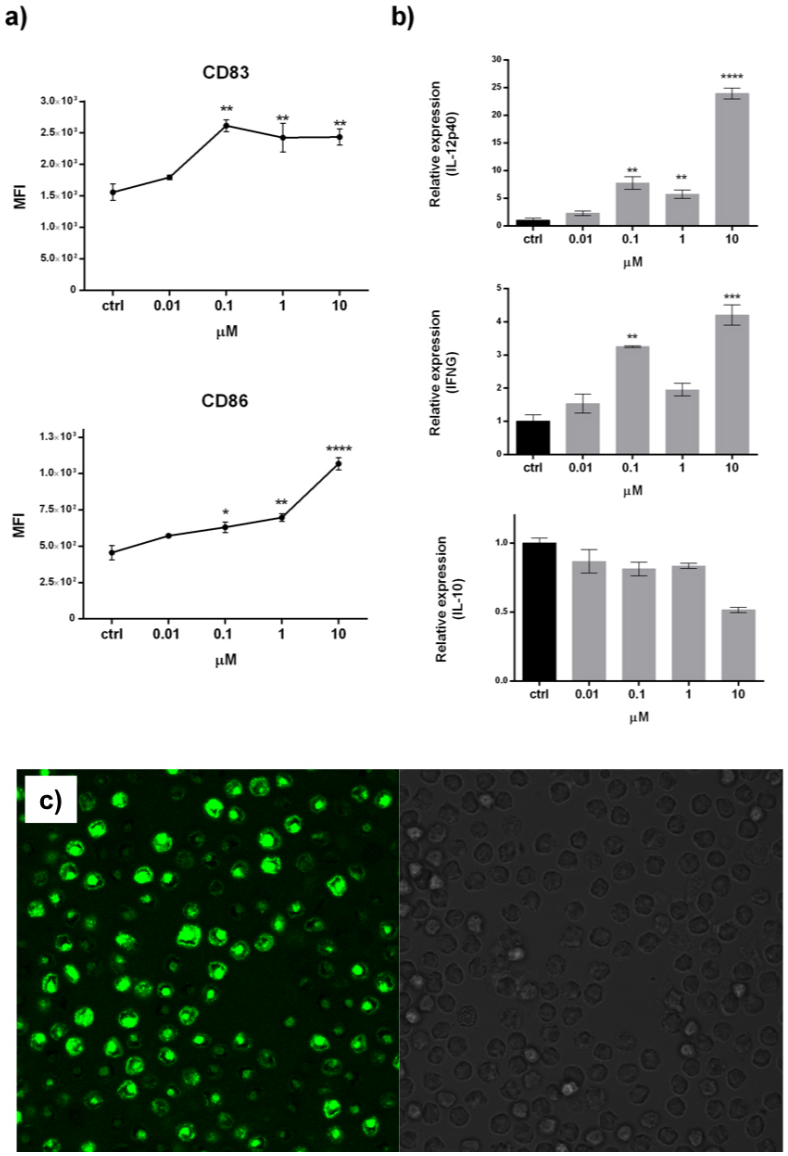

Figure 2.41 a) Flow cytometric analysis of moDCs: moDCs were stimulated with fluorescent molecule in the range of concentration 0.01-10 µM b) Relative cytokine gene expression c) Confocal microscopy image of Sulfavant R-Me$_4$BODIPY in cell culture

2.5.4 Conclusions

A molecular-level understanding of the processes by which Sulfavants show their ability to induce an immune response, is a crucial factor for the development of this new class of molecular adjuvants.

Molecular imaging offers a powerful approach to investigate on the interaction between drugs and their cellular targets and to monitor at the same time the biodistribution and the metabolism of drugs *in vitro* and *in vivo*.

The preparation of fluorescent analogues of Sulfavants is an advantageous tool for further investigation on their biological behaviour.

In this paragraph is reported the diastereoselective and versatile synthetic strategy employed for the synthesis of the adduct Sulfavant R-Me_4BODIPY, involving glycosylation of trichloroacetimidate-sugar donor and (*R*)-1,2-*O*-isopropylidene glycerol acceptor, with subsequent introduction of stearic acid on primary hydroxyl group on glycerol moiety. After the oxidation step to achieve the sulfonic function on carbon 6', the Me_4BODIPY undecanoyl moiety, previously prepared, has been linked to secondary hydroxyl group on glycerol moiety.

This strategy can be applied to other sulfolipids and in particular the other Sulfavants, opening the opportunity to prepare a wide range of fluorescent derivatives, essential for the comprehension of the complex biological mechanisms of Sulfavants.

Preliminary biological assays of Sulfavant R-Me_4BODIPY showed the capability of this compound to elicit the moDcs maturation in comparable manner to that of Sulfavants, stimulating up-regulation of the surface markers CD83 and CD86, costimulatory molecules involved in T cells priming, and showing also an effect on the gene expression of IL12p40 and IFNγ, demonstrating the maintenance of the immunomodulatory effect of the fluorescent compound.

2.6 Synthesis of 1-*O*-alkyl-2-*O*-(2'-*O*-β-D-glucopyranosyl-β-D-xylopyranosyl)-glycerol.

As introduced in the first chapter, this work involved an internship at University of British Columbia (UBC) in Vancouver (Canada), at laboratories of Professor Raymond Andersen. Andersen and co-workers isolated a natural mixture from a Canadian sponge (species to classify), containing high percentage of a glycolipid, 1-*O*-alkyl-2-*O*-(2'-*O*-β-D-glucopyranosyl-β-D-xylopyranosyl)-glycerol (Figure 2.42), whose preliminary bioactivity evaluation showed an interesting pharmacological potential.

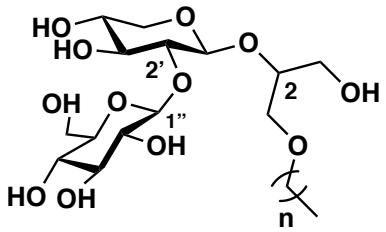

Figure 2.42: 1-*O*-alkyl-2-*O*-(2'-*O*-β-D-glucopyranosyl-β-D-xylopyranosyl)-glycerol

As well known, in depth studies on the biological activity of a component of a natural mixture are a complicated step considering the difficulties to obtain a single and pure molecule to examine. Frequently these studies require to be supported by the chemical synthesis that allow the preparation of the molecule of interest. Therefore, in order to investigate on the molecule found out by Andersen and co-workers, during the internship at UBC, a synthetic strategy for the preparation of this molecule has been designed.

More details about the biological activity of this molecule and the nature of the alkyl chains are forbidden because of patent pending by Professor Andersen and co-workers, therefore in this paragraph will be discussed only the synthetic aspects of this thematic.

The main challenges in the development of a synthetic strategy for the preparation of 1-*O*-alkyl-2-*O*-(2'-*O*-β-D-glucopyranosyl-β-D-xylopyranosyl)-glycerol (Figure 2.42), were in the requirement of a chemical approach comprising of the β-glycosidic bond with glycerol moiety and the β interglycosidic linkage in position 2'→1'' between xylose and glucose.

The synthetic approach designed was based on the synthesis of three main synthons (Scheme 2.10), with subsequent formation of the interglycosidic linkage, thus, activation of the disaccharide moiety and coupling reaction with the glyceridic moiety.

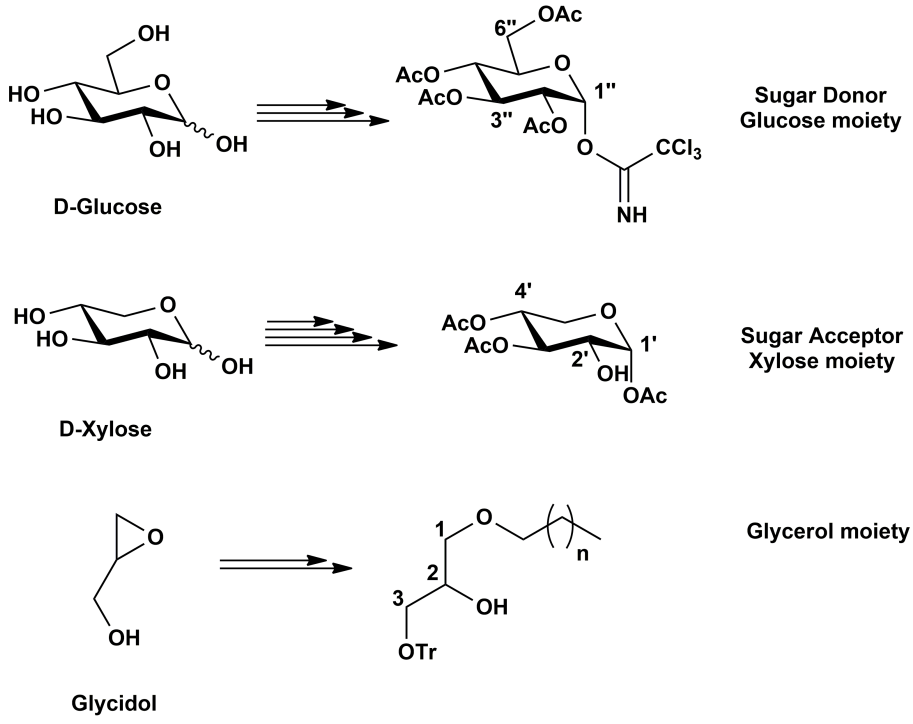

Scheme 2.10: Main synthones involved in the 1-O-alkyl-2-O(2'-O-β-D-glucopyranosyl-β-D-xylopyranosyl)-glycerol synthesis

Sugar donor synthesis (Scheme 2.11) started with the acetylation of D-glucose, followed by selective deacetylation at the anomeric position with benzylamine and derivatization with trichloroacetimidate.

The use of acetate as protecting groups and trichloroacetimidate as leaving group has been already employed in the synthesis of Sulfavants.

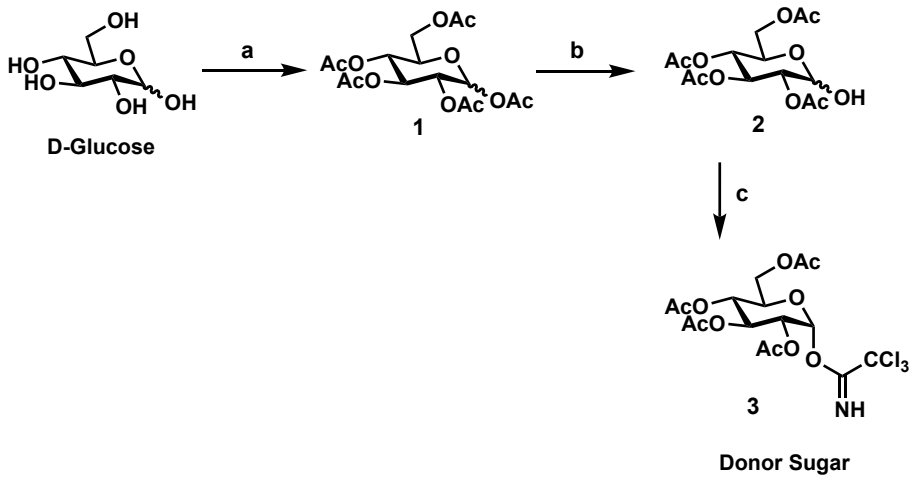

Scheme 2.11: Glycosyl donor preparation
(all experimental conditions are reported in Chap. 4)

The acceptor sugar had to be characterized by only one free hydroxyl group in position 2'. In order to obtain this synthon, the strategy (Scheme 2.12) involved a first acetylation of D-xylose with subsequent bromination at anomeric position. The bromide intermediate (**44**) was particularly unstable, and it was necessary to proceed very quickly with the following formation of the methyl orthoester (**45**).

The reaction of peracetylated xylopyranosyl bromide (**44**) with methanol, tetrabutylammonium bromide and sodium bicarbonate in dry acetonitrile solvent gave the 1,2 orthoester derivative (**45**) subsequently opened by hydrolysis with acetic acid/water 95/5 to give a free hydroxyl group in position 2' as required.

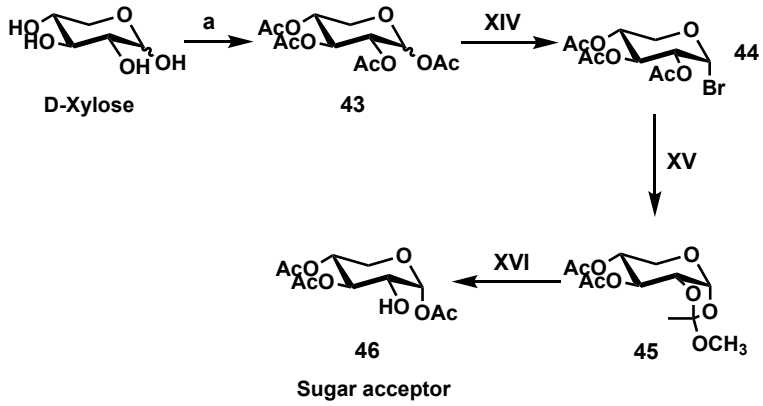

Scheme 2.12: Glycosyl acceptor formation
(all experimental conditions are reported in Chap. 4)

The final synthon to be synthesised was the glycerol acceptor (Scheme 2.13): the commercially available glycidol was tritylated with trityl chloride in presence of *N,N*-dimethylaminopyridine and trimethylamine; the subsequent opening of the epoxide under basic conditions allowed the introduction of the fatty alcohol to the less substituted position [204].

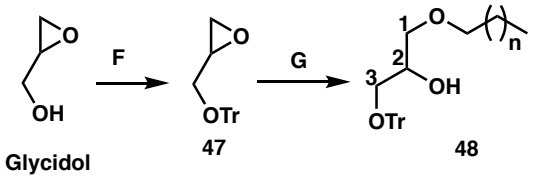

Scheme 2.13: Glycerol moiety formation
(all experimental conditions are reported in Chap. 4)

Thereafter, the coupling reaction (Scheme 2.14), between the two sugar derivatives, has been carried out by Schmidt methodology [122, 123] with a good yield.

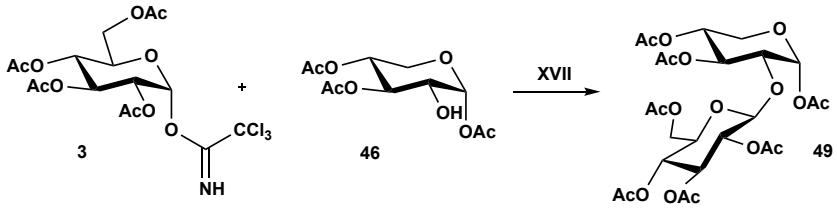

Scheme 2.14: Coupling reaction between sugar donor and acceptor
(all experimental conditions are reported in Chap. 4)

Once the disaccharide was synthetized, the designed synthetic strategy (Scheme 2.15) involved the deprotection of the anomeric position of the xylose in order to proceed with the formation of the second glycosyl acceptor to link to the glycerol moiety. Unfortunately, the hydroxyl deprotection in basic condition did not work as expected even though it was carried out with different reaction conditions (Scheme 2.15, step XVIII), in fact, as alternative to the deprotection by benzylamine in tetrahydrofuran, this reaction was carried out using dimethylamine in tetrahydrofuran and diethylamine in acetonitrile and for each reaction different temperatures, time and amounts of reagents were employed, without any improvement of the outcome.

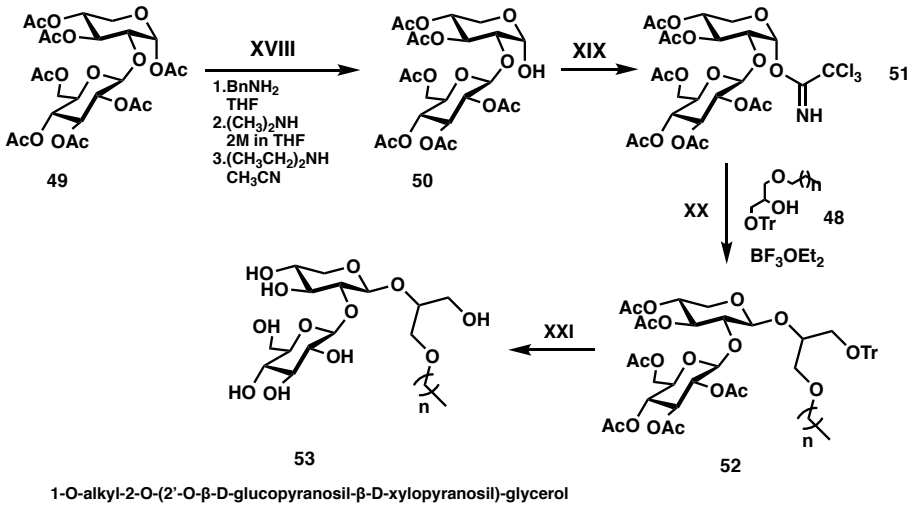

Scheme 2.15: Chemical strategy planned for synthesis of 1-*O*-alkyl-2-*O*-(2'-*O*-β-D-glucopyranosyl-β-D-xylopyranosyl)-glycerol.

Considering this setback, other synthetic strategies have been searched for the achievement of 1-O-alkyl-2-O-(2'-O-β-D-glucopyranosyl-β-D-xylopyranosyl)-glycerol, one of them involved the introduction of different protecting groups (acetonide) on the xylose moiety in the synthesis of the sugar acceptor synthon (Scheme 2.12), but also in this case, the unusual xylose instability lead to several by-products that obstructed the continuation of the total synthesis.

The last designed strategy involved a direct bromination of the position 1' after the formation of the disaccharide in order to proceed with the coupling reaction with the glycerol moiety following the Koening and Knorr reaction [206, 207] (Scheme 2.16). This attempt will be accomplished within a successive collaboration with Professor Andersen.

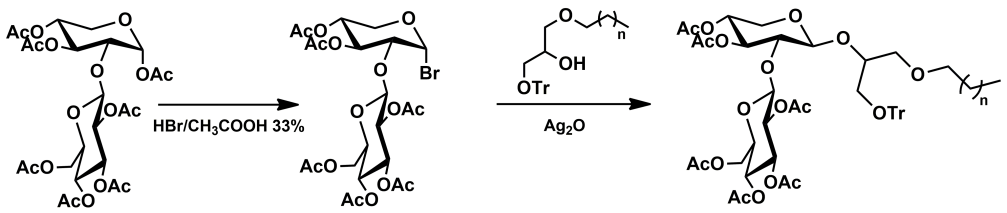

Scheme 2.16: Improvement of the synthetic strategy designed for the synthesis of 1-*O*-alkyl-2-*O*-(2'-*O*-β-D-glucopyranosyl-β-D-xylopyranosyl)-glycerol.

2.6.1 Conclusions

The synthetic strategy for the preparation of the bioactive 1-*O*-alkyl-2-*O*-(2'-*O*-β-D-glucopyranosyl-β-D-xylopyranosyl)-glycerol was designed partially concluded.

The choice of acetate group on the glucose donor synthon, with the introduction of the trichloroacetimidate as leaving group, as well as described by Schmidt [122], allowed to achieve a good β stereoselectivity in the formation of the interglycosidic bond (**49**).

Due to the xylose bromide (**44**) intermediate instability, the synthesis of the sugar acceptor did not show high yield, but the insertion of bromine was necessary for the subsequent formation of the orthoester (**45**) that allowed to free the only position 2' on the xylose moiety (**46**) [208].

At the same time, the glycerol moiety was prepared starting from the commercial glycidol and after tritylation, the opening of the epoxide under basic conditions, in presence of the desired alcohol, lead to the third synthon with the alkyl chain linked to the less substituted position of the trityl glycerol (**48**).

Despite several different experimental conditions used to deprotect the anomeric position of the disaccharide in order to proceed with the coupling reaction with the glycerol moiety, no method worked.

Successively an alternative strategy has been planned, involving the use of acetonide as protecting group for the xylose, but due to the xylose particular chemistry [207], this method was not efficient, leading to the formation of a lot of by-products.

For a future development of this synthesis, an alternative way to achieve the 1-*O*-alkyl-2-*O*-(2'-*O*-β-D-glucopyranosyl-β-D-xylopyranosyl)-glycerol was designed, including the direct bromination of the disaccharide in order to prepare the donor for the Koening and Knorr glycosylation [205, 206]. This new strategy will be carried out within further collaboration with Professor Andersen.

2.7 Modification of the Sulfavants synthetic strategy for the preparation of pure Sulfavant S

As discussed in the paragraph 2.3.1, the two diasteropure compounds, Sulfavant R and Sulfavant S, were achieved by the same improved synthetic strategy employed for the preparation of Sulfavant A (Scheme 2.6); this was possible carrying out the coupling reaction between the sugar trichloroacetimidate derivative and the (*R*) or (*S*) 1,2-*O*-isopropylidene glycerol enantiomer, respectively (Scheme 2.7).

An unresolved aspect of this strategy was the partial epimerization that occurred throughout the preparation of Sulfavant S due to a diasteroselective opening and closing of the acetonide during the glycosylation step: the synthetic Sulfavant S included about 20% of Sulfavant R.

In order to avoid this issue, an alternative synthetic strategy was planned for the preparation of 100% pure Sulfavant S. With this aim and to avoid the acetonide opening and closing side reaction, the (*S*)-1,2-*O*-distearoyl glycerol, new acceptor in the coupling step with sugar, has been prepared (Scheme 2.17).

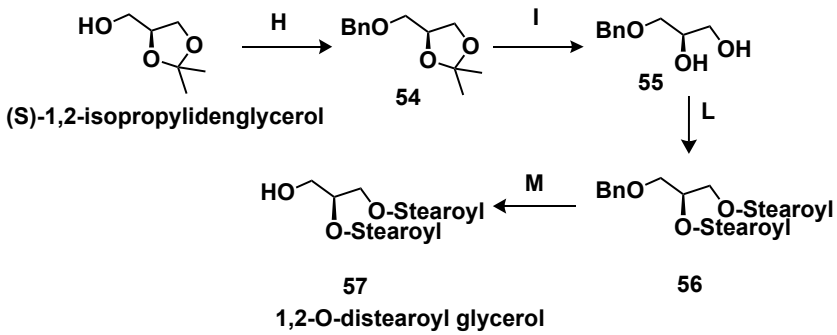

(S)-1,2-isopropylidenglycerol

54

55

57

1,2-O-distearoyl glycerol

56

Scheme 2.17: Synthetic method used to prepare the new acceptor (*S*)-1,2-*O*-distearoyl glycerol
(all experimental conditions are reported in Chap. 4)

Thereafter, (*S*)-1,2-*O*-distearoyl glycerol acceptor (**57**) was directly coupled with the trichloroacetimidate derivative (**3**) and the synthetic strategy proceeded in the same way previously discussed (Scheme 2.18).

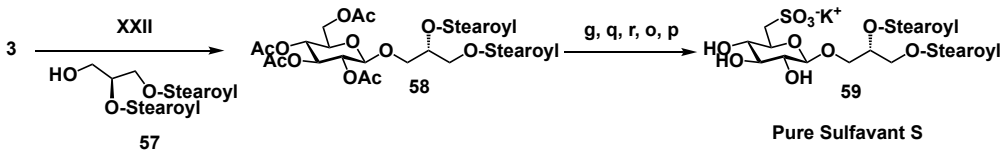

Scheme 2.18: Synthesis of pure Sulfavant S
(all experimental conditions are reported in Chap. 4)

2.7.1 Conclusions

Sulfavant S, as well Sulfavant R, is a diasteropure analogue of Sulfavant A, the prototype of this new class of molecular adjuvants.

As widely discussed in this work, in order to investigate the interesting biological activity of these sulfolipids, the synthesis of different structural analogues was mandatory. Despite the improvement of the synthetic strategy shown above, Sulfavant S was subject to a partial epimerization during the coupling reaction between the sugar donor and (*S*)-1,2-*O*-ispropylidene glycerol acceptor, avoiding the possibility to get a pure Sulfavant S epimer.

Since the important results obtained by the biological evaluation of the diasteropure compounds, it was crucial to synthetize the pure Sulfavant S.

This aim was achieved by a little modification of the synthetic strategy, involving the preparation of (*S*)-1,2-*O*-distearoyl glycerol (**57**) as acceptor for the glycosylation reaction.

The biological activity of the pure Sulfavant S will be evaluated for further investigation, even if, from preliminary biological data of not pure Sulfavant S and considering in the same time the close structural similarity with Sulfavant R, it's plausible that its biological behaviour will not deviate much from that of Sulfavant R.

2.8 Scale-up of the synthesis of Sulfavant A

Sulfavants are promising molecular adjuvants considering their efficient capability to stimulate DCs maturation combined with the absence of side effects [38].

Further biological investigation on this class of molecule represent a crucial point for their pharmacological development and the improvement of the synthetic strategy, in order to produce higher amount of product, is a mandatory requirement for future clinical developments.

Despite the previous synthesis of Sulfavants (discussed in paragraph 2.3) was characterized by clean and efficient steps, some modifications had to be implemented to obtain a more simple, efficient and scalable synthetic strategy applicable on grams scale.

2.8.1 Scalable synthetic strategy for Sulfavants

In a brief description of the standard synthetic procedure (paragraph 2.3), Sulfavant A was prepared from an acetylation of D-glucose, followed by selective deacetylation of the anomeric hydroxyl group with benzylamine; coupling with 1,2-*O*-isopropylidene glycerol by trichloroacetimidate methodology gave 3-*O*-(2',3',4',6'-tetracetyl)-β-D-glucosyl-glycerol that was acylated with stearic acid to obtain the intermediate 1,2-distearoyl-3-*O*-β-D-glucosyl glycerol after selective deacetylation by hydrazine; subsequent iodination, thioacetylation and oxidation gave finally the Sulfavant A after a further hydrazinolysis.

Apparently, the above-mentioned strategy looked ready to a large amount production of the Sulfavants, but some difficulties were encountered during the transition to gram scale. The main complication, indeed, concerned the employing of hydrazine for both two selective deacetylation steps. In detail, the use of a greater amount of hydrazine in the scaling up, caused several difficulties for the corresponding hydrazinolysis products purification (both 1,2-distearoyl-3-*O*- β -D-glucosyl and Sulfavant A); these complications were overcome performing at least three subsequent silica gel

chromatography aimed to remove the hydrazine excess. Nevertheless, a decreasing in the total yield to about 5.6% (half of that expected on analytical basis) was determined and not totally pure Sulfavant A was achieved (traces of hydrazine were still present). In order to make the preparation of Sulfavants scalable, avoiding the decrease in the total yield, each step was reviewed and ameliorated with profound changes involving the hydrazinolysis steps, main responsible for the limited applicability to the large scale.

In particular, the improved procedure showed (Scheme 2.19) common steps to the previous strategy but with fundamental changes regarding the reaction conditions and the work-up procedures. Concerning the first four steps, leading to 1,2-isopropylidene-3-*O*-(2',3',4',6'-tetracetyl)-β-D-glucose, were ameliorated with a great improvement about the yield for the anomeric deacetylation (from 79% to 96%) thanks to the use of 0.3 more equivalents of benzylamine and longer reaction time (40 hours).

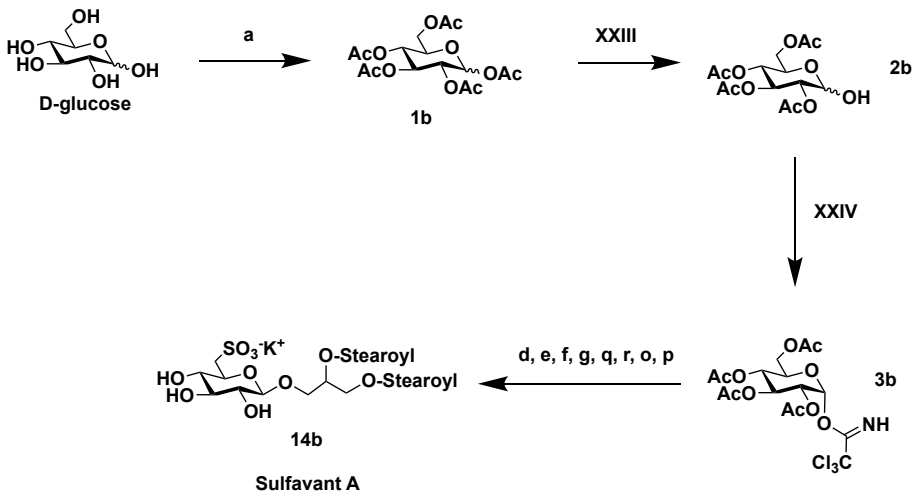

Scheme 2.19: Scale-up procedure for the preparation of Sulfavant A on large scale.
(all experimental conditions are reported in Chap. 4)

Moreover, the trichloroacetimidate preparation, performed under strictly anhydrous conditions allowed an increased yield (from 81% to 91%) in addition to the lower cost due to the remarkable reduction of the tricloroacetonitrile reagent (from 10 to 3 equivalents).

Moreover, an important improvement of this strategy was correlated with the final hydrazinolysis step, where, before the purification by silica gel, the hydrazine excess was removed by centrifuge extraction through cold water precipitation of Sulfavant A, avoiding any further hydrazine contamination,

2.8.2 Conclusions

Sulfavant A is the prototype of a new class of molecular adjuvants based on a sulfoquinovoside-glycerol skeleton, and its potential pharmacological applications as future commercial adjuvant need to be supported by further clinical studies. As commonly known, one of the main goals for the clinical development of new drug candidates is the advancement in the chemical synthesis aimed to a large-scale preparation.

In order to move towards this purpose, starting from the previous synthetic strategy, an improved and scalable synthetic process was developed; this improved approach, made the procedure simpler, efficient and workable, ensuring the purity of final products even on a large scale.

Employing exactly the same strategy developed for analytical preparation the overall yield was negatively affected by the raised quantity of reagents used that involved the formation of several by-products and impurities difficult to remove by simple purification practice. With some experimental adjustments regarding the used equivalents of reactants and reaction times in some reactions, it was possible to raise the yield of some steps. Moreover, the most relevant modifications were realized on the final step of purification: since the excess of monohydrate hydrazine used in the last step of the synthesis brought to several correlated by-products, the simple silica gel purification was not enough to lead to a purified compound; improving this step

by centrifuge extraction through cold water precipitation of Sulfavant A, it was possible to remove the hydrazine excess, making the purification on silica gel easier and more performant.

Chapter 3: Conclusions and Future Perspectives

This PhD thesis was aimed on the identification of new bioactive species, with particular attention on the immunomodulant properties of natural glycoglycerolipid analogues.

In the laboratory where this thesis was carried out, starting from natural substances and considering the positive results obtained by fractions of different diatom species containing glycolipids, the species *Talassiosira weissiflogii* was one of the main objects of study.

In particular, a mixture including high level of *α*-sulfoquinovosyl diacylglycerols (α-SQDGs), showed promising immunomodulant activity.

This PhD project was based on the chemical preparation of SQDGs analogues and the investigation of the structure/activity relationship of these compounds.

Considering the chemical structure of natural α-SQDGs (Figure 3.1), the new synthetic analogues presented the peculiar sulfonic group in position 6' of the sugar and the β configuration at the anomeric position, inspired by the anomeric configuration of known immunogenic bacterial glycolipids.

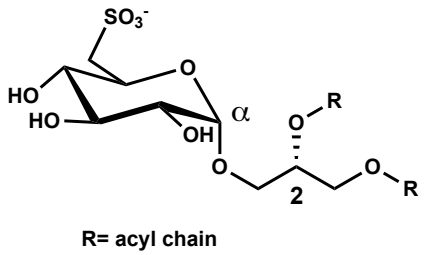

Figure 3.1: Generic chemical structure of natural α-SQDGs

As far as the glycerol portion was concerned, during this thesis several sulfolipids were prepared differing from each other in the length of the acyl chains linked to the glycerol and in the configuration of the carbon in position 2.

In detail, the effect of different acyl chains was explored with the synthesis of β-SQDG16, β-SQDG18 β-SQDG19 (Figure 3.2) and for each one the epimeric mixture at carbon 2 and the respective diasteropure analogues were prepared.

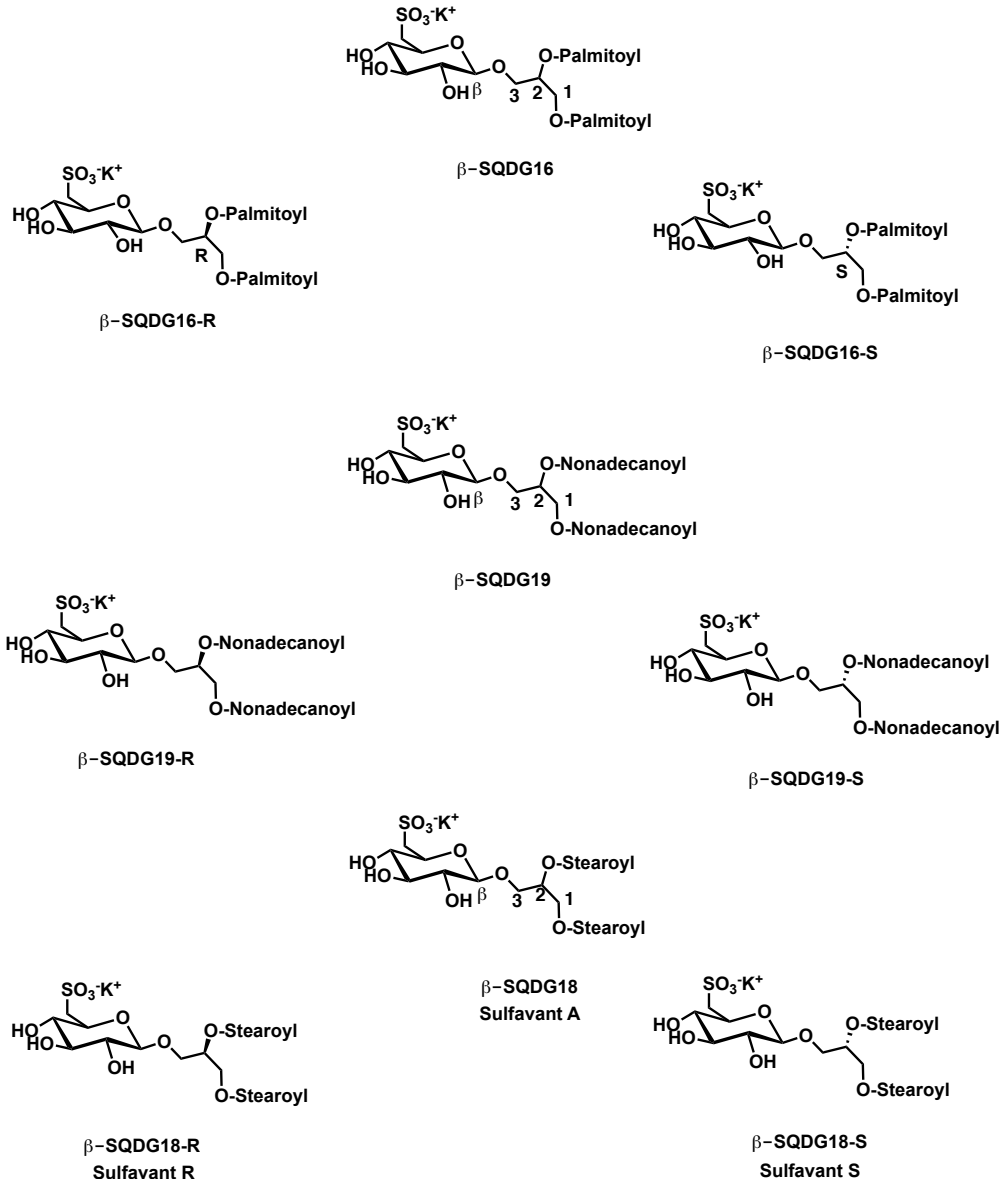

Figure 3.2: Chemical structure of the sulfoquinovosyldiacylglycerols synthesised in this PhD thesis.

The synthetic strategy for the chemical preparation of β-SQDGs was planned and successively optimized during this thesis. Finally, an efficient and versatile strategy,

relevant for the synthesis of several glycoglycerolipids, was achieved, both with same and different acyl chains linked to the glycerol moiety.

The immunomodulant activity of each compound was tested for the evaluation of their ability to stimulate DCs maturation. DCs are fully involved in the immune response and they represent sentinel able to activate naïve T cells. Their process of maturation, once activated, was followed by the analysis of the levels of expression of some surface phenotypic markers as well as of some proinflammatory cytokines.

Within the synthetic compounds, only those featured by stearoyl chains (Sulfavant A, Sulfavant S, Sulfavant R) showed a promising immunomodulant activity.

In fact, Sulfavant A was the first molecule investigated in this doctoral thesis, and since the good biological response obtained, further investigation on its immunomodulant activity were carried out. Comparing its chemical structure with that of other immunogenic bacterial glycolipids (e.g. LPS) it was possible they could act in the same manner (through interaction with TLRs); therefore, Sulfavant A was tested in a cell-based assay with HEK293 stably co-transfected to express full-length human TLR-2 or TLR-4. These bioassays highlighted, for Sulfavant A, a TLRs-independent mechanism of action, differently from some common adjuvants, and the next step was to evaluate the adjuvant activity in immunization assays *in vivo*.

A first experiment was carried out using OVA as antigen and comparing the results with TM and CFA. It was demonstrated that Sulfavant A owned the ability to stimulate the same type and the same level of Igs stimulated by the two commercial adjuvants.

Moreover, a second experiment of immunization involved the evaluation of the effect of Sulfavant A in a model of cancer vaccine against a murine B16F10 melanoma cell line using $hgp100_{25–33}$ as melanoma antigen. The results underlined the efficient adjuvant effect of Sulfavant A that induced a delay and a reduction of the tumour growth overall.

Looking at all the results as a whole, it is possible to define Sulfavant A as a prototype of a new class of molecular adjuvants and it is worth proceeding with further investigation on the mechanisms underlying its bioactivity.

It was exactly for this reason that this PhD thesis involved the synthesis of several β-SQDGs analogues, and a very interesting bioactivity was found out for Sulfavant R and Sulfavant S.

In detail, biological assays showed an enhancement of the immunomodulatory activity of the diasteropure compounds. Sulfavant S and Sulfavant R triggered maturation of the innate immune DCs at concentration one thousand-fold lower than the activity concentration of Sulfavant A, showing the peculiar bell-shaped dose-response curve as well as the epimeric mixture (Figure 3.3).

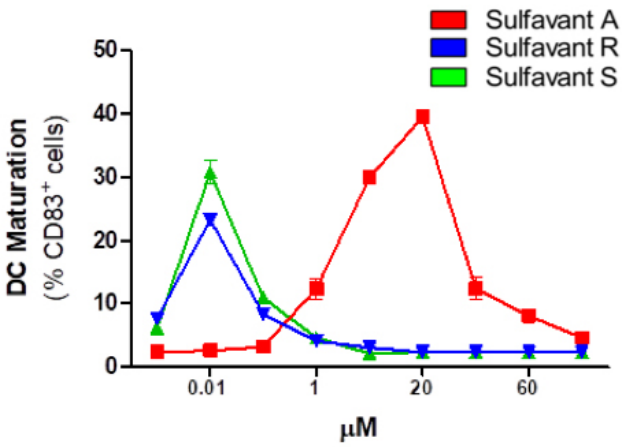

Figure 3.3: Percentage of $CD83^+$ cells stimulated by Sulfavant A (red line), Sulfavant R (blue line) and Sulfavant S (green line)

Therefore, part of this PhD thesis was focused on the explanation of the different activity concentration of Sulfavants and the characteristic shape of their bioactivity curves.

Considering the amphiphilic nature of these sulfolipids, it was possible that they arranged themselves in aqueous solution in supramolecular aggregates in order to avoid the direct contact between the polar solvent and the hydrophobic tails.

The possible self-assembling will provoke a changing of the bioavailability of monomers (or small oligomers such as dimers or trimers), that can freely diffuse and interact with cell targets, affecting the biological response. This hypothesis and the structural slight differences of Sulfavant A, R and S let think that these molecules can self-assemble in water forming different colloidal particles.

Using several techniques, analysis of the chemo-physical properties of Sulfavants in water was performed.

In detail, by means of DLS, the first evidence that these sulfolipids aggregated in water was achieved and the evaluation of the hydrodynamic radius suggested the formation of aggregates differing in size; in fact, the pure epimers formed colloidal particles smaller than Sulfavant A.

Since this study aimed to obtain information on the possible aggregation of Sulfavants at the concentration at which they showed their maximum activity, during this work many difficulties were faced in the study of very low concentrations.

Throughout the CMC evaluation of these molecules by means of surface tension measurements and fluorescence spectroscopy, not only the differences between the epimeric mixture and its diasteropure analogues were confirmed, but the results also suggested that among the monomers (or dimers/trimers) and the 'large final aggregate' there were several equilibria between different types of aggregates (from the smallest to the largest).

Final evidences and great support for the correlation between self-assembling and bioactivity of Sulfavants have been achieved by electron microscopy analysis at 10 nM and 10 μM concentration.

Confirming the first hypothesis, it seems that at 10 nM Sulfavant R formed micelles in rapid equilibrium with monomers (or dimers/trimers) allowing easier interaction with the cell target, while Sulfavant A aggregated as vesicles with a slower

equilibrium with monomers (or dimers/trimers), making DCs activation more complicated.

On the other hand, at 10 µM both Sulfavants (A and R) appeared as vesicles, but Sulfavant A formed less cohesive aggregates supporting a sufficient bioavailability of monomers (or dimers/trimers) in order to promote DCs maturation (Figure 3.4).

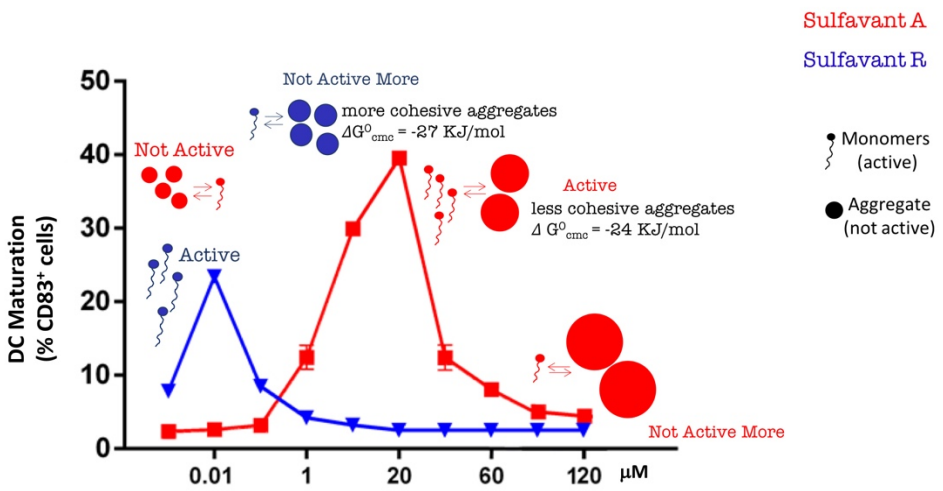

Figure 3.4: Correlation between Sulfavnt A (red line) and Sulfavant R (blue line) self-assembling and their biological activity

The demonstration that self-assembling negatively influenced the biological activity of Sulfavants was obtained by evaluating the effect of both the addition of a detergent agent and the modification of the sample preparation protocol on Sulfavants ability to promote CD83 up-regulation: inducing a breakdown of the aggregates, the maximum activation has undergone a shift to lower concentrations.

Further molecular docking experiments could allow to explore this issue at molecular level, explaining the differences between the molecular packing of the three sulfolipids.

The study of the mechanisms underlying the immunogenic properties of Sulfavants was another of the crucial points of this thesis and, in particular, bio-imaging techniques represent a powerful tool for a thorough biological study. In this regard, a fluorescent analogue of Sulfavant R was synthesised.

The fluorescent probe selected for this purpose was a BODIPY derivative, considering the suitable features of this class of compounds. Therefore, Me_4BODIPY has been linked to the hydrophobic portion of Sulfavant R with a synthetic strategy inspired by Sulfavant A methodology.

The introduction of the fluorescent probe on the sulfolipid did not affect the immunomodulant activation as suggested by biological assays performed on Sulfavant R-Me_4BODIPY highlighting the potential of this molecule in future analysis on the biological mechanisms Sulfavants act with.

As underlined more than once, specific and detailed studies aimed to the pharmacological development of this new class of molecular adjuvants require the production of high amount of product. For this purpose, during the PhD thesis the scale-up of the synthetic strategy was carried out. The methodology employed for the analytical preparation of Sulfavant A was already enough suitable to be scaled-up, but using exactly the same experimental conditions the overall yield suffered a substantial reduction, especially for the difficulties into the purification of some intermediates; after same modifications and optimization of the experimental conditions it was achieved the crucial target to produce grams of Sulfavant A.

According to this PhD project, part of this thesis was developed at the University of British Columbia (Vancouver-Canada), where recently Professor Andersen and his co-workers isolated an interesting natural mixture from a Canadian sponge (to be classified). In order to evaluate the potential bioactivity of the main component (1-*O*-alkyl-2-*O*-(2'-*O*-β-D-glucopyranosyl-β-D-xylopyranosyl)-glycerol Figure 3.5), its synthesis was planned within this thesis.

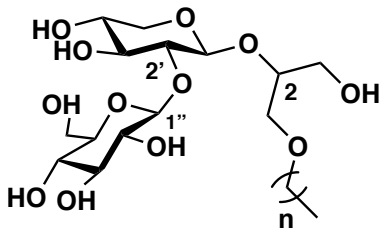

Figure 3.5: Chemical structure of 1-*O*-alkyl-2-*O*-(2'-*O*-β-D-glucopyranosyl-β-D-xylopyranosyl)-glycerol

Because of the unusual xylose instability and its peculiar reactivity, the synthetic method designed for this aim was not finalised. In detail, the poor stability of some intermediates reduced the total yield leading to several by-products, and after the disaccharide was synthetized (without the glyceridic aglycon), it did not react with the any reactant employed to proceed with the synthetic preparation. Even if different modifications to the strategy were done, no method worked. Finally, a new method has been designed, and surely it will be accomplished in collaboration with Professor Andersen.

Chapter 4: Experimental section

4.1 General Experimental Procedures

1D- and 2D-NMR spectra were recorded on a Bruker Avance-400 (400.13 MHz) and on a Bruker DRX-600 equipped with a TXI CryoProbe in $CDCl_3$ and CD_3OD (δ values are referred to $C\underline{H}Cl_3$ and $C\underline{H}_3OH$ at 7.26 and 3.34 ppm respectively) and ^{13}C NMR spectra were recorded on a Bruker Avance-400 (400.13 MHz) (δ values are referred to $\underline{C}DCl_3$ and $\underline{C}D_3OD$ at 77.0 and 49.0 ppm respectively).

ESI-MS was conducted on a Micromass Q-TOF micro. TLC plates (Kieselgel 60 F_{254}) and silica gel powder (Kieselgel 60, 0.063-0.200 mm) were from Merck.

All the reagents were purchased from Sigma-Aldrich and used without any further purification.

All the synthetic intermediates were characterized by NMR spectroscopy.

4.2 Synthesis of Sulfavant A

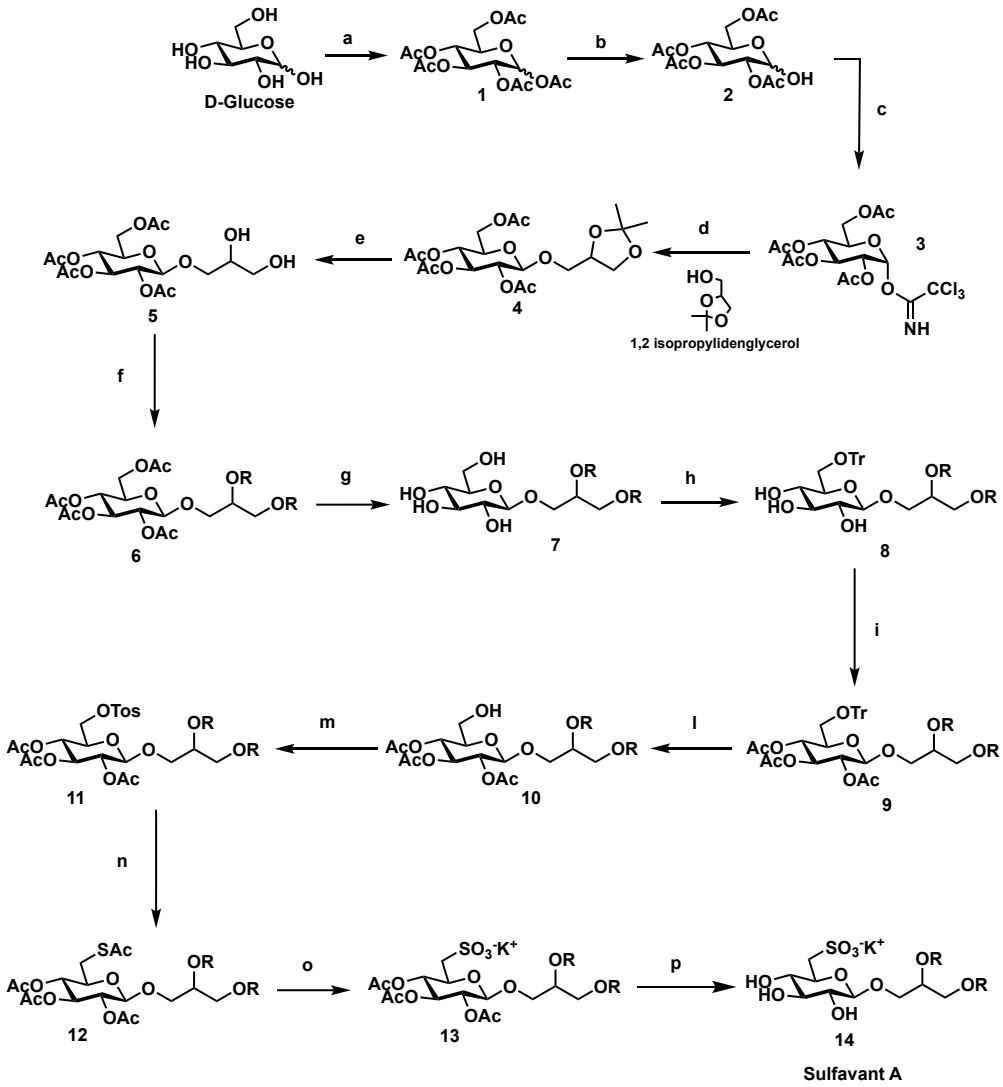

Scheme 2.1 Total synthesis of 1,2-*O*-distearoyl-3-*O*- β-D-sulfoquinovosylglycerol (Sulfavant A)

1,2-(R/S)-*O*- isopropylidene glycerol: glycerol (2 g, 0.0022 mol) was dissolved in *N,N*-Dimethylformamide (4.0 mL); 2,2-dimethoxypropane (4.0 mL) and *p*-toluensulfonic acid (0.3 g, 0.0017 mol) were added; after stirring overnight at 25°C, the mixture was portioned between cold distilled water and dichloromethane; the organic phase was purified by silica gel chromatography using a gradient of petroleum ether/diethyl ether to give 1,2-*O*-isopropylidene glycerol (2 g, 0.015 mol, 70%). ^{1}H-NMR (400 MHz, $CDCl_3$): δ 4.24 (1H, m, H-2), 4.09 (1H, dd, *J*= 6.7, 8.5 Hz, H-1a), 3.82 (1H, dd, *J*= 6.4, 8.5 Hz, H-1b), 3.65 (2H, m, H_2-1), 1.46 (3H, s, CH_3), 1.40 (3H, s, CH_3); HRESIMS m/z 155.0699 $[M+Na]^+$ (calcd for $C_6H_{12}O_3Na$, 155.0684).

a)

Compound 1: D-glucose (2.00 g, 0.0112 mol) was dissolved in pyridine (26 mL) and acetic anhydride (10 mL) was added; the reaction mixture was stirred for 3 h at 25ºC; after portioning between water and chloroform, the organic phase was evaporated under reduced pressure and purified by silica gel chromatography using a light petroleum ether/diethyl ether gradient to give compound **1** (4.20 g, 0.011 mol, 95%) as pale yellow oil; ^{1}H-NMR (400 MHz, $CDCl_3$): δ 6.32 (1H, d, *J*=3.3 Hz, H-1', α-form), 5.71 (1H, d, *J*= 8.18 Hz, H-1', β-form), 5.46 (1H, dd, *J*= 9.7, 9.7 Hz, H-4'), 5.12 (1H, overlapped, H-2'), 5.11 (1H, overlapped, H-3'), 4.29 (1H, m, H-5'), 4.26 (1H, dd, *J*= 6.37, 11.1 Hz, H-6'a), 4.11 (1H, dd, *J*= 6.7, 11.1 Hz, H-6'b), 2.17-2.00 (15H, -$COCH_3$); ESIMS *m/z* 413.1039 $[M+Na]^+$ (calcd for $C16H_{22}O_{11}Na$, 413.1054).

b)

Compound 2: compound **1** (4.20 g, 0.011 mol) was dissolved in tetrahydrofuran (40 mL) and 1.5 equiv. of benzylamine were added; the reaction mixture was stirred overnight at 25ºC; after portioning between water and chloroform, the organic phase was evaporated under reduced pressure and purified by silica gel chromatography using a light petroleum ether/diethyl ether gradient to give compound **2** (2.78 g, 0.0080 mol, 74%); ^{1}H-NMR (400 MHz, $CDCl_3$): δ 5.38 (1H, dd, *J*= 3.4, 12.7 Hz, H-

3'), 5.31 (1H, dd, *J*= 3.4, 11.0 Hz, H-4'), 5.03 (1H, dd, *J*= 3.4, 10.8 Hz, H-2'), 4.79 (1H, d, *J*= 4.48 Hz, H-1', α-form), 4.65 (1H, d, *J*= 7.4 Hz, H-1', β-form), 4.05-3.76 (3H, overlapped, H-5', H_2-6'), 2.05 (1H, s, OAc), 2.00 (1H, s, OAc), 1.95 (1H, s, OAc), 1.90 (1H, s, OAc); ESIMS *m/z* 371.0942 $[M+Na]^+$ (calcd for $C16H22O11Na$, 371.0949).

c)

Compound 3: compound **2** (2.78 g, 0.0080 mol) was dissolved in anhydrous dichloromethane (24 mL); 10 equiv. of trichloroacetonitrile and 0.2 equiv. of 1,8-Diazabiciclo[5.4.0]undec-7-ene (DBU) were added; the reaction mixture was stirred for 2 h at 0°C on activated 3 Å molecular sieves; after filtration on celite and evaporation under reduced pressure, the mixture was purified by silica gel chromatography using a gradient of *n*-hexane/ethyl acetate to give compound **3** (3.12 g, 0.0065 mol, 81%) as pale yellow oil. ^{1}H-NMR (400 MHz, $CDCl_3$): δ 6.56 (1H, d, *J*=3.8 Hz, H-1'), 5.57 (1H, dd, *J*= 9.2, 9.2 Hz, H-3'), 5.18 (1H, dd, *J*= 9.2, 9.2 Hz, H-4'), 5.14 (1H, dd, *J*= 3.5, 9.2 Hz, H-2'), 4.28 (1H, m, H-6'a), 4.26 (1H, m, H-5'), 4.13 (1H, m, H_2-6'b), 2.09-2.01 (12H, $COCH_3$); HRESIMS *m/z* 514.0040 $[M+Na]^+$ (calcd for $C16H20O10Cl3NNa$, 514.0045).

d)

Compound 4: compound **3** (3.12 g, 0.0065 mol) was dissolved in anhydrous dichloromethane (24 mL) and 1.5 equiv. of 1,2-(R/S)-*O*- isopropylidene glycerol was added; the reaction mixture was kept at -20°C on activated 3 Å molecular sieves under argon; boron trifluoride etherate (0.2 equiv.) was added and stirring was maintained for 2 h; after another addition of boron trifluoride etherate (0.2 equiv.), the temperature was raised to -10°C and the reaction mixture was stirred for 16h. After neutralization with triethylamine (540 µL) and filtration on celite, the mixture was evaporated under reduced pressure and purified by silica gel chromatography using a light petroleum ether/diethyl ether gradient to give

compound **4** (2.50 g, 0.0054 mol, 82%) as pale yellow oil; ^{1}H-NMR (400 MHz, $CDCl_3$): δ 5.19 (1H, bt, *J*= 9.4 Hz, H-3'), 5.06 (1H, bt, *J*= 9.9 Hz, H-4'), 4.99 (1H, bt, *J*= 8.4 Hz, H-2'), 4.60 (1H, d, *J*= 7.8 Hz, H-1'), 4.25 (1H, dd, *J* = 5.0, 12 Hz, H-1a), 4.14-3.69 (6H, overlapped, H-1b, H-2, H_2-6', H-5', H-3a), 3.62 (1H, dd, *J*= 5.9, 10.7 Hz, H-3b), 2.08 (3H, s, OAc), 2.04 (3H, s, OAc), 2.01 (3H, s, OAc), 1.99 (3H, s, OAc), 1.40 (3H, s, CH_3), 1.33 (3H, s, CH_3); HRESIMS *m/z* 485.1639 $[M+Na]^+$ (calcd for $C_{20}H_{30}O_{12}Na$, 485.1635).

e)

Compound 5: compound **4** (2.50 g, 0.0054 mol) was dissolved in acetonitrile (18 mL) and 5 equiv. of zinc nitrate hexahydrate was added; the reaction mixture was heated at 50°C and kept under stirring for 6 h; after evaporation of the organic solvent under reduced pressure, the mixture was partitioned between water and chloroform, the organic phase was evaporated and purified by silica gel chromatography using a gradient of petroleum ether/ethyl acetate to give compound **5** (1.75 g, 0.004 mol, 77%) as pale yellow oil. ^{1}H-NMR (400 MHz, $CDCl_3$): δ 5.23 (1H, dd, J=9.4 and 9.3 Hz), 5.09 (1H, dd, J=9.4 and 9.5 Hz), 5.02 (1H, dd, J=9.4 and 7.5 Hz), 4,56 (1H, d, 7.8 Hz), 4.22 (2H, bs), 3.52-3.95 (6H), 2.01-2.10 (12H); HRESIMS 445.1319 $[M+Na]^+$ (calcd for $C_{17}H_{26}O_{12}Na$, 445.1322).

f)

Compound 6: compound **5** (1.75 g, 0.004 mol) was dissolved in anhydrous dichloromethane (16 mL) prior to addition 1.1 equiv. of stearic acid, DCC (1.6 g, 0.008 mol) and DMAP (0.1 g, 0.0008 mol) under argon. The reaction mixture was stirred for 16h at 25ºC; after evaporation under reduced pressure, the mixture was purified by silica gel chromatography using a gradient of petroleum ether/diethyl ether to give compound **6** (3.8 g, 0.004 mol, 90%) as pale-yellow oil. ^{1}H-NMR (400 MHz, $CDCl_3$): δ 5.12 (1H, m), 5.10 (1H, overlapped), 5.05 (1H, t, J=9.5 Hz), 4.96 (1H, dd,

J=9.5 and 7.9 Hz), 4.5 (1H, d), 4.19–4.32 (2H, m), 4.03–4.17 (2H, m),.3.92 (1H, dd, J=11.0 and 4.9 Hz), 3.6-3.7 (2H, m), 2.3 (4H, m) 1.9-2.0 (12H, bt), 1.55 (4H, m), 1.1-1.3 (56H), 0.9 (6H, t, J=6.9); HRESIMS 977.6545 $[M+Na]^+$ (calcd for $C_{53}H_{94}O_{14}Na$, 977.6541).

g)

Compound 7: compound **6** (3.8 g, 0.004 mol) was dissolved in aqueous ethanol (85%) (35 mL) and 1.2 equiv. of hydrazine mono-hydrate were added. The reaction mixture was stirred for 6h at 44°C. After evaporation under a stream of nitrogen, the mixture was purified by silica gel chromatography using a gradient of chloroform/methanol to give compound **7** (2.60 g, 0.0032 mol, 81%). ^{1}H-NMR (400 MHz, $CDCl_3$): δ 5.24 (1H, m, H-2), 4.35 (1H, bd, H=11, H-1b), 4.28 8, d, J=7.8, H-1'), 4.06 (1H, dd, J=12 and 6.7, H-1a), 3.85, (1H, bd, J=10.5, H-3b), 3.79 (2H, bs, H-6'ab), 3.62 (1H, dd, J=10.7 and 6.4, 3-Ha), 3.60 (1H, m, H-3'), 3.57 (1H, m, H-4'), 3.39 (1H, m, H-2'), 3.32 (1H, m, H-5'), 2.3 (4H, bt, J=6.9, α-methylene), 1.57 (4H, m, β-methylene), 1.2-1.4 (56H), 0.83 (6H, bt, J=6.7, CH_3); HRESIMS 809.6123 $[M+Na]^+$ (calcd for $C_{45}H_{86}O_{10}Na$, 809.6119).

h)

Compound 8: compound **7** (2.60 g, 0.0032 mol) were treated with 1.6 equiv. of trityl chloride and 0.4 equiv. of DMAP in dry pyridine (25 mL). The reaction mixture was stirred for 3 h at 60 °C and then the organic solvent was evaporated under a stream of nitrogen. The residue was purified by silica gel chromatography using a chloroform/methanol gradient to give compound **8** (2.14 g, 0.0020 mol, 77%) as pale yellow oil; ^{1}H-NMR (400 MHz, $CDCl_3$): δ 7.52-7.15 (15H, m, trityl portion), 5.22 (1H, m, H-2), 4.33 (1H, m, H-1a), 4.32 (1H, d, *J*= 7.0 Hz, H-1′), 4.09 (1H, m, H-1b), 4.02 (1H, m, H-3a), 3.71 (1H, m, H-3b), 3.42 (1H, m, H-3'), 3.41 (1H, H-4'), 3.40 (1H, m, H-2'), 3.40 (1H, m, H-6'a), 3.29 (1H, m, H-6'b), 2.11 (2H, t, *J*= 7.9 Hz, α-

methylene), 2.09 (2H, t, *J*= 7.8 Hz, α-methylene), 1.51 (4H, m, β-methylene), 1.28-1.15 (56H, acyl chain), 0.83 (6H, t, *J*= 7.0 Hz, 2 CH_3); HRESIMS *m/z* 1051.7204 $[M+Na]^+$ (calcd for $C_{64}H_{10}O_{10}Na$, 1051.7201).

i)

Compound 9: compound **8** (2.14 g, 0.0020 mol) was dissolved in pyridine (20 mL) and acetic anhydride (10 mL). The reaction mixture was stirred for 3h at 25ºC and then extracted with distilled water and chloroform. The resulting organic phase was evaporated under reduced pressure and purified by silica gel chromatography using a light petroleum ether/diethyl ether gradient to give compound **9** (2.20 g, 0.0018 mol, 90%). ^{1}H-NMR (400 MHz, $CDCl_3$): δ 7.47-7.18 (15H, m, trityl portion), 5.23 (1H, m, H-2), 5.15 (1H, m, H-4'), 5.14 (1H, m, H-3'), 5.05 (1H, m, H-2'), 4.54 (1H, d, *J*= 7.7 Hz, H-1'), 4.34 (1H, dd, *J*= 4.1, 12.0 Hz, H-1a), 4.13 (1H, dd, *J*= 5.9, 12.0 Hz, H-1b), 4.03 (1H, dd, *J*= 4.9, 11.1 Hz, H-3a), 3.74 (1H, dd, *J*= 5.1, 11.1 Hz, H-3b), 3.55 (1H, m, H-5'), 3.27 (1H, bd, *J*=10.2 Hz, H-6'a), 3.09 (1H, dd, *J*=2.3, 10.2, H-6'b), 2.31 (2H, t, *J*= 7.5 Hz, α-methylene), 2.16 (2H, t, *J*= 7.8 Hz, α-methylene), 1.54 (4H, m, β-methylene), 1.28-1.15 (acyl chain), 0.86 (6H, t, *J*= 7.0 Hz, 2CH_3); HRESIMS *m/z* 1177.7507 $[M+Na]^+$ (calcd for $C_{70}H_{106}O_{13}Na$, 1177.7505).

l)

Compound 10: compound **9** (2.20 g, 0.0018 mol) was dissolved in iodine methanol solution (40 mL, 1%). After stirring for 6 h at 60 °C, the mixture was concentrated and purified by silica gel chromatography using a gradient of petroleum ether/diethyl ether to give compound **10** (1.23 g, 0.0014 mol, 74%) as a pale yellow oil; ^{1}H-NMR (400 MHz, $CDCl_3$): δ 5.31-5.28 (2H, overlapped, H-2, H-3'), 5.08-5.00 (2H, m, H-2', H-4'), 4.61 (1H, d, *J*= 7.8 Hz, H-1'), 4.36 (1H, m, H-1a), 4.16 (1H, m, H-1b), 3.92 (1H, m, H-3a), 3.78 (1H, m, H-3b), 3.74 (1H, m, H-6'a), 3.60 (1H, m, H-6'b), 3.54 (1H, m, H-5'), 2.41-2.29 (4H, m, α-methylene), 2.10-2.01 (9H, s, 3 OAc), 1.62-1.52

(4H, m, β-methylene), 1.33-1.15 (acyl chain), 0.90 (6H, t, *J*= 7.0 Hz, $2CH_3$); HRESIMS *m/z* 935.6399 $[M+Na]^+$ (calcd for $C_{51}H_{92}O_{13}Na$, 935.6403).

m)

Compound 11: compound **10** (1.23 g, 0.0014 mol) was dissolved in anhydrous pyridine (20 mL), 1.1 equiv. of *p*-Tosylchloride and DMAP (0.18 g, 0.0015 mol) were added at 0 °C under argon and the reaction mixture was stirred for 16h at 25 ºC. After evaporation under a stream of nitrogen, the mixture was purified by silica gel chromatography using a gradient of petroleum ether/diethyl ether to give compound **11** (1.16 g, 0.0011 mol, 80%) as a pale yellow oil; ^{1}H-NMR (400 MHz, $CDCl_3$): δ 7.77 (2H, d, *J*= 8.3 Hz, aromatic methynes), 7.34 (2H, d, *J*= 8.3 Hz, aromatic methynes), 5.18-5.13 (2H, m, H-2, H-3′), 4.96-4.89 (2H, m, H-2', H-4'), 4.48 (1H, d, *J*= 7.9 Hz, H-1′), 4.26 (1H, m, H-1a), 4.08-4.01 (3H, overlapped, H-1b, H_2-6′a), 3.87 (1H, dd, *J*=5.1, 10.8 Hz, H-3a), 3.61 (1H, dd, J= 5.4, 10.8 Hz, H-3b), 2.44 (3H, s, aromatic methyl), 2.31-2.28 (4H, m, α-methylene), 2.04-1.97 (9H, s, 3 OAc), 1.60-1.54 (4H, m, β-methylene), 1.39-1.23 (acyl chain), 0.91-0.87 (6H, overlapped, $2CH_3$); HRESIMS *m/z* 1089.6501 $[M+Na]^+$ (calcd for $C_{58}H_{98}O_{15}NaS$, 1089.6505).

n)

Compound 12: compound **11** (1.16 g, 0.0011 mol) was dissolved in 2-butanone (50 mL) and potassium thioacetate (0.31 g, 0.0027 mol). The reaction mixture was stirred at 80°C for 2.5h and then the solvent was evaporated at reduced pressure. The resulting material was purified by silica gel chromatography using a light petroleum ether/diethyl ether gradient to give compound **12** (0.88 g, 0.00091 mol, 84%) as a colourless oil; ^{1}H-NMR (400 MHz, $CDCl_3$): δ 5.18-5.14 (2H, m, H-2, H-3′), 4.96-4.89 (2H, m, H-2', H-4'), 4.50 (1H, d, *J*= 8.0 Hz, H-1′), 4.28 (1H, dd, *J*= 4.1, 11.8 Hz, H-1a), 4.08 (1H, dd, J= 5.7, 11.8 Hz, H-1b), 3.91 (1H, dd, *J*=4.5, 11.1 Hz, H-3a), 3.65 (1H, dd, J= 5.4, 11.1 Hz, H-3b), 3.62 (1H, m, H-5'), 3.24 (1H, bd, *J*= 11.4 Hz, H-6'a),

3.05 (1H, dd, *J*= 2.4 Hz, 11.4 Hz), 2.33-2.29 (4H, m, α-methylene), 2.13-1.98 (9H, s, 3 OAc), 1.64-1.57 (4H, m, β-methylene), 1.32-1.23 (acyl chain), 0.91-0.87 (6H, overlapped, $2CH_3$); HRESIMS *m/z* 993.6322 $[M+Na]^+$ (calcd for $C_{53}H_{94}O_{13}NaS$, 993.6320).

o)

Compound 13: compound **12** (0.88 g, 0.00091 mol) was dissolved in potassium acetate (0.44 g, 0.0044 mol), 34% (w/v) H_2O_2 (2.20 mL) and acetic acid (25 mL). The reaction mixture was for 16h at 40 °C. After evaporation under a stream of nitrogen, the oily residue was purified by silica gel chromatography using a gradient of chloroform/methanol to give compound **13** (0.68 g, 0.00066 mol, 70%) as a colourless oil; ^{1}H-NMR (400 MHz, $CDCl_3$): δ 5.27 (1H. m, H-2), 5.18 (1H, dd, 8.9, 8.9 Hz, H-3), 5.08-4.99 (2H, m, H-2', H-4′), 4.68 (1H, d, 7.3 Hz, H-1'), 4.31 (1H, dd, *J*= 5.1, 11.1 Hz, H-1a), 4.15-4.06 (3H, overlapped, H-1b, H-3a, H-5'), 3.75 (1H, m, H-3b), 3.20 (2H, overlapped, H_2-6'), 2.33-2.28 (4H, m, α-methylene), 2.06-1.98 (9H, s, 3 OAc), 1.64-1.55 (4H, m, β-methylene), 1.34-1.22 (acyl chain), 0.91-0.88 (6H, overlapped, $2CH_3$); HRESIMS *m/z* 975.6108 $[M]^-$ (calcd for $C_{51}H_{91}O_{15}S^-$, 975.6111).

p)

Compound 14 (Sulfavant A): compound **13** (0.68 g, 0.00066 mol) was dissolved in aqueous ethanol (85%) (50 mL), 2.4 equiv. of hydrazine monohydrate was added, and the reaction mixture was stirred for 6h at 44°C. After evaporation under a stream of nitrogen, the mixture was purified by silica gel chromatography using a gradient of chloroform/methanol to give compound **14** (**Sulfavant A**) (0.35 g, 0.00040 mol, 60%) as a white solid; ^{1}H-NMR (400 MHz, $CDCl_3/CD_3OD$ 1/1): ^{1}H-NMR (400 MHz, $CDCl_3/CD_3OD$ 1/1): δ 5.29 (1H, m, H-2), 4.47 (1H, m, H-1a), 4.34 and 4.32 (each for 1H, d, 7.8 Hz, H-1'), 4.19 (1H, m, H-1b), 4.13-4.03 (1H, m, H-1a), 3.79-3.75 (2H, m, H-3b, H-5'), 3.42 (1H, m, H-3'), 3.32 (1H, m, H-6'a), 3.26 (1H, m, H-2'), 3.14

(1H, m, H-4'), 2.98 (1H, m, H-6'b), 2.43-2.35 (4H, m, α-methylene), 1.69-1.58 (4H, m, β-methylene), 1.43-1.29 (acyl chain), 0.94 (6H, overlapped, $2CH_3$); HRESIMS *m/z* 849.5761 $[M]^-$ (calcd for $C_{51}H_{91}O_{15}S^-$, 849.5767).

4.3 Modification of Synthetic Strategy of Sulfavant A for the preparation of β-SQDG16

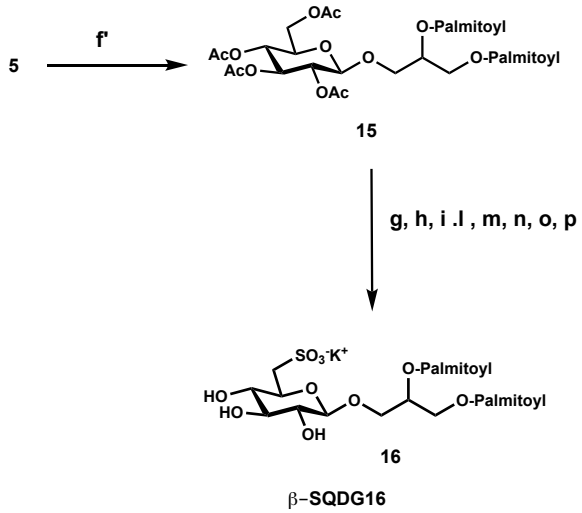

Scheme 2.2: Modification of synthetic strategy of Sulfavant A in order to obtain β-SQDG16

f')

Compound 15: Compound **5** (2.1 g, 0.005 mol) was dissolved in anhydrous dichloromethane (20 mL) and 1.1 equiv. of palmitic acid, 1 equiv. of DCC and 0.2 equiv. of DMAP were added under argon atmosphere. The reaction mixture was stirred for 16h at 25ºC; after evaporation under reduced pressure, the mixture was purified by silica gel chromatography using a gradient of petroleum ether/diethyl ether to give compound **15** (4.04 g, 0.0045 mol, 90%) as pale-yellow oil. ^{1}H-NMR (400 MHz, $CDCl_3$): δ 5.12 (1H, ss, J=9.4 and 7.2 Hz), 5.10 (1H, overlapped), 5.05 (1H, t, J=9.5 Hz), 4.96 (1H, dd, J=9.5 and 7.9 Hz), 4.5 (1H, d), 4.19–4.32 (2H, m), 4.03–4.17 (2H, m),.3.92 (1H, dd, J=11.0 and 4.9 Hz), 3.6-3.7 (2H, m), 2.3 (4H, m) 1.9-2.0 (12H, bt), 1.55 (4H, m), 1.1-1.3 (54H), 0.9 (6H, t, J=6.9); HRESIMS 921.6545 $[M+Na]^+$ (calcd for $C_{53}H_{94}O_{14}Na$, 921.6541).

4.4 Modification of the Synthetic Strategy for the preparation of β-SQDG16-R and β-SQDG16-S

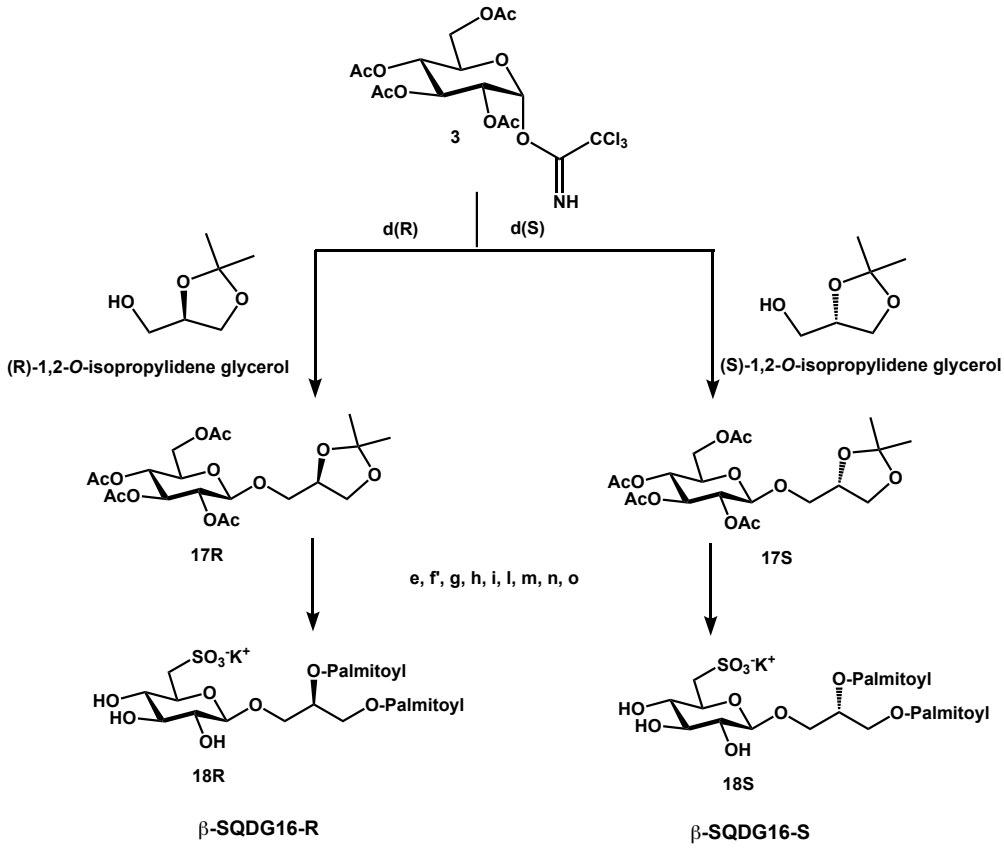

Scheme 2.3: Modification of the synthetic strategy previous discussed for the preparation of β-SQDG16-R and β-SQDG16-S

d (R)

Compound 17R: 1'-*O*-trichloroacetimidate-2',3',4',6'-tetra-acetyl-glucose (**3**) (2.3 g, 0.0047 mol) was dissolved in anhydrous dichloromethane (18 mL) and 1.5

equivalents of 1,2-*(R)*-*O*-isopropylidene glycerol was added; the reaction mixture was kept at -20°C on activated 3 Å molecular sieves under argon; boron trifluoride etherate (252 µL, 1.03 mmol) was added and stirring was maintained for 2 h; after another addition of boron trifluoride etherate (252 µL, 1.03 mmol), the temperature was raised to -10°C and the reaction mixture was stirred overnight at that temperature. After neutralization with triethylamine (400 µL) and filtration on celite, the mixture was evaporated under reduced pressure and purified by silica gel chromatography using a light petroleum ether/diethyl ether gradient to give compound **17R** (1.77 g, 0.0039 mol, 82%) as pale yellow oil; ^{1}H-NMR (400 MHz, $CDCl_3$): δ 5.19 (1H, bt, *J*= 9.4 Hz, H-3'), 5.06 (1H, bt, *J*= 9.9 Hz, H-4'), 4.99 (1H, bt, *J*= 8.4 Hz, H-2'), 4.60 (1H, d, *J*= 7.8 Hz, H-1'), 4.25 (1H, dd, *J* = 5.0, 12 Hz, H-1a), 4.14-3.69 (6H, overlapped, H-1b, H-2, H_2-6', H-5', H-3a), 3.62 (1H, dd, *J*= 5.9, 10.7 Hz, H-3b), 2.08 (3H, s, OAc), 2.04 (3H, s, OAc), 2.01 (3H, s, OAc), 1.99 (3H, s, OAc), 1.40 (3H, s, CH_3), 1.33 (3H, s, CH_3); HRESIMS *m/z* 485.1641 $[M+Na]^+$ (calcd for $C_{20}H_{30}O_{12}Na$, 485.1635).

d (S)

Compound 17S: 1'-*O*-trichloroacetimidate-2',3',4',6'-tetra-acetyl-glucose (**3**) (2.0 g, 0.0040 mol) was dissolved in anhydrous dichloromethane (15 mL) and 1.5 equivalents of 1,2-(*S*)-*O*-isopropylidene glycerol was added; the reaction mixture was kept at -20°C on activated 3 Å molecular sieves under argon; boron trifluoride etherate (220 µL, 0.9 mmol) was added and stirring was maintained for 2 h; after another addition of boron trifluoride etherate (220 µL, 0.9 mmol), the temperature was raised to -10°C and the reaction mixture was stirred overnight at that temperature. After neutralization with triethylamine (350 µL) and filtration on celite, the mixture was evaporated under reduced pressure and purified by silica gel chromatography using a light petroleum ether/diethyl ether gradient to give compound **17S** (1.5 g, 0.003 mol, 82%) as pale yellow oil (0.57 g, 0.0012 mol, 82%) as pale yellow oil; ^{1}H-NMR (400 MHz, $CDCl_3$): δ 5.19 (1H, bt, *J*= 9.4 Hz,

H-3'), 5.06 (1H, bt, *J*= 9.9 Hz, H-4'), 4.99 (1H, bt, *J*= 8.4 Hz, H-2'), 4.60 (1H, d, *J*= 7.8 Hz, H-1'), 4.25 (1H, dd, *J* = 5.0, 12 Hz, H-1a), 4.14-3.69 (6H, overlapped, H-1b, H-2, H_2-6', H-5', H-3a), 3.62 (1H, dd, *J*= 5.9, 10.7 Hz, H-3b), 2.08 (3H, s, OAc), 2.04 (3H, s, OAc), 2.01 (3H, s, OAc), 1.99 (3H, s, OAc), 1.40 (3H, s, CH_3), 1.33 (3H, s, CH_3); HRESIMS *m/z* 485.1639 $[M+Na]^+$ (calcd for $C_{20}H_{30}O_{12}Na$, 485.1635).

4.5 Modification of Synthetic Strategy of Sulfavant A for the preparation of β-SQDG19

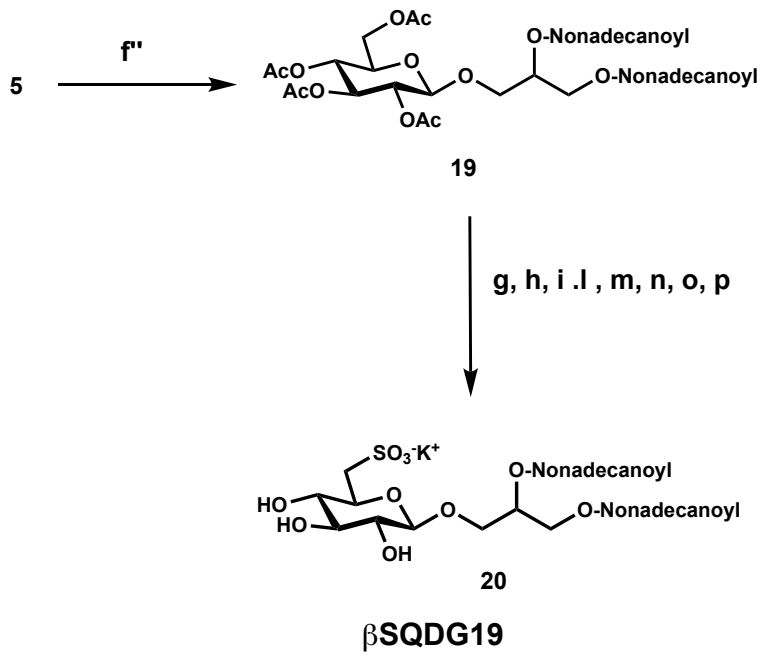

Scheme 2.4: Modification of synthetic strategy of Sulfavant A in order to obtain β-SQDG19

f'')

Compound 19: Compound **5** (1.7 g, 0.004 mol) was dissolved in anhydrous dichloromethane (16 mL) and 1.1 equiv. of palmitic acid, 1 equiv. of DCC and 0.2 equiv. of DMAP were added under argon atmosphere. The reaction mixture was stirred for 16 h at 25ºC; after evaporation under reduced pressure, the mixture was purified by silica gel chromatography using a gradient of petroleum ether/diethyl ether to give compound **19** (3.5 g, 0.0036 mol, 90%) as pale-yellow oil. ^{1}H-NMR (400 MHz, $CDCl_3$): δ 5.12 (1H, ss, J=9.4 and 7.2 Hz), 5.10 (1H, overlapped), 5.05 (1H, t, J=9.5 Hz), 4.96 (1H, dd, J=9.5 and 7.9 Hz), 4.5 (1H, d), 4.19–4.32 (2H, m), 4.03–4.17

(2H, m),.3.92 (1H, dd, J=11.0 and 4.9 Hz), 3.6-3.7 (2H, m), 2.3 (4H, m) 1.9-2.0 (12H, bt), 1.55 (4H, m), 1.1-1.3 (66H), 0.9 (6H, t, J=6.9); HRESIMS 1005.7039 $[M+Na]^+$ (calcd for $C_{53}H_{94}O_{14}Na$, 1005.7045).

4.6 Improvement of the Synthetic Strategy for the preparation of Sulfavant A

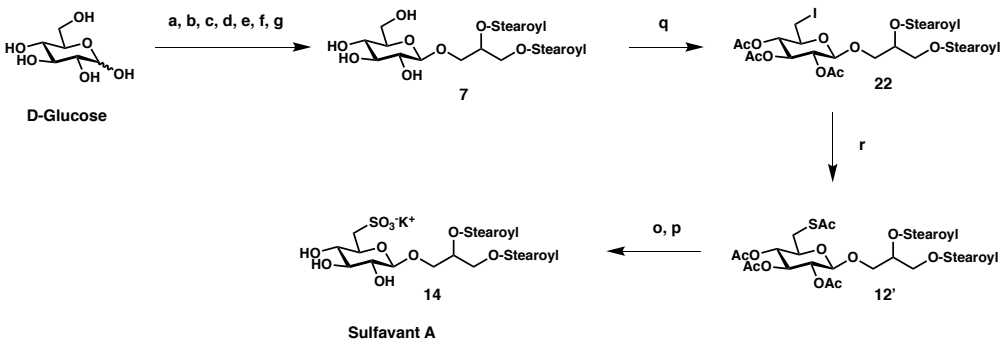

Improvement of the synthetic strategy

q)

Compound 22: Iodine (49 mg, 0.191 mmol) was added to a mixture of 1,2-distearoyl-3-*O*-β-D- glucosyl glycerol (**7**) (100 mg, 0.127 mmol), triphenylphosphine (50 mg, 0.191 mmol) and 2,6-dimethylpyridine (450 mg, 4.2 mmol) at 80 °C; the mixture was stirred for 30 min at 80 °C and subsequently acetylated by addition of pyridine (0.5 mL) and acetic anhydride (0.5 mL); after evaporation of the solvent under a stream of nitrogen, the mixture was purified by silica gel chromatography using a gradient of petroleum ether/diethylether to give compound **22** (195 mg, 0.191 mmol, 100%) as a colorless oil; ^{1}H NMR (400 MHz, $CDCl_3$): δ 5.21−5.16 (2H, overlapped, H-2, H-3′), 4.99−4.94 (1H, m, H-2′), 4.87 (t, J = 8.03 Hz, H-4′), 4.56 and 4.55 (each 1H, d, J = 8.1 Hz, H-1′ of the two epimers), 4.33−428 (1H, m, H-1a), 4.17−4.09 (1H, m, H-1b), 4.02−3.97 (1H, m, H-3a), 3.78−3.71 (1H, m, H-3b), 3.52 (1H, m, H-5′), 3.28 (1H, dd, J = 3.06, 11.1 Hz, H-6′a), 3.13 (1H, dd, J = 8.4, 11.1 Hz, H-6′b), 2.35−2.26 (4H, overlapped, α- methylenes of stearoyl portions), 2.07−1.97 (9H, s, OAc), 1.64−1.58 (4H, overlapped, β-methylenes of stearoyl portions), 1.33−1.21 (60H, aliphatic

methylenes), 0.91−0.84 (6H, overlapped, $2CH_3$); HRESIMS m/z: 1045.5460 $[M + Na]^+$ (calcd for $C_{51}H_{91}NaO_{12}I$, 1045.5453).

r)

Compound 12'. Compound **22** (195 mg, 0.191 mmol) was dissolved in 2-butanone (15 mL) and potassium thioacetate (108 mg, 0.953 mmol). The reaction mixture was stirred at 80 °C for 2 h and then the solvent was evaporated under reduced pressure. The resulting material was purified by silica gel chromatography using a light petroleum ether/diethyl ether gradient to give compound **12** (184.7 mg, 0.191 mmol, 100%) as a colorless oil; ^{1}H NMR (400 MHz,$CDCl_3$): δ 5.20−5.14 (2H, m, H-2, H-3′), 4.96−4.89 (2H, m, H-2′, H-4′), 4.50 (1H, d, J = 8.0 Hz, H-1′), 4.28 (1H, dd, J = 4.1, 11.8 Hz, H-1a), 4.09 (1H, dd, J = 5.7, 11.8 Hz, H-1b), 3.91 (1H, dd, J = 4.5, 11.1 Hz, H-3a), 3.65 (1H, dd, J = 5.4, 11.1 Hz, H-3b), 3.62 (1H, m, H-5′), 3.25 (1H, bd, J = 11.4 Hz, H-6′a), 3.06 (1H, dd, J = 2.4 Hz, 11.4 Hz), 2.35 (3H, s, SAc), 2.33−2.29 (4H, m, α-methylene of stearoyl portion), 2.13−1.99 (9H, s, 3OAc), 1.64−1.57 (4H, m, β-methylene of stearoyl portion), 1.32−1.23 (60H, aliphatic methylenes), 0.93−0.87 (6H, overlapped, $2CH_3$); HRESIMS m/z: 993.6329 $[M + Na]^+$ (calcd for $C_{53}H_{94}O_{13}NaS$, 993.6313).

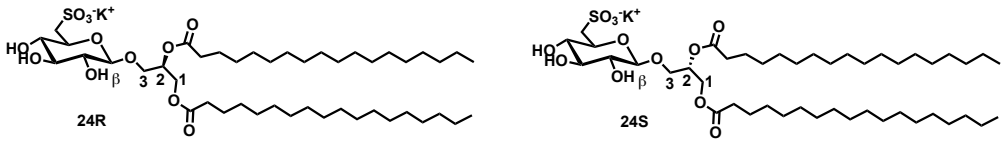

Sulfavant R Sulfavant S

Compound 24R and 24 S (synthesised with this synthetic strategy)

Sulfavant S (24S): white solid; ^{1}H-NMR (400 MHz, $CD_3OD/CDCl_3$ 1/1): δ values are referred to CH_3OH (3.34 ppm and 49.0 ppm): δ 5.28 (1H, m, H-2), 4.40 (1H, dd, *J*= 2.7, 12.0 Hz, H-1a), 4.31 (1H, d, *J*= 7.6 H-1'), 4.24 (1H, dd, *J*= 6.9, 12.0 Hz, H-1b), 4.05 (1H, dd, *J*= 5.4, 11.0 Hz, H-3a), 3.79-3.71 (3H, H-3b, H-3', H-4'), 3.41 (1H, bt, *J*= 8.9 Hz, H-2'), 3.26 (1H, H-6'a), 3.25 (1H, H-5'), 3.09 (1H, dd, *J*= 7.2, 15.7 Hz, H-6'b), 2.36-2.27 (4H, α-methylenes of stearoyl portions), 1.65-1.56 (4H, β-methylenes of stearoyl portions), 1.36-1.20 (aliphatic methylenes), 0.89 (6H, bt, *J*= 6.0 Hz, $2CH_3$); ^{13}C-NMR (100MHz, $CD_3OD/CDCl_3$ 1/1): δ 174.1, 173.7 (C, acyl esters of stearoyl part), 103.2 (CH, C1′), 76.1 (CH, C2′), 73.8 (CH, C5′), 72.4 (CH, C3'), 72.3 (CH, C4'), 70.2 (CH, C2), 68.2 (CH_2, C3), 63.2 (CH_2, C1), 53.6 (CH_2, C6'), 34.2 (CH_2, α-methylene of stearoyl portion), 32.2-29.0 (CH_2, methylenes of stearoyl portion), 24.9 (CH_2, β-methylene of stearoyl portion), 13.8 (CH_3, methyls of stearoyl portion); HRESIMS *m/z* 849.5772 $[M]^-$ (calcd for $C_{45}H_{85}O_{12}S^-$, 849.5767).

Sulfavant R (24R): white solid; ^{1}H-NMR (400 MHz, $CD_3OD/CDCl_3$ 1/1): δ values are referred to CH_3OH at 3.34 ppm and 49.0 ppm): δ 5.28 (1H, m, H-2), 4.45 (1H, dd, *J*= 2.6, 12.1 Hz, H-1a), 4.31 (1H, d, *J*= 7.7 Hz, H-1'), 4.17 (1H, dd, *J*= 6.7, 12.1 Hz, H-1b), 4.05 (1H, dd, *J*= 5.2, 11.1 Hz, H-3a), 3.78-3.71 (3H, overlapped, H-3b, H-3', H-4'), 3.40 (1H, bt, *J*= 8.7 Hz, H-2'), 3.26 (1H, H-5'), 3.24 (1H, H-6'a), 3.09 (1H, dd, *J*= 7.2, 15.7 Hz, H-6'b), 2.35-2.29 (4H, α-methylenes of stearoyl portions), 1.64-1.57 (4H, β-methylenes of stearoyl portions), 1.32-1.22 (aliphatic methylenes), 0.88 (6H, bt, *J*= 6.9 Hz, $2CH_3$); ^{13}C-NMR (100MHz, $CD_3OD/CDCl_3$ 1/1): δ 174.0, 173.8 (C, acyl esters of stearoyl part), 103.1 (CH, C1′), 76.3 (CH, C2′), 73.5 (CH, C5′), 72.3 (CH, C3'), 72.2 (CH, C4'), 70.5 (CH, C2), 68.1 (CH_2, C3), 63.1 (CH_2, C1), 53.2 (CH_2, C6'), 34.1 (CH_2, α-methylene of stearoyl portion), 32.5-29.2 (CH_2, methylenes of stearoyl portion), 24.8 (CH_2, β-methylene of stearoyl portion), 13.7 (CH_3, methyls of stearoyl portion); HRESIMS *m/z* 849.5775 $[M]^-$ (calcd for $C_{45}H_{85}O_{12}S^-$, 849.5767).

4.7 Synthesis of Sulfavant R-Me$_4$BODIPY

- Preparation of Me$_4$BODIPY-undecanoic acid

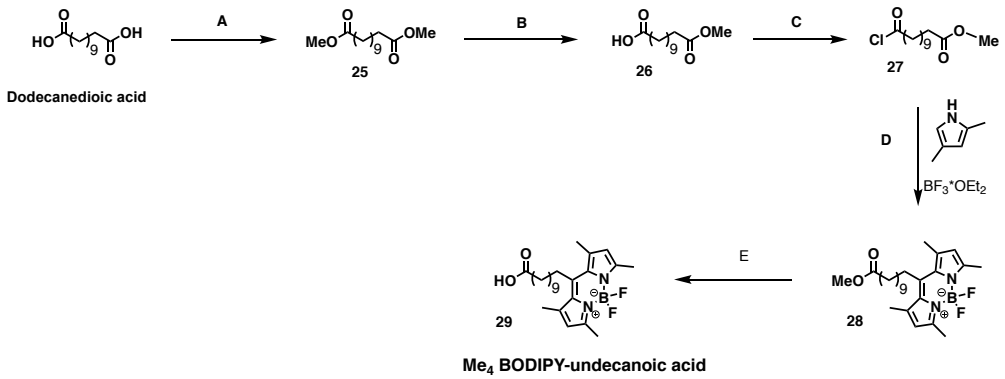

Scheme 2.8: Synthetic procedure employed for the preparation of Me$_4$BODIPY-undecanoic acid

A)

Compound 25: Dodecanedioic acid (6 g, 0,026 mol) was dissolved in CH_3OH/HCl (0.5M) (40 mL). The reaction mixture was stirred for 2 h at 25ºC and then the solvent was evaporated under reduced pressure. The resulting material was purified by silica gel chromatography to obtain compound **25** (6.7 g, 0.026 mol, 100%); ^{1}H-NMR (400 MHz, $CDCl_3$): δ 3.62 (6H, s, OCH_3), 2.27 (4H, t, J=6.9 Hz), 1.57 (4H, m), 1.26 (10H, m). HRESIMS m/z: 279.1965 $[M + Na]^+$ (calcd for $C_{15}H_{28}O_3Na^+$, 279.1931).

B)

Compound 26: compound **25** (6.7 g, 0.026 mol) was dissolved in $CH_3CN/(CH_3CH_2)_2O$ 1/1 (44 mL) and then KOH (1.6 g, 0.028 mol) and CH_3OH (6 mL) were added at 0ºC. The reaction mixture was stirred for 50 h at 4ºC and then extracted with distilled water and diethyl ether. The aqueous phase was extracted

again with ethyl acetate. The organic phase was evaporated under reduced pressure and purified by silica gel chromatography to obtain compound **26** (3.87 g, 0.0158 mol), 62%; ^{1}H-NMR (400 MHz, $CDCl_3$): δ 3.67 (3H, s, OCH_3), 2.32 (2H, t, overlapped), 2.30 (2H, t, overlapped), 1.62 (4H, m), 1.30 (10H, m). HRESIMS m/z: 279.1780 $[M + Na]^+$ (calcd for $C_{14}H_{26}O_3Na^+$, 265.1774).

C)

Compound 27: compound **26** (3.87 g, 0.0158 mol) was dissolved in anhydrous CH_2Cl_2 and 1.5 equiv. of thionyl chloride were added: the reaction mixture was stirred at 50ºC for 16 h and then evaporated under reduced pressure and purified by silica gel chromatography to obtain compound **27** (2.17 g, 0.0085 mol, 52%); ^{1}H-NMR (400 MHz, $CDCl_3$): δ 3.65 (3H, s, OCH_3), 2.87 (2H, t, J= 7.1 Hz), 2.29 (2H, t, J= 6.9 Hz), 1.69 (2H, m), 1.51 (2H, m), 1.31 (10H, m). HRESIMS m/z: 283.1429 $[M + Na]^+$ (calcd for $C_{14}H_{25}ClO_2Na^+$, 283.1435).

D)

Compound 28: compound **27** (2,17 g, 0,008 mol) was dissolved in anhydrous CH_2Cl_2 and 2 equiv. of 2,4-dimethylpyrrol (previously dissolved in CH_2Cl_2 16 mL) were added slowly at 25ºC. The reaction mixture was stirred under reflux condition (50ºC) for 4 h; successively *N*-hexane (100 mL) was added and then the solvent was evaporated under reduced pressure. The oily product was dissolved in anhydrous CH_2Cl_2 (40 mL) and 2 equiv. of triethylamine were added, after stirring for 15 min, 4 equiv. of boron trifluoride etherate were added. The reaction mixture was stirred for 2h at 24ºC; the crude product was extracted with distilled water/$NaHCO_3$ (sat.) and CH_2Cl_2. The organic phase was dried at reduced pressure and purified by silica gel chromatography using a gradient of petroleum ether/diethylether to give compound **28** (0.8 g, 0.002 mol, 25%); ^{1}H-NMR (400 MHz, $CDCl_3$): δ 6.08 (2H, s), 3.70 (3H, s, OCH_3), 2.96 (2H, m), 2.55 (6H, s, CH_3), 2.43 (6H, s, CH_3), 2.32 (2H, t, J=7.0 Hz),

1.62 (2H, m), 1.32 (10H, m). HRESIMS *m/z* 446.2910 $[M-H]^-$ (calcd for $C_{25}H_{37}BF_2N_2O_2^-$, 446.2916).

E)

Compound 29: compound **28** (0.8 g, 0.002 mol) was dissolved in isopropanol (13 mL) and 3 equiv. of KOH (0.296 g) in distilled water (1.8 mL); the reaction mixture was stirred for 5h at 25ºC and then 100 mL of distilled water were added, and the solution was acidified adding HCl 1M. after extraction with ethyl acetate, the organic phase was dried at reduced pressure and purified by silica gel chromatography using a gradient of petroleum ether/diethylether to give compound **29 (**0.46 g, 0.0011 mol, 54%); ^{1}H-NMR (400 MHz, $CDCl_3$): δ 6.07 (2H, s), 2.93 (2H, m), 2.51 (6H, s, methyls), 2.41 (6H, s, methyls), 2.34 (2H, t, J= 7.4 Hz, α-methylene), 1.56 (2H, m, β-methylene), 1.36-1.44 (14H, overlapped); HRESIMS *m/z* 431.2696 $[M-H]^-$ (calcd for $C_{24}H_{34}BF_2N_2O_2^-$, 431.2687).

- Total synthesis of Sulfavant R-Me_4BODIPY

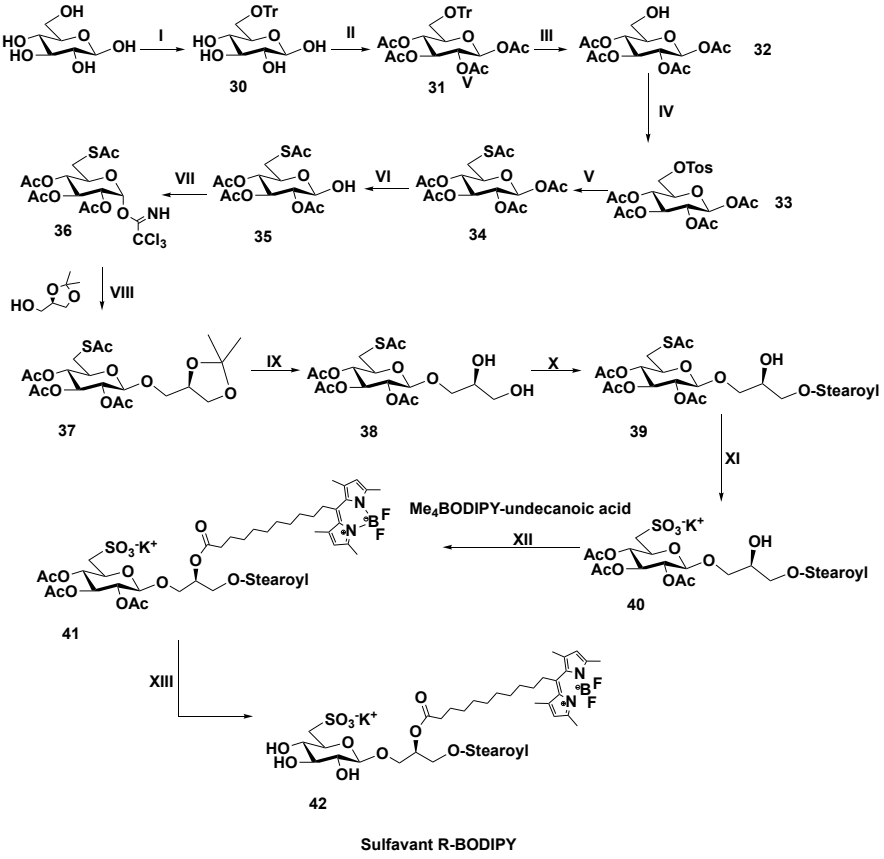

Scheme 2.9: Synthetic strategy for the preparation of Sulfavant R-BODIPY

I)

Compound 30: D-glucose (3.0 g, 0.017 mol) were treated with 3.0 equiv. of trityl chloride (14.2 g, 0.051 mol) and 1.0 equiv. of triethylamine (10 mL, 0.017 mol) in dry pyridine (30 mL). The reaction mixture was stirred for 16 h at 70 °C and then the organic solvent was evaporated under a stream of nitrogen. The residue was purified by silica gel chromatography using a chloroform/methanol gradient to give **30** (5.54 g, 0.0131 mol, 77%). HRESIMS m/z 445.1628 $[M+Na]^+$ (calcd for $C_{25}H_{26}O_6Na^+$, 445.1622).

II)

Compound 31: compound **30** (5.54 g, 0.0131 mol) was dissolved in pyridine (15 mL) and acetic anhydride (6 mL) was added; the reaction mixture was stirred for 3h at 25ºC; after portioning in water and chloroform, the organic phase was evaporated under reduced pressure and purified by silica gel chromatography using a light petroleum ether/diethyl ether gradient to give **31** (7.39 g, 0.0125 mol, 95%). ^{1}H-NMR (400 MHz, $CDCl_3$): δ 7.48-7.16 (15H, aromatic protons), 6.44 (1H, bd, *J*=3.3 Hz, α-anomeric proton), 5.73 (1H, d, *J*=7.9 Hz, β-anomeric proton), 5.41 (1H, t, *J*= 9.5 Hz), 5.31 (1H, t, *J*= 9.5 Hz), 5.26-5.14 (2H, overlapped), 4.02 (1H, m), 3.69 (1H, m), 3.43 (1H, m), 3.06 (1H, m), 2.16 (3H, s, OAc), 2.04 (3H, s, OAc), 2.03 (3H, s, OAc), 2.02 (3H, s, OAc), 1.98 (3H, s, OAc); HRESIMS *m/z* 613.2056 $[M+Na]^+$ (calcd for $C_{33}H_{34}O_{10}Na$, 613.2050).

III)

Compound 32: compound **31** (7.39 g, 0.0125 mol) was dissolved in anhydrous acetonitrile (90 mL) prior to addition of sodium iodide (5.77 g, 0.038 mol) and chlorotrimethylsilane (4.10 g, 0.038 mol). The reaction mixture was stirred for 2h at 0°C; after dilution with diethylether (200 mL) the mixture was portioned with aqueous solution of sodium thiosulfate and the organic phase was purified by silica gel chromatography using a gradient of petroleum ether/diethyl ether to give **32** (2.13 g, 0.0062 mol, 52%). ^{1}H-NMR (400 MHz, $CDCl_3$): δ 6.15 (1H, d, *J*=2.9 Hz, α-anomeric proton), 5.58 (1H, bd, *J*= 8.2 Hz, β-anomeric proton), 5.32 (1H, t, *J*= 9.3 Hz), 5.14 (1H, t, *J*= 8.4 Hz), 4.98-4.87 (2H, overlapped), 3.78 (1H, m), 3.58-3.51 (2H, m), 3.46-3.38 (1H, m), 2.01 (3H, s, OAc), 1.94 (3H, s, OAc), 1.89 (3H, s, OAc), 1.86 (3H, s, OAc), 1.84 (3H, s, OAc); HRESIMS *m/z* 371.0948 $[M+Na]^+$ (calcd for $C_{16}H_{22}O_{11}Na$, 371.0954).

IV)

Compound 33: compound **32** (2.13 g, 0.0062 mol) was dissolved in anhydrous pyridine (20 mL). *p*-Tosylchloride (5.25 g, 0.031 mol) and DMAP (0.74 g, 0.0062 mol) were slowly added and the reaction mixture was stirred for 16h at 25ºC. After evaporation under a stream of nitrogen, the mixture was purified by silica gel chromatography using a gradient of petroleum ether/diethyl ether to give **34** (1.87 g, 0.0038 mol, 68%); ^{1}H-NMR (400 MHz, $CDCl_3$): δ 7.69 (2H, d, *J*= 8.3 Hz, aromatic methynes), 7.28 (2H, d, *J*= 8.3 Hz, aromatic methynes), 6.13 (1H, bd, *J*= 3.6 Hz), 5.34 (1H, t, J= 10.3 Hz), 4.88 (1H, dd, *J*= 3.4, 10.3 Hz), 4.09-3.98 (3H, overlapped), 2.38 (3H, s, aromatic methyl), 2.07 (3H, s, OAc), 1.93 (3H, s, OAc), 1.92 (3H, s, OAc), 1.91 (3H, s, OAc); HRESIMS *m/z* 525.1050 $[M+Na]^+$ (calcd for $C_{21}H_{26}O_{12}NaS$, 525.1043).

V)

Compound 34: Compound **33** (1.87 g, 0.0038 mol) was dissolved in 2-butanone (140 mL) and potassium thioacetate (2.19 g, 0.019 mol). The reaction mixture was stirred at 80°C for 2.5h and then the solvent was evaporated under reduced pressure. The resulting material was purified by silica gel chromatography using a light petroleum ether/diethyl ether gradient to give **34** (1.19 g, 0.0031 mol, 82%); ^{1}H-NMR (400 MHz, $CDCl_3$): δ 6.2 (1H, d, *J*= 3.7 Hz), 5.36 (1H, t, *J*= 9.6 Hz), 5.00-4.92 (2H, overlapped), 2.27 (3H, s, SAc), 2.10 (3H, s, OAc), 2.02 (3H, s, OAc), 1.95 (3H, s, OAc), 1.94 (3H, s, OAc); HRESIMS *m/z* 429.0822 $[M+Na]^+$ (calcd for $C_{16}H_{22}O_{10}NaS$, 429.0831).

VI)

Compound 35: compound **34** (1.19 g, 0.0031 mol) was dissolved in tetrahydrofuran (10 mL) and 1.1 equiv. of benzylamine were added; the reaction mixture was stirred for 3h at 25ºC; after evaporation of the solvent, the residue was purified by silica gel chromatography using a light petroleum ether/diethyl ether gradient to give compound **35** (0.56 g, 0.0016 mol, 53%); ^{1}H-NMR (400 MHz, $CDCl_3$): δ 5.49 (1H, t, *J*= 10.6

Hz), 5.41 (1H, bs), 4.96 (1H, t, *J*= 8.8 Hz), 4.87 (1H, dd, *J*= 3.6, 10.6 Hz), 4.24 (1H, m), 3.19 (1H, dd, *J*= 3.2, 14.6 Hz), 3.11 (1H, d, *J*= 5.9, 14.6 Hz), 2.34 (3H, s, SAc), 2.08 (3H, s, OAc), 2.07 (3H, s, OAc), 2.00 (3H, s, OAc); HRESIMS *m/z* 387.0726 $[M+Na]^+$ (calcd for $C_{14}H_{20}O_9NaS$, 387.0726).

VII)

Compound 36: compound **35** (0.56 g, 0.0016 mol) was dissolved in anhydrous dichloromethane (6 mL); 6 equiv. of trichloroacetonitrile and 0.3 equivalents of 1,8-Diazabiciclo[5.4.0]undec-7-ene (DBU) were added; the reaction mixture was stirred for 2h at 0°C on activated 3 Å molecular sieves; after evaporation under reduced pressure, the mixture was purified by silica gel chromatography using a gradient of petroleum ether/diethyl ether to give compound **36** (0.51 g, 0.00104 mol, 65%). ^{1}H-NMR (400 MHz, $CDCl_3$): δ 8.71 (1H, s, NH), 6.54 (1H, d, *J*= 3.5 Hz), 5.56 (1H, t, *J*= 9.9 Hz), 5.15-5.06 (2H, overlapped), 4.25 (1H, m), 3.23 (2H, overlapped), 2.35 (3H, s, SAc), 2.13 (3H, s, OAc), 2.05 (3H, s, OAc), 2.04 (3H, s, OAc); HRESIMS *m/z* 515.9781 $[M+Na]^+$ (calcd for $C_{16}H_{20}O_9Cl_3NaS$, 515.9791).

VIII)

Compound 37: compound **36** (0.51 g, 0.00104 mol) was dissolved in anhydrous dichloromethane (8 mL) and 1.5 equiv. of (*R*)-1,2-*O*-isopropylidene glycerol (2.04 g, 0.0225 mol) was added; the reaction mixture was kept at -20°C on activated 4 Å molecular sieves under argon; boron trifluoride etherate (0.2 equiv.) was added and stirring was maintained for 2 h; after another addition of boron trifluoride etherate (0.2 equiv.), the temperature was raised to -10°C and the reaction mixture was stirred for 16h at -10°C. After neutralization with triethylamine (0.035 mL), the mixture was evaporated under reduced pressure and purified by silica gel chromatography using a light petroleum ether/diethyl ether gradient to give **37** (0.28 g, 0.00062 mol, 60%); (400 MHz, $CDCl_3$): δ 5.19 (1H, t, *J*=9.8 Hz), 5.02-4.95 (2H, overlapped), 4.57 (1H, d, *J*= 8.4 Hz), 4.25 (1H, m), 4.06 (1H, m), 3.83-3.70 (2H, m), 3.68-3.59 (2H, m), 3.27

(1H, bd, *J*= 14.4 Hz), 3.08 (1H, dd, *J*= 6.8, 14.4 Hz), 2.36 (3H, s, SAc), 2.10 (3H, s, OAc), 2.06 (3H, s, OAc), 2.01 (3H, s, OAc), 1.43 (3H, s, acetonide methyl), 1.37 (3H, s, acetonide methyl); HRESIMS *m/z* 501.1414 $[M+Na]^+$ (calcd for $C_{20}H_{30}O_{11}NaS$, 501.1407).

IX)

Compound 38: compound **37** (0.28 g, 0.00062 mol) was dissolved in 10 mL of MeOH/H_2O (97/3); DOWEX-H^+ (3.7 g) was added and the reaction mixture was stirred for 3h at 25ºC; after filtration, the evaporation of the solvent under reduced pressure gave **10** (0.24 g, 0.00057 mol, 92%); (400 MHz, $CDCl_3$): δ 5.17 (1H, t, *J*=9.2 Hz), 4.98-4.92 (2H, overlapped), 4.50 (1H, d, *J*= 8.3 Hz), 3.86-3.80 (2H, m), 3.69-3.54 (3H, m), 3.25 (1H, dd, *J*= 3.3, 14.3 Hz), 3.03 (1H, dd, *J*= 6.8, 14.3 Hz), 2.34 (3H, s, SAc), 2.07 (3H, s, OAc), 2.03 (3H, s, OAc), 1.98 (3H, s, OAc); HRESIMS *m/z* 461.1100 $[M+Na]^+$ (calcd for $C_{17}H_{26}O_{11}NaS$, 461.1094).

X)

Compound 39: compound **38** (0.24 g, 0.00057 mol) was dissolved in anhydrous dichloromethane (11 mL) prior to addition at 0°C of stearic acid (0.161 g, 0.00057 mol), *N,N*-dicyclohexylcarbodiimide (0.118 g, 0.00057 mol) and DMAP (0.068 g, 0.00057 mol). The reaction mixture was stirred overnight at 4°C; after evaporation under reduced pressure, the mixture was purified by silica gel chromatography using a gradient of petroleum ether/diethyl ether to give **39** (0.269 g, 0.00039 mol, 69%); ^{1}H-NMR (400 MHz, $CDCl_3$): δ 5.17 (1H, t, 9.7 Hz), 4.97 (2H, overlapped), 4.51 (1H, d, 7.9 Hz), 4.11 (1H, dd, *J*= 5.6, 10.7 Hz), 3.98 (1H, m), 3.86 (1H, dd, *J*= 3.9, 10.7 Hz), 3.67-3.60 (2H, m), 3.26 (1H, dd, *J*= 3.4, 14.7 Hz), 3.04 (1H, dd, *J*= 6.4, 14.7 Hz), 2.34 (3H, s, SAc), 2.34-2.31 (2H, overlapped), 2.08 (3H, s, OAc), 2.04 (3H, s, OAc), 2.00 (3H, s, OAc), 1.64-1.55 (2H, m, β-methylene), 1.34-1.23 (acyl chain methylenes), 0.88 (3H, t, *J*= 6.7 Hz, CH_3); HRESIMS *m/z* 727.3710 $[M+Na]^+$ (calcd for $C_{35}H_{60}O_{12}NaS$, 727.3703).

XI)

Compound 40: compound **39** (0.269 g, 0.00039 mol) was dissolved in potassium acetate (0.54 g), 34% (w/v) H_2O_2 (0.57 mL) and acetic acid (2 mL). The reaction mixture was stirred for 16h at 40 °C. After evaporation under a stream of nitrogen, the oily residue was purified by silica gel chromatography using a gradient of chloroform/methanol to give **40** (0.19 g, 0.00027 mol, 70%); ^{1}H-NMR (400 MHz, $CDCl_3$/MeOD 1/1): δ (1H, t, 9.6 Hz), 5.00-4.92 (2H, overlapped), 4.12-4.05 (2H, overlapped), 3.99 (1H, m), 3.92 (1H, dd, 3.5, 11.4 Hz), 3.74 (1H, dd, *J*= 5.0, 11.4 Hz), 3.07-3.00 (2H, overlapped), 2.36 (2H, t, *J*= 6.8 Hz, α-methylene), 2.09 (3H, s, OAc), 2.03 (3H, s, OAc), 2.00 (3H, s, OAc), 1.64-1.60 (2H, m, β-methylene), 1.35-1.24 (acyl chain methylenes), 0.90 (3H, t, *J*= 6.7 Hz, CH_3); HRESIMS *m/z* 709.3461 $[M]^-$ (calcd for $C_{33}H_{57}O_{14}S^-$, 709.3469).

XII)

Compound 41: compound **40** (0.19 g, 0.00027 mol) was dissolved in anhydrous dichloromethane (12 mL) prior to addition of BODIPY-undecanoic acid (**29**) (0.185 g, 0.00043 mol), *N,N*-dicyclohexylcarbodiimide (0.167 g, 0.00081 mol) and DMAP (0.064 g, 0.00054 mol). The reaction mixture was stirred for 16h at 60°C; after evaporation under reduced pressure, the mixture was purified by silica gel chromatography using a gradient of chloroform/methanol to give **41** (0.161 g, 0.00018 mol, 68%); ^{1}H-NMR (400 MHz, $CDCl_3$): δ 6.04 (2H, s), 5.23 (1H, m), 5.18 (1H, t, *J*= 9.7 Hz), 4.97 (2H, m), 4.61 (1H, d, 7.8 Hz), 4.27 (1H, dd, *J*= 3.4, 11.3 Hz), 4.14-4.05 (3H, overlapped), 3.75 (1H, m), 3.12 (2H, overlapped), 2.93 (2H, m), 2.51 (6H, bs, Me_4BODIPY methyls), 2.41 (6H, bs, Me_4BODIPY methyls), 2.33-2.25 (4H, m, α-methylenes), 2.04-1.98 (9H, s, 3 OAc), 1.64-1.55 (4H, m, β-methylenes), 1.32-1.21 (acyl chain methylenes), 0.88 (3H, t, *J*= 6.7 Hz, CH_3); HRESIMS *m/z* 1123.6114 $[M]^-$ (calcd for $C_{57}H_{90}BF_2N_2O_{15}S^-$, 1123.6123).

XIII)

Compound 42: compound **41** (0.161 g, 0.00018 mol) was dissolved in aq. ethanol (85%) (40 mL) and hydrazine mono-hydrate (0.101 g, 0.00216 mol) was added. The reaction mixture was stirred for 16h at 44°C. After evaporation under a stream of nitrogen, the mixture was purified by silica gel chromatography using a gradient of chloroform/methanol to give **42 (Sulfavant R-Me$_4$BODIPY)** (0.077 g, 0.0001 mol, 58%); ^{1}H-NMR (400 MHz, $CDCl_3$/MeOD 1/1): δ 6.17 (2H, s, Me$_4$BODIPY methynes), 5.29 (1H, m, H-2), 4.48 (1H, dd, *J*= 2.9, 12.0 Hz, H-1a), 4.32 (1H, d, *J*= 7.7 Hz, H-1'), 4.18 (1H, dd, 6.3, 11.6 Hz, H-1b), 4.09 (1H, dd, *J*= 5.0, 10.5 Hz, H-3a), 3.77-3.72 (2H, overlapped, H-3b, H-5'), 3.39 (1H, overlapped, H-6'a), 3.36 (1H, overlapped, H-3'), 3.20 (1H, t, *J*= 8.0 Hz, H-2'), 3.13 (1H, t, *J*= 9.0 Hz, H-4'), 3.06 (2H, m), 2.99 (1H, dd, J= 9.0, 14.0 Hz, H-6'b), 2.49 (6H, bs, Me$_4$BODIPY methyls), 2.47 (6H, bs, Me$_4$BODIPY methyls), 2.33-2.25 (4H, m, α-methylenes), 1.72-1.56 (8H, m), 1.45-1.32 (acyl chain methylenes), 0.92 (3H, t, *J*= 7.0 Hz, CH_3); ^{13}C-NMR (100 MHz, $CDCl_3$/MeOD 1/1): δ 174.5 (C), 174.3 (C), 154.2 (C), 147.6 (C), 141.0 (C), 131.8 (C), 122.2 (CH), 104.5 (CH, C-1'), 77.7 (CH), 75.0 (CH), 74.7 (CH), 74.1 (CH), 71.4 (CH), 68.7 (CH_2), 64.1 (CH_2), 54.5 (CH_2), 35.0 (CH_2), 32.7 (CH_2), 30.5-29.4 (acyl chains CH_2), 14.2 (CH_3); HRESIMS *m/z* 997.5800 $[M]^-$ (calcd for $C_{51}H_{84}BF_2N_2O_{12}S^-$, 997.5806).

4.8 Synthesis of 1-*O*-alkyl-2-*O*-(2'-*O*-β-D-glucopyranosyl-β-D-xylopyranosyl)-glycerol

- Preparation of the glyceride moiety:

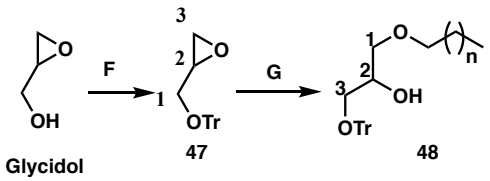

Scheme 2.13: Glycerol moiety preparation

F)

Compound 47: Trityl chloride (2 g, 0.0072 mol), was dissolved in dichloromethane (10 mL) and triethylamine (1.4 mL, 0.01 mol). The solution was kept at 0ºC and 2,3-Epoxy-1-propanol (0.5 g, 0.007 mol) was added dropwise. Successively DMAP (0.050 g, 0.0004 mol) were added and the temperature was raised to 25ºC. The reaction mixture was stirred for 16h at 25ºC and then it was quenched with distilled water and neutralized adding HCl (1M). The mixture was partitioned between water and chloroform, the organic phase was evaporated and purified by silica gel chromatography using a gradient of hexane/diethyl ether to give compound **47** (1.3 g, 0.0042 mol, 60%). ^{1}H-NMR (400 MHz, $CDCl_3$): δ 7.55 (6H, d, H-Ph), 7.4 (9H, m, H-Ph), 3.52 (2H, dd, H-1), 3.28 (1H, m, H-2), 2.77 (1H, t, H-3a), 2.65 (1H, m, H-3b). HRESIMS *m/z* 339.1360 $[M+Na]^+$ (calcd for $C_{22}H_{20}O_2Na^+$, 339.1356).

G)

Compound 48: potassium *tert*-butoxide (1.9 g, 0.017 mol) and alcohol (0.008 mmol) were added to a solution of compound **47** (1.3 g, 0.0042 mol) in DMF (22 mL). The reaction mixture was stirred for 2h at 100°C and then it was extracted with distilled water and diethyl ether. The organic layer was evaporated under reduced pressure and

the resulting residue was purified by silica gel chromatography using a gradient of hexane/ diethyl ether to give compound **48** (0.0031 mol, 75%). ^{1}H-NMR (400 MHz, $CDCl_3$): δ 7.55 (6H, d, H-Ph), 7.4 (9H, m, H-Ph), 3.9 (1H, m, H-2), 3.5 (2H, dd, H-3), 3.4 (2H, m, H-1), 3.2 (2H, t, CH_2 α alkyl chain), 1.5 (2H, m, CH_2 β alkyl chain), 1.1-1.2 (nH, aliphatic methylenes), 0.8 (3H, t, CH_3)

- The glycosyl donor was prepared with the same experimental procedures employed for the synthesis of Sulfavant A

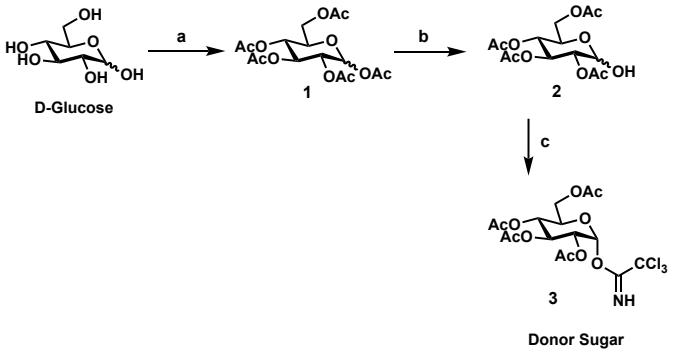

Scheme 2.11: Glycosyl donor preparation

- Preparation of the glycosyl acceptor:

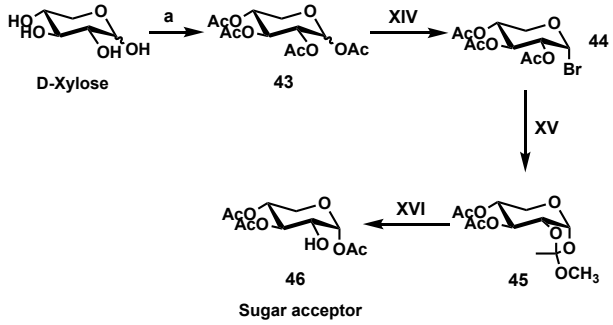

Scheme 2.12: Synthesis of Glycosyl acceptor

XIV-XV)

Compound 44 and 45: compound **43** (1.1 g**,** 0.0035 mol) was dissolved in CH_2Cl_2 (3.5 mL) and a solution HBr/CH_3COOH 33% (2 mL) was added drop by drop at 0ºC. The reaction mixture was stirred for 3h at 25ºC on activated 4 Å molecular sieves under argon atmosphere.

Then aqueous solution of saturated $NaHCO_3$ was added at 0ºC to quench the reaction and after a very fast extraction with CH_2Cl_2 the organic phase was dried under a stream of nitrogen. The acetobromo glycoside (**44**) was dissolved in dry acetonitrile (10 mL) and tetrabutylammonium bromide (0.80 g, 0.0025 mol), anhydrous sodium bicarbonate (0.60 g, 0.007 mol) and anhydrous methanol (1.4 mL, 0.010 mol) were added. The reaction mixture was stirred for 16h at 25ºC on activated 4 Å molecular sieves under argon atmosphere. The solvent was evaporated to dryness under reduced pressure and the residue was purified by silica gel chromatography using a gradient of hexane/diethyl ether to give compound **45** (0.4 g, 0.0014 mol, 40%); ^{1}H-NMR (400 MHz, $CDCl_3$: δ 5.58 (1H, d, H-1'), 5.25 (1H, t, H-3'), 4.8 (1H, m, H-4'), 4.2 (1H, m, H-2'), 3.9 (1H, dd, H-5'a), 3.7 (1H, dd, H-5'b), 3.27 (3H, s, CH_3O-), 2,08 (3H, s, CH_3CO-), 2.15 (3H, s, CH_3CO-), 1.7 (3H, s, -CH_3). HRESIMS *m/z*313.0901 $[M+Na]^+$ (calcd for $C_{12}H_{18}O_8Na^+$, 313.0894).

XVI)

Compound 46: compound **45** (0.4 g, 0.0014 mol) was dissolved in 95% aqueous acetic acid (1.8 mL) and the reaction mixture was stirred for 1h at 25ºC. The solvent was removed under a stream of nitrogen. The colorless oil obtained was dissolved in diethyl ether and was crystallized adding *n*-hexane to provide compound **46** (0.20 g, 0.00072 mol, 52%). %); ^{1}H-NMR (400 MHz, $CDCl_3$): δ 6.1 (1H, d, H-1'), 5.22 (1H, t, H-3') 4.95 (1H, m, H-4'), 3.86 (1H, dd, H-5'a), 3.81 (1H, dd, H-2'), 3.6 (1H, t, H-5'b). HRESIMS *m/z* 299.0731 $[M+Na]^+$ (calcd for $C_{11}H_{16}O_8Na^+$, 299.0737).

- Coupling reaction between Glycosyl donor and acceptor:

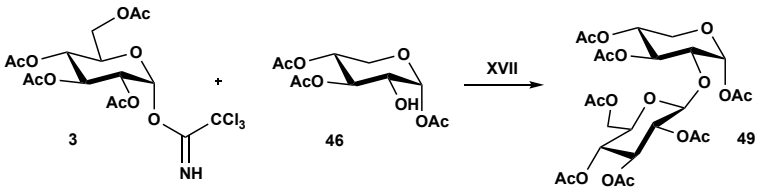

Scheme 2.14 Coupling reaction between sugar donor and acceptor

XVII)

Compound 49: 1'-*O*-trichloroacetimidate-2',3',4',6'-tetra-acetyl-glucose (**3**) (0.260 g, 0.00053 mol) was dissolved in anhydrous dichloromethane (4 mL) and 1.5 equiv. of **46** (0.220 g, 0.0008 mol) were added; the reaction mixture was kept at -20°C on activated 3 Å molecular sieves under argon; 0.2 equiv. of boron trifluoride etherate were added and stirring was maintained for 2 h; after another addition of boron trifluoride etherate (0.2 equiv.), the temperature was raised to -10°C and the reaction mixture was stirred overnight at that temperature. After neutralization with triethylamine (48 μL) and filtration on celite, the mixture was evaporated under reduced pressure and purified by silica gel chromatography using a hexane/diethyl ether gradient to give compound **49.** ^{1}H-NMR (400 MHz, $CDCl_3$): δ 6.2 (1H, d, H-1', J=3.7 Hz), 5.36 (1H, t, H-3'), 5.1 (1H, t, H-3''), 5.00 (1H, t, H-4''), 4.9-4.8 (2H, m, overlapped signals, H-4', H-2''), 4.57 (1H, d, H1'', J=7.9 Hz), 4.12 (2H, m, H-6''a, H-6''b), 3.8 (2H, m, overlapped signals, H-2', H-5'a), 3.64 (1H, m, H-5''), 3.58 (1H, t, H-5'b), 2.12-1.9 (21H, $COCH_3$). HRESIMS *m/z* 629.1680 $[M+Na]^+$ (calcd for $C_{25}H_{34}O_{17}Na^+$, 629.1688).

4.9 Modification of the Sulfavants Synthetic Strategy for the preparation of pure Sulfavant S

- Synthesis of (*S*)-1,2-*O*-distearoyl glycerol acceptor

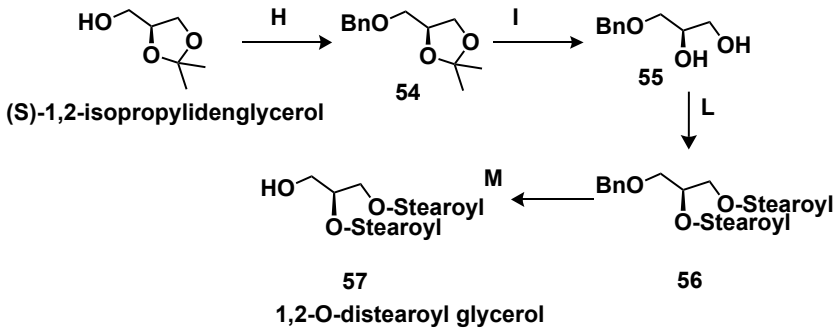

Scheme 2.17: Synthetic method used to prepare the new acceptor (*S*)-1,2-*O*-distearoyl glycerol

H)

Compound 54: Sodium hydride (0.235 g, 0.01 mol) was portion-wise added to (*S*)-(+)-1,2-isopropylideneglycerol (0.6 g, 0.00457 mol) dissolved in THF (7.5 mL) and after 30 min of stirring benzyl bromide (0.85 g, 0.005 mol) was added; after stirring for 20 h at 60°C the mixture was purified by silica gel chromatography using a light petroleum ether/diethyl ether gradient to give **54** (1 g, 0.0045 mol, 93%); ^{1}H-NMR (400 MHz, $CDCl_3$): δ 7.19-7.08 (5H, overlapped), 4.38 (2H, bs), 4.12 (1H, m), 3.86 (1H, m), 3.58 (1H, m), 3.38 (1H, m), 3.30 (1H, m), 1.27 (3H, s), 1.20 (3H, s). HRESIMS *m/z* 245.1140 $[M+Na]^+$ (calcd for $C_{13}H_{18}O_3Na^+$, 245.1148).

I)

Compound 55: Compound **54** (1 g, 0.0045 mol) was dissolved in methanol/water 95/5 (7 mL) and Dowex H^+ (7.3 g) was added; after 1.5h of stirring the mixture was filtered and evaporated giving compound **55** (0.762 g, 0.0042 mol, 93%); ^{1}H-NMR (400 MHz, $CDCl_3$): δ 7.29-7.17 (5H, overlapped, Ph), 4.58 (2H, bs), 3.86 (1H, m), 3.60 (1H, m), 3.52 (1H, m), 3.44 (2H, m). HRESIMS *m/z* 205.0829 $[M+Na]^+$ (calcd for $C_{10}H_{14}O_3Na^+$, 205.0835).

L)

Compound 56: compound **55** (0.762 g, 0.0042 mol) was dissolved in anhydrous dichloromethane (7 mL) prior to addition 1.1 equiv. of stearic acid, DCC (1 g, 0.008 mol) and DMAP (0.51 g, 0.0042 mol) under argon. The reaction mixture was stirred for 16h at 25ºC; after evaporation under reduced pressure, the mixture was purified by silica gel chromatography using a gradient of petroleum ether/diethyl ether to give compound **56** (2.76 g, 0.0039 mol, 92%) as pale-yellow oil. ^{1}H-NMR (400 MHz, $CDCl_3$): δ 7.29-7.17 (5H, overlapped, Ph), 5.28, (1H, m, H-2), 4.57 (2H, CH_2Bn), 4,39 (1H, dd, J=3.76 and 11.8 Hz, H-1a), 4.23 (1H, dd, J=6.4 and 11.8 Hz, H-1b), 3.63 (2H, bd, J=5.2 Hz, H-3), 2.33 (2H, m, α-methylene), 1.63 (2H, m, β-methylene), 1.28-1,32 (56H, m, CH_2 acyl chains), 0.83 (6H, m, CH_3 acyl chains). HRESIMS *m/z* 737.6062 $[M+Na]^+$ (calcd for $C_{46}H_{82}O_5Na^+$, 737.6054).

M)

Compound 57: Compound **56** (2.76 g, 0.0039 mol) was dissolved in THF/MeOH 1/1 (25 mL) and Pd-C (10%) (0.350 g) was added; after stirring for 16h at 25ºC the mixture was filtered, evaporated and purified by silica gel chromatography using a light petroleum ether/ethyl acetate gradient to give **57** (0.625 g, 0.001 mol, 25%); ^{1}H-NMR (400 MHz, $CDCl_3$): δ 5.1 (1H, m, H-2), 4.32 (1H, dd, J=4.4 and 11.9 Hz, H-1a), 4.23 (1H, dd, J=5.8 and 11.9 Hz, H-1b), 3.72 (2H, bd, J=4.8 Hz, H-3), 2.33 (2H,

m, α-methylene), 1.63 (2H, m, β-methylene), 1.21-1,35 (56H, m, CH_2 acyl chains), 0.85 (6H, m, CH_3 acyl chains). HRESIMS *m/z* 647.5591 $[M+Na]^+$ (calcd for $C_{39}H_{76}O_5Na^+$, 647.5585).

- coupling reaction for the preparation of pure Sulfavant S

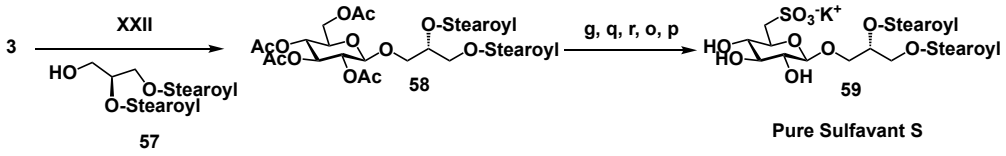

Scheme 2.18: Synthesis of pure Sulfavant S

XXII)

Compound 58: Compound 3 (0.491 g, 0.001 mol) and compound 57 (0.625 g, 0.001 mol) were dissolved in dried dichloromethane (15 mL) and the solution was kept at 0ºC, then TMSOTf (35 µL in 1,5 mL of CH_2Cl_2) was added dropwise. The reaction mixture was stirred on activated 3 Å molecular sieves under argon for 5h at 0ºC. the reaction was quenched adding triethylamine (150 µL) and the crude product was dried under reduced pressure and successively purified by silica gel chromatography using a gradient of petroleum ether/diethyl ether to give compound **58** (0.430 g, 0.00045 mol, 45%). ^{1}H-NMR (400 MHz, $CDCl_3$): δ 5.19 (1H, m), 5.06 (1H, overlapped), 4.99 (1H, t, J=9.5 Hz), 4.88 (1H, dd, J=9.5 and 7.9 Hz), 4.52 (1H, d), 4.02–4.32 (4H, overlapped), 3.93 (1H, dd, J=11.0 and 4.9 Hz), 3.68 (2H, m), 2.3 (4H, m) 1.98-2.02 (12H, bt), 1.60 (4H, m), 1.32-1.22 (56H), 0.89 (6H, t, J=6.9); HRESIMS 977.6545 $[M+Na]^+$ (calcd for $C_{53}H_{94}O_{14}Na$, 977.6541).

4.10 Scale-up of the Synthesis of Sulfavant A

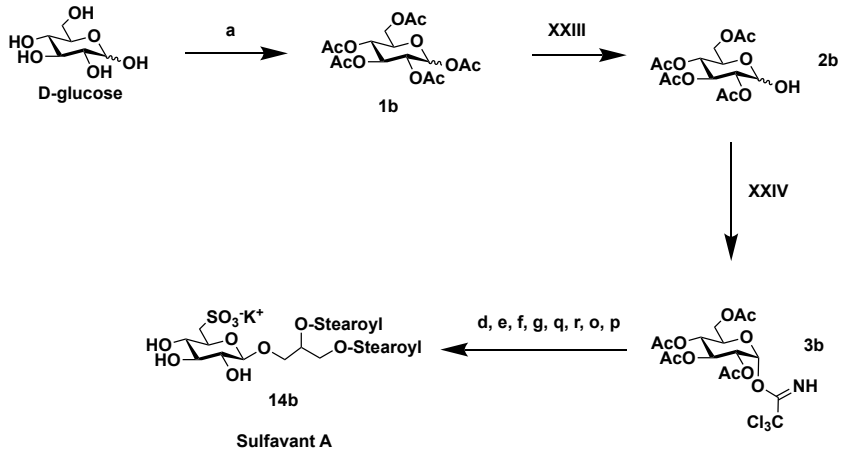

XXIII)

Compound 2b: Peracetylated glucose **(1b)** (40.9 g, 0.105 mol) was dissolved in tetrahydrofuran (50 mL) and 1.5 equiv. of Benzylamine were added dropwise; the reaction mixture was stirred for 24h at 25ºC. After 24h further 0.3 equiv. of Benzylamine were added dropwise and the reaction mixture was stirred overnight at 25ºC. After 40h the mixture was portioned in water and chloroform, the organic phase was evaporated under reduced pressure and purified by silica gel chromatography using a light petroleum ether/diethyl ether gradient to give compound **2b** (36.5 g, 0.105 mol, 96%).

XXIV)

Compound 3b: compound **2b** (36.5 g, 0.105 mol) was dissolved in anhydrous dichloromethane (100 mL); 3.0 equiv. of trichloroacetonitrile and 0.2 equiv. of 1,8-Diazabiciclo[5.4.0]undec-7-ene (DBU) were added; under Argon atmosphere the

reaction mixture was stirred for 2 h at 0°C on activated 3 Å molecular sieves; after evaporation under reduced pressure, the mixture was purified by silica gel chromatography using a light petroleum ether/diethyl ether gradient to give 1'-*O*-trichloroacetimidate-2',3',4',6'-tetra-acetyl-glucose (46.4 g, 0.095 mol, 90%).

4.11 Characterization of Sulfavants colloid nanoparticles

- Samples preparation for DLS Analysis:
  in collaboration with Professor Luigi Paduano from University of Naples Federico II, Dept of Chemical Sciences

After purification by HPLC, samples were prepared in 1 ml of Millipore water filtered on 0.22 μm pore size syringe filter at different concentration of each Sulfavant.
Initially, after sonication for 40 minutes at 35°C, the solutions were analysed immediately and after 2, 4, 24, 48h.
Successively, the ideal protocol was defined:
After sonication for 40 minutes at 35°C, the solutions maintained at room temperature (25°C) for 24 h. The mean diffusion coefficients were obtained as an average of at least three measurements at 25°C. Stability of the systems over time (1 week) was systematically controlled by the reproducibility of the diffusion coefficients.

- Samples preparation for CMC determination by surface tension:
  in collaboration with Professor Luigi Paduano from University of Naples Federico II, Dept of Chemical Sciences

2.5 mg of each Sulfavant was suspended in 10 mL of Millipore water filtered on 0.22 μm pore size syringe filter. All solutions were sonicated for 40 minutes at 35°C.
The surface tension of aqueous Sulfavant samples was measured with a Sigma 70 tensiometer (KSV, Stockholm, Sweden) using the Du Noüy ring method. Successive aliquots of the stock Sulfavant solutions, freshly prepared, were added to the vessel with a known volume of water. The CMCs were obtained as an average of at least three measurements at 25°C.

- Effect of detergent agents on aqueous solution of Sulfavants

4,25 µg of Sulfavant A were dissolved in 1 mL of D_2O. The solution was sonicated for 40 minutes at 35°C. After 24h the ^1H NMR spectrum was recorded on a Bruker DRX-600 equipped with a TXI CryoProbe.
At this sample 1,5 µL of a solution of TritonX100 (81 mg in 750 µL of D_2O) was added. 25h after sonication for 15 minutes, the ^1H NMR spectrum was recorded on a Bruker DRX-600 equipped with a TXI CryoProbe.

For the evaluation of the effect of Kolliphor RH40 on the biological activity of Sulfavant A, 100 µµµng of the detergent were added to various amounts of Sulfavant A dissolved in a total volume of 1 ml of PBS.

- Samples preparation for CMC determination by Fluorescence spectroscopy:

10 µL of 0.5 mM DPH dissolved in THF were added to various amounts of detergent dissolved in a total volume of 1 ml of Millipore water filtered on 0.22 µm pore size syringe filter. Before adding DPH, Sulfavant A solutions were sonicated for 40 minutes at 35ºC.
Tubes were incubated for 1 h in the dark at room temperature before measurement of fluorescence. The experiments were done with triplicate sets of samples and average fluorescence was evaluated.
Fluorescence intensity at 25°C was measured using an FP-8300 fluorometer (Jasco, Easton, MD): excitation wavelength: 390-550 nm, emission wavelength: 358nm.

- Samples preparation for cryo-TEM analysis:
  in collaboration with Professor Luigi Paduano from University of Naples Federico II, Dept of Chemical Sciences, Professor Piero Lupetti from University of Siena, Dept of Life Sciences and with Dr. Marie-Sousai

Appavou of Jülich Centre for Neutron Science JCNS at Heinz Maier-Leibnitz Zentrum (MLZ) - 85748 Garching – Germany.

For these experiments the following solutions were prepared in a total volume of 1 mL of Millipore water filtered on 0.22 μm pore size syringe filter:

- Sulfavant A 10 nM;
- Sulfavant R 10 nM;
- Sulfavant A 10 μM;
- Sulfavant R 10 μM.

The samples were sonicated for 40 minutes at 35ºC and the cryo-TEM images were acquired at least 24h after sonication.

Another sample preparation protocol was conducted for these analyses: Sulfavant A 10 μM and Sulfavant R 10 μM, suspended in 1 mL of Millipore water filtered on a 0.22 μm pore size syringe filter, were subjected to sonication for 40 minutes at 35ºC. cryo-TEM images were acquired at least 24h after sonication.

4.12 Biological activity evaluation

- Human monocyte-dendritic cell differentation.

For each assay human peripheral blood mononuclear cells were isolated from two healthy donors by routine Ficoll density gradient centrifugation. Monocytes were purified from human peripheral blood mononuclear cells using MACS CD14 microbeads (Miltenyi Biotech, Auburn, CA) according to the manufacturer's recommendation. Purity was checked by staining with a FITC-conjugated anti-CD14 antibody (Milteny Biotech) and FACS analysis and was routinely found to be greater than 98%. Immature DCs were obtained by incubating monocytes at $7 \cdot 10^5$cell/mL in RPMI 1640 medium supplemented with 10% fetal calf serum, 1% L-glutamine 2 mM, 1% penicillin and streptomycin, human IL-4 (5 ng/mL) and human GM-CSF (100 ng/mL) for five days.

- Cells Staining and stimulation.

After five days in culture, surface staining was performed on monocyte-derived dendritic cells for flow cytometry analysis. moDCs were stained by using the following conjugated mAbs from BD- Biosciences: CD14Fitc, CD1a-BUV121, CD86 BV650, CD83BUV737, HLA-DRBV786, CD11c- BUV395, CD3 BV510, CD54Pe, CD1c Alexa Fluor 647, CD4- PeCys7, and analysed by flow-cytometer (BD LSR Fortessa X-20, BD Bioscience, Milano, Italy) according to standard protocol. moDCs were then incubated with synthetic compounds in 12-wells at concentration of 0.01-0.1-1-10 μg mL^{-1}. Stimulation with PAM2CSK4 1μg mL^{-1} (Invivogen) was used as positive control. After 24 hours expression of all surface markers was estimated again by fluorochrome-conjugated antibodies.

- Real Time PCR analysis.

Total RNA was isolated using Trizol Reagent, according to the manufacturer's protocol. RNA quantity and purity were measured with a NanoDrop 2000 spectrophotometer (Thermo Scientific). Sample purity was checked by A260/A280 ratios between 1.80 and 2.00. Extracted RNAs from all preparations were in this range. Cytokines mRNA expression was measured by quantitative Real Time-PCR (QuantStudio 7 Flex Real-Time PCR System; Thermo Scientific). All data were analysed by two-way ANOVA followed by the Tukey test for multiple comparison test. A p-value less than 0.05 was considered as statistically significant. All analyses were performed using the GraphPad Prism 6.00 for Windows software (GraphPad Software, San Diego California, USA).

- PCR Array analysis.

About 200 ng RNA was subjected to reverse transcription reaction using the RT2 first strand kit (Qiagen, Hilden, Germany) according to the manufacturer’s instructions. e qRT-PCR analysis was performed in triplicate using the RT2 Profiler PCR Array kit (Qiagen, Hilden, Germany), in order to analyse the expression of inflammatory cytokines and receptors on dendritic cells stimulated. Plates were run on an Applied Biosystem ViiA 7 Real-Time PCR System (384 well blocks) (Thermo Scientific, Waltham, MA, USA) by Standard Fast PCR Cycling protocol with 10 µl reaction volumes. Cycling conditions used were: 1 cycle initiation at 95.0 °C for 10 min followed by amplification for 40 cycles at 95.0 °C for 15 s and 60.0 °C for 1 min. Amplification data were collected via A ViiA 7 RUO So ware (Applied Biosystems). e cycle threshold (Ct)-values were analysed with PCR array data analysis online so ware (Qiagen, Hilden, Germany).

- TLR assay.

Human TLR-4/NF-kB/SEAP and TLR2/ NF-kB/SEAP (SEAPorterTM) HEK 293 reporter cells (Novus Biologicals, Littleton, CO, USA) were plated in 24-well plates at 2×105 cells/well. After 16 hours, for functional assays, TLR4 cells, cells were transiently transfected with MD2/CD14 plasmid vector (Invivogen, San Diego, CA, USA) for 24 hours. Cells were then stimulated with Sulfavant A for 24 hours. LPS for TLR-4 cell line and Pam2CSK4 for TLR-2 cell line were used as positive control under the same conditions. SEAP was analysed using the SEAPorter Assay (Novus Biologicals, Littleton, CO, USA) in according to manufacturer's instructions. Quantitative data (ng/mL) were obtained by a standard curve for the SEAP protein.

- Immunization protocol.

Immunization of C56BL/6 mice (four groups of three individuals) was carried out by injecting twice 5 μg Ovalbumin (OVA) (Hyglos GmbH, Bernried am Starnberger See, Germany) together with 2.5 mg of Sulfavant A according to published protocols. OVA-specific Ig production was measured by ELISA according to Leung S *et al*.61. Titermax and Complete Freund's Adjuvant (Sigma Aldrich, St. Louis, MO, USA) were used according to manufacturer instructions. Statistical analyses were performed by ANOVA using the GraphPad Prism 4.0 So ware (GraphPad So ware, Inc, La Jolla, CA).

- Comparative analysis of cancer vaccine formulations.

Experiments were carried out according to the published protocol45 by challenging C57BL/6 J mice with subcutaneously injection of B16F10 melanoma cells (1 × 105 cells/mouse). Prior to challenge, the animals were immunized three times at days −14, −7 and 0 by subcutaneous injection of $hgp100_{25–33}$ peptide (100 μg/mouse injection) in association with one of the following products: CpG (30 μg) (Tib MolBiol, Genoa,

Italy), Freund's adjuvant (1:1 v/v) (Sigma Aldrich, St. Louis, MO), Sulfavant A (600 μg). Formulations were carried out according to manufacturers' instructions. For Sulfavant A, the melanoma antigen was simply added to a stable emulsion of the sulfolipid in phosphate buffer prior to injection. Experiments were carried out on groups of 8 animals each. Tumour masses were measured with a calliper at 2–3 days intervals by measuring long and short axes. Volume was calculated according to the formula: tumour volume = 1⁄2 (length × width^2) in cm^3. Mice were sacrificed when either tumours reached > 1 cm^3, when ulceration/bleeding developed, or after 30 days from the tumour challenge. Mice treated with hgp100$_{25–33}$ peptide alone prior to challenging with B16F10 cells (1 × 105 cells/mouse) were used as negative control. Statistical analyses were performed by the Mann-Whitney unpaired T test for nonparametric measures using the GraphPad Prism 4.0 So ware (GraphPad So ware, Inc, La Jolla, CA).

- Cytotoxic assay on moDcs

Cells were incubated in 12-well plates (7x10^5 cells/well) with compounds at concentration of 0.01- 0.1-1-10 μg/mL, vehicle and PAM2CSK4. After 24 hours, cells were collected and were stained with Annexin V-FITC and propidium iodide (PI) according to the manufacturer's instructions (Dead Cell Apoptosis Kit with Annexin V FITC and PI, for flow cytometry; Invitrogen). Untreated cells were used as the control for double staining. The cells were analysed immediately after staining using a FACScan flow cytometer (BD Accuri C6). For each measurement, at least 10,000 cells were counted. After staining apoptotic cells show green fluorescence, dead cells (late apoptotic) show red and green fluorescence, and live cells show little or no fluorescence.

References

1. [BOOK] Sasaki, D. (2008). Glycolipids: new research. Nova Publishers.
2. [BOOK] Vance, D. E., Vance, J. E. (Eds.). (1996). Biochemistry of lipids, lipoproteins and membranes. Elsevier.
3. Hölzl, G., Dörmann, P. (2007). Structure and function of glycoglycerolipids in plants and bacteria. Progress in lipid research, 46(5), 225-243.
4. Oshima, Y., Yamada, S. H., Matsunaga, K., Moriya, T., Ohizumi, Y. (1994). A monogalactosyl diacylglycerol from a cultured marine dinoflagellate, Scrippsidla trochoidea. Journal of natural products, 57(4), 534-536.
5. Nakata, K., Guo, C. T., Matsufuji, M., Yoshimoto, A., Trmgnlri, M., Higuchi, R., Suzuki, Y. (2000). Influenza A virus-binding activity of glycoglycerolipids of aquatic bacteria. The Journal of Biochemistry, 127(2), 191-198.
6. Costantino, V., Fattorusso, E., Menna, M., Taglialatela-Scafati, O. (2004). Chemical diversity of bioactive marine natural products: an illustrative case study. Current medicinal chemistry, 11(13), 1671-1692.
7. Gaspar, H., Cutignano, A., Grauso, L., Neng, N., Cachatra, V., Fontana, A., Xavier, J., Cerejo, M., Vieira, H., Santos, S. (2016). Erylusamides: Novel Atypical Glycolipids from Erylus cf. deficiens. Marine drugs, 14(10), 179.
8. Powers, D. A. (1989). Fish as model systems. Science, 246(4928), 352-358.
9. Bule, M. H., Ahmed, I., Maqbool, F., Bilal, M., Iqbal, H. M. N. (2018). Microalgae as a source of high-value bioactive compounds. Front. Biosci.(Sch. Ed.), 10, 197-216.
10. García-Vilas, J., Martínez-Poveda, B., Quesada, A., Medina, M. (2016). Aeroplysinin-1, a sponge-derived multi-targeted bioactive marine drug. Marine drugs, 14(1), 1.

11. Bule, M. H., Ahmed, I., Maqbool, F., Bilal, M., Iqbal, H. M. (2018). Microalgae as a source of high-value bioactive compounds. Frontiers in Bioscience, 10, 197-216.
12. Romano, G., Costantini, M., Sansone, C., Lauritano, C., Ruocco, N., Ianora, A. (2017). Marine microorganisms as a promising and sustainable source of bioactive molecules. Marine environmental research, 128, 58-69.
13. Borowitzka, M. A. (1995). Microalgae as sources of pharmaceuticals and other biologically active compounds. Journal of Applied Phycology, 7(1), 3-15.
14. Vinayak, V., Manoylov, K., Gateau, H., Blanckaert, V., Hérault, J., Pencréac'h, G., Marchand, J., Gordon, R., Schoefs, B. (2015). Diatom milking: a review and new approaches. Marine drugs, 13(5), 2629-2665.
15. Sahu, A., Pancha, I., Jain, D., Paliwal, C., Ghosh, T., Patidar, S., Bhattacharya, S., Mishra, S. (2013). Fatty acids as biomarkers of microalgae. Phytochemistry, 89, 53-58.
16. Benson, A. A., Daniel, H., Wiser, R. (1959). A sulfolipid in plants. Proceedings of the National Academy of Sciences of the United States of America, 45(11), 1582.
17. Wintermans, J. F. G. M. (1960). Concentrations of phosphatides and glycolipids in leaves and chloroplasts. Biochimica et biophysica acta, 44, 49-54.
18. Benson, A. A. (1963). The plant sulfolipid. In Advances in lipid research (Vol. 1, pp. 387-394). Elsevier.
19. Haines, T. H. (1973). Halogen-and sulfur-containing lipids of Ochromonas. Annual Reviews in Microbiology, 27(1), 403-412.
20. Bishop, D. G., Sparace, S. A., Mudd, J. B. (1985). Biosynthesis of sulfoquinovosyldiacylglycerol in higher plants: The origin of the diacylglycerol moiety. Archives of biochemistry and biophysics, 240(2), 851-858.

21. Kates, M. (1970). Plant phospholipids and glycolipids. In Advances in lipid research (Vol. 8, pp. 225-265). Elsevier.
22. Elbein, A. D. (1982). Glycolipids and other glycosides. In Plant Carbohydrates I (pp. 601-612). Springer, Berlin, Heidelberg.
23. Haines, T. H. (1983). Anionic lipid headgroups as a proton-conducting pathway along the surface of membranes: a hypothesis. Proceedings of the National Academy of Sciences, 80(1), 160-164.
24. Morimoto, T., Nagatsu, A., Murakami, N., Sakakibara, J., Tokuda, H., Nishino, H., Iwashima, A. (1995). Anti-tumour-promoting glyceroglycolipids from the green alga, Chlorella vulgaris. Phytochemistry, 40(5), 1433-1437.
25. Andrianasolo, E. H., Haramaty, L., Vardi, A., White, E., Lutz, R., Falkowski, P. (2008). Apoptosis-inducing galactolipids from a cultured marine diatom, Phaeodactylum tricornutum. Journal of natural products, 71(7), 1197-1201.
26. Maeda, N., Hada, T., Yoshida, H., Mizushina, Y. (2007). Inhibitory effect on replicative DNA polymerases, human cancer cell proliferation, and in vivo anti-tumor activity by glycolipids from spinach. Current medicinal chemistry, 14(9), 955-967.
27. Farokhi, F., Wielgosz-Collin, G., Robic, A., Debitus, C., Malleter, M., Roussakis, C., Kornprobst, M., Barnathan, G. (2012). Antiproliferative activity against human non-small cell lung cancer of two O-alkyl-diglycosylglycerols from the marine sponges Myrmekioderma dendyi and Trikentrion laeve. European journal of medicinal chemistry, 49, 406-410.
28. Brady, R. C., Bernstein, D. I. (2004). Treatment of herpes simplex virus infections. Antiviral research, 61(2), 73-81.
29. Morfin, F., Thouvenot, D. (2003). Herpes simplex virus resistance to antiviral drugs. Journal of Clinical Virology, 26(1), 29-37.
30. Bacon, T. H., Levin, M. J., Leary, J. J., Sarisky, R. T., Sutton, D. (2003). Herpes simplex virus resistance to acyclovir and penciclovir after two decades of antiviral therapy. Clinical microbiology reviews, 16(1), 114-128.

31. Vo, T. S., Ngo, D. H., Van Ta, Q., Kim, S. K. (2011). Marine organisms as a therapeutic source against herpes simplex virus infection. European Journal of Pharmaceutical Sciences, 44(1-2), 11-20.
32. Plouguerné, E., de Souza, L., Sassaki, G., Cavalcanti, J., Villela Romanos, M., da Gama, B., Pereira, R.C., Barreto-Bergter, E. (2013). Antiviral sulfoquinovosyldiacylglycerols (SQDGs) from the Brazilian brown seaweed Sargassum vulgare. Marine drugs, 11(11), 4628-4640.
33. Mattos, B. B., Romanos, M. T. V., Souza, L. M. D., Sassaki, G., Barreto-Bergter, E. (2011). Glycolipids from macroalgae: potential biomolecules for marine biotechnology?. Revista Brasileira de Farmacognosia, 21(2), 244-247.
34. Reshef, V., Mizrachi, E., Maretzki, T., Silberstein, C., Loya, S., Hizi, A., Carmeli, S. (1997). New acylated sulfoglycolipids and digalactolipids and related known glycolipids from cyanobacteria with a potential to inhibit the reverse transcriptase of HIV-1. Journal of natural products, 60(12), 1251-1260.
35. Bruno, A., Rossi, C., Marcolongo, G., Di Lena, A., Venzo, A., Berrie, C. P., Corda, D. (2005). Selective in vivo anti-inflammatory action of the galactolipid monogalactosyldiacylglycerol. European journal of pharmacology, 524(1-3), 159-168.
36. Larsen, E., Kharazmi, A., Christensen, L. P., Christensen, S. B. (2003). An Antiinflammatory Galactolipid from Rose Hip (Rosa c anina) that Inhibits Chemotaxis of Human Peripheral Blood Neutrophils in Vitro. Journal of Natural Products, 66(7), 994-995.
37. Matsumoto, Y., Sahara, H., Fujita, T., Shimozawa, K., Takenouchi, M., Torigoe, T., Hanashima, S., Yamazaki, T., Takahashi, S., Sugawara, F., Mizushina, Y. Ohta, K., Takahashi, N., Gasa, S., Jimbow, K., Sakaguchi, K., Sato, N. (2002). An immunosuppressive effect by synthetic sulfonolipids

deduced from sulfonoquinovosyl diacylglycerols of sea urchin. Transplantation, 74(2), 261-267.

38. Manzo, E., Cutignano, A., Pagano, D., Gallo, C., Barra, G., Nuzzo, G., Sansone, C., Ianora, A., Urbanek, K., Fenoglio, D., Ferrera, F., Bernardi, C., Parodi, A., Pasquale, G., Leonardi, A., Filaci, G., De Palma, R., Fontana, A. (2017). A new marine-derived sulfoglycolipid triggers dendritic cell activation and immune adjuvant response. Scientific reports, 7(1), 6286.
39. [BOOK] Abbas, A. K., Lichtman, A. H., Pillai, S. (2014). Basic immunology: functions and disorders of the immune system. Elsevier Health Sciences.
40. [BOOK] Janeway Jr, C. A., Travers, P., Walport, M., Shlomchik, M. J. (2001). Immunobiology: The Immune System in Health and Disease. 5th edition. Garland Science.
41. Berard, M., Tough, D. F. (2002). Qualitative differences between naive and memory T cells. Immunology, 106(2), 127-138.
42. Corthay, A. (2009). How do regulatory T cells work?. Scandinavian journal of immunology, 70(4), 326-336.
43. Lewis, D. E., Blutt, S. E. (2019). Organization of the immune system. In Clinical Immunology, 19-38.
44. Schroeder Jr, H. W., Cavacini, L. (2010). Structure and function of immunoglobulins. Journal of Allergy and Clinical Immunology, 125(2), S41-S52.
45. Karlmark, K., Tacke, F., Dunay, I. (2012). Monocytes in health and disease—Minireview. European Journal of Microbiology and Immunology, 2(2), 97-102.
46. Breedveld, A., Groot Kormelink, T., van Egmond, M., de Jong, E. C. (2017). Granulocytes as modulators of dendritic cell function. Journal of leukocyte biology, 102(4), 1003-1016.

47. Lee, D. M., Friend, D. S., Gurish, M. F., Benoist, C., Mathis, D., Brenner, M. B. (2002). Mast cells: a cellular link between autoantibodies and inflammatory arthritis. Science, 297(5587), 1689-1692.
48. Zhang, J. M., An, J. (2007). Cytokines, inflammation and pain. International anesthesiology clinics, 45(2), 27.
49. Berger, A. (2000). Th1 and Th2 responses: what are they?. British Medical Journal, 321(7258), 424.
50. Parkin, J., Cohen, B. (2001). An overview of the immune system. The Lancet, 357(9270), 1777-1789.
51. [BOOK] Janeway Jr, C. A., Travers, P., Walport, M., Shlomchik, M. J. (2001). The complement system and innate immunity. In Immunobiology: The Immune System in Health and Disease. 5th edition. Garland Science.
52. Ehrnthaller, C., Ignatius, A., Gebhard, F., Huber-Lang, M. (2011). New insights of an old defense system: structure, function, and clinical relevance of the complement system. Molecular medicine, 17(3), 317.
53. Nesargikar, P., Spiller, B., Chavez, R. (2012). The complement system: history, pathways, cascade and inhibitors. European Journal of Microbiology and Immunology, 2(2), 103-111.
54. Stahl, G. L., Xu, Y., Hao, L., Miller, M., Buras, J. A., Fung, M., Zhao, H. (2003). Role for the alternative complement pathway in ischemia/reperfusion injury. The American journal of pathology, 162(2), 449-455.
55. Vorup-Jensen, T., Petersen, S. V., Hansen, A. G., Poulsen, K., Schwaeble, W., Sim, R. B., Reid, K. B. M., Simon J. Davis, S. J., Thiel, S., Jensenius, J. C. (2000). Distinct pathways of mannan-binding lectin (MBL)-and C1-complex autoactivation revealed by reconstitution of MBL with recombinant MBL-associated serine protease-2. The Journal of Immunology, 165(4), 2093-2100.

56. Beck, S., Trowsdale, J. (2000). The human major histocompatibility complex: lessons from the DNA sequence. Annual review of genomics and human genetics, 1(1), 117-137.
57. Gruen, J. R., Weissman, S. M. (2001). Human MHC class III and IV genes and disease associations. Frontiers in Bioscience, 6, D960-972.
58. Hewitt, E. W. (2003). The MHC class I antigen presentation pathway: strategies for viral immune evasion. Immunology, 110(2), 163-169.
59. Hansen, T. H., Bouvier, M. (2009). MHC class I antigen presentation: learning from viral evasion strategies. Nature Reviews Immunology, 9(7), 503.
60. Rodriguez, A., Regnault, A., Kleijmeer, M., Ricciardi-Castagnoli, P., Amigorena, S. (1999). Selective transport of internalized antigens to the cytosol for MHC class I presentation in dendritic cells. Nature cell biology, 1(6), 362.
61. Roche, P. A., Furuta, K. (2015). The ins and outs of MHC class II-mediated antigen processing and presentation. Nature Reviews Immunology, 15(4), 203.
62. Unanue, E. R. (2002). Perspective on antigen processing and presentation. Immunological reviews, 185(1), 86-102.
63. Steinman, R. M., Cohn, Z. A. (1974). Identification of a novel cell type in peripheral lymphoid organs of mice: II. Functional properties in vitro. Journal of Experimental Medicine, 139(2), 380-397
64. https://www.nobelprize.org/prizes/medicine/2011/steinman/biographical/
65. Steinman, R. M., Banchereau, J. (2007). Taking dendritic cells into medicine. Nature, 449(7161), 419.
66. Ochando, J. C., Homma, C., Yang, Y., Hidalgo, A., Garin, A., Tacke, F., Angeli, V., Li, Y., Boros, P., Ding, Y., Jessberger, R., Trinchieri, G., Lira, S. A., Randolph, G. J., Bromberg, J. S. (2006). Alloantigen-presenting

plasmacytoid dendritic cells mediate tolerance to vascularized grafts. Nature immunology, 7(6), 652.

67. Goubier, A., Dubois, B., Gheit, H., Joubert, G., Villard-Truc, F., Asselin-Paturel, C., Trinchieri, G., Kaiserlian, D. (2008). Plasmacytoid dendritic cells mediate oral tolerance. Immunity, 29(3), 464-475.
68. Van Brussel, I., Berneman, Z. N., Cools, N. (2012). Optimizing dendritic cell-based immunotherapy: tackling the complexity of different arms of the immune system. Mediators of inflammation, 2012.
69. Dalod, M., Chelbi, R., Malissen, B., Lawrence, T. (2014). Dendritic cell maturation: functional specialization through signaling specificity and transcriptional programming. The EMBO journal, 33(10), 1104-1116.
70. Sabado, R. L., Bhardwaj, N. (2010). Directing dendritic cell immunotherapy towards successful cancer treatment. Immunotherapy, 2(1), 37-56.
71. Geijtenbeek, T. B., Torensma, R., van Vliet, S. J., van Duijnhoven, G. C., Adema, G. J., van Kooyk, Y., Figdor, C. G. (2000). Identification of DC-SIGN, a novel dendritic cell–specific ICAM-3 receptor that supports primary immune responses. Cell, 100(5), 575-585.
72. Mbongue, J. C., Nieves, H. A., Torrez, T. W., Langridge, W. H. (2017). The role of dendritic cell maturation in the induction of insulin-dependent diabetes mellitus. Frontiers in immunology, 8, 327.
73. Hubo, M., Trinschek, B., Kryczanowsky, F., Tuettenberg, A., Steinbrink, K., Jonuleit, H. (2013). Costimulatory molecules on immunogenic versus tolerogenic human dendritic cells. Frontiers in immunology, 4, 82.
74. Nestle, F. O., Alijagic, S., Gilliet, M., Sun, Y., Grabbe, S., Dummer, R., Burg, G., Schadendorf, D. (1998). Vaccination of melanoma patients with peptide- or tumorlysate-pulsed dendritic cells. Nature medicine, 4(3), 328.
75. Dhodapkar, M. V., Steinman, R. M., Sapp, M., Desai, H., Fossella, C., Krasovsky, J., Donahoe, S. M., Dunbar, P. R., Cerundolo, V., Nixon, D. F., Bhardwaj, N. (1999). Rapid generation of broad T-cell immunity in humans

after a single injection of mature dendritic cells. The Journal of clinical investigation, 104(2), 173-180.

76. Steinman, R. M. (2007). Dendritic cells: understanding immunogenicity. European journal of immunology, 37(S1), S53-S60.
77. Vandebriel, R. J., Hoefnagel, M. H. (2012). Dendritic cell-based in vitro assays for vaccine immunogenicity. Human vaccines & immunotherapeutics, 8(9), 1323-1325.
78. Mizumoto, N., Gao, J., Matsushima, H., Ogawa, Y., Tanaka, H., Takashima, A. (2005). Discovery of novel immunostimulants by dendritic-cell–based functional screening. Blood, 106(9), 3082-3089.
79. Rey-Ladino, J., Ross, A. G., Cripps, A. W., McManus, D. P., Quinn, R. (2011). Natural products and the search for novel vaccine adjuvants. Vac
80. Dowds, C. M., Kornell, S. C., Blumberg, R. S., Zeissig, S. (2014). Lipid antigens in immunity. Biological chemistry, 395(1), 61-81.
81. De Libero, G., Mori, L. (2014). The T-cell response to lipid antigens of Mycobacterium tuberculosis. Frontiers in immunology, 5, 219.
82. De Libero, G., Mori, L. (2010). How the immune system detects lipid antigens. Progress in lipid research, 49(2), 120-127.
83. Chang, Y. J., Huang, J. R., Tsai, Y. C., Hung, J. T., Wu, D., Fujio, M., Wong, C-H., Alice, L. Y. (2007). Potent immune-modulating and anticancer effects of NKT cell stimulatory glycolipids. Proceedings of the National Academy of Sciences, 104(25), 10299-10304.
84. Vartabedian, V. F., Savage, P. B., Teyton, L. (2016). The processing and presentation of lipids and glycolipids to the immune system. Immunological reviews, 272(1), 109-119.
85. Mattner, J., DeBord, K. L., Ismail, N., Goff, R. D., Cantu III, C., Zhou, D., Saint-Mezard, P., Wang, V., Gao, Y., Yin, N., Hoebe, K., Schneewind, O., Walker, D., Beutler, B., Teyton, L., Savage, P. B., Bendelac, A. (2005).

Exogenous and endogenous glycolipid antigens activate NKT cells during microbial infections. Nature, 434(7032), 525.

86. Johnson, D. A. (2008). Synthetic TLR4-active glycolipids as vaccine adjuvants and stand-alone immunotherapeutics. Current topics in medicinal chemistry, 8(2), 64-79.
87. E. Tritto, F. Mosca, E. De Gregorio, E "Mechanism of action of licensed vaccine adjuvants" Vaccine, 27 (25-26) (2009), 3331-3334.
88. R. Rappuoli, M. Pizza, G. Del Giudice, E. De Gregorio "Vaccines, new opportunities for a new society" Proceedings of the National Academy of Sciences, 111(34) (2014), 12288-12293.
89. T. Olafsdottir, M. Lindqvist, A. M. Harandi "Molecular signatures of vaccine adjuvants" Vaccine, 33(40) (2015) 5302-5307.
90. Di Pasquale, S. Preiss, F.T. Da Silva, N. Garcon, "Vaccine Adjuvants: From 1920 to 2015 and Beyond" Vaccines, 3 (2015) 320–343
91. Riedel, S. (2005, January). Edward Jenner and the history of smallpox and vaccination. In Baylor University Medical Center Proceedings (Vol. 18, No. 1, pp. 21-25). Taylor & Francis.
92. Gross, C. P., Sepkowitz, K. A. (1998). The myth of the medical breakthrough: smallpox, vaccination, and Jenner reconsidered. International journal of infectious diseases, 3(1), 54-60.
93. Stearns, R. P., Pasti, G. (1950). Remarks upon the introduction of inoculation for smallpox in England. Bulletin of the History of Medicine, 24, 103.
94. Bhattacharya, S. (2008). The World Health Organization and global smallpox eradication. Journal of Epidemiology & Community Health, 62(10), 909-912.
95. Cherry, J. D. (1996). Historical review of pertussis and the classical vaccine. Journal of Infectious Diseases, 174(Supplement_3), S259-S263.
96. Marciani, D. J. (2003). Vaccine adjuvants: role and mechanisms of action in vaccine immunogenicity. Drug discovery today, 8(20), 934-943.

97. Savelkoul, H., Ferro, V., Strioga, M., Schijns, V. (2015). Choice and design of adjuvants for parenteral and mucosal vaccines. Vaccines, 3(1), 148-171.
98. Apostólico, J. D. S., Lunardelli, V. A. S., Coirada, F. C., Boscardin, S. B., Rosa, D. S. (2016). Adjuvants: classification, modus operandi, and licensing. Journal of immunology research, 2016.
99. Sokolovska, A., Hem, S. L., HogenEsch, H. (2007). Activation of dendritic cells and induction of CD4+ T cell differentiation by aluminum-containing adjuvants. Vaccine, 25(23), 4575-4585.
100. Hem, S. L., HogenEsch, H. (2007). Relationship between physical and chemical properties of aluminum-containing adjuvants and immunopotentiation. Expert review of vaccines, 6(5), 685-698.
101. Ulanova, M., Tarkowski, A., Hahn-Zoric, M., Hanson, L. Å. (2001). The common vaccine adjuvant aluminum hydroxide up-regulates accessory properties of human monocytes via an interleukin-4-dependent mechanism. Infection and immunity, 69(2), 1151-1159.
102. Billiau, A., Matthys, P. (2001). Modes of action of Freund's adjuvants in experimental models of autoimmune diseases. Journal of leukocyte biology, 70(6), 849-860.
103. Salk, J. E., Laurent, A. M. (1952). The use of adjuvants in studies on influenza immunization: I. Measurements in monkeys of the dimensions of antigenicity of virus-mineral oil emulsions. Journal of Experimental Medicine, 95(5), 429-447.
104. [BOOK] Karandikar, S., Mirani, A., Waybhase, V., Patravale, V. B., Patankar, S. (2017). Nanovaccines for oral delivery-formulation strategies and challenges. In Nanostructures for Oral Medicine, 263-293. Elsevier.
105. Sun, H. X., Xie, Y., Ye, Y. P. (2009). Advances in saponin-based adjuvants. Vaccine, 27(12), 1787-1796.
106. Takeshita, F., Leifer, C. A., Gursel, I., Ishii, K. J., Takeshita, S., Gursel, M., Klinman, D. M. (2001). Cutting edge: role of Toll-like receptor 9

in CpG DNA-induced activation of human cells. The Journal of Immunology, 167(7), 3555-3558.

107. Wagner, H. (1999). Bacterial CpG DNA activates immune cells to signal infectious danger. In Advances in immunology, 73, 329-368. Academic Press.

108. Klinman, D. M., Conover, J., Coban, C. (1999). Repeated administration of synthetic oligodeoxynucleotides expressing CpG motifs provides long-term protection against bacterial infection. Infection and immunity, 67(11), 5658-5663.

109. Singh, M., Ott, G., Kazzaz, J., Ugozzoli, M., Briones, M., Donnelly, J., (2001). Cationic microparticles are an effective delivery system for immune stimulatory CpG DNA. Pharmaceutical research, 18(10), 1476-1479.

110. Kalvodova, L. (2010). Squalene-based oil-in-water emulsion adjuvants perturb metabolism of neutral lipids and enhance lipid droplet formation. Biochemical and biophysical research communications, 393(3), 350-355.

111. Calabro, S., Tritto, E., Pezzotti, A., Taccone, M., Muzzi, A., Bertholet, S., De Gregorio, E., O'Hagan, D. T., Seubert, A. (2013). The adjuvant effect of MF59 is due to the oil-in-water emulsion formulation, none of the individual components induce a comparable adjuvant effect. Vaccine, 31(33), 3363-3369.

112. Rappuoli, R., Mandl, C. W., Black, S., De Gregorio, E. (2011). Vaccines for the twenty-first century society. Nature reviews immunology, 11(12), 865.

113. Pagano, D., Cutignano, A., Manzo, E., Tinto, F., Fontana, A. (2016). Glycolipids synthesis: Improved hydrazinolysis conditions for preparation of 1, 2-polyunsaturated fatty acyl-β-monogalactosyl-glycerols. Carbohydrate research, 424, 21-23.

114. Manzo, E., Gallo, C., Fioretto, L., Nuzzo, G., Barra, G., Pagano, D., Russo Krauss, I., Paduano, L., Ziaco, M., DellaGreca, M., De Palma, R., Fontana, A. (2019). Diasteroselective Colloidal Self-Assembly Affects the Immunological Response of the Molecular Adjuvant Sulfavant. ACS Omega, 4(4), 7807-7814.

115. Motabar, O., Goldin, E., Leister, W., Liu, K., Southall, N., Huang, W., Marugan, J. J., Sidransky, E., Zheng, W. (2012). A high throughput glucocerebrosidase assay using the natural substrate glucosylceramide. Analytical and bioanalytical chemistry, 402(2), 731-739.

116. [BOOK] O'Hagan, D. T., Singh, M. (2007). MF59: a safe and potent oil-in-water emulsion adjuvant (pp. 115-129). John Wiley & Sons: Hoboken, NJ, USA.

117. Hanashima, S., Mizushina, Y., Yamazaki, T., Ohta, K., Takahashi, S., Sahara, H., Sagakuchi, K. Sugawara, F. (2001). Synthesis of sulfoquinovosylacylglycerols, inhibitors of eukaryotic DNA polymerase α and β. Bioorganic & medicinal chemistry, 9(2), 367-376.

118. Gigg, R., Penglis, A. A., Conant, R. (1980). Synthesis of 3-O-(6-deoxy-6-sulpho-α-D-glucopyranosyl)-1, 2-di-O-hexadecanoyl-L-glycerol, 'sulphoquinovosyl diglyceride'. Journal of the Chemical Society, Perkin Transactions 1, 2490-2493.

119. Yamazaki, T., Aoki, S., Ohta, K., Hyuma, S., Sakaguchi, K., Sugawara, F. (2004). Synthesis of an immunosuppressant SQAG9 and determination of the binding peptide by T7 phage display. Bioorganic & medicinal chemistry letters, 14(16), 4343-4346.

120. Manzo, E., Ciavatta, M. L., Pagano, D., Fontana, A. (2012). An efficient and versatile chemical synthesis of bioactive glyco-glycerolipids. Tetrahedron Letters, 53(7), 879-881.

121. Manzo, E., Fioretto, L., Pagano, D., Nuzzo, G., Gallo, C., De Palma, R., Fontana, A. (2017). Chemical synthesis of marine-derived

sulfoglycolipids, a new class of molecular adjuvants. Marine drugs, 15(9), 288.

122. Schmidt, R. R., Michel, J. (1980). Facile synthesis of α-and β-O-glycosyl imidates; preparation of glycosides and disaccharides. Angewandte Chemie International Edition in English, 19(9), 731-732.

123. Schmidt, R. R. (1986). New Methods for the Synthesis of Glycosides and Oligosaccharides—Are There Alternatives to the Koenigs-Knorr Method? [New Synthetic Methods (56)]. Angewandte Chemie International Edition in English, 25(3), 212-235.

124. Mannock, D. A., Lewis, R. N., McElhaney, R. N. (1987). An improved procedure for the preparation of 1, 2-di-O-acyl-3-O-(β-D-glucopyranosyl)-sn-glycerols. Chemistry and physics of lipids, 43(2), 113-127.

125. Sallusto, F., Lanzavecchia, A. (1994). Efficient presentation of soluble antigen by cultured human dendritic cells is maintained by granulocyte/macrophage colony-stimulating factor plus interleukin 4 and downregulated by tumor necrosis factor alpha. Journal of Experimental Medicine, 179(4), 1109-1118.

126. Qu, C., Brinck-Jensen, N. S., Zang, M., Chen, K. (2014). Monocyte-derived dendritic cells: targets as potent antigen-presenting cells for the design of vaccines against infectious diseases. International Journal of Infectious Diseases, 19, 1-5.

127. Zhou, L. J., Tedder, T. F. (1996). CD14+ blood monocytes can differentiate into functionally mature CD83+ dendritic cells. Proceedings of the National Academy of Sciences, 93(6), 2588-2592.

128. Zhou, L. J., Tedder, T. F. (1995). Human blood dendritic cells selectively express CD83, a member of the immunoglobulin superfamily. The Journal of Immunology, 154(8), 3821-3835.

129. Coffman, R. L., Sher, A., Seder, R. A. (2010). Vaccine adjuvants: putting innate immunity to work. Immunity, 33(4), 492-503.

130. Tze, L. E., Horikawa, K., Domaschenz, H., Howard, D. R., Roots, C. M., Rigby, R. J., Way, D.A., Ohmura-Hoshino, M., Ishido, S., Degli-Esposti, M. A., Goodnow, C. C. (2011). CD83 increases MHC II and CD86 on dendritic cells by opposing IL-10–driven MARCH1-mediated ubiquitination and degradation. Journal of Experimental Medicine, 208(1), 149-165.

131. Prechtel, A. T., Turza, N. M., Theodoridis, A. A., Steinkasserer, A. (2007). CD83 knockdown in monocyte-derived dendritic cells by small interfering RNA leads to a diminished T cell stimulation. The Journal of Immunology, 178(9), 5454-5464.

132. Aerts-Toegaert, C., Heirman, C., Tuyaerts, S., Corthals, J., Aerts, J. L., Bonehill, A., Breckpot, K. (2007). CD83 expression on dendritic cells and T cells: correlation with effective immune responses. European journal of immunology, 37(3), 686-695.

133. Heufler, C., Koch, F., Stanzl, U., Topar, G., Wysocka, M., Trinchieri, G., Steinmen, R.M., Romani, N., Schuler, G. (1996). Interleukin-12 is produced by dendritic cells and mediates T helper 1 development as well as interferon-γ production by T helper 1 cells. European journal of immunology, 26(3), 659-668.

134. Steinhagen, F., Kinjo, T., Bode, C., Klinman, D. M. (2011). TLR-based immune adjuvants. Vaccine, 29(17), 3341-3355.

135. Collins, A. M. (2016). IgG subclass co-expression brings harmony to the quartet model of murine IgG function. Immunology and cell biology, 94(10), 949-954.

136. Nativi, C., Renaudet, O. (2014). Recent progress in antitumoral synthetic vaccines.

137. Strioga, M. M., Felzmann, T., Powell Jr, D. J., Ostapenko, V., Dobrovolskiene, N. T., Matuskova, M., Michalek, J., Schijns, V. E. (2013).

Therapeutic Dendritic Cell− Based Cancer Vaccines: The State of the Art. Critical Reviews™ in Immunology, 33(6).

138. Ya, Z., Hailemichael, Y., Overwijk, W., Restifo, N. P. (2015). Mouse model for Pre-Clinical study of human cancer immunotherapy. Current protocols in immunology, 108(1), 20-1.

139. Schwartzentruber, D. J., Lawson, D. H., Richards, J. M., Conry, R. M., Miller, D. M., Treisman, J., Gailani, F., Riley, L., Conlon, K., Pockaj, B., Kendra, K. L., White, R. L. (2011). gp100 peptide vaccine and interleukin-2 in patients with advanced melanoma. New England Journal of Medicine, 364(22), 2119-2127.

140. Kalli, F., Machiorlatti, R., Battaglia, F., Parodi, A., Conteduca, G., Ferrera, F., Proietti, M., Tardito, S., Sanguineti, M., Millo, E., Fenoglio, D., De Palma, R., Inghirami, G., Filaci, G. (2013). Comparative analysis of cancer vaccine settings for the selection of an effective protocol in mice. Journal of translational medicine, 11(1), 120.

141. De Gregorio, E., D'Oro, U., Wack, A. (2009). Immunology of TLR-independent vaccine adjuvants. Current opinion in immunology, 21(3), 339-345.

142. Traboni, S., Bedini, E., Iadonisi, A. (2018). Solvent-Free Conversion of Alcohols to Alkyl Iodides and One-Pot Elaborations Thereof. ChemistrySelect, 3(6), 1616-1622.

143. Teng, M. W., Bowman, E. P., McElwee, J. J., Smyth, M. J., Casanova, J. L., Cooper, A. M., Cua, D. J. (2015). IL-12 and IL-23 cytokines: from discovery to targeted therapies for immune-mediated inflammatory diseases. Nature medicine, 21(7), 719.

144. Kaka, A. S., Foster, A. E., Weiss, H. L., Rooney, C. M., Leen, A. M. (2008). Using dendritic cell maturation and IL-12 producing capacity as markers of function: a cautionary tale. Journal of immunotherapy (Hagerstown, Md.: 1997), 31(4), 359.

145. Pearce, E. J., Everts, B. (2015). Dendritic cell metabolism. Nature Reviews Immunology, 15(1), 18.

146. Couper, K. N., Blount, D. G., Riley, E. M. (2008). IL-10: the master regulator of immunity to infection. The Journal of Immunology, 180(9), 5771-5777.

147. Owen, S. C., Doak, A. K., Ganesh, A. N., Nedyalkova, L., McLaughlin, C. K., Shoichet, B. K., Shoichet, M. S. (2014). Colloidal drug formulations can explain "bell-shaped" concentration–response curves. ACS chemical biology, 9(3), 777-784.

148. Yamamoto, Y., Sahara, H., Takenouchi, M., Matsumoto, Y., Imai, A., Fujita, T., Tamura, Y., Takahashi, N., Gasa, S., Matsumoto, K., Ohta, K., Sugawara, F., Sakaguchi, K., Jimbow, K., Sato, N. (2004). Inhibition of CD62L+ T-cell response in vitro via a novel sulfo-glycolipid, β-SQAG9 liposome that binds to CD62L molecule on the cell surface. Cellular immunology, 232(1-2), 105-115.

149. Aoki, S., Ohta, K., Matsumoto, K., Sakai, H., Abe, M., Miura, M., Sugawara, F., Sakaguchi, K. (2006). An emulsion of sulfoquinovosylacylglycerol with long-chain alkanes increases its permeability to tumor cells. The Journal of membrane biology, 213(1), 11-18.

150. Matsumoto, K., Takenouchi, M., Ohta, K., Ohta, Y., Imura, T., Oshige, M., Yamamoto, Y., Sahara, H., Sakai, H., Abe, M., Sugawara, F., Sato, N., Sakaguchi, K. (2004). Design of vesicles of 1, 2-di-O-acyl-3-O-(β-d-sulfoquinovosyl)-glyceride bearing two stearic acids (β-SQDG-C18), a novel immunosuppressive drug. Biochemical pharmacology, 68(12), 2379-2386.

151. [BOOK] Cosgrove, T. (Ed.). (2010). Colloid science: principles, methods and applications. John Wiley & Sons.

152. [BOOK] Tadros, T. F. (Ed.). (2013). Encyclopedia of colloid and interface science (pp. 492-492). Berlin: Springer.

153. Nagarajan, R., Ruckenstein, E. (1991). Theory of surfactant self-assembly: a predictive molecular thermodynamic approach. Langmuir, 7(12), 2934-2969.

154. Matsumoto, K., Sakai, H., Takeuchi, R., Tsuchiya, K., Ohta, K., Sugawara, F., Abe, M., Sakaguchi, K. (2005). Effective form of sulfoquinovosyldiacyglycerol (SQDG) vesicles for DNA polymerase inhibition. Colloids and Surfaces B: Biointerfaces, 46(3), 175-181.

155. [BOOK] Lomakin, A., Teplow, D. B., Benedek, G. B. (2005). Quasielastic light scattering for protein assembly studies. In Amyloid Proteins (pp. 153-174). Humana Press.

156. Stetefeld, J., McKenna, S. A., Patel, T. R. (2016). Dynamic light scattering: a practical guide and applications in biomedical sciences. Biophysical reviews, 8(4), 409-427.

157. Foord, R., Jakeman, E., Oliver, C. J., Pike, E. R., Blagrove, R. J., Wood, E., Peacocke, A. R. (1970). Determination of diffusion coefficients of haemocyanin at low concentration by intensity fluctuation spectroscopy of scattered laser light. Nature, 227(5255), 242.

158. Santos, F. K. G., Neto, E. L. B., Moura, M. C. P., Dantas, T. N. C., Neto, A. A. D. (2009). Molecular behavior of ionic and nonionic surfactants in saline medium. Colloids and Surfaces A: Physicochemical and Engineering Aspects, 333(1-3), 156-162.

159. [BOOK] Tanford, C. (1980). The hydrophobic effect: formation of micelles and biological membranes 2d ed. J. Wiley.

160. Lipinski, C. A. (2000). Drug-like properties and the causes of poor solubility and poor permeability. Journal of pharmacological and toxicological methods, 44(1), 235-249.

161. Wan, L. S., Lee, P. F. (1974). CMC of polysorbates. Journal of pharmaceutical sciences, 63(1), 136-137.

162. Garcia-Mateos, I., Mercedes Velazquez, M., Rodriguez, L. J. (1990). Critical micelle concentration determination in binary mixtures of ionic surfactants by deconvolution of conductivity/concentration curves. Langmuir, 6(6), 1078-1083.

163. Chattopadhyay, A., London, E. (1984). Fluorimetric determination of critical micelle concentration avoiding interference from detergent charge. Analytical biochemistry, 139(2), 408-412.

164. Aguiar, J., Carpena, P., Molina-Bolıvar, J. A., Ruiz, C. C. (2003). On the determination of the critical micelle concentration by the pyrene 1: 3 ratio method. Journal of Colloid and Interface Science, 258(1), 116-122.

165. Cai, L., Gochin, M., Liu, K. (2011). A facile surfactant critical micelle concentration determination. Chemical Communications, 47(19), 5527-5529.

166. Cerichelli, G., Mancinit, G. (1997). NMR techniques applied to micellar systems. Current opinion in colloid & interface science, 2(6), 641-648

167. LaPlante, S. R., Carson, R., Gillard, J., Aubry, N., Coulombe, R., Bordeleau, S., Bonneau, P., Little, M., O'Meara, J., Beaulieu, P. L. (2013). Compound aggregation in drug discovery: implementing a practical NMR assay for chemists. Journal of medicinal chemistry, 56(12), 5142-5150.

168. Strickley, R. G. (2004). Solubilizing excipients in oral and injectable formulations. Pharmaceutical research, 21(2), 201-230.

169. Grant, R. L., Yao, C., Gabaldon, D., Acosta, D. (1992). Evaluation of surfactant cytotoxicity potential by primary cultures of ocular tissues: I. Characterization of rabbit corneal epithelial cells and initial injury and delayed toxicity studies. Toxicology, 76(2), 153-176.

170. Gelderblom, H., Verweij, J., Nooter, K., Sparreboom, A. (2001). Cremophor EL: the drawbacks and advantages of vehicle selection for drug formulation. European journal of cancer, 37(13), 1590-1598.

171. Kiss, L., Walter, F. R., Bocsik, A., Veszelka, S., Ózsvári, B., Puskás, L. G., Szabó-Révész, P., Deli, M. A. (2013). Kinetic analysis of the toxicity of pharmaceutical excipients Cremophor EL and RH40 on endothelial and epithelial cells. Journal of pharmaceutical sciences, 102(4), 1173-1181.

172. Szutkowski, K., Kołodziejska, Ż., Pietralik, Z., Zhukov, I., Skrzypczak, A., Materna, K., Kozak, M. (2018). Clear distinction between CAC and CMC revealed by high-resolution NMR diffusometry for a series of bis-imidazolium gemini surfactants in aqueous solutions. RSC advances, 8(67), 38470-38482.

173. Brito, R. M., Vaz, W. L. (1986). Determination of the critical micelle concentration of surfactants using the fluorescent probe N-phenyl-1-naphthylamine. Analytical biochemistry, 152(2), 250-255.

174. Kalyanasundaram, K. (1988). Pyrene fluorescence as a probe of fluorocarbon micelles and their mixed micelles with hydrocarbon surfactants. Langmuir, 4(4), 942-945.

175. London, E., Feigenson, G. W. (1978). A convenient and sensitive fluorescence assay for phospholipid vesicles using diphenylhexatriene. Analytical biochemistry, 88(1), 203-211

176. Laan, A. C., Denkova, A. G. (2017). Cryogenic transmission electron microscopy: the technique of choice for the characterization of polymeric nanocarriers. EJNMMI research, 7(1), 44.

177. Franken, L. E., Boekema, E. J., Stuart, M. C. (2017). Transmission electron microscopy as a tool for the characterization of soft materials: application and interpretation. Advanced Science, 4(5), 1600476.

178. Dubochet, J., Adrian, M., Chang, J. J., Homo, J. C., Lepault, J., McDowall, A. W., Schultz, P. (1988). Cryo-electron microscopy of vitrified specimens. Quarterly reviews of biophysics, 21(2), 129-228.

179. Friedrich, H., Frederik, P. M., de With, G., Sommerdijk, N. A. (2010). Imaging of self-assembled structures: interpretation of TEM and Cryo-TEM images. Angewandte Chemie International Edition, 49(43), 7850-7858.

180. Aniansson, E. A. G., Wall, S. N., Almgren, M., Hoffmann, H., Kielmann, I., Ulbricht, W., Zana, R., Lang, J., Tondre, C. (1976). Theory of the kinetics of micellar equilibria and quantitative interpretation of chemical relaxation studies of micellar solutions of ionic surfactants. The Journal of Physical Chemistry, 80(9), 905-922.

181. Morigaki, K., Walde, P., Misran, M., Robinson, B. H. (2003). Thermodynamic and kinetic stability. Properties of micelles and vesicles formed by the decanoic acid/decanoate system. Colloids and Surfaces A: Physicochemical and Engineering Aspects, 213(1), 37-44.

182. Dushkin, C. D., Ivanov, I. B., Kralchevsky, P. A. (1991). The kinetics of the surface tension of micellar surfactant solutions. Colloids and surfaces, 60, 235-261.

183. Yan, H., Yalagala, R. S., Yan, F. (2015). Fluorescently labelled glycans and their applications. Glycoconjugate journal, 32(8), 559-574.

184. Liu, Y., Bittman, R. (2006). Synthesis of fluorescent lactosylceramide stereoisomers. Chemistry and physics of lipids, 142(1-2), 58-69.

185. Gretskaya, N. M., Bezuglov, V. V. (2013). Synthesis of BODIPY® FL C 5-Labeled D-erythro-and L-threo-Lactosylceramides. Chemistry of natural compounds, 49(1), 17-20.

186. Vo-Hoang, Y., Micouin, L., Ronet, C., Gachelin, G., Bonin, M. (2003). Total Enantioselective Synthesis and In Vivo Biological Evaluation of a Novel Fluorescent BODIPY α-Galactosylceramide. ChemBioChem, 4(1), 27-33.

187. Cheng, J. M., Chee, S. H., Knight, D. A., Acha-Orbea, H., Hermans, I. F., Timmer, M. S., Stocker, B. L. (2011). An improved synthesis of dansylated α-galactosylceramide and its use as a fluorescent probe for the monitoring of glycolipid uptake by cells. Carbohydrate research, 346(7), 914-926.

188. Daikoku, S., Ono, Y., Ohtake, A., Hasegawa, Y., Fukusaki, E., Suzuki, K., Ito, Y., Goto, S., Kanie, O. (2011). Fluorescence-monitored zero dead-volume nanoLC-microESI-QIT-TOF MS for analysis of fluorescently tagged glycosphingolipids. Analyst, 136(5), 1046-1050.

189. Rudin, M., Weissleder, R. (2003). Molecular imaging in drug discovery and development. Nature reviews Drug discovery, 2(2), 123.

190. Manzo, E., D'Ippolito, G., Pagano, D., Tinto, F., Fontana, A. (2014). Design and synthesis of fluorescent galactolipid probes. Tetrahedron letters, 55(25), 3521-3524.

191. Molotkovsky, J. G., Mikhalyov, I. I., Imbs, A. B., Bergelson, L. D. (1991). Synthesis and characterization of new fluorescent glycolipid probes. Molecular organisation of glycosphingolipids in mixed-composition lipid bilayers. Chemistry and physics of lipids, 58(3), 199-212.

192. Boldyrev, I. A., Zhai, X., Momsen, M. M., Brockman, H. L., Brown, R. E., Molotkovsky, J. G. (2007). New BODIPY lipid probes for fluorescence studies of membranes. Journal of lipid research, 48(7), 1518-1532.

193. Boldyrev, I. A., Molotkovsky, J. G. (2010). New 4, 4-difluoro-3a, 4a-diaza-s-indacene (BODIPY)-labeled sphingolipids for membrane studies. Russian journal of bioorganic chemistry, 36(4), 508-511.

194. Rasmussen, J. A. M., Hermetter, A. (2008). Chemical synthesis of fluorescent glycero-and sphingolipids. Progress in lipid research, 47(6), 436-460.

195. Bittman, R. (2004). The 2003 ASBMB-Avanti award in lipids address: applications of novel synthetic lipids to biological problems. Chemistry and physics of lipids, 129(2), 111-131.

196. Pagano, R. E., Martin, O. C., Kang, H. C., Haugland, R. P. (1991). A novel fluorescent ceramide analogue for studying membrane traffic in animal cells: accumulation at the Golgi apparatus results in altered spectral properties of the sphingolipid precursor. The Journal of cell biology, 113(6), 1267-1279.

197. Boens, N., Leen, V., Dehaen, W. (2012). Fluorescent indicators based on BODIPY. Chemical Society Reviews, 41(3), 1130-1172.

198. Johnson, I. D., Kang, H. C., Haugland, R. P. (1991). Fluorescent membrane probes incorporating dipyrrometheneboron difluoride fluorophores. Analytical biochemistry, 198(2), 228-237.

199. Karolin, J., Johansson, L. B. A., Strandberg, L., Ny, T. (1994). Fluorescence and absorption spectroscopic properties of dipyrrometheneboron difluoride (BODIPY) derivatives in liquids, lipid membranes, and proteins. Journal of the American Chemical Society, 116(17), 7801-7806.

200. Ni, Y., Wu, J. (2014). Far-red and near infrared BODIPY dyes: synthesis and applications for fluorescent pH probes and bio-imaging. Organic & biomolecular chemistry, 12(23), 3774-3791.

201. Pagano, R. E., Puri, V., Dominguez, M., Marks, D. L. (2000). Membrane traffic in sphingolipid storage diseases. Traffic, 1(11), 807-815.

202. Boldyrev, I. A., Molotkovsky, J. G. (2006). A synthesis and properties of new 4, 4-difluoro-3a, 4a-diaza-s-indacene (BODIPY)-labeled lipids. Russian Journal of Bioorganic Chemistry, 32(1), 78-83.

203. Lenschow, D. J., Walunas, T. L., Bluestone, J. A. (1996). CD28/B7 system of T cell costimulation. Annual review of immunology, 14(1), 233-258

204. Manzo, E., Carbone, M., Mollo, E., Irace, C., Di Pascale, A., Li, Y., Ciavatta, M. L., Cimino, G., Guo, Y. W., Gavagnin, M. (2011). Structure and synthesis of a unique isonitrile lipid isolated from the marine mollusk Actinocyclus papillatus. Organic letters, 13(8), 1897-1899.

205. Koenigs, W., Knorr, E. (1901). Ueber einige Derivate des Traubenzuckers und der Galactose. Berichte der deutschen chemischen Gesellschaft, 34(1), 957-981.

206. Igarashi, K. (1977). The Koenigs-Knorr reaction. In Advances in Carbohydrate Chemistry and Biochemistry (Vol. 34, pp. 243-283). Academic Press.

207. Thorsheim, K., Siegbahn, A., Johnsson, R. E., Stålbrand, H., Manner, S., Widmalm, G., Ellervik, U. (2015). Chemistry of xylopyranosides. Carbohydrate research, 418, 65-88.

208. Lemieux, R. U., Driguez, H. (1975). Chemical synthesis of 2-O-(α-L-fucopyranosyl)-3-O-(α-D-galactopyranosyl)-D-galactose. Terminal structure of the blood-group B antigenic determinant. Journal of the American Chemical Society, 97(14), 4069-4075.

Acknowledgements

First and foremost, I would like to thank the European Union (PON Ricerca e Innovazione 2014-2020) for founding this PhD project and giving me a great opportunity to pursue my dreams.

I would like to express my gratitude to my supervisors: prof. Marina Della Greca, for her patience and several advices, prof. Raymond Andersen, for his warm hospitality during my internship at UBC in Vancouver and in particular dr. Emiliano Manzo for his moral and scientific support, it was a great privilege to work under his guidance.
Besides my advisors, I would like to thank my examiner, prof. Emiliano Bedini for his insightful comments and our helpful meeting during these three years.
My sincere thanks also goes to all people involved in this thesis, in particular prof. Luigi Paduano, dr. Carmen Gallo, dr. Jenny Nuzzo, dr. Marcello Ziaco and dr. Angelo Fontana, who provided me an opportunity to join their team as intern, who gave access to the laboratory and research facilities and who completed my research with additional data. Without their valuable support, this research would not have been possible.

Thanks to all my colleagues, we are a great team, always ready to encourage each other!
A special thanks to my first labmates, you have been an essential part of my growth in this field!
To all my friends, academic and not, old and new, thank you to make this life more bearable!

I am extremely grateful to my whole family, for their love, understanding, and continuous support throughout my life, even when being by my side was tiring. I

would like to dedicate all my victories to my parents, without their sacrifices for educate and prepare me for my future I would not be here today. My soul (mom), my strength (dad)... my deep gratitude goes to you! For my courage, my sister, thank you because you are who you are... the best sister ever, I will always be by your side!
Special thanks to my brothers-in-law and to my sister-in-law for their friendship, empathy and great sense of humour, you are my family!
For my nephew and my niece (to be), all my life is for you, you are my light in the darkness, my smile in the sadness, my hope for a better future... I love you!
Last but not least, I would like to thank my husband, you are every moment of my days, thank you for supporting me and enduring me, you encouraged me to undertake this journey, you were with me every time I wanted to leave everything, because you know me best of all, maybe better than me. Love u!

For my stars... always with me, always with you!

“The PhD candidate wish to thank European Union (FSE, PON Ricerca e Innovazione 2014-2020, Azione I.1 “Dottorati Innovativi con caratterizzazione Industriale”), for funding a Ph.D. grant to Laura Fioretto”

La borsa di dottorato è stata cofinanziata con risorse del
Programma Operativo Nazionale Ricerca e Innovazione 2014-2020 (CCI 2014IT16M2OP005),
Fondo Sociale Europeo, Azione I.1 “Dottorati Innovativi con caratterizzazione Industriale”

UNIONE EUROPEA
Fondo Sociale Europeo

Ministero dell’Istruzione, dell’Università e della Ricerca

PON RICERCA E INNOVAZIONE 2014 - 2020